ISSN 0280-6819

KAROLINSKA INSTITUTET

TECHNICAL AUDIOLOGY

Report TA128
Oct 1993

Predicting hearing aid response in real ears

Per-Eric Sanborn

KAROLINSKA INSTITUTET
Teknisk Audiologi
Dept. of Technical Audiology

ISSN 0280-6819
TA128, Oct 1993

Predicting hearing aid response in real ears

Per-Eric Sanborn

ABSTRACT

A hearing aid fitted to different ears will produce very different sound pressure spectra in the ear canal. In addition, this variation in response is different among hearing aids.

A description in terms of an electrical analog model of the ear and hearing aid system is given. The applicability of this model is tested via series of measurements. The measurement and prediction procedure was first verified on a coupler (ear simulator) with good results from 300 Hz to 8000 Hz. Three types of hearing-aids were then measured and used on five different human ears. Where the measured and predicted response was compared a fairly good agreement was obtained from 300 Hz to approximately 6000 Hz. The errors are mainly caused by probe misalignments. The theoretical description given in the present work is shown to be valid from low frequencies to at least 10 kHz. The level dependence, due to the contraction of the stapedius muscle, of the ear input impedance is shown to have no significant importance in the prediction of the hearing aid response.

Although solutions for related problems has been given for low frequencies, a solution of the hearing aid fitting problem has not been published earlier.

Keywords: hearing aid, ear, impedance

This work was supported by the Swedish National Board for Industrial and Technical Development (NUTEK), grant No 623-90-1175

Mailing address:
Teknisk Audiologi / KI
Box 70025
S-100 44 STOCKHOLM
Sweden

Visiting address:
Teknisk Audiologi
Lindstedtsvägen 7
Kungliga Tekniska Högskolan
Stockholm

Telephone:
Nat.: 08-411 66 60
Int.: +46 8 411 66 60

Fax:
Nat.: 08-791 71 30
Int.: +46 8 791 71 30

ISSN 0280-6819
TA128, Oct 1993

CONTENTS

ISSN 0280-6819
TA128, Oct 1993

CONTENTS (continued)

1.INTRODUCTION

The response from a hearing aid may show great variations when used on different ears. The variation may reach 20 dB at high frequencies [Olsson, 1985]. This is a major problem when fitting hearing-aids. The basis for selecting hearing-aids is measurements on a coupler (ear simulator), which does not give enough information about the final response on an individual ear. Approximately 90 different models of hearing aids are used in Sweden at present. When fitting hearing aids the hearing aid response is compared to the individual hearing loss. The fact that the hearing aid response is not unique makes the hearing aid fitting time consuming.

In order to estimate the variations a study was made at three hospitals in Stockholm [Berninger et al., 1989]. The result from tests in the frequency range 500 Hz to 4 kHz with one aid on 16 ears was large variations throughout the entire range. One possible explanation for these large variations is the fact that the output impedance of various hearing aids are different, and that the input impedance of the human ears also vary between individuals.

A literature survey that preceded the present project [Sanborn, 1990] revealed two works that were treating problems close to the present one [Egolf et al., 1977, Hara et al., 1988]. In the present work a description in terms of an electrical analog model of the ear and hearing-aid system is given. This model is verified by measurements on a number of hearing aids and human ears.

2.DEFINITIONS

Acoustical impedance is defined as

$$Z = \frac{P}{U},$$

where P is the complex amplitude of the sound pressure and U is the complex amplitude of the volume velocity.

Admittance is the inverse of impedance. Immittance is short for admittance or impedance.

SI-units are used and the time factor is $e^{+j\omega t}$ unless otherwise specified.

3.THEORETICAL DESCRIPTION

The aim of the present work was to give a description of the acoustical system "hearing aid and ear". It should be accurate enough to describe the acoustical parameters involved with sufficient accuracy and yet simple enough for easy applications at the clinics. The frequency range of interest is that of hearing aids today with some margin for further developments.

The theoretical model used in this work is shown in Figure 1. This electrical analogy is a low frequency model expected to be valid for plane waves (below the first cut-on frequency). However, it may also include the effects of nearfield modes.

The model describes the hearing aid (including tube and mold) as a sound pressure generator and an output impedance (Thevenin parameters). The ear is described with an (input) impedance. It is important to notice that this model has no geometrical spread. The parameters involved are valid only at the point of connection between the hearing aid and the ear.

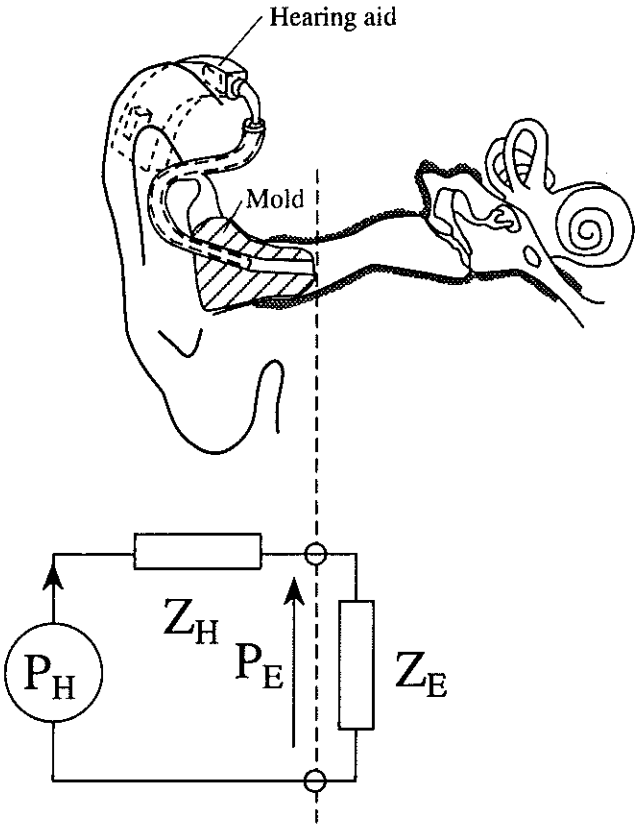

Figure 1. Theoretical model of the acoustical system "hearing aid and ear".

In order to determine the impedances for the system "hearing aid and ear" a so called "impedance probe" is used. This impedance probe is also modelled by an electrical analog circuit as shown in section 4. To determine the hearing aid Thevenin pressure, a measurement proceedure involving a coupler, is used as described in sections 6 and 8.

Measurements and calculations for verification of the model have been carried out in the frequency range 100 Hz to 10 kHz. The verification consists of determining the pressure generator and impedances, calculating the sound pressure in the ear canal and measuring the sound pressure for comparison.

4.IMPEDANCE MEASUREMENT METHOD

The impedance probe consists of an insert earphone (EAR-3A by Etymotic Research) and a probe microphone (ER-7C by Etymotic Research), Figure 2. The earphone is emitting sound into the ear canal through the mold and the microphone is measuring the sound pressure at a position remote to the mold. The earphone and microphone together are calibrated and used as an impedance probe. With the Thevenin parameters of the impedance probe known, the impedance of an object can be calculated from a measurement.

With the assumption that the earphone is giving (approximately) constant volume velocity this configuration of impedance probe has been in use since the 1950's, see "two tube method" in [Sanborn, 1990]. In the present work a more complete description of the probe is used. The impedance probe is modeled as an electrical analog with complex valued Thevenin parameters consisting of a pressure generator (P_0) and an internal impedance (Z_0) as given by Figure 2. For determining the two Thevenin parameters two measurements on two known impedances are required. However, the accuracy of such a calibration is limited near anti-resonance dips.

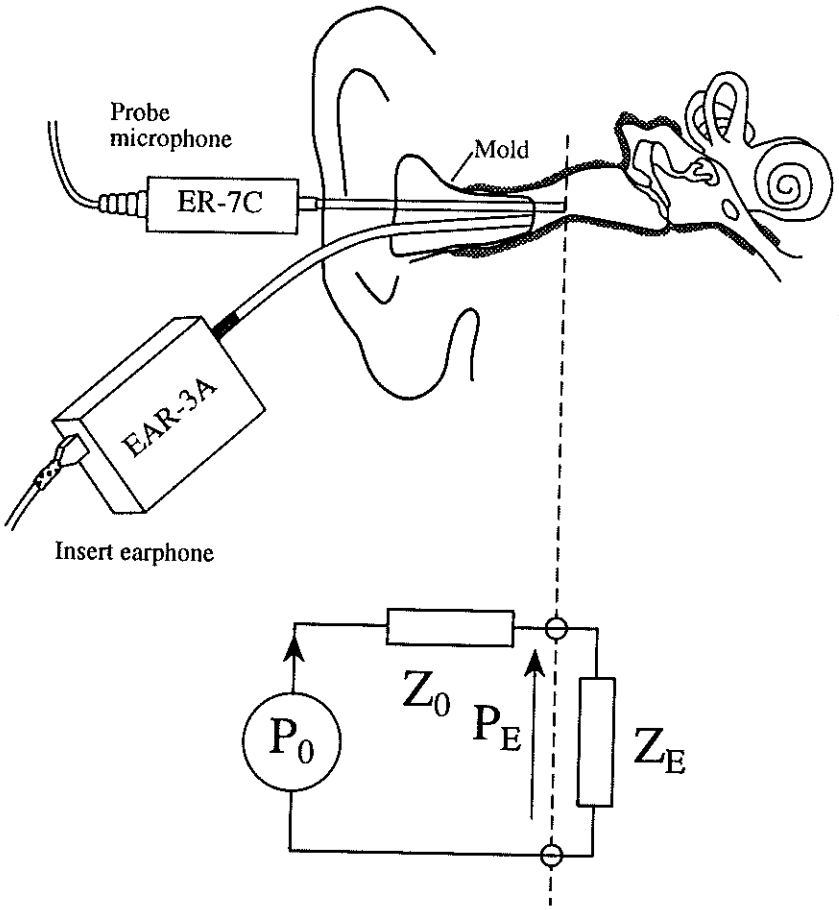

Figure 2. Theoretical model of the "impedance probe and ear".

A calibration procedure useful for a wider frequency range has been presented by Allen, 1985. Allen's procedure makes use of calibration measurements on four known impedances. This will give a overdetermined system for determination of the Thevenin parameters (solved with a Least Mean Square (LMS) -method) leading to a more robust calibration. Keefe et al. has been using this method with some changes and their version of it is used in the present work [Keefe et al. 1992]. This method for increasing the accuracy of measurements is also in use in the area of engineering acoustics, for instance with the multiple load method for measuring source characteristics of fluid machines [Bodén, 1991].

The known impedances are in this investigation those of circular uniform brass tubes with rigid ends. Kirchhoff's solution for sound in a tube with rigid walls includes the effects of both viscosity and heath conduction on acoustic propagation through a rigid cylindrical tube. It assumes that the ocsillatory flow is laminar, nonlinear terms in the equation of motion is negligible, and that the inner wall is isothermal. For use in the present work the input impedance and propagation wave number of these tubes are calculated with a high frequency (small acoustic boundary layer) approximation of Kirchhoff's exact solution given by [Keefe 1984]. Consider a smooth cylindrical duct with isothermal walls whose axis extends along the z axis. For frequencies below the first cut on we have for the acoustic pressure P(z) and volume flow U(z), using the equation of motion and the equation of mass continuity

$$\frac{\partial P}{\partial z} = -ZU, \qquad (1)$$

$$\frac{\partial U}{\partial z} = -YP, \tag{2}$$

where the series impedance Z and the shunt admittance Y per unit length along the z axis of the tube are

$$Z = \frac{j\omega R_0}{c(1-F_v)}, \tag{3}$$

$$Y = \frac{j\omega}{cR_0}(1+(\gamma-1)F_t). \tag{4}$$

Here ω is the angular frequency, c is the speed of sound and R_0 is the characteristic impedance of the tube (acoustic transmission line) in the absence of thermal and viscous dissipation defined as

$$R_0 = \frac{\rho c}{\pi a^2}, \tag{5}$$

where a is the tube radius and ρ is the equilibrium gas density. The quantity γ is given below. The quantity F_V in eq.3 is given by Kirchhoff's solution and is

$$F_v = \frac{2J_1(r_v\sqrt{-j})}{r_v\sqrt{-j}J_0(r_v\sqrt{-j})}, \tag{6}$$

where J_0 and J_1 are Bessel functions and the dimensionless parameter r_V (ratio of tube radius to viscous boundary layer) is

$$r_v = a\sqrt{\frac{\rho\omega}{\eta}}. \tag{7}$$

Here η is the dynamic shear viscosity coefficient. The quantity F_t in eq.4 is

$$F_t = \frac{2J_1(r_t\sqrt{-j})}{r_t\sqrt{-j}J_0(r_t\sqrt{-j})}, \tag{8}$$

where

$$r_t = \nu r_v \tag{9}$$

(the ratio of tube radius to thermal boundary layer) and ν is the square root of the Prandtl number defined as

$$\nu = \sqrt{\frac{\eta C_p}{\kappa}}. \tag{10}$$

Here C_p is the coefficient of specific heat of the gas at constant pressure, and κ is the gas thermal conductivity.

With characteristic acoustic impedance Z_{ci}, propagation wave number Γ_i and tube length L_i, the acoustic impedance of brass tube no. i is given by (Keefe et al., January 1992)

$$Z_i(k) = Z_{ci}(k)\coth(\Gamma_i(k)L_i). \tag{11}$$

When the impedance probe is connected to the impedance to be measured, Z_X, the relation between P_X (the sound pressure measured by the microphone), Z_X and the Thevenin parameters of the probe is

$$P_x = P_0 \frac{Z_x}{Z_0 + Z_x}. \tag{12}$$

Suppose the calibration is carried out with M known impedances (in the present work M = 10). Eq.12 used for each of the M measurements in the calibration gives the system

$$\begin{bmatrix} Z_1 & -P_1 \\ Z_2 & -P_2 \\ \vdots & \vdots \\ Z_M & -P_M \end{bmatrix} \begin{bmatrix} P_0 \\ Z_0 \end{bmatrix} = \begin{bmatrix} P_1 Z_1 \\ P_2 Z_2 \\ \vdots \\ P_M Z_M \end{bmatrix}. \tag{13}$$

Explicit reference to frequency is suppressed in the system equations, and it is understood that they must be solved separately for each frequency. For optimization of this system the error function $\varepsilon(n)$ is first calculated for each frequency n as

$$\varepsilon(n) = \sum_{i=1}^{M} \left| Z_i P_0 - P_i Z_0 - P_i Z_i \right|^2. \tag{14}$$

Whatever values are chosen for the lengths, they must be applied for all frequencies when computing the Thevenin parameters. For visualizing the error, it is convenient to define a non-dimensional error function $N(n)$

$$N(n) = \frac{\varepsilon(n)}{\sum_{i=1}^{M} \left| P_i Z_i \right|^2} \tag{15}$$

The average normalized error N_T quantifies the error across the optimization bandwith, and is defined to be

$$N_T = \frac{1}{n_2 - n_1 + 1} \sum_{n=n_1}^{n_2} N(n). \tag{16}$$

The error function N_T is a function of the M closed tube lengths, and the lengths L_i are chosen such that N_T is minimized. This may be regarded as a weighted least-squares method where the weighting coefficient is the denominator of equation 15.

The minimization method used in the M-dimensional space is the modified Powell's method. In each dimension the minimization technique of Brent is used [Press et al.1986]. The result of the optimization is depending on the starting values of the tube lengths. In [Keefe et al. 1992] the starting values of the tube lengths were calculated from the resonance peaks of measured sound pressure spectra in the tubes. In the present work the initial tube lengths were instead measured with a rule.

When the optimization is through, P_0 and Z_0 are given by the LMS-solution [Allen 1985]:

$$\begin{bmatrix} P_0 \\ Z_0 \end{bmatrix} = \frac{1}{\Delta} \begin{bmatrix} \sum_{i=1}^{M} |P_i|^2 & -\sum_{i=1}^{M} \overline{Z_i} P_i \\ \sum_{i=1}^{M} \overline{P_i} Z_i & -\sum_{i=1}^{M} |Z_i|^2 \end{bmatrix} \begin{bmatrix} \sum_{i=1}^{M} |Z_i|^2 P_i \\ \sum_{i=1}^{M} |P_i|^2 Z_i \end{bmatrix} \tag{17a}$$

with

$$\Delta = \left(\sum_{i=1}^{M} |Z_i|^2 \right) \left(\sum_{i=1}^{M} |P_i|^2 \right) - \left(\sum_{i=1}^{M} \overline{P_i} Z_i \right) \left(\sum_{i=1}^{M} \overline{Z_i} P_i \right). \tag{17b}$$

This LMS-solution is derived in appendix 3.

The tip of the probe microphone extends approximately 5 mm past the flush surface of the plastic insert (see Figure 2), in order to reduce the contribution of the evanescent mode coupling between the earphone source and the probe tip. This leaves a cavity between the probe tip and the surface of the plastic surface. This cavity will have a volume depending on the tube diameter. The calibration will therefore give different results in terms of P_0 and Z_0 depending on the tube diameter. The calibration was therefore carried out for diameters 7.5 mm, corresponding approximately to the outer part of the earcanal, and 3 mm, corresponding to the canal in the mold (see Figure 1).

In order to improve the measurement accuracy at different diameters of the measured object the calibration tube diameters were given a variation around nominal values.

The LMS solution in eq.17 is based on the assumption that the matrix on the left hand of eq.13 is not singular or close to singular. One simple way of preventing this is to use one tube that is significantly shorter than the remaining tubes. To be even more sure that this is the case 3 short tubes were used, see Table 1.

A resistance $\mathrm{Re}(Z_0)$ less than zero was not accepted as this would mean that the internal impedance of the earphone is active. At frequencies were this happened $\mathrm{Re}(Z_0)$ was put equal to zero.

5.APPROXIMATIONS AND VALUES OF PHYSICAL CONSTANTS

The following approximations for the thermodynamic constants for air are used in this investigation [Keefe, 1984]:

$$\rho = 1.1769(1 - 0.00335\Delta T'), \tag{18}$$

$$\eta = 1.846 \cdot 10^{-5}(1 + 0.0025\Delta T'), \tag{19}$$

$$\gamma = 1.4017(1 - 0.00002\Delta T'), \tag{20}$$

$$\nu = 0.8410(1 - 0.0002\Delta T), \tag{21}$$

$$c = 347.23(1 + 0.00166\Delta T'), \tag{22}$$

where ΔT is the temperature difference relative to 26.85 $^{\circ}C$. These equations are believed to be accurate within ± 10 $^{\circ}C$ of that temperature.

The characteristic impedance Z_c of the transmission line is defined to be the input impedance looking into a infinite length of cylindrical tubing and is

$$Z_c = \sqrt{\frac{Z}{Y}}. \tag{23}$$

The propagation wavenumber Γ of the transmission line is defined to be the phase change per unit length at a fixed time along an infinite cylindrical tube and is

$$\Gamma = \alpha + j(\frac{\omega}{v_p}) = \sqrt{ZY}, \tag{24}$$

where v_p is the phase velocity.

The large r_v approximation is computed using an asymptotic expansion of the Bessel functions which converges asymptotically to the exact result as r assumes large values. For air at 26.85 °C and atmospheric pressure we get

$$\mathrm{Re}(Z_c) = R_o(1 + \frac{0.369}{r_v}), \tag{25}$$

$$\mathrm{Im}(Z_c) = -R_0(\frac{0.369}{r_v} + \frac{1.149}{(r_v)^2} + \frac{0.303}{(r_v)^3}), \tag{26}$$

$$\alpha = (\frac{\omega}{c})(\frac{1.045}{r_v} + \frac{1.080}{(r_v)^2} + \frac{0.750}{(r_v)^3}), \tag{27}$$

$$v_p = \frac{c}{(1 + \frac{1.045}{r_v})}. \tag{28}$$

From the asymptotic expansion of the Bessel functions, the lower limit for this high frequency approximation can be calculated. With an accuracy of 1% we get for a tube radius of 1.5 mm the limit at 26.7 Hz and for radius 3.5 mm the limit is 4.90 Hz.

6.THE MEASUREMENT PROCEDURE IN BRIEF

In order to check the validity of the model in Figure 1, P_H, Z_H and Z_E were calculated from measurements, the predicted pressure P_{EPRED} calculated and then measured for verification.

P_H was calculated from the response obtained when the hearing aid was connected to a IEC 711 coupler (see Figure 12). This requires knowledge of the coupler input impedance and transfer function.

Z_H and Z_E were measured with the impedance measurement method described in section 4.

In practice the calibration measurements were carried out first. Second the prediction check and ear impedance were measured on each subject. Last the measurements for P_H and Z_H were carried out on each hearing aid with individual mold. P_H was determined with the same electrical input signal as in the prediction check measurement.

All measurement devices were expected to have properties independent of signal level.

7. PROBLEMS AND LIMITATIONS OF THE METHOD

Different sources of error may distort the results. Those expected to dominate were checked and are discussed below.

7.1 Otoacoustic emission

When stimulated by external sounds the ear will give a low level response to this stimulation. In the present project measurement levels where high except in the frequency range 7 kHz-9 kHz. However the levels of the otoacoustic emission are usually below 30 dB SPL at the particular frequencies and stimulus levels used [Norton, 1993]. Otoacoustic emission is therefore not expected to cause any errors in our mesurements.

7.2 Stapedius contraction

At high sound pressure levels the stapedius muscle is contracted. The muscle will pull the ossicle chain in such a way that the eardrum is pulled inwards and becomes stiff. This will in turn increase the input impedance of the middle ear. For sinusoidal stimulus the threshold of contraction is 90-95 dB SPL [Margolis, 1993]. It has been shown that the sound pressure level in the ear canal is increased approximatly 2.5 dB when the stimulus tone was increased from 85 to 110 dB Hearing Level [Anderson, 1969].

The stapedius reflex is active throughout long-term exposure to an industrial noise which is variable with respect to frequency and amplitude [Borg et al. 1979]. In the present work the stimulus signal was a sinewave stepped in frequency over the measurement range. It has not been found in the literature whether or not a change in frequency only will reactivate the stapedius muscle. If the stapedius was not reactivated from a frequency shift only it may have caused problems turning on and off during our measurements.

In order to check the reactivation from frequency shifts, measurements were therefore carried out on two persons with normal audiograms. The stapedius reflex is bilateral, that is a sufficiently high sound level into one ear will cause a contraction in both ears. In Figure 3 a schematic picture of the inter-aural measurement is given. The stimulus is emitted into the left ear, from the generator via amplifier, attenuators and earphone. The stimulus level is monitored through a probe microphone and a measurement amplifier. On the right side the same type of equipment for monitoring the change in impedance is connected. The impedance itself was not measured but the change in sound pressure due to the change in impedance.

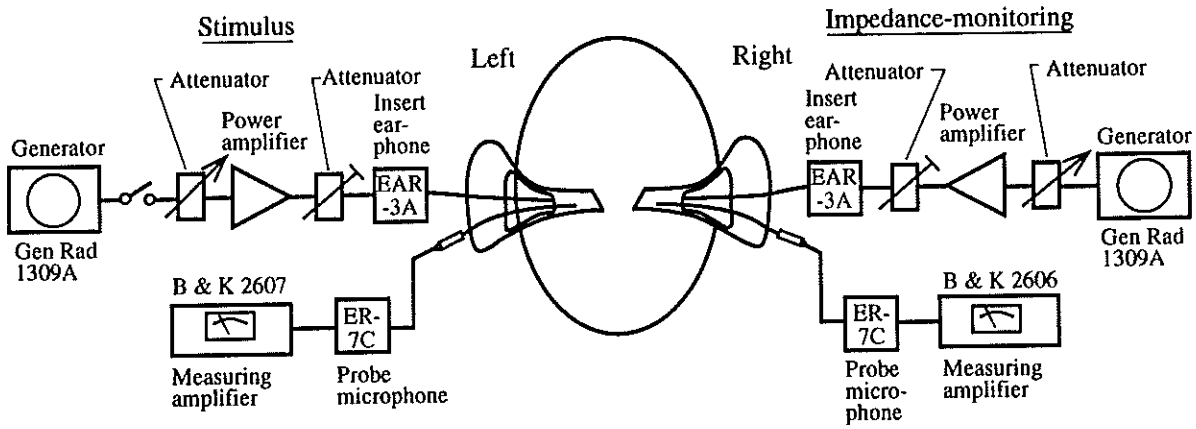

Figure 3. Shematic view of measurement setup for stapedius contraction check.

In the first experiment the stimulus tone was 500 Hz, 110 dB SPL for 10 sek. The probe tone was 800 Hz 65 dB. Over the 10 sek. period the probe tone level decreased approximatly 0.5 dB. This indicates that the stapedius is contracted at the onset of the stimulus tone and is released over the measurement time.

In the second experiment the stimulus tone was 300 Hz - 1 kHz in 25 Hz steps, 3 sec. for each frequency, 110 dB SPL. The frequency step and time is that of most measurements in the main investigations in this project. The probe tone was the same as in the first experiment. In this case there was no significant change in the level of the probe tone. This indicates that the stapedius is reactivated by the change in frequency only. Although not found in the literature this result was expected.

7.3 Probe location in the ear canal

While making measurements in the ear canal it is important to know the position of the probe end. As will be shown below it is important to measure the input impedance of the ear and the sound pressure (for comparison) in the same point. This problem was to a large degree solved by making identical molds for hearing aid and impedance probe on each ear.

A simulation model using MathCAD was made for checking the dependence of probe position in the hearing aid Thevenin impedance on the predicted sound pressure level. The hearing aid receiver is modeled as a resistor (10^9 acoustic ohms), the middle ear is modeled with Shaw's electrical analog [Shaw and Stinson, 1981]. The tube (diam. 2 mm, length 60 mm) and ear canal (diam. 7 mm, length 15 mm) are modeled as loss-free straight tubes of constant crossection. An impedance translation proceedure, chapter 3-7 in [Pierce, 1981], was used for sound propagation in the tubes.

In Figure 4 the real part (Figure 4a) and the imaginary part (Figure 4b) of the hearing aid Thevenin impedance is given. The left-most curves are valid for the correct position of the impedance probe. The right-most curves are valid for a probe position 1 mm closer to the hearing aid. In Figure 4c the difference in predicted sound pressure level in the ear canal of theses two cases are given. The calculations are given in Appendix 1.

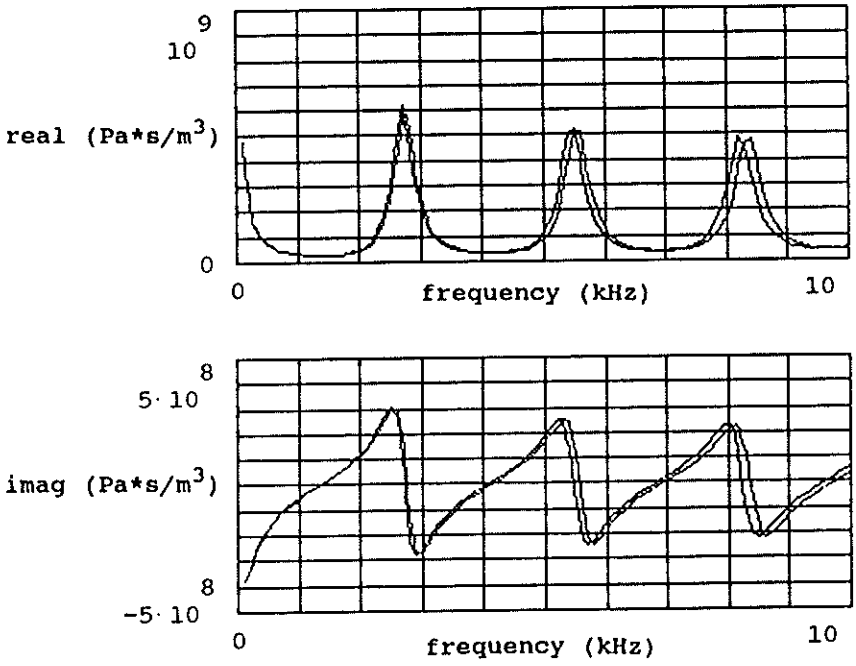

Figure 4a,b. Probe positioning error in impedance measurement of the hearing aid. Real part (upper) and imaginary part (lower) of hearing aid Thevenin impedance (in Pa·s/m^3). Left-most curves are valid for correct probe position, right-most curves are valid for a probe position 1mm closer to the ear drum.

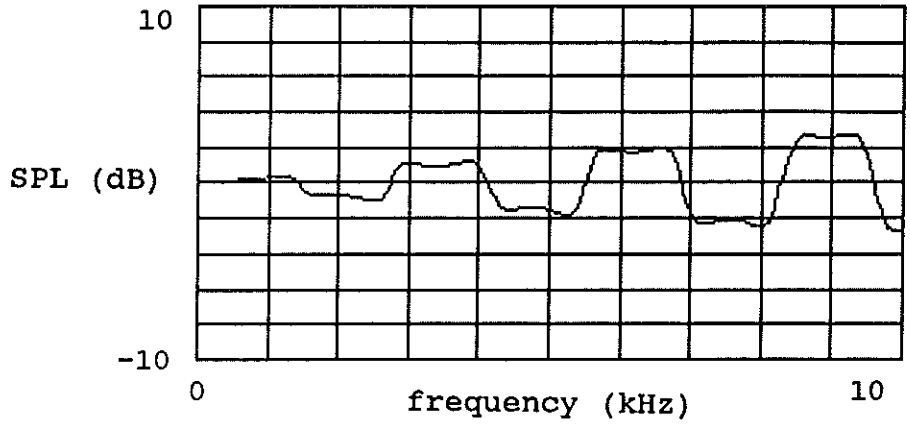

Figure 4c. Probe positioning error in impedance measurement of the hearing aid
Resulting error in predicted sound pressure level (dB) from 1 mm probe position error.

The corresponding error caused by an impedance probe missalignment in the ear canal is given in Figure 5. The same situation as in Figure 4 is assumed. The difference in predicted sound pressure level between a correct measurement and a measurement with the impedance probe 1 mm closer to the ear is shown.

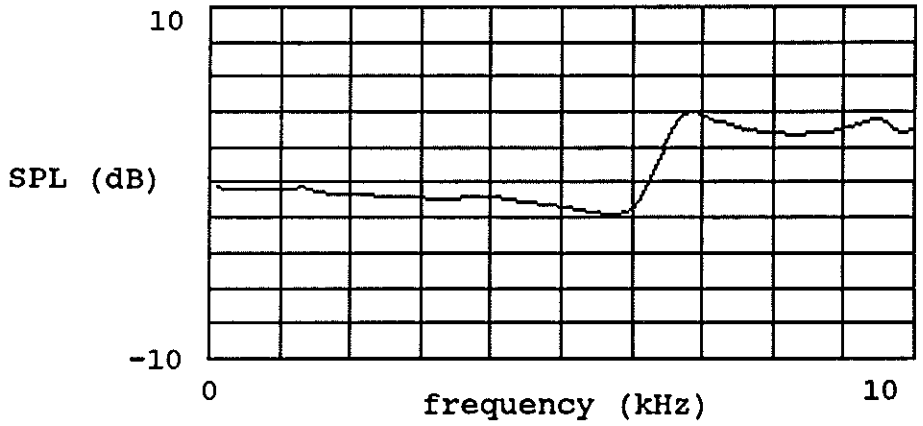

Figure 5. Probe positioning error in impedance measurement of the hearing aid

Resulting error in predicted sound pressure level (dB) from 1 mm probe position error.

7.4 Nearfield modes

Propagating higher modes in the human ear canal are not present below the first cut-on frequency. This is expected to be approximatly 18 kHz [Rabbitt, 1988] for adults. For children this frequency limit is even higher. Higher modes in the sense of nearfield modes (primarily near the ear canal entrance and the eardrum) may be found above 2.5 kHz [Rabinowitz, 1981]. According to Hudde [1989], the nearfield modes may exist as low as 1/10 of the first cut on frequency but there is no distinct limit. This would mean nearfield effects from approximately 1.5 kHz.

The step in crossectional area between the sound canal of the mold and the ear canal will also produce nearfield modes. These modes are commonly described as a mass loading the mold canal or as an extension of the mold canal. From an impedance point of view this can easily be taken into account [Karal, 1953]. Measurements in these nearfields will however give

nonpredictable results and therefore measurements are taken some distance from these area steps.

A MathCAD simulation model was made in order to study the extension of the nearfield modes. Consider a tube of infinite length terminated in one end by a rigid wall with a circular symmetric hole. Through the hole a source is emitting sound into the tube. The nearfield modes will have different amplitudes but will decrease at the same rate with distance from the tube ending. In Figure 6 the amplitude of the first nearfield (trapped) mode relative to its value at the tube end (z=0) is given. The tube diameter is 7 mm and the amplitude is given as a function of distance (0-10 mm) from the tube ending. In the plot 10 lines are shown representing 1 kHz to 10 kHz. The lower line represents 1 kHz and the upper line 10 kHz, indicating that the frequency dependence is very low.

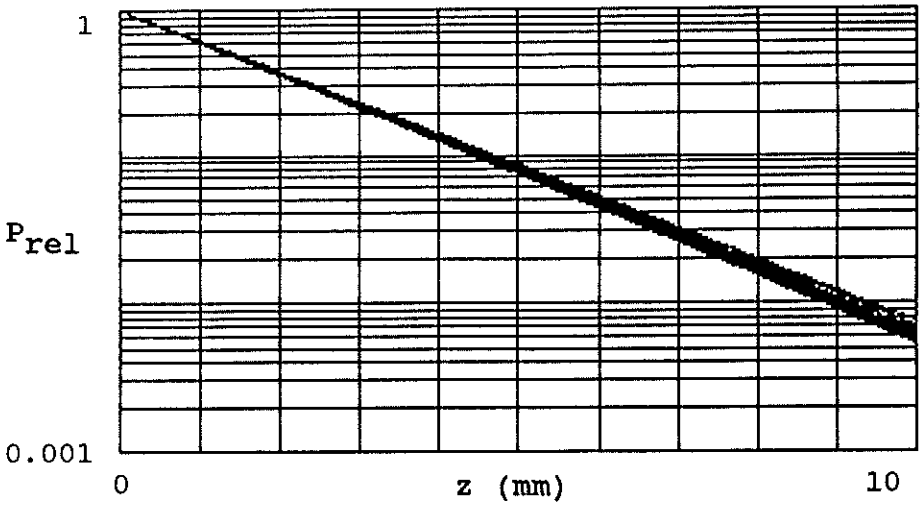

Figure 6. Relative amplitude of the first nearfield mode at end of tube with opening in the tube ending.

At z=5 mm the amplitude is 0.1 (-20 dB) of the amplitude at z=0 (the mold end). This is considered sufficiently low for the present work.

7.5 Nonlinear acoustic effects

Hearing-aids are often used at high levels (120 dB SPL is not unusual). It was therefore checked if nonlinear acoustic effects are present. High sound levels through a crossectional area step was investigated in [Cummings, 1984]. The mechanism of energy absorption present in this situation is the conversion, via acoustic interaction with a shear layer, of acoustic energy into vortical energy and its subsequent dissipation into heath without significant acoustic regeneration. This type of energy absorption can be expected even at low velocities of mean flow, but also, as in the present work, without mean flow if the sound level is high.

Calculations at 1 kHz and 10 kHz reveal (besides an added mass reactance) a relative increase in the acoustic resistance of $3*10^{-5}$. This is of course negligible.

8. A DETAILED DESCRIPTION OF MEASUREMENT AND CALIBRATION PROCEDURES

The measurement system used was Tektronix 2630 in swept sine mode. All measurements were carried out in 397 frequency points (100 Hz - 10 kHz in 25 Hz steps). Usually a bandwith of 100 Hz was used with the tracking filter and an average of 5 measurements. From the measurements transfer functions, auto-spectra functions (channel 2 in Figures 7-12, 14, 15)

and coherence functions were used. For the calculation of complex valued parameters the transfer function is necessary. However, the reference is in this case the output signal of the analyzer. In order to get a sound pressure level with $20*10^{-6}$ Pascal as a reference the autospectrum from the calibrated probe microphone was used. The requirement in coherence was set to 0.99, giving a maximum error in level of 0.1 dB for each measurement [Herlufsen, 1984]. This requirement was nearly always met.

For the calculations in the impedance calibration a program was written in Turbo Pascal. For the other calculations "Matlab" was used. All calculations were performed on a PC.

8.1 Calibration measurements

8.1.1 Calibration of sound pressure probe

In order to calculate the sound pressure level from the auto-spectrum the transfer function of the probe microphone is needed. If only the difference between measured and predicted sound pressure levels is of interest this transfer function is of no interest since it is canceled out in the calculations.

The calibration of the probe microphone, including the amplifier/ equalizer delivered with it, was made through comparison with a 1/2" Bruel and Kjaer 4134 microphone, Figure 7. The reference microphone was used with grazing incidence and will in that position give a flat spectrum except for a 1 dB rise above 7 kHz. No correction was made for the reference microphone response nor that of the measurement amplifier. Two different 4134 microphones were used in order to check that the result was reliable. The measurements were carried out in an anechoic chamber.

Probe microphone and reference microphone were measured separately with the analyzer giving the transfer functions (for explanation of the symbols, see list of symbols)

$$Xfer_{PP} = k_A k_{7C} G_{PP} \tag{29}$$

and

$$Xfer_{PR} = k_A k_{REF} G_{PR}, \tag{30}$$

respectively, see Figure 7. From this we get

$$k_{7C} = -k_{REF} \frac{Xfer_{PP} G_{PR}}{Xfer_{PR} G_{PP}}, \tag{31}$$

the minus sign taking into account that the reference microphone is inverting.

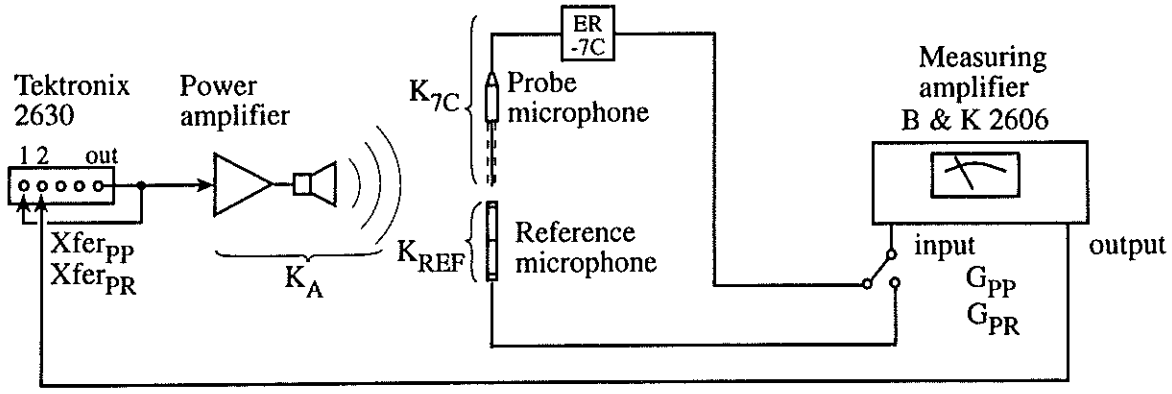

Figure 7. Measurement setup for calibration measurements of the probe microphone.

The magnitude of the sound pressure is given by

$$P = \frac{\sqrt{Aspec_{PR}}}{k_{REF} G_{PR}} = \frac{\sqrt{Aspec_{PP}}}{|k_{7C}| G_{PP}}. \qquad (32)$$

The result is given in Figure 16. The sensitivity is flat within ±2 dB except near 100 Hz.

8.1.2 Calibration of impedance probe

The measurement setup for measurements on tubes for calibrating the impedance probe is shown in Figure 8. The variable attenuator was included in order to reduce the analyzer output signal below 3 mV but was adjusted for 6.6 dB attenuation throughout all measurements in the project. The power amplifier and the 700 Ohm attenuator acted as driver for the 10 Ohm ER-3A insert earphone. The ER-7C probe microphone with the measurement amplifier with gain G_{P0Z0} (same value for all measurements) measured the sound pressure response.

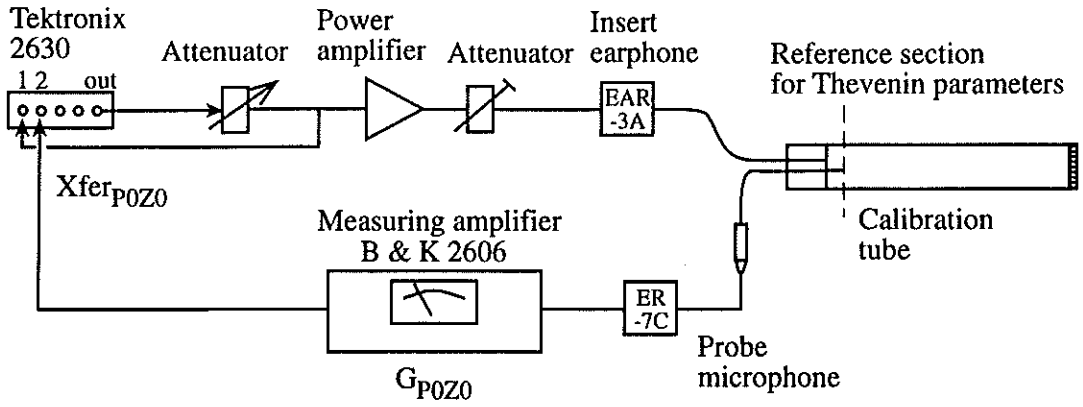

Figure 8. Measurement setup for impedance probe measurements on tubes.

At the input end of the calibration tube there will be an air volume defined by the tube wall and the free part of the probe tube extending into the calibration tube. As this volume is depending on the diameter of the calibration tube two sets of calibration tubes were used, one for the ear canal ($\phi \approx 7.5$mm) and one for the mold canal ($\phi \approx 3$mm). Tube dimensions are given in table 1. The tube diameters were chosen arbitrarily around the nominal 3 and 7 mm but covering the expected range of diameters on the test objects. The tube lengths were picked out in such a way that the dips in magnitude of tube impedance would not overlap.

The tube responses give a large difference in level between peaks and valleys (sometimes in excess of 70 dB). Although the measurement method includes a bandpass filtering it was necessary to use as high level as possible in order to get a good coherence. The limit was given by the probe microphone that will give distorted output above 126 dB SPL.

From the transfer functions $Xferp_{0Z0}$ (analyzer input/analyser output) from the measurements on each tube, $Xferp_0$ (the transfer function resulting from the optimization, representing P0) and Z_0 are calculated as described in section 4.

An exampel of a transfer function of a tube used for the impedance probe calibration is given in Figure 17. The coherence was good except for tube 2 and 3 for which the coherence was slightly below 0.99 at low frequencies.

Tube number	Internal length (mm)	Internal diam. (mm)
1	64	8
2	76	8
3	84.5	9.7
4	347	8
5	374	8.9
6	390	7.5
7	407	8
8	423	6
9	440	7.5
10	458	8
11	65	3.9
12	76	3.2
13	85	3.9
14	346	3.9
15	374	3.9
16	389	3.9
17	407	3.0
18	423	3.9
19	440	3.0
20	458	3.0

Table 1. Calibration tube dimensions.

$Xferp_0$ and Z_0 are given in Figures 18,19 for the small diameter tubes and in Figures 20, 21 for the large diameter tubes. Where the real part of Z_0 was negative it was put equal to 0. These negative values are errors due to insufficient accuracy in the initial tube lengths put into the optimization.

The optimization routine was run twice to obtain a better result. The tube lengths calculated in the first optimization was used as input in the second one. This improved the accuracy slightly. As the same measurement system is used in measurements of both Z_H and Z_E, systematic errors in the measurement system will have a relatively small impact in the predicted sound pressure level.

8.1.3 Comparison with calculated tube impedance

In order to evaluate the errors in the impedance measurements, a comparison between measured and calculated input impedance of two tubes was carried out. Tube dimensions not used in the calibration measurements were used.

Measured and calculated tube impedance is given in Figure 22 for a small diameter tube (ø=3mm, length=403mm). At low frequencies the difference is small increasing at high frequencies and is large in the range 7.5 kHz - 9.5 kHz. In this range the EAR-3A earphone is giving a low output level. The coherence is more than 0.999 throughout the frequency range for the tube measurement and all calibration measurement involved. However, the earphone response makes the autospectrum fall from approximatly 3 kHz and is 30 dB down at 8 kHz. The damping in the tube is also increasing with frequency.

In Figure 23 measured and calculated impedance is given for a large diameter tube (ø=7.5mm, length=380mm). The damping is less in this tube and the result is better. The phase plot does reveal sharp peaks at 4.5 kHz and 9 kHz in addition to other minor errors. These peaks may be due to the fact that some of the calibration tubes has impedance dips very close with the tube length determined by the calibration program.

8.1.4 Measurement of coupler input impedance

The coupler response of the hearing-aid is used for determining the Thevenin pressure parameter P_H. In order to do this the coupler input impedance and transfer function are required.

The IEC 711 coupler (Bruel and Kjaer type 4157) was used with a specially designed adapter for the impedance probe. The measurement setup is given by Figure 9 and the coupler input impedance is given by

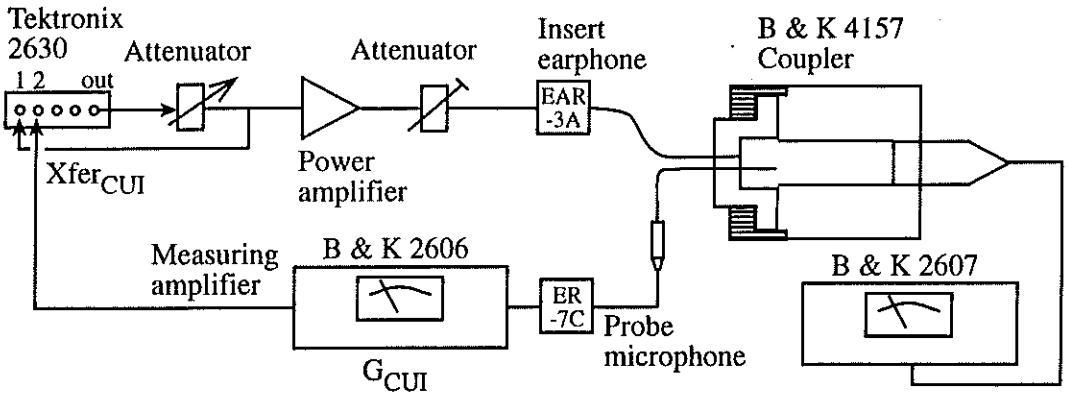

Figure 9. Measurement setup for coupler input impedance measurement.

$$Z_{CU} = Z_0 \frac{Xfer_{CUI} / G_{CUI}}{Xfer_{P0} / G_{P0Z0} - Xfer_{CUI} / G_{CUI}}. \qquad (33)$$

The magnitude of the sound pressure at the coupler input is given by

$$P = \frac{\sqrt{Aspec_{CUI}}}{|k_{TC}| G_{CUI}}. \qquad (34)$$

The measurements were carried out at approximately 105 dB SPL.

A resistance Re(Z_{CU}) less than zero was not accepted as this would mean that the coupler is generating sound. At frequencies were this happened Re(Z_{CU}) was put equal to zero.

The reproducibility of the coupler impedance measurement was good.

The coupler impedance is given in Figure 24.

8.1.5 Measurement of coupler transfer function

The transfer function of the coupler is defined as

$$k_{CU} = \frac{P_{CO}}{P_{CI}}, \qquad (35)$$

were P_{CO} is the sound pressure measured by the coupler built-in microphone and P_{CI} is the sound pressure at the coupler input measured by the probe microphone. The measurement setup in given by Figure 10.

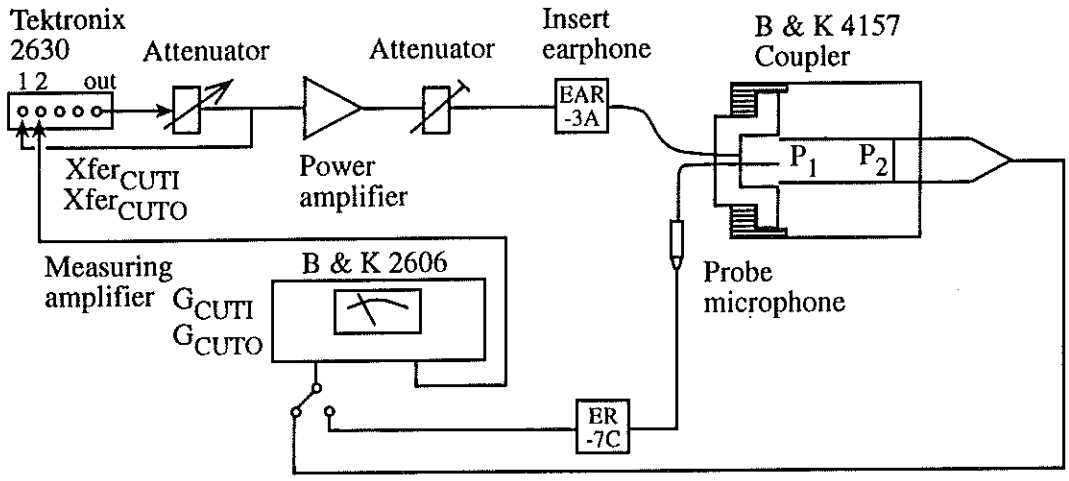

Figure 10. Measurement setup for coupler transfer function measurement.

The P_{CO}- and P_{CI}-signals were measured separately with the analyzer giving the transfer functions

$$Xfer_{CUTI} = k_{ERP} k_{CU} k_{1C} G_{CUTI} \tag{36}$$

and

$$Xfer_{CUTO} = k_{ERP} k_{CU} k_{REF} G_{CUTO}, \tag{37}$$

respectively. From this we get

$$k_{CU} = -\frac{Xfer_{CUTO} G_{CUTI} k_{1C}}{Xfer_{CUTI} G_{CUTO} k_{REF}}, \tag{38}$$

the minus sign taking into account that the reference microphone is inverting the signal. The magnitude of the sound pressure at the coupler input is given by

$$P_{CI} = \frac{\sqrt{Aspec_{CUTI}}}{|k_{1C}| G_{CUTI}}, \tag{39}$$

and at the coupler output by

$$P_{CO} = \frac{\sqrt{Aspec_{CUTO}}}{|k_{REF}| G_{CUTO}}. \tag{40}$$

The measurements were carried out at approximatly 105 dB SPL. The reproducibility was good. The coupler transfer function is given by Figure 25. For a pure cavity the real part tends to unity as the frequency decreases to low frequencies. However, the IEC 711 coupler includes a vent.

8.2 Measurements on hearing aid

8.2.1 Measurement of hearing aid Thevenin impedance

If the Thevenin model is valid for the hearing aid plus tube and mold the Thevenin impedance can be measured through measuring the impedance at the mold end towards the hearing aid. The Thevenin impedance of the hearing aid is thus measured with the method described in section 4.

A specially designed adapter for fitting the impedance probe to the mold was used, Figure 11. It includes screws for holding the mold in correct position and a soft rubber for tightening the end of the mold to the adapter.

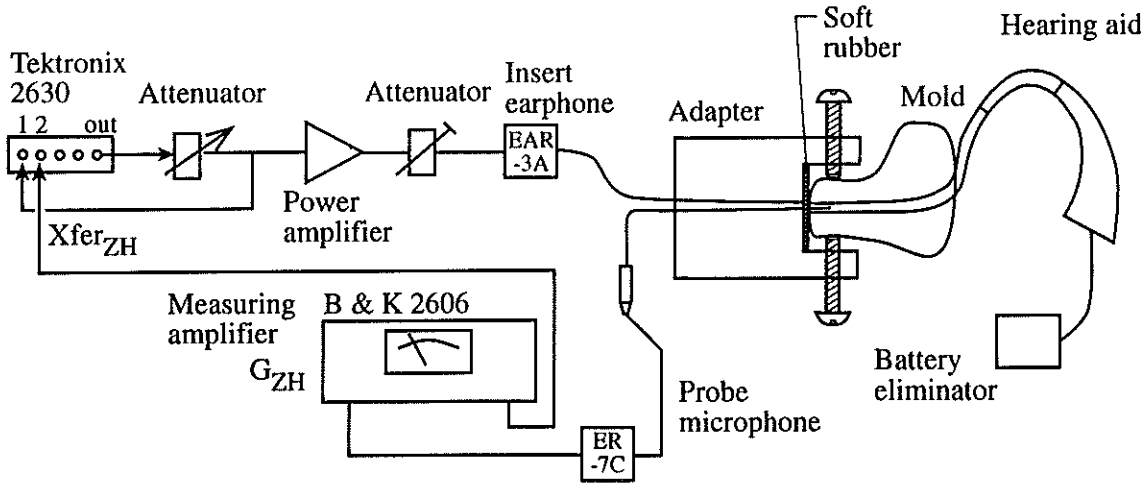

Figure 11. Measurement setup for hearing aid Thevenin impedance measurement.

The Thevenin impedance of the hearing aid is given by

$$Z_H = Z_0 \frac{Xfer_{ZH} / G_{ZH}}{Xfer_{P0} / G_{P0Z0} - Xfer_{ZH} / G_{ZH}}. \qquad (41)$$

The magnitude of the sound pressure is given by

$$P = \frac{\sqrt{Aspec_{ZH}}}{|k_{7C}| G_{ZH}}. \qquad (42)$$

8.2.2 Measurement of hearing aid Thevenin pressure

The Thevenin pressure is determined by measuring the sound pressure from the hearing aid in a known impedance, in this case a coupler (IEC 711). The construction of the coupler makes it impossible to extend the microphone probe from the mold into the coupler. Therefore the built-in microphone of the coupler was used. To calculate the sound pressure at the end of the mold the coupler transfer function and input impedance are required. The Thevenin pressure is determined at the mold end, as opposed to the Thevenin impedance, P_H is therefore denoted P_{HM} below.

In order to get a well defined input signal to the hearing aid an electrical input signal was used. A plastic compound was used between the mold and the coupler to get an airtight seal. The measurement setup is shown in Figure 12.

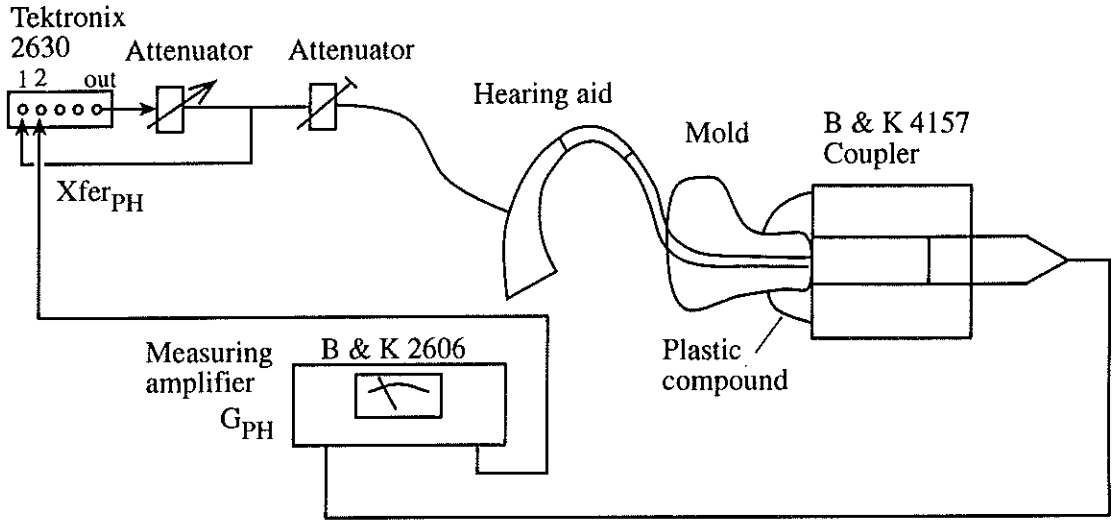

Figure 12. Measurement setup for hearing aid Thevenin pressure measurement.

The hearing aid Thevenin pressure is given by

$$P_{HM} = P_{CI}\frac{Z_{CU} + Z_{HM}}{Z_{CU}}, \tag{43}$$

or

$$P_{HM} = -Xfer_{PHM}\frac{Z_{CU} + Z_{HM}}{G_{PHM}k_{REF}k_{CU}Z_{CU}}. \tag{44}$$

The sound pressure at the coupler microphone is

$$P_{CO} = \frac{\sqrt{Aspec_{PHM}}}{k_{REF}G_{PHM}}. \tag{45}$$

8.2.3 Translation of the hearing aid Thevenin parameters

As the probe microphone is extending some distance into the tube were the impedance is measured, the result has to be translated. The translations given below are valid with the assumption that the tubes are straight, without damping and of constant crossection.

The Thevenin impedance of the hearing aid is first translated to the end of the mold. This is done by the "impedance translation theorem" given in [Pierce, 1981]

$$Z_{HM} = \frac{Z_H\cos(kL_M) - \frac{jc}{S_M}\sin(kL_M)}{\cos(kL_M) - Z_H\frac{jS_M}{c}\sin(kL_M)}. \tag{46}$$

The Thevenin pressure, P_{HM}, is already determined at the end of the mold, see Figure 13. At this point the end correction due to the crossectional area step between the mold canal and the ear canal is added. At this discontinuity the air is regarded as incompressible. This means that the discontinuity can be described by a mass type impedance defined by

$$Z_K = \frac{P_{0+} - P_{0-}}{U_{HM}}, \tag{47}$$

where P_{0+} and P_{0-} are the sound pressures immediately to the left and right of the discontinuity. The impedance is given by [Karal, 1953]

$$Z_K = j2\pi f \frac{4\rho}{3\pi^2 D_M} H(m), \tag{48}$$

with $m = D_M/D_E$ and H approximated by

$$H(m) = 0.982 - 1.19m + 0.02e^{-\frac{m}{0.03}} + 0.0008e^{\frac{m}{0.18}}. \tag{49}$$

D_M and D_E were estimated from measurements of the mold canal and mold outer dimensions. Finally, P_{HM} and Z_{HM} are translated to the point of comparison with the measured result some distance outside the mold as described below. The sound pressure amplitude, P_{HR} and the acoustic impedance,Z_{HR} at the remote location of comparison are given by the transfer matrix representation:

$$\begin{bmatrix} P_{HM} \\ U_{HM} \end{bmatrix} = \begin{bmatrix} \cos(kL_E) & \frac{jc}{S_E}\sin(kL_E) \\ \frac{jS_E}{c}\sin(kL_E) & \cos(kL_E) \end{bmatrix} \begin{bmatrix} P_{HR} \\ U_{HR} \end{bmatrix}. \tag{50}$$

Solving this we get:

$$P_{HR} = P_{HM}\cos(kL_E) - \frac{P_{HM} jc}{Z_{HM} S_E}\sin(kL_E) \tag{51}$$

and

$$Z_{HR} = \frac{Z_{HM}\cos(kL_E) - \frac{jc}{S_E}\sin(kL_E)}{\cos(kL_E) - Z_{HM}\frac{jS_E}{c}\sin(kL_E)}. \tag{52}$$

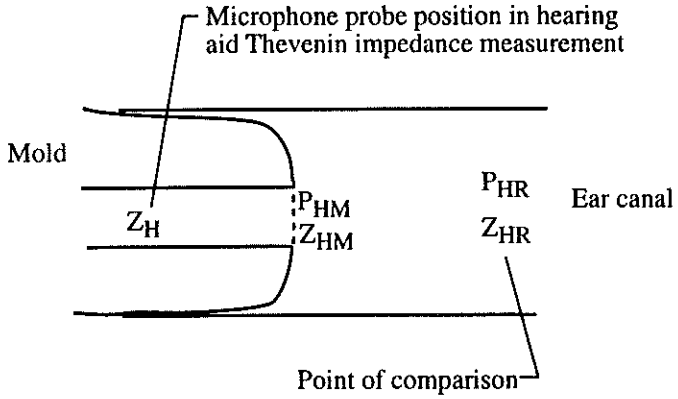

Figure 13. Positions of calculated hearing aid Thevenin parameters.

A resistance $Re(Z_{HR})$ less than zero was not accepted. At those frequencies were this happened $Re(Z_{HR})$ was put equal to zero.

8.3 Measurements on the ear

8.3.1 Measurement of the ear impedance

In order to find the correct position for impedance measurements in the ear canal four identical molds were made from the same cast. One for the impedance measurement and the others for use with the hearing aids.

The measurement setup is given in Figure 14. For the impedance of the ear we get

$$Z_E = Z_0 \frac{Xfer_{ZE} / G_{ZE}}{Xfer_{PO} / G_{POZO} - Xfer_{ZE} / G_{ZE}}. \qquad (53)$$

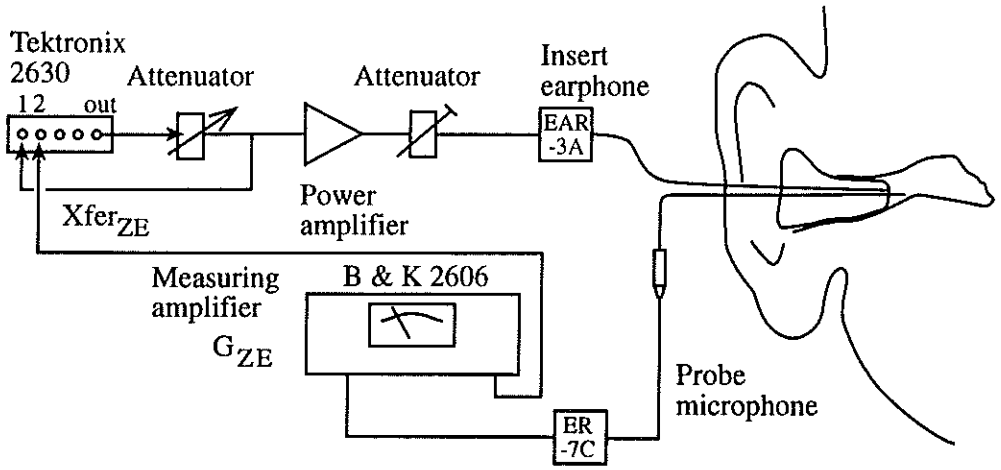

Figure 14. Measurement setup for ear input impedance measurement.

The magnitude of the sound pressure is given by

$$P = \frac{\sqrt{Aspec_{ZE}}}{|k_{7C}| G_{ZE}}. \qquad (54)$$

8.3.2 Measurement for prediction check

In order to verify the model the pressure in the point of comparison was measured and compared to the predicted pressure. The input electrical signal and attenuatur settings must of course be the same as in the measurement of the hearing aid Thevenin pressure.

The maximum sound pressure level was 105 dB. The measurement setup is given in Figure 15.

The sound pressure predicted from transfer function measurements is related to the analyzer output signal. In order to relate it to $20*10^{-6}$ Pascal a comparison was made between autospectrum at 1 kHz and the transfer function at 1 kHz. The ratio of the sound pressures given by these two functions is

$$P_{ERAT} = \frac{\sqrt{Aspec_{PC}}}{|Xfer_{PC}|}. \qquad (55)$$

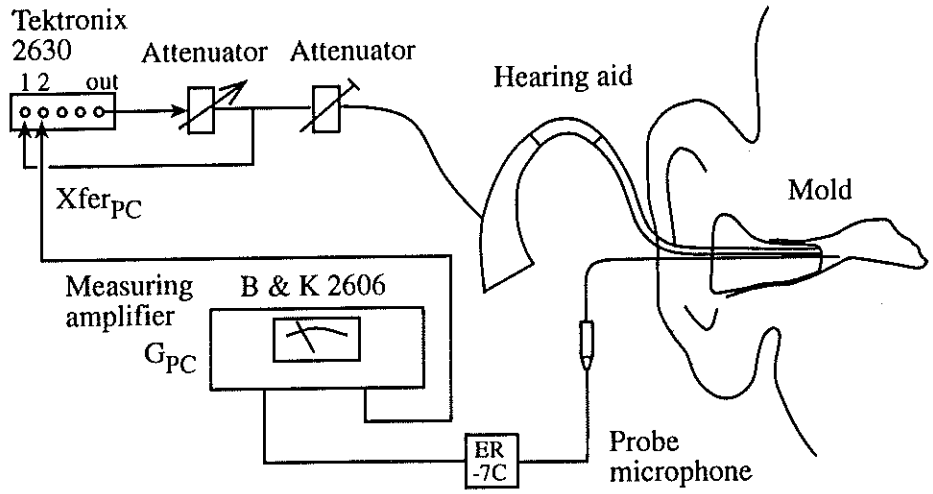

Figure 15. Measurement setup for prediction check measurement.

The predicted complex sound pressure is given by

$$P_{EPRED} = P_{HR} P_{ERAT} \frac{Z_E}{Z_E + Z_{HR}}. \tag{56}$$

The complex sound pressure measured for comparison is given by

$$P_{EMEAS} = P_{ERAT} \frac{Xfer_{PC}}{k_{7C} G_{PC}}. \tag{57}$$

9. TEST OBJECTS

9.1 Hearing aids

For all hearing aids the microphone was disconnected and the stimulus signal was connected to the preamplifier input. The linearity in output level was checked prior to the investigations. The input was changed in 20 dB steps and the output signal was measured at a fixed frequency giving maximum output level. The following three hearing aids were used with adjustments as given below.

Widex ES1, denoted E in this report.

P1 (Bass cut H-N)	: Normal
P2 (Max output -10 - 0)	: 0 dB
Volume (1-4)	: 2.5
Microphone-telecoil	: Microphone

Linearity check: Input	Output
3mV	79dB
30mV	100dB
300mV	120dB

Philips M49, denoted M in this report.

Bass cut (H-N)	: Normal
P (Max output 101-121)	: 121
Volume (1-7)	: 4
Microphone-telecoil (M-T-0)	: Microphone

Linearity check: Input	Output
10mV	83dB
100mV	104dB
1V	124dB

Phonak Pico SC, denoted P in this report.

SSPL (1-3)	: 3
Volume (1-4)	: 3
Microphone-telecoil (L-H-T)	: L (Microphone)

Linearity check: Input	Output
3mV	75dB
30mV	95dB
300mV	114dB

9.2 Subjects

Five hearing-impared subjects, denoted A-E, with hearing loss were used in this project. Their hearing status were as follows:

A: Pure tone audiogram jan. 1992; total deafness on right ear, on left ear a flat loss around the 40 dB level up to 3 kHz, thereafter descending steeply.
PTA (Pure Tone Average, 500Hz-1kHz-2kHz) 0 dB on right ear, 40 dB on left ear.
Impedance audiometry sep. 1977; normal on both ears.
Latest note on mold is from feb. 1991.
The mold was not tight and audible leakage was noted. As opposed to the other subjects A's molds were not tightened with vaseline during the measurements.

B: Pure Tone Audiometry mar.1993; Normal hearing at low frequencies, thereafter severe loss down to the 100 dB-level at 1kHz, at higher frequencies no measurable hearing.
PTA 85 dB on right ear, 88 dB on left ear.
Speech audiometry; 40% on right ear, 42% on left ear.
The hearing loss has been unchanged over the last years.
No information on impedance audiometry.
No information on the age of the mold.

C: Pure Tone Audiometry aug.1991 is showing combined hearing loss with a steep descent at high frequencies, somewhat more on the left than on the right ear.
PTA for air conduction 51 dB on right and 68 dB on left ear.
Bone conduction 41 dB on right and 45 dB on left ear.
Speech audiogram normal.
Impedance audiometry jan.1989; normal reflexion in the eardrum bilateral. Bilateral threshold of stapedius-contraction at an increased level.
Brainstem audiometry feb.1989; cochlear hearing loss.
No relevant information on molds.

D: Pure Tone Audiogram is showing symmetric neural hearing loss, normal hearing at low frequencies, steeply descending hearing loss down to the 80 dB level at 1 kHz thereafter flat hearing loss at this level at high frequencies.
PTA 63 dB on right and 66 dB on left ear.
The hearing loss has been unchanged over the last years.
Impedance audiometry okt.1981 shows that left eardrum and left middle ear ossicle chain are OK. On the right side the eardrum is OK.
Complete absence of stapedius contraction indicates a fixation of the middle ear ossicle chain in the right ear.
New molds were made in mar.1992 and in feb.1993.

E: Pure Tone Audiometry shows symmetric, neural hearing loss at 80-90 dB.
PTA is 93 dB on right ear and 85 dB on left ear.
Speech discrimination; 22% on right and 40% on left ear.
The hearing loss has been unchanged over the last years.
No information on impedance audiometry.
Latest notes on molds are from jun.1990.

In this investigation the left ear of subject A and right ear of subject B-E were used.

The age of the mold may have an impact in the results of this project. The ear canal of the hearing aid user will change in size and shape over time. Therefore a fresh cast giving a mold that fits tightly is essential.

10. RESULTS

10.1 Prediction on a coupler

The measurement and prediction procedure was first carried out with the IEC 711 coupler (ear simulator) used instead of the human ear. The results are given by Figures 26 - 33 and comments are given below.

10.1.1 Hearing aid Thevenin impedance

The Thevenin impedance of Philips M49 with tube and mold is given by Figure 26. In order to check the reproducibility all measurements were carried out three times. In Figure 27 the Thevenin impedance from three measurements is given. The real part is zero in some frequency bands. This is due to calibration errors of the impedance probe. The coherence is very good in these measurements except for the very lowest frequencies.

The Thevenin impedance is depending not only on the receiver, tube and mold but also on the output impedance of the hearing aid amplifier. In figure 28 the Thevenin impedance of Philips M49 is given with power turned on (solid line) and power turned off (dashed line). There is a difference between 1 kHz and 5.3 kHz, however none of the curves is consistently higher.

10.1.2 Hearing aid Thevenin pressure

The Thevenin pressure of the hearing aid is given in Figure 29. The result is depending not only on the same parameters as the Thevenin impedance but also on the signal processing of the hearing aid (and the microphone characteristics if used).

The measurement was carried out with the same hearing aid input signal as in the prediction check below.

The coherence function was good in these measurements except below 400 Hz.

10.1.3 Coupler impedance

In the prediction with the ear replaced by a coupler the coupler input impedance from the calibration measurements shown in Figure 24 was used.

10.1.4 Prediction check

Four measurements of each parameter were carried out. Figures 30 and 31 are showing measured and predicted sound pressure levels in coupler for best and worst result respectively. In Figures 32 and 33 the differences are given for the same prediction checks. From 230 Hz to 8 kHz the error is within ±5 dB. Above this frequency range large errors occurs.

The coherence was in excess of 0.9995 except in measurement 2 (Figure 30) were a large dip occurs at 300 Hz.

10.2 Prediction on real ears

For verification of the model on real ears three hearing aids and five ears as described in section 9 where used.

10.2.1 Hearing aid Thevenin impedance

Examples of Thevenin impedances for the three hearing aids are given in Figures 34-36. The molds were identical but the length of the tubes were somewhat different.

The sound pressure level in these measurements does not show large variations between measurements on the same object. An example of one measurement for the Widex ES1 hearing aid is given in Figure 37a. The coherence was in excess of 0.999 with some exceptions at a few frequencies. An example of the coherence function from the same measurement as Figure 37a is given in Figure 37b.

The reproducibility is limited. Two examples of the hearing aid Thevenin impedance are given in Figures 38 and 39 with three measurements of each.

10.2.2 Hearing aid Thevenin pressure

The measurement was carried out with the same hearing aid input signal as in the prediction check in section 10.2.4.

The coherence function was in excess of 0.999 in these measurements except in the frequency range were the hearing aid output level is low. An example of the sound pressure level from a measurement on the Widex ES1 type is given in Figure 40a. The corresponding coherence function is given in Figure 40b. The transfer functions $Xferp_0$ representing P0 as translated to the end of the mold (see section 8.2.3) are given for the three hearing aids in Figures 41-43.

An example of the reproducibility is given for Widex ES1 and Philips M49 in Figures 44 and 45 with three measurements of each.

10.2.3 Ear impedance

All real ears used in the main investigations of this project are pathological. Results from the impedance-audiometry gives an idea of whether or not the ear input impedance is normal. Of the five real ears used only subject A has got a documented normal result from the impedance-audiometry.

Due to the stapedius contraction the human ear is expected to have an input impedance varying with sound level. Impedance measurements on the ear were therefore carried out at two different sound pressure levels. SPL(max) denotes the maximum sound pressure level in one

measurement. In Figures 46-50 mean, max and min from three measurements at 100-105 dB SPL(max) are given for the five ears. In Figures 51-55 the same results are given for the measurements at 80-85 dB SPL(max).

In some of the results the reactance differs substantially from the expected cavity shape. This occurs for the high level measurements in cases A,B,C,E and for the low level measurements in cases A,B,E. The reason for this is likely to be leakage. However, another possible reason is that parts of the ear canal wall are loose and moving with the sound field. This latter explanation may be valid for the case C, in which this deviation is shown only at high levels. The six impedance measurements on each ear were carried out in pairs, one measurement at each level without remounting the probe.

The coherence function from these measurements exceeds 0.99 except for the frequency range 7 kHz - 9 kHz were it somtimes was as low as 0.7. This is caused by the responce of the EAR-3A earphone in combination with the quater wave resonance of the ear canal.

10.2.4 Prediction check

In Figures 56-58 examples of measured and predicted response is given for the three hearing aids on subject A. The measurements were carried out over a wider frequency range than the hearing aids are expected to be used at. Noise problems were experienced at the low levels in the high frequency dips. An example of the coherence function from these measurements is given in Figure 59. This can be considered as a worst case.

As all parameters above were calculated from three different measurements, the prediction check was also carried out three times. The error "predicted sound pressure level minus measured sound pressure level" is given for all hearing aids on all ears in Figures 60-74. Maximum, minimum and average (in dB-values) out of three measurements and calculations of each parameter are given. Subjects D and E show better reproducability than the others, this may be due to molds of later date than in the other cases. For these two subjects a good mold fit was noted.

In general, there is a low-frequency region and a high-frequency region with large spread. A mid-frequency region, 1 kHz - 6 kHz usually reveals better accuracy (approximatly ±5 dB in most cases).

Average, maximum and minimum are also calculated for each hearing aid over all subjects and for each subject over all hearing aids. Results for each hearing aid are given in Figure 75 for Widex ES1, in Figure 76 for Philips M49, in Figure 77 for Phonak Pico SC. Results for each subject A-E are given in Figures 78-82.

The hearing aids are expected to have Thevenin parameters independent of sound pressure level as mentioned earlier. The human ear is expexted to have an input impedance varying with sound pressure level. The prediction check was therefore carried out in two cases, with ear impedance measured at 80-85 dB(max) and 100-105 dB(max). Average, maximum and minimum over all subjects and hearing aids are given in Figure 83 for ear impedance measured at 100-105 dB(max) and in Figure 84 for ear impedance measured at 80-85-dB(max). The difference between averages at 100-105 dB(max) and 80-85 dB(max) are given in Figure 85. There is no significant difference between the results at the two levels.

11. DISCUSSION AND CONCLUSTIONS

An electrical analog model (Figure 1) has been given as a theoretical description of the acoustical system "hearing aid and ear". This model has been tested in the frequency range 100 Hz - 10 kHz.

The comparison between predicted and measured sound pressure level on coupler is clearly showing the influence of probe misalignmet in Figures 31 and 33. The error is in the order of 4 dB up to 8 kHz. Apart from this type of error the result is good from 300 Hz up to 8 kHz, see Figures 30 and 32. Large errors occur at 8 kHz - 9 kHz. These are due to calibration errors in this frequency range of the impedance probe at small tube diameters, see Figure 22. Calibration problems with small tube diameters has been mentioned by [Keefe, 1993]. The errorrs are increesed in frequency range 8 kHz - 9 kHz due to the response of the EAR-3A earphone.

The prediction check on real ears show larger errors as expected. Below 250 Hz large errors occur in all measurements. The impedance measurement check in Figures 22 and 23 doesn't show any large errors at low frequencies, but Keefe has mentioned the same problem [Keefe 1993] in his impedance measurements. A more important problem at low frequencies (< 1 kHz) is leakage. This seems to be present with subjects A,B and C but not D and E. A good mold fit, and thus a tight mold, was noted on subjects D and E.

In the frequency range 1 kHz - 6 kHz the average predicted sound pressure level is within approximately ±3 dB of the measured level. However the maximum error is 13 dB, see Figures 83 and 84. The coherence functions from the Z_H measurements are exceeding 0.999. In the $Xfer_{PH}$ measurements it is exceeding 0.999 except for the frequency range were the hearing aid output is low (7 kHz - 9 kHz). The coherence functions from Z_E measurements exceeded 0.999 except for frequencies above 7 kHz were it was somtimes as low as 0.7. The reproducibility of Z_H (Figure 27), $Xfer_{PH}$ (Figures 44 and 45) and Z_E (Figures 46-55) is not excellent. However the influence in detail of each parameter on the prediction error is not allways easily detected since all parameters involved are varying between different prediction results. An alternative way of comparison would be to study the variation of one parameter at a time with the other parameters fixed. Since the fixed parameters would be estimates of the real ones, the results of such a comparison would be unsertain. The comparison used in the present work simulates the results obtained in a measurement situation at a clinic. Some relations between parameters are easily detected: Z_E for subject C is showing large variations below 1.3 kHz. It causes the deviation in this frequency range in the predictions in Figure 66 - 68. Z_E for subject E reveals variations in the frequency range 4.5 kHz - 6.5 kHz. This is causing the deviations in this frequency range in the predicted result, see Figures 72 - 74.

The large variations in the frequency range 6 kHz - 9 kHz are caused partly by the low sound pressure levels in the $Xfer_{PH}$- , Z_E- and P_{EMEAS}- measurements. This causes problems since the noise level of the probe microphone is rather high (55 dB SPL equivalent, 20 Hz to 20 kHz bandwith). The variations are caused partly by the error in impedance probe calibration mentioned in section 8.1.3 and shown in Figure 22. It is also important to point out that all measurements including prediction check also includes errors from probe misalignment, see appendix 1 and 2. In Figures 78-82 prediction error for all hearing aids on each subject is given, Above 6 kHz large errors occur with the exception of hearing aid M on subject E. In general the reproducability is bad at high frequencies but is somewhat better on subjects D and E. As these two subjects revealed a better mold fit than the others this indicates the importance of a good mold fit and thus an accurate probe alignment.

The overall shape of the averaged prediction error curves, negative at low frequencies and positive at high frequencies, may be given by probe misalignments. However this would mean that this type of error is systematic. The example in Figure 58 shows dips at different frequencies for measured and predicted result. This error is probably caused by probe misalignment. These errors are simulated for the case of Z_H and Z_E measurements in appendix 1 and 2.

Measurements of Z_E and P_{EMEAS} reveal errors in the frequency range 7 kHz - 9 kHz. This is due to the frequency response of the insert earphone and the hearing aids. The tube earphone model ER-3A has the response of the TDH-39 supra-aural earphone. This means low levels at high frequencies. The EAR-3A was chosen for its high level capabilities. As it has been shown in this project that the sound pressure level used is not critical in the prediction of hearing aid

response, insert earphones for use at lower levels may be used. In that case earphone models with a more flat frequency responce are available.

A main reason for the bad result at high frequencies is the low hearing aid response. The hearing aids used in this project were chosen from their "deviation in response on different ears" [Svärd, 1993] as this is of primary importance. The development in hearing aid technology is moving towards better high-frequency response. The measurement- and calculation-procedure given in this report is thus expected to give at better result as development goes on.

Summing up sources of errors:

- Calibration errors. In the present work the calibration tube lengths were measured with a rule. The acoustical measurement of calibration tube lengths in [Keefe et al. 1992] should be used.

- Response of EAR-3A earphone. Measurements can be carried out at lower sound pressure levels. This means that an earphone with a more flat response can be used.

- Noise level of ER-7C probe microphone. The noise from the probe microphone causes errors in the frequency ranges were the sound pressure level is low.

- Response of hearing aids. At high frequencies the output level is low. In combination with a rather high microphone noise this causes problem.

- Probe misalignments. Misalignments causes errors increasing with frequency. Molds made from individual casts of the ear canal is necessary.

To conclude, the described measurement- and calculation-procedure is useful between approximately 300 Hz and 6 kHz. In this frequency range probe positioning errors dominate. At higher frequencies large errors occurs, mainly due to the response of the hearing aids and insert earphone used. The theoretical model used is found valid up to 10 kHz.

12. ACKNOWLEDGMENTS

The author owes many thanks to Dr.Mats Åbom at Technical Acoustics, Dept. of vehicle technology/ Royal Institute of Technology, Stockholm. The many long discussions with Mats have been most essential to the project as well as the use of the Tektronix 2630 measurement system, at Technical Acoustics.

Thanks to the five patients for their participation. Thanks to Mr Ingmar Svärd/ Karolinska Sjukhuset for providing contact with these nice people and also for supplying the project with hearing aids for the main investigations.

Many thanks to Mr Göran Lundberg at Dept. of Technical Audiology/ Karolinska Institutet for support with the Turbo Pascal-programming.

Thanks also to Mr Åke Svanberg/ Philips försäljning AB for providing a Philips M46 hearing aid for the preliminary investgations of this project.

This work was supported by the Swedish National Board for Industrial and Technical Development (NUTEK).

13. LIST OF SYMBOLS

a	Tube radius
$Aspec_{CUI}$	Autospectrum function of coupler input impedance measurement
$Aspec_{CUTI}$	Autospectrum function at coupler input of coupler transfer function measurement
$Aspec_{CUTO}$	Autospectrum function at coupler output of coupler transfer function measurement
$Aspec_{PC}$	Autospectrum from prediction check measurement
$Aspec_{PHM}$	Autospectrum from hearing aid Thevenin pressure measurement
$Aspec_{PP}$	Autospectrum function in probe microphone measurement of sound probe calibration.
$Aspec_{PR}$	Autospectrum function in reference microphone measurement of sound probe calibration.
$Aspec_{ZE}$	Autospectrum from ear impedance measurement.
$Aspec_{ZH}$	Autospectrum from hearing aid Thevenin impedance measurement.
c	Speed of sound
C_p	Specific heat of the gas at constant pressure.
D_E	Ear canal diameter
D_M	Mold canal diameter
f	Frequency
Fv,Ft	Quantities given by Kirchhoff's solution.
G_{CUI}	Amplifier gain in coupler input impedance measurement.
G_{CUTI}	Amplifier gain in probe microphone measurement of coupler transfer function measurement.
G_{CUTO}	Amplifier gain in built-in microphone measurement of coupler transfer function measurement.
G_{PC}	Amplifier gain in prediction check measurement.
G_{PHM}	Amplifier gain in hearing aid Thevenin pressure measurement.
G_{P0Z0}	Amplifier gain in impedance probe calibration measurement.
G_{PP}	Amplifier gain in probe microphone measurement of sound probe calibration.
G_{PR}	Amplifier gain in reference microphone measurement of sound probe calibration.
G_{ZE}	Amplifier gain in ear impedance measurement.
G_{ZH}	Amplifier gain in hearing aid Thevenin impedance measurement.
H	Discontinuity inductance correction factor according to Karal.
j	Imaginary unit
J_0	Bessel function of order zero.
J_1	Bessel function of order one.
k	Wave number
k_A	Transfer function of power amplifier, loudspeaker and air path.
k_{CU}	Coupler transfer function
k_{ERP}	Transfer function of power amplifier + attenuator + ER-3A earphone.
k_{REF}	Sensitivity of the reference microphone.
k_{7C}	Transfer function of the probe microphone.
L_E	Legnth of probe microphone tube extending into ear canal.
L_i	Length of calibration tube i.
L_M	Length of probe microphone tube extending into the mold canal.
m	Ration of mold canal diameter to ear canal diameter.
M	Number of known impedances (calibration tubes) in impedance probe calibration.
n	Frequency number
n1, n2	Frequency number limits.
N(n)	Nondimensional error function
N_T	Average normalized error
P	Sound pressure
P_0	Thevenin pressure of impedance probe.

P_{0+}	Sound pressure an infinitly small distance to the left of the discontinuity.
P_{0-}	Sound pressure an infinitly small distance to the right of the discontinuity.
P_{CO}	Sound pressure at coupler output (built-in microphone).
P_{CI}	Sound pressure at coupler input
P_{EMEAS}	Measured complex sound pressure in prediction check measurement.
P_{EPRED}	Predicted complex sound pressure in point of comparison.
P_{ERAT}	Ratio of $(Aspec_{PC})^{1/2}$ to $\|Xfer_{PC}\|$.
P_H	Thevenin pressure of hearing aid.
P_{HM}	Thevenin pressure of hearing aid at mold end.
P_{HR}	Thevenin pressure at the point of comparison, remote from the mold.
P_i	Sound pressure measured in impedance probe calibration tube i.
P_x	Sound pressure in impedance measurement.
R_0	Characteristic impedance of the acoustic transmission line in the absence of thermal and viscous dissipation.
r_v	Ratio of tube radius to viscous boundary layer.
r_t	Ratio of tube radius to thermal boundary layer.
S_E	Crossectional area of ear canal.
S_M	Crossectional area of mold canal minus crossectional area of probe microphone tube.
t	Time
U	Volume velocity
U_{HM}	Volume velocity at mold end.
U_{HR}	Volume velocity at point of comparison.
v_p	Phase velocity
$Xfer_{CUI}$	Transfer function from coupler input impedance measurement.
$Xfer_{CUTI}$	Transfer function from input measurement of coupler transfer function measurement.
$Xfer_{CUTO}$	Transfer function from output measurement of coupler transfer function measurement.
$Xfer_{PC}$	Transfer function from prediction check measurement.
$Xfer_{PHM}$	Transfer function from hearing aid Thevenin pressure measurement.
$Xfer_{P0}$	Transfer function representing impedance probe Thevenin pressure.
$Xfer_{P0Z0}$	Transfer function from impedance calibration measurement.
$Xfer_{PP}$	Transfer function in probe microphone measurement of sound probe calibration measurement.
$Xfer_{PR}$	Transfer function in reference microphone measurement of sound probe calibration measurement.
$Xfer_{ZE}$	Transfer function from ear impedance measurement.
$Xfer_{ZH}$	Transfer function from hearing aid Thevenin impedance measurement.
Y	Shunt admittance/ unit length
z	Room coordinate
Z	Acoustical impedance
Z	Series impedance/ unit length (eqs.1,3,16,17)
Z_0	Thevenin impedance of impedance probe.
Z_c	Characteristic acoustic impedance
Z_{ci}	Characteristic impedance of tube i.
Z_{CU}	Coupler input impedance
Z_E	Ear input impedance
Z_H	Thevenin impedance of hearing aid.
Z_{HM}	Hearing aid Thevenin impedance at mold end.
Z_{HR}	Hearing aid Thevenin impedance at the point of comparison.
Z_i	Input impedance of calibration tube i.
Z_K	End correction impedance according to Karal.
Z_x	Impedance to be determined.

α	Real part of propagation wave number
γ	Termodynamic konstant
Γ	Propagation wave number
Γ_i	Propagation wave number of tube i
Δ	Determinant in LMS-solution
ΔT	Temperature difference relative to 26.85 °C
ε	Error function
η	Dynamic viscosity coefficient
κ	Gas thermal conductivity
ν	Square root of the Prandtl number
ρ	Mean density of medium
ω	Angle velocity

14. REFERENCES

Allen, J.B. 1985. Measurement for eardrum acoustic impedance. *Peripheral auditory mechanisms*, Springer 1985.

Anderson, H. 1969. Acoustic intra-aural reflexes in clinical diagnosis. Doctoral thesis, Dept.of Audiology and Otolaryngology, The Karolinska Hospital, Stockholm.

Berninger, E., Ovegård, A. & Svärd, I. 1992. Coupler-related real ear gain. *Scandinavian Audiology 21*, 15-22.

Bodén, H. 1991. The multiple load method for measuring the source characteristics of time-variant sources. *Journal of Sound and Vibration 148(3)*, 437-453.

Borg, E., Nilsson, R. & Lidén, G. 1979. Fatigue and recovery of the human acoustic stapedius reflex in industrial noise. *Journal of the Acoustical Society of America* 65(3), 846-848.

Cummings, A. 1984. Acoustic nonlinearities and power losses at orifices. *AIAA Journal 22(6)*, 786-792

Egolf, D.P. & Leonard, R.G. 1977. Experimental scheme for analyzing the dynamic behavior of electro-acoustic transducers. *Journal of the Acoustical Society of America 62(4)*, 1013-1023.

Hara, M., Itami, E., Okabe, K., Hamada, H. & Miura, T. 1988. Prediction of the insertion gain on canal type hearing-aid. *Hearing Aid Fitting* (Edited by Janne Hartvig Jensen), 13th Danavox Symposium, Odense, Denmark.

Herlufsen, H. 1984. Dual channel FFT analysis (part 1). *Technical Review 1*, Bruel&Kjaer.

Hudde, H. 1989. Acoustical higher-order mode scattering matrix of circular nonuniform lossy tubes without flow. *Journal of the Acoustical Society of America 85(6)*, 2316-2330.

Ingård, U 1948. On the radiation of sound into a circular tube, with an application to resonators. *Journal of the Acoustical Society of America 20(5)*, 665-682.

Karal, F.C. 1953. The analogous acoustical impedance for discontinuities and constrictions of circular cross section. *Journal of the Acoustical Society of America 25(2)*, 327-334.

Keefe, D.H. 1984. Acoustical wave propagation in cylindrical ducts: Transmission line parameter approximations for isothermal and nonisothermal boundary conditions. *Journal of the Acoustical Society of America 75(1)*, 58-62.

Keefe, D.H., Ling, R. & Bulen, J.C. 1992. Method to measure acoustic impedance and reflection coefficient. *Journal of the Acoustical Society of America 91(1)*, 470-485.

Keefe, D.H. 1993. Personal communication.

Margolis, R.H. 1993. Detection of Hearing Impairment with the Acoustic Reflex. *Ear and Hearing 14(1)*, 3-10.

Norton, S.J. 1993. Application of Transient Evoked Otoacoustic Emissions to Pediatric Populations. *Ear and Hearing 14(1)*, 64-73.

Olsson, U. 1985. Hearing-aid measurements on occluded-ear simulator compared to simulated in-situ and in-situ measurements. Report no 111, Department of Technical Audiology, Karolinska Institutet, Stockholm.

Pierce, A.D. 1981. Acoustics, An Introduction to Its Physical Principles and Applications. Acoustical Society of America, ISBN 0-88318-612-8.

Press, W.H., Flannery, B.P., Teukolsky, S.A. & Vetterling, W.T. 1986. Numerical recipes. Cambridge univ. press, ISBN 0-521-30811-9.

Rabbitt, R.D. 1988. High-frequency plane waves in the ear canal: Application of a simple asymptotic theory. *Journal of the Acoustical Society of America 84(6)*, 2070-2080.

Rabinowitz, W.M. 1981. Measurement of the acoustic input immittance of the human ear. *Journal of the Acoustical Society of America 70(4)*, 1025-1035.

Sanborn, P-E. 1990. Hearing-aid to ear impedance-matching: A literature survey. Report no 118, Department of Technical Audiology, Karolinska Institutet, Stockholm.

Shaw, E.A.G. & Stinson, M.R. 1981. Network concepts and energy flow in the human middle-ear. The 101st Meeting of the Acoustical Society of America, 19-22 May, Invited paper T2.

Svärd, I. 1993. Coupler-related real ear gain, part 2. To be published.

15. FIGURES 16-85

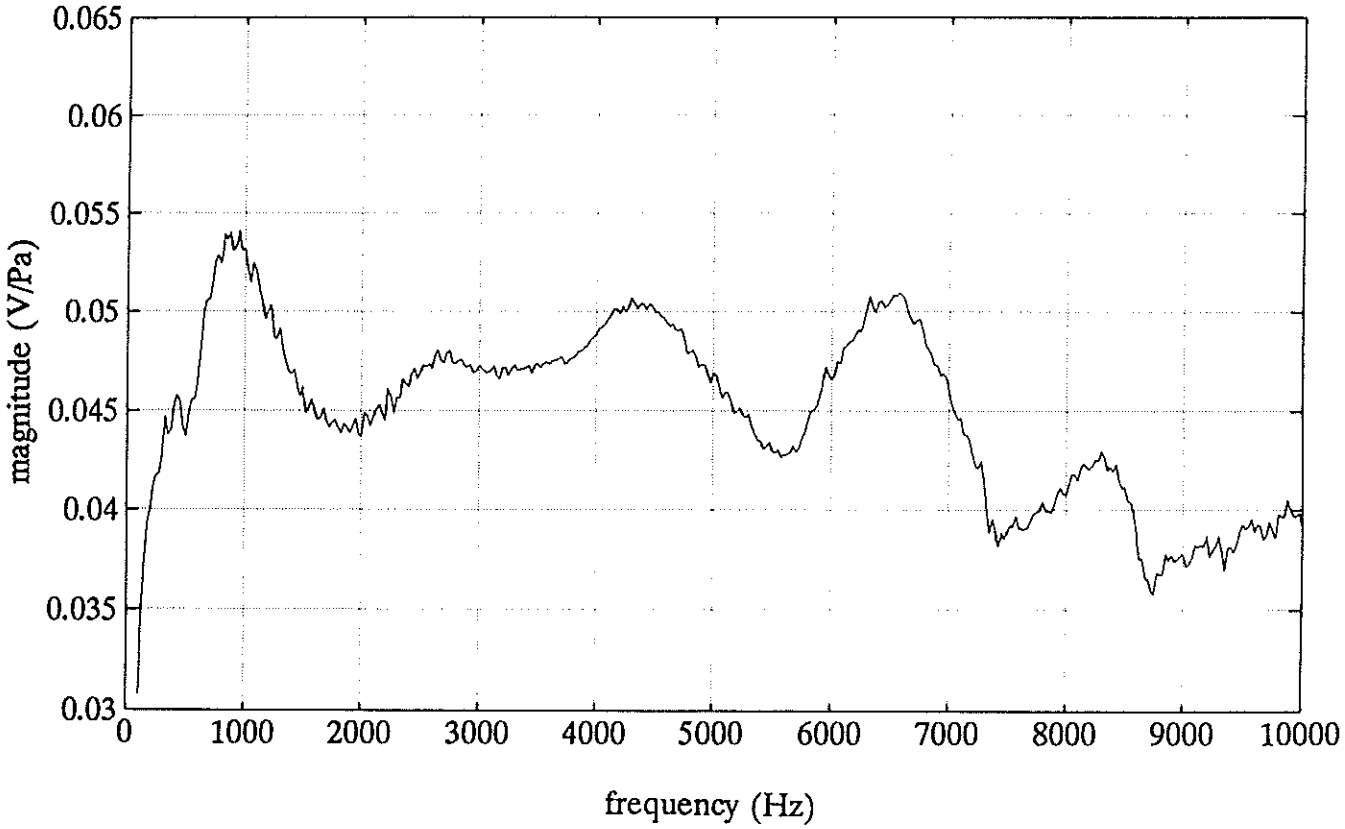

Figure 16a. Magnitude of the sensitivity of ER-7C probe microphone no 87583.

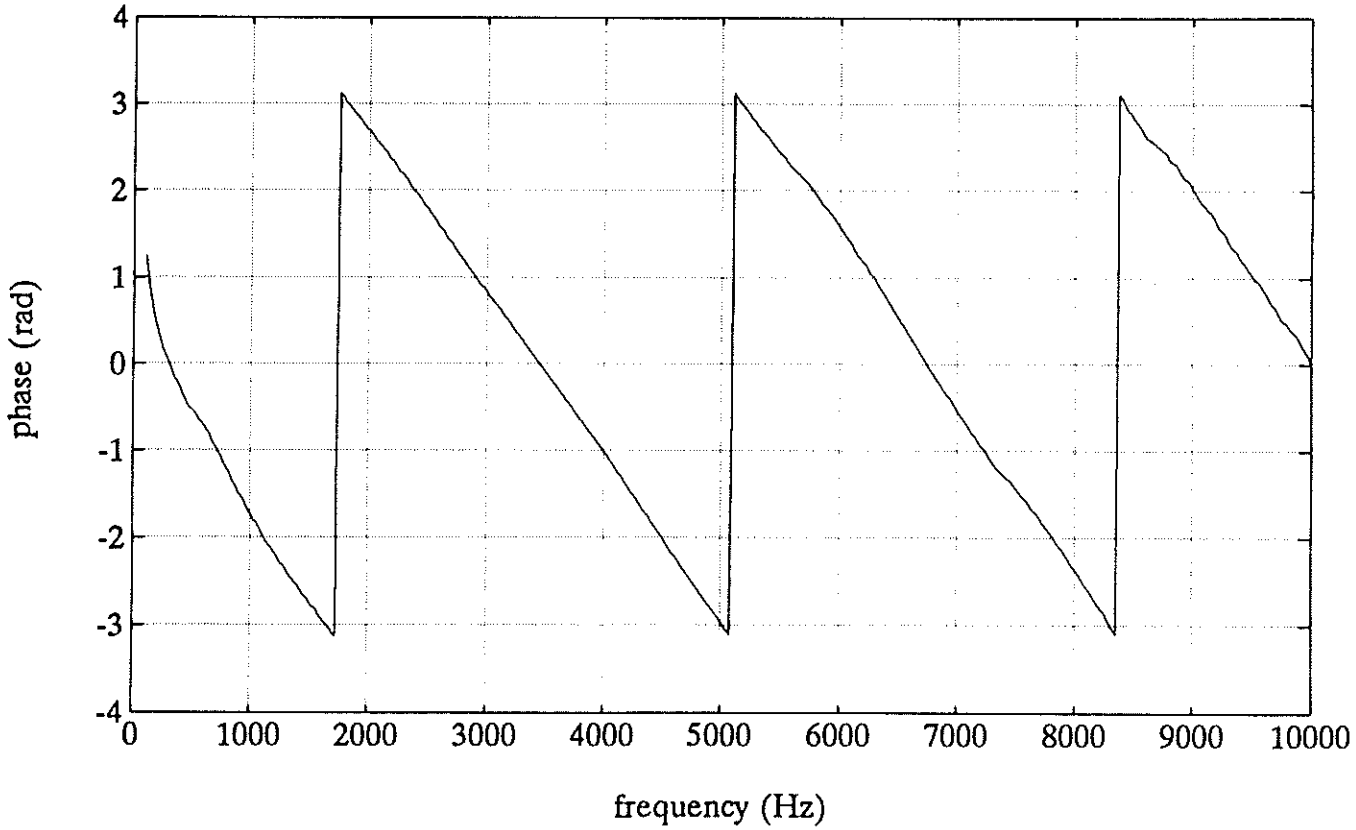

Figure 16b. Phase of the sensitivity of ER-7C probe microphone no 87583.

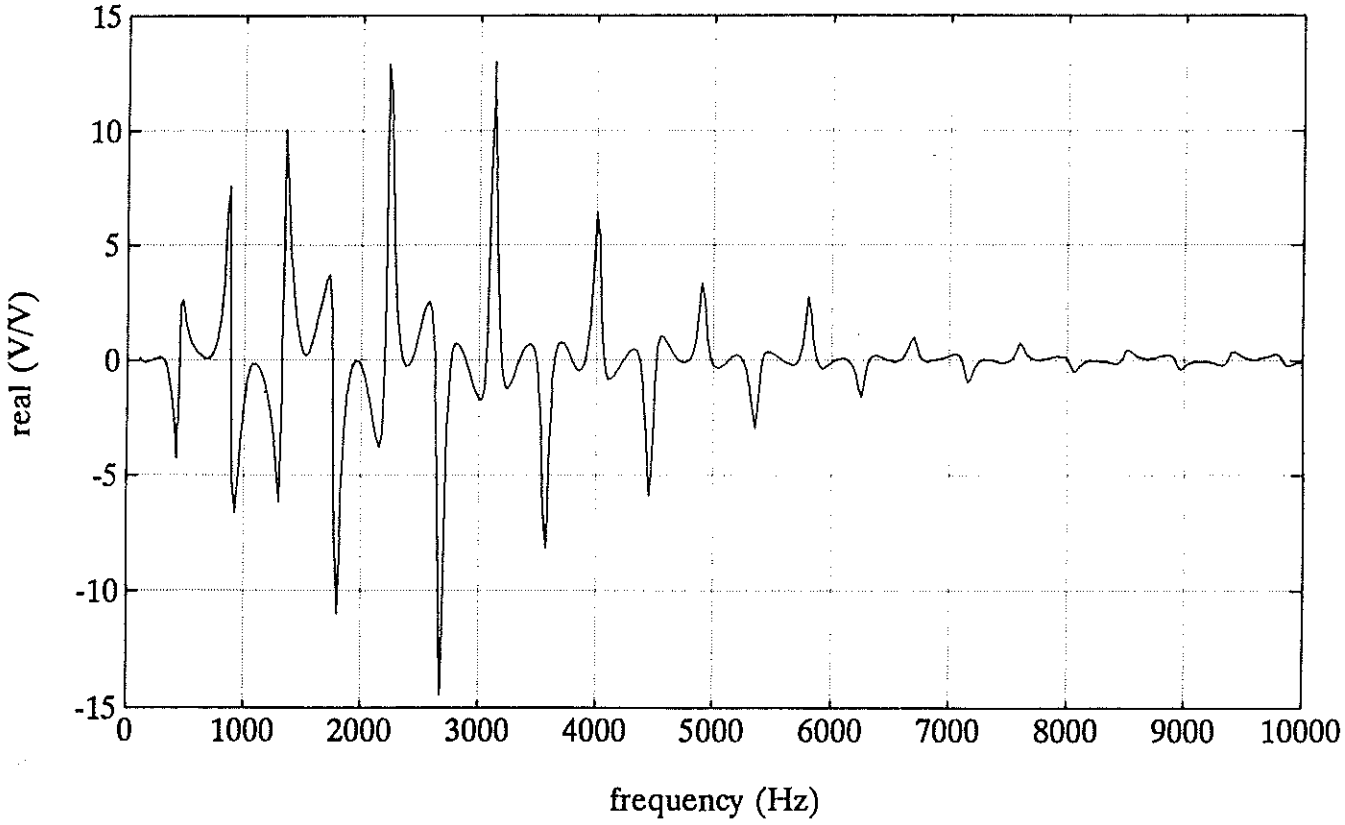

Figure 17a. Real part of transfer function from measurement on calibration tube No 6.

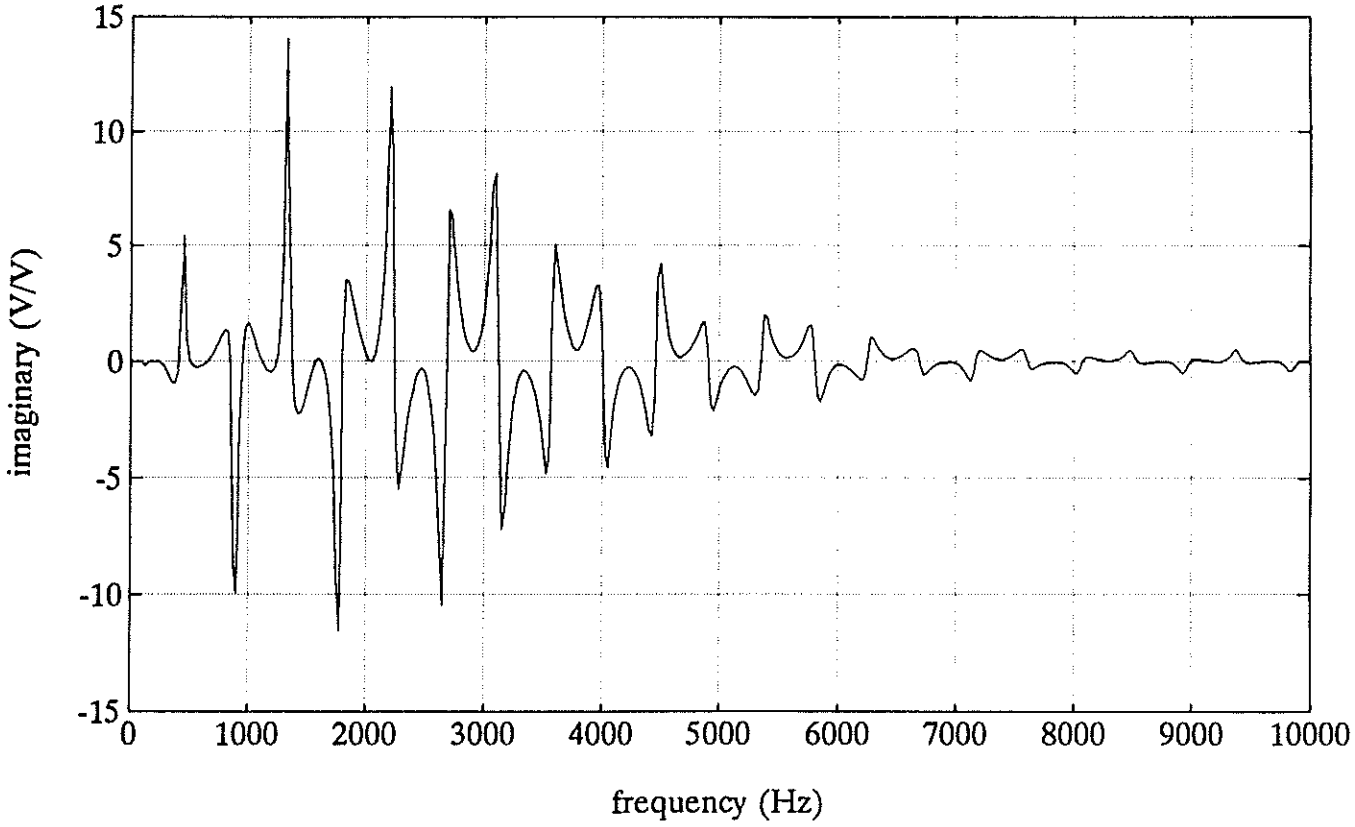

Figure 17b. Imaginary part of transfer function from measurement on calibration tube No 6.

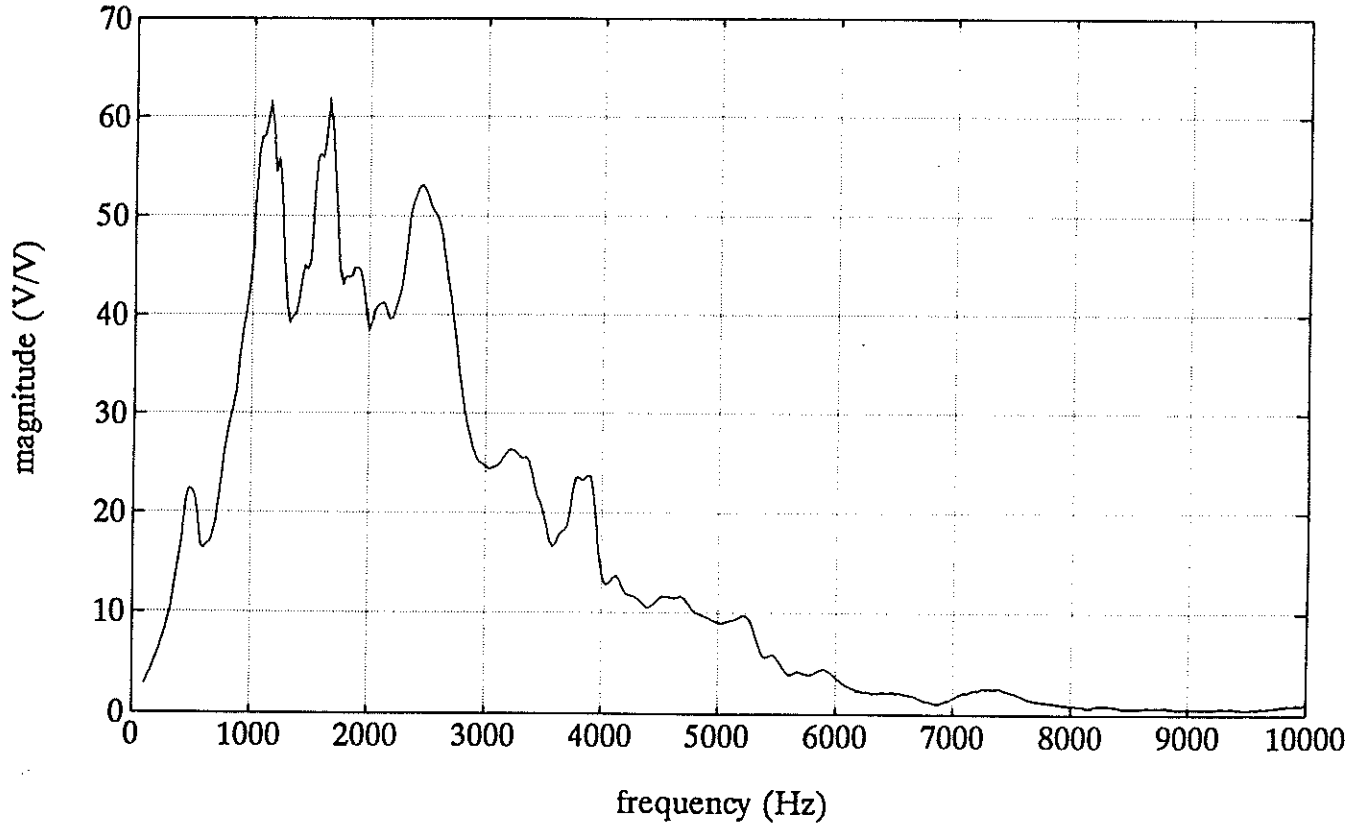

Figure 18a. Magnitude of $Xferp_0$ for small diameter calibration.

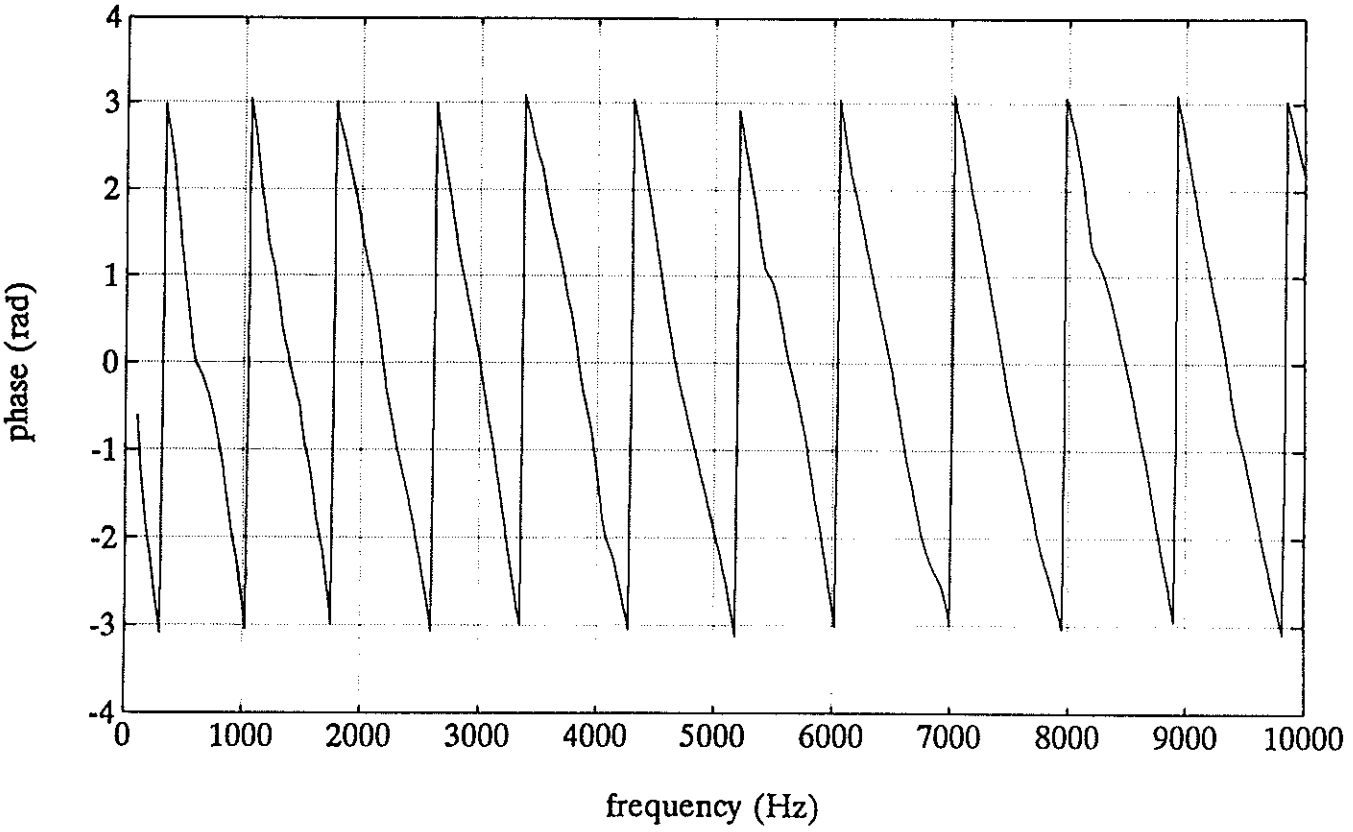

Figure 18b. Phase of $Xferp_0$ for small diameter calibration.

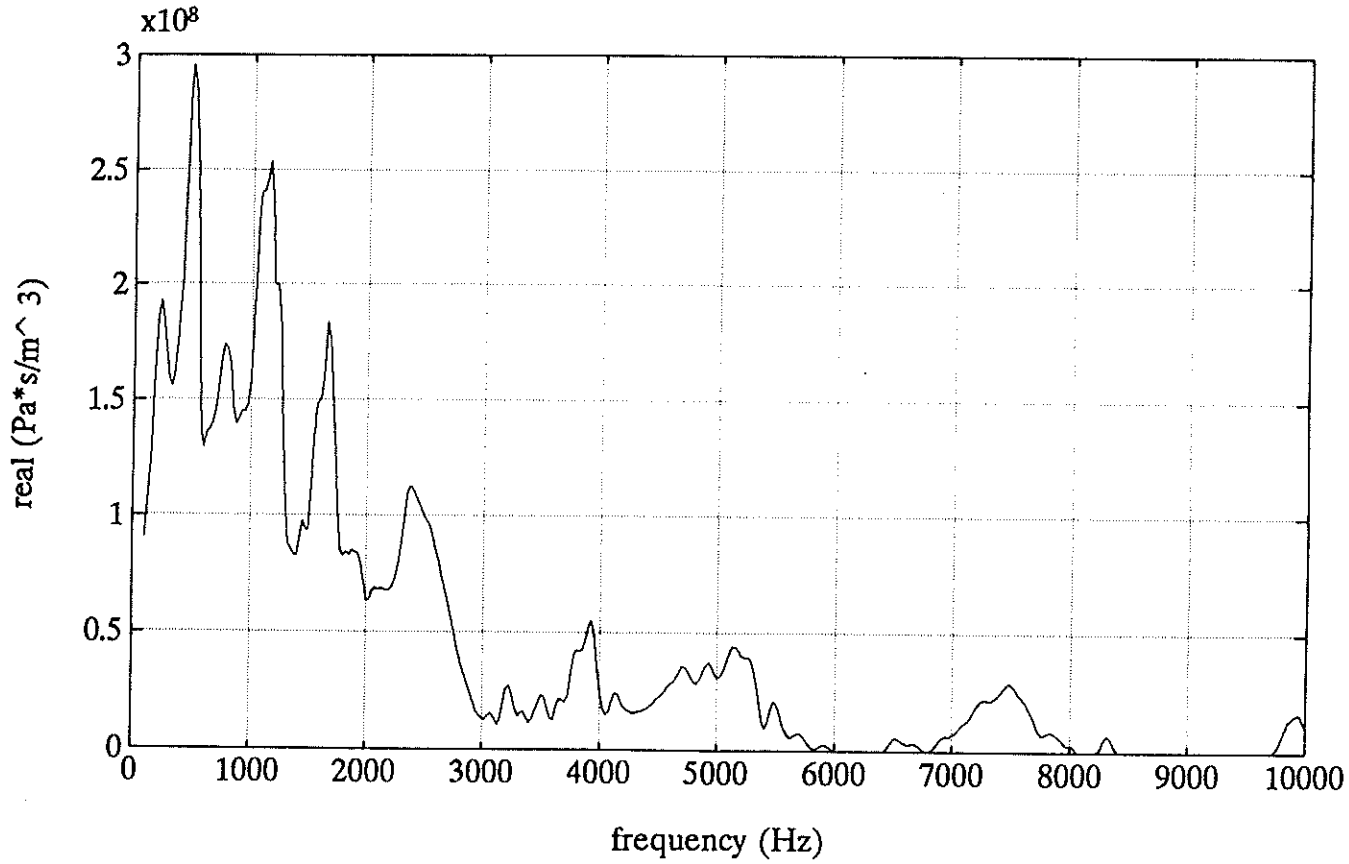

Figure 19a. Real part of Z0 for small diameter calibration.

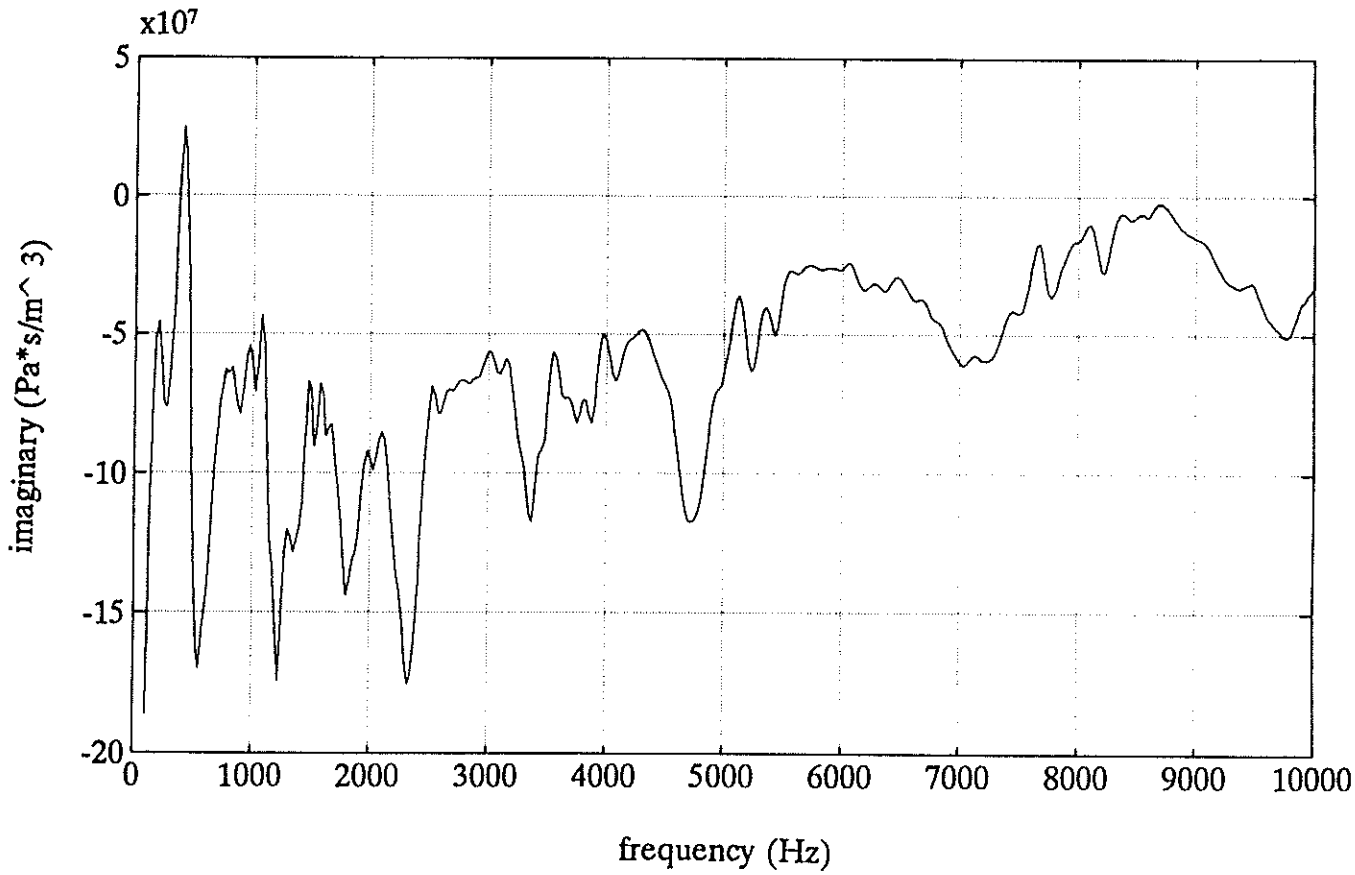

Figure 19b. Imaginary part of Z0 for small diameter calibration.

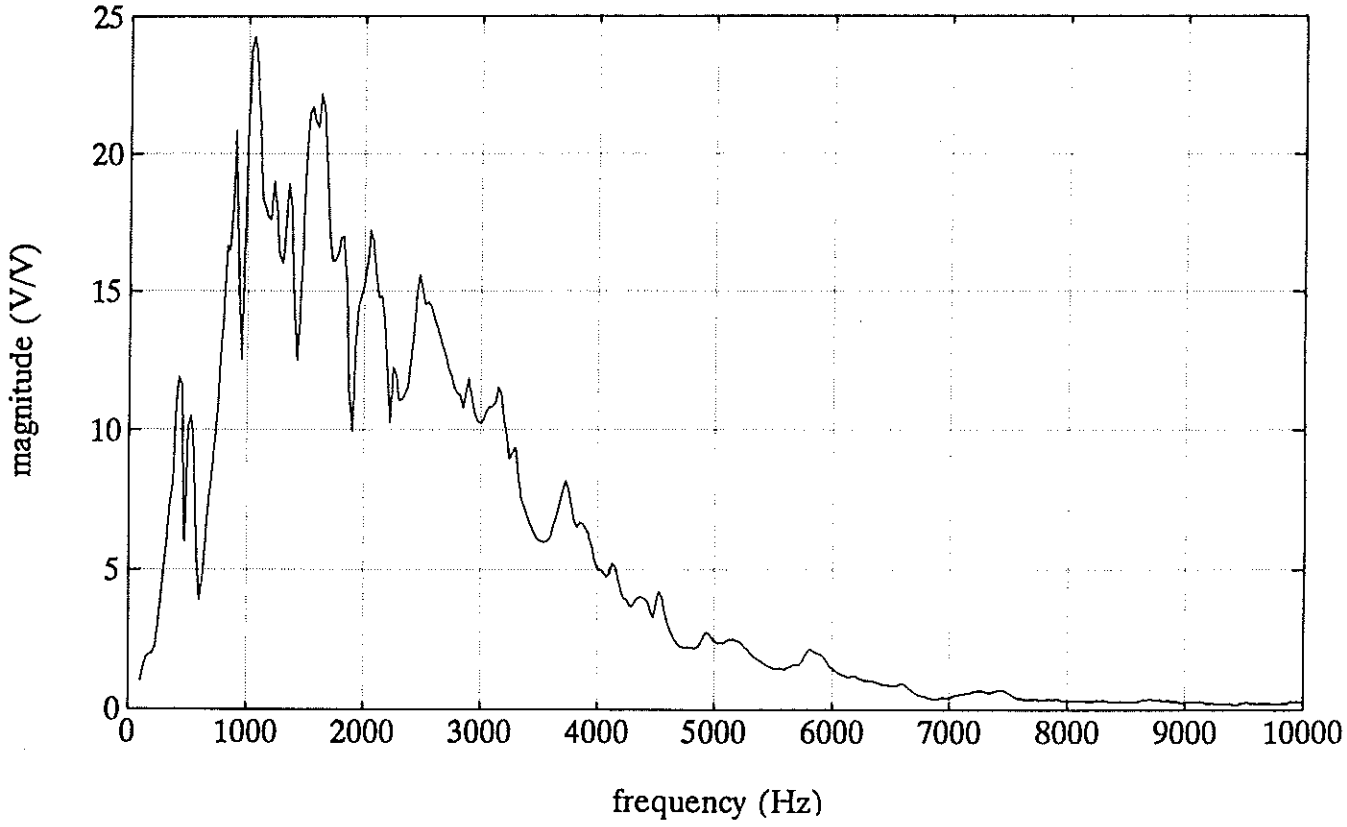

Figure 20a. Magnitude of $Xferp_0$ for large diameter calibration.

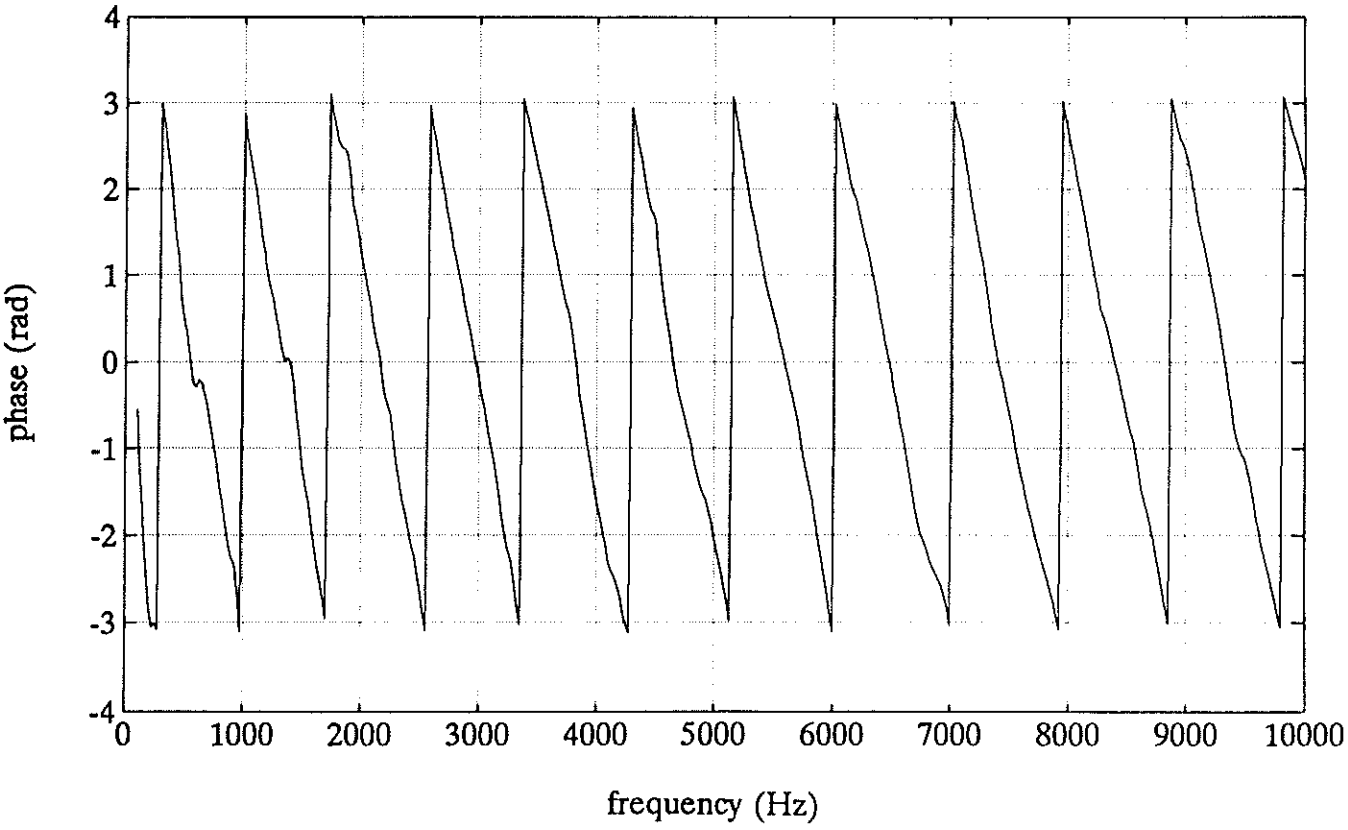

Figure 20b. Phase of $Xferp_0$ for large diameter calibration.

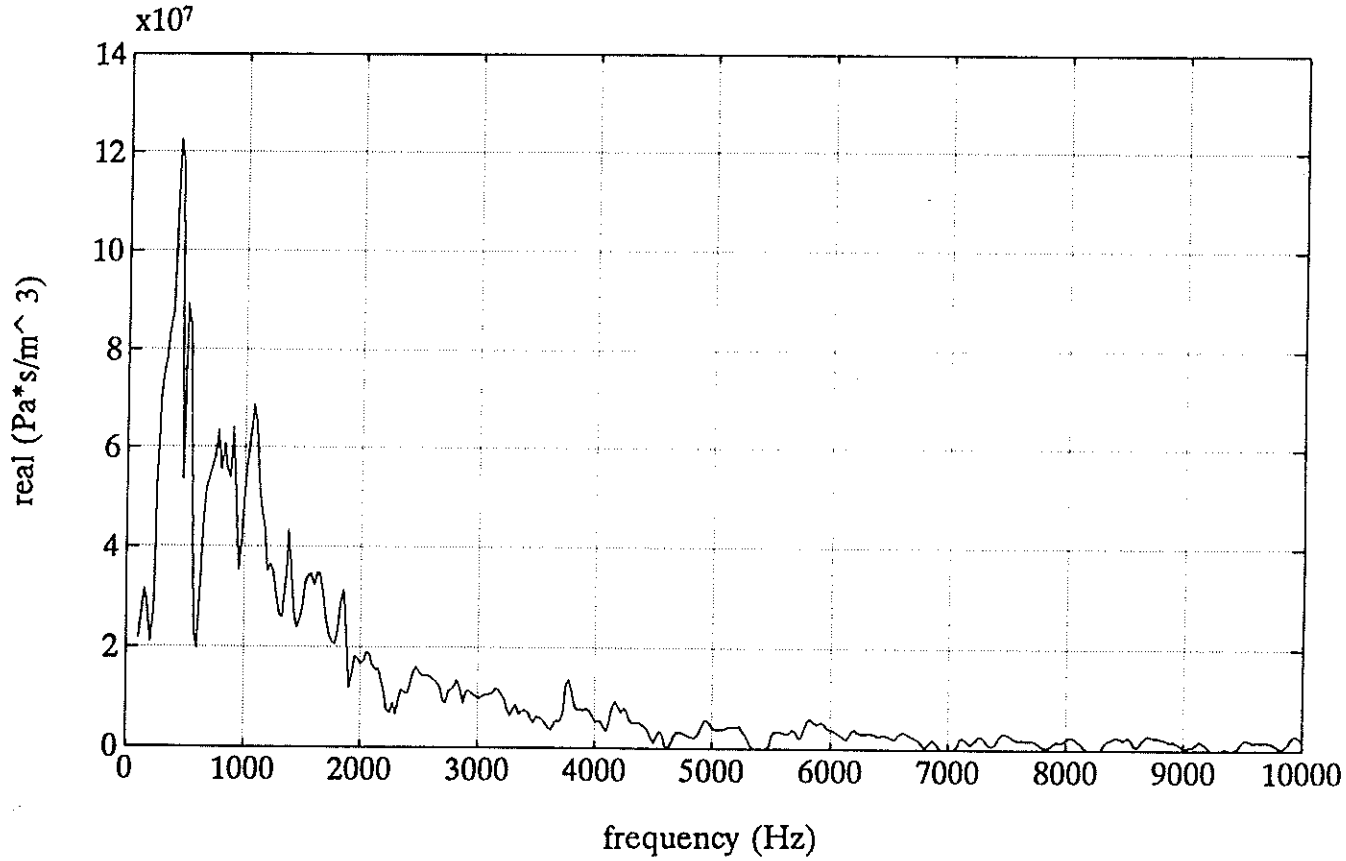

Figure 21a. Real part of Z0 for large diameter calibration.

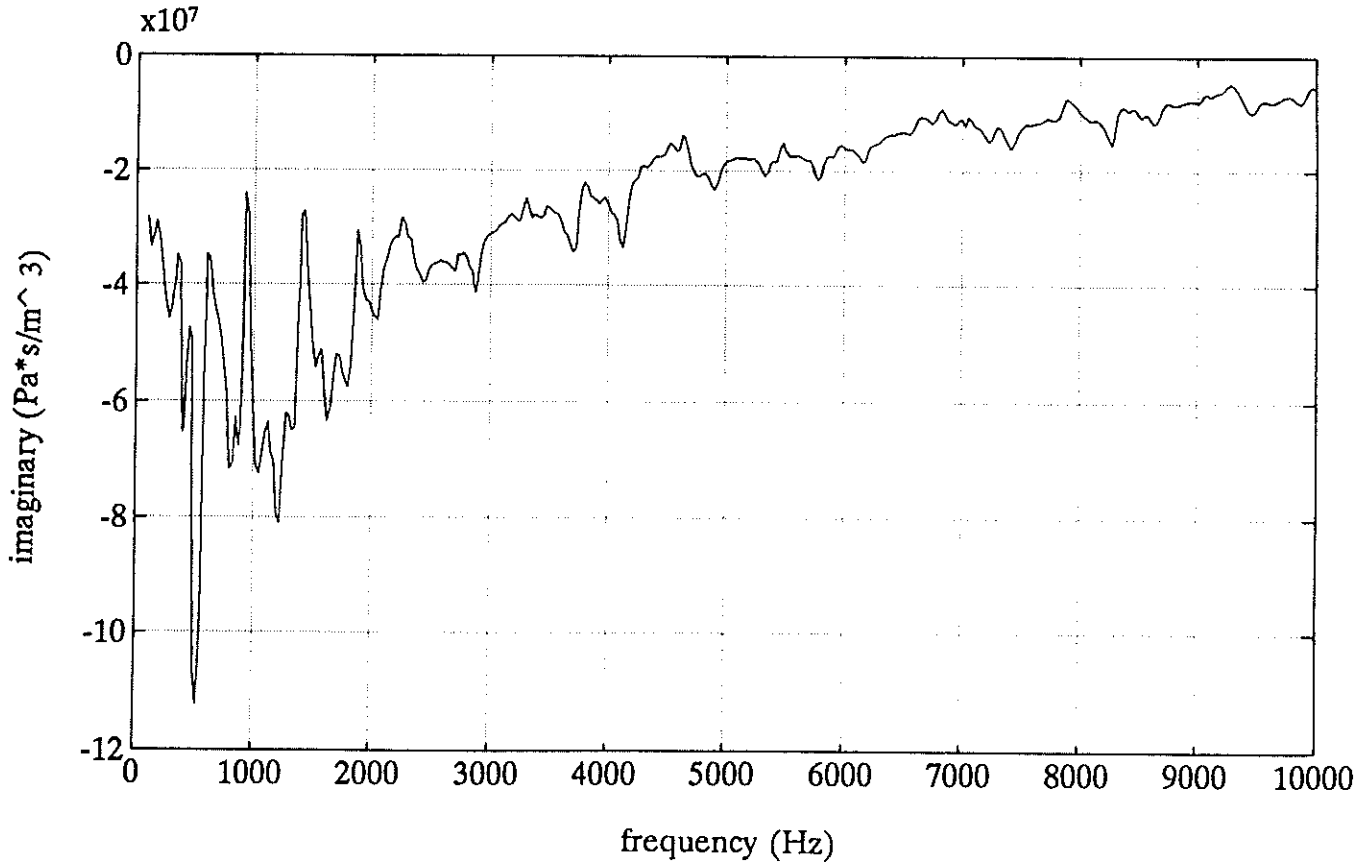

Figure 21b. Imaginary part of Z0 for large diameter calibration.

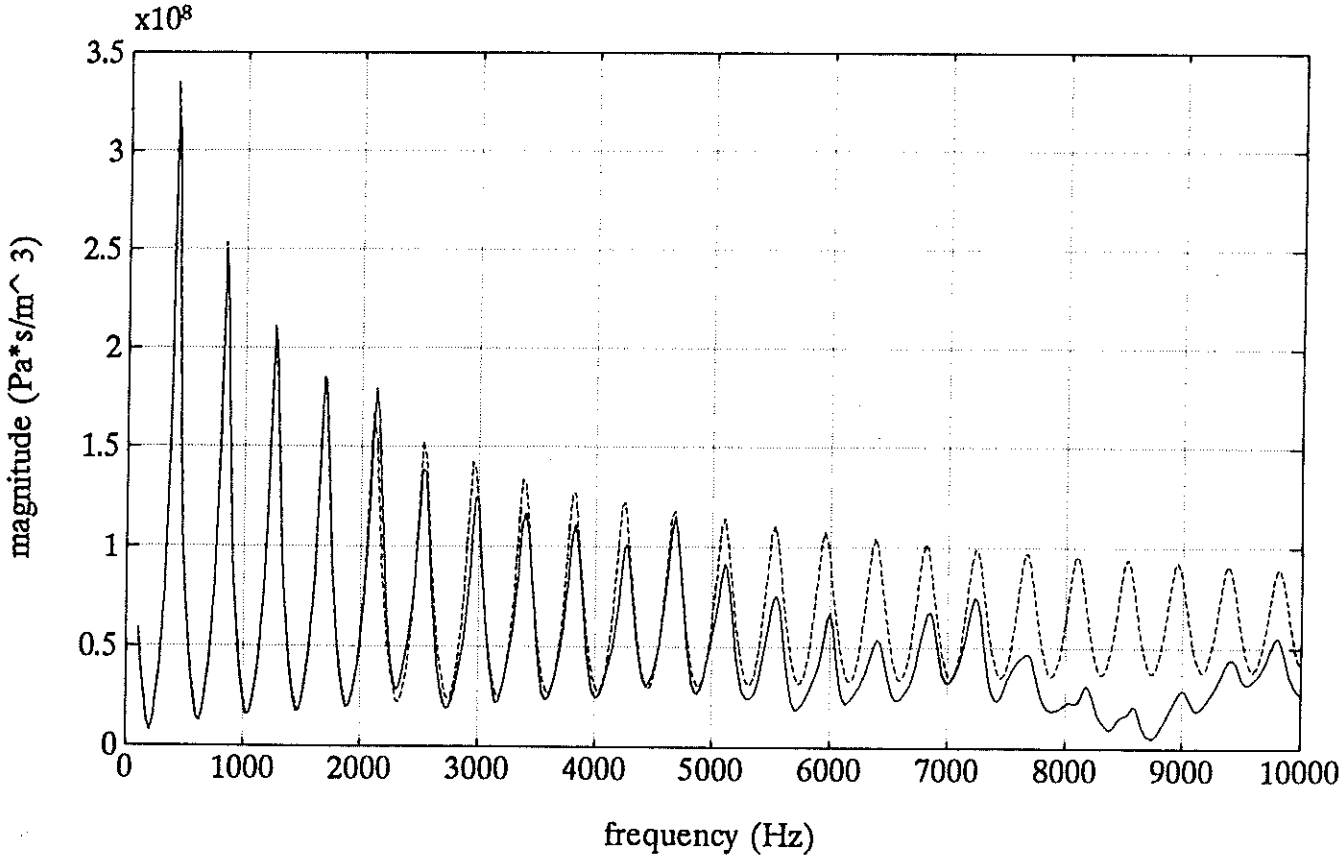

Figure 22a. Magnitude of measured (solid) and calculated (dashed) input impedance of small diameter tube, No 17.

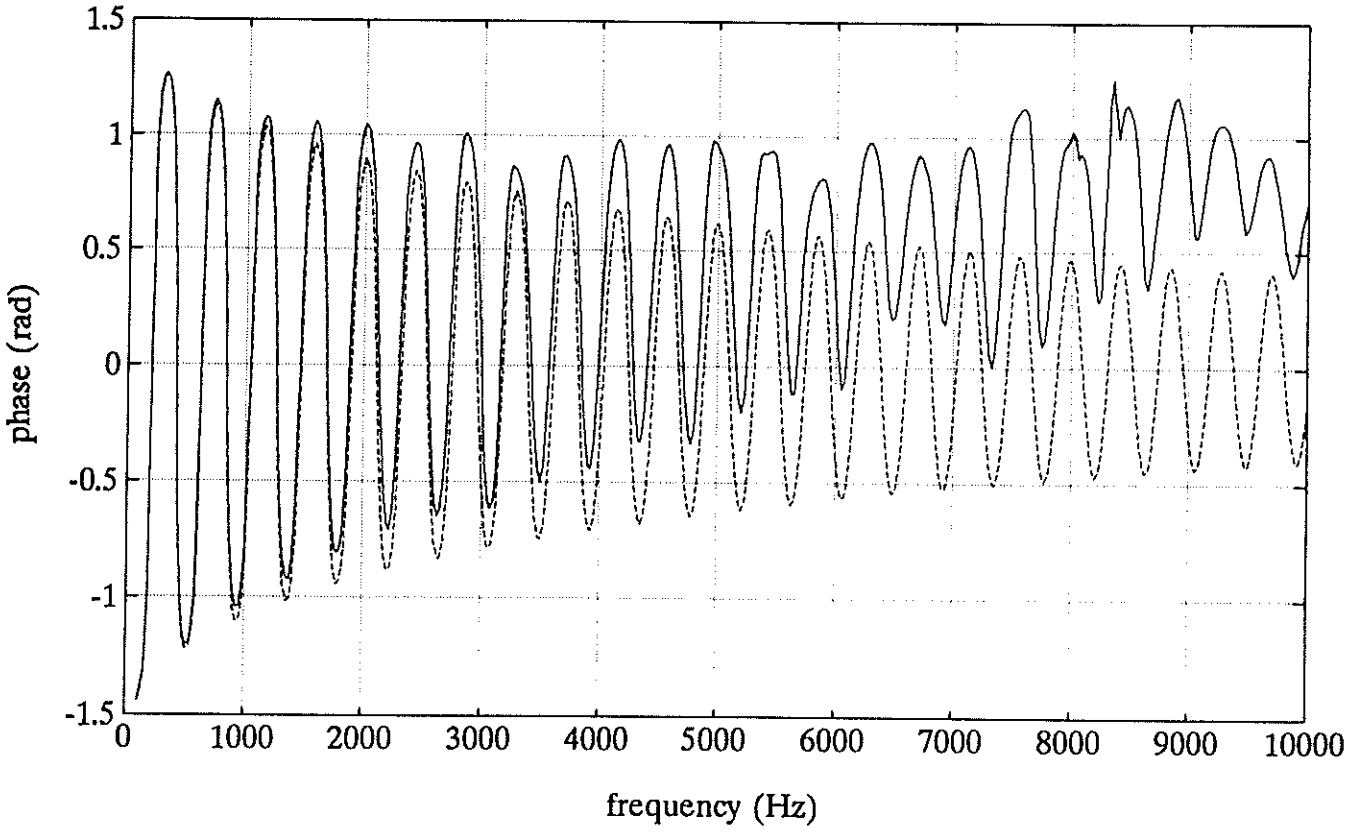

Figure 22b. Phase of measured (solid) and calculated (dashed) input impedance of small diameter tube, No 17.

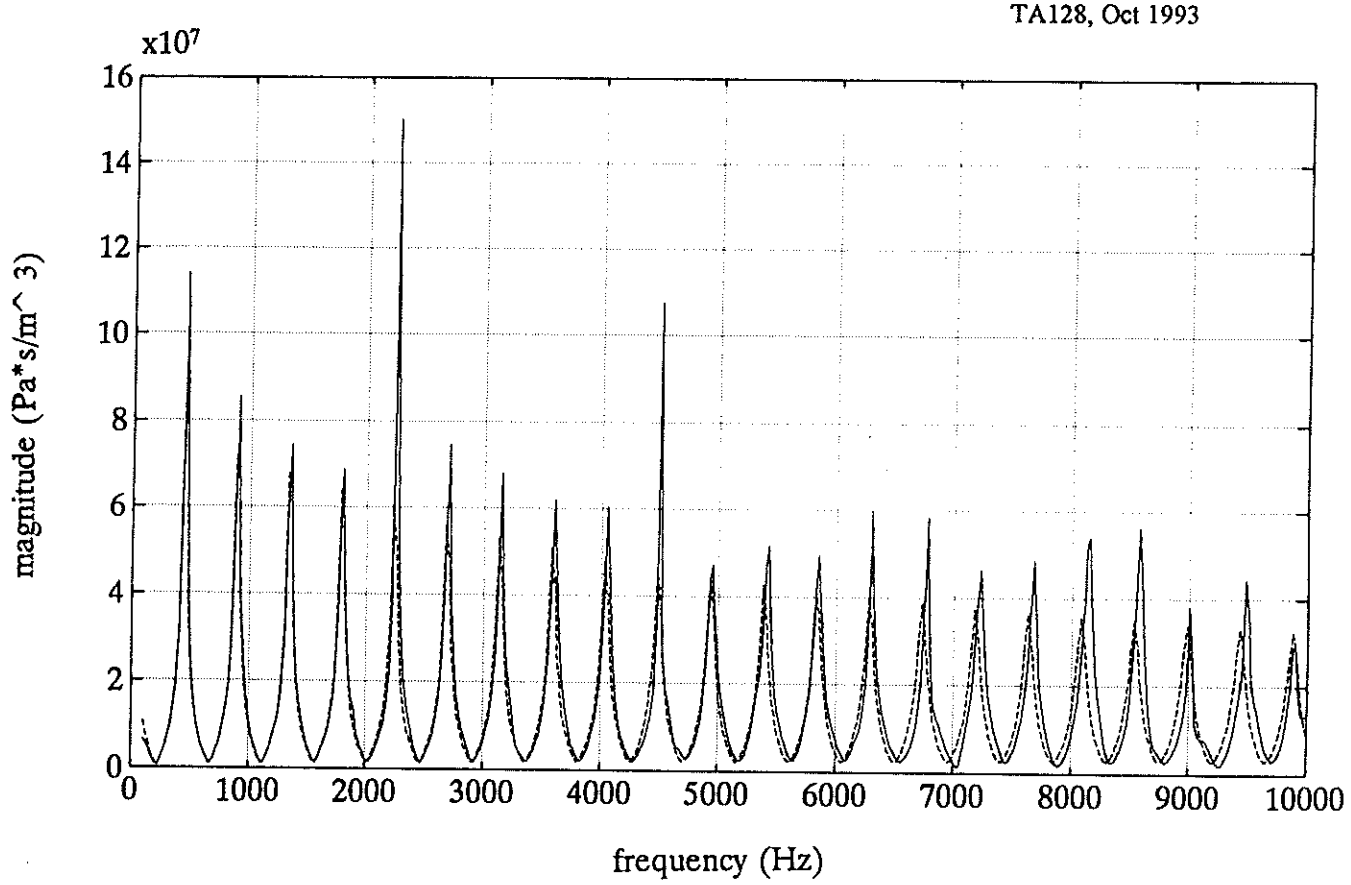

Figure 23a. Magnitude of measured (solid) and calculated (dashed) input impedance of large diameter tube, No 6.

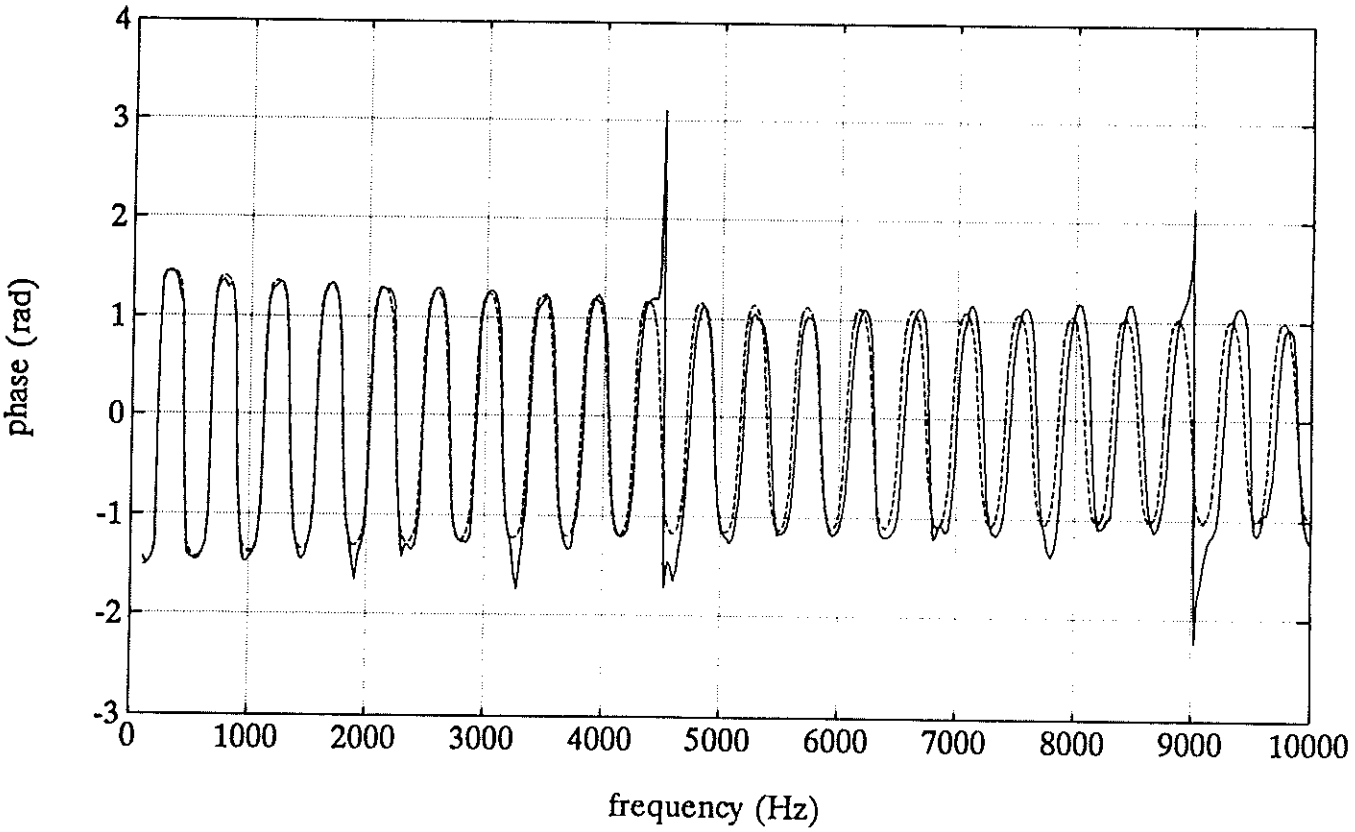

Figure 23b. Phase of measured (solid) and calculated (dashed) input impedance of large diameter tube, No 6.

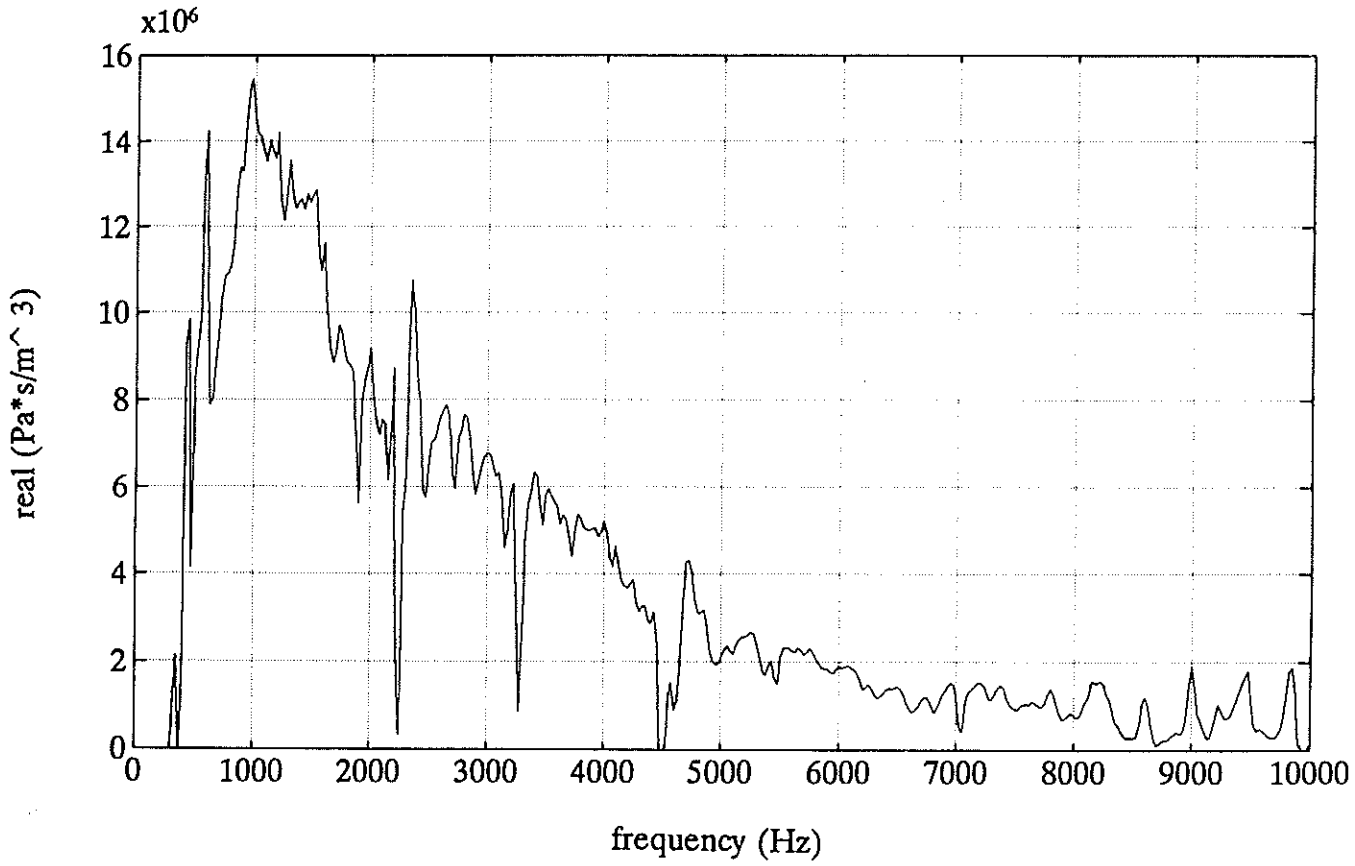

Figure 24a. Real part of coupler input impedance.

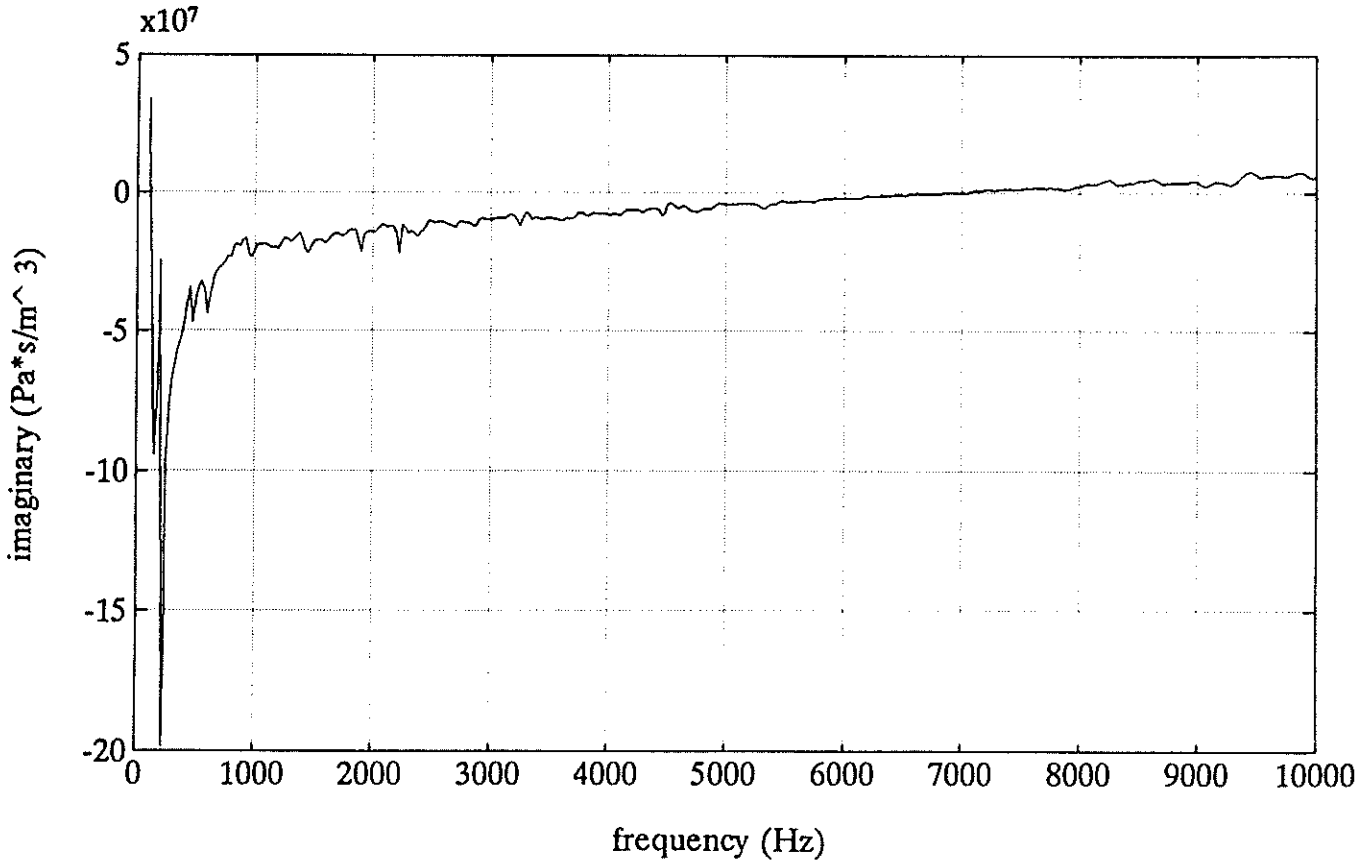

Figure 24b. Imaginary part of coupler input impedance.

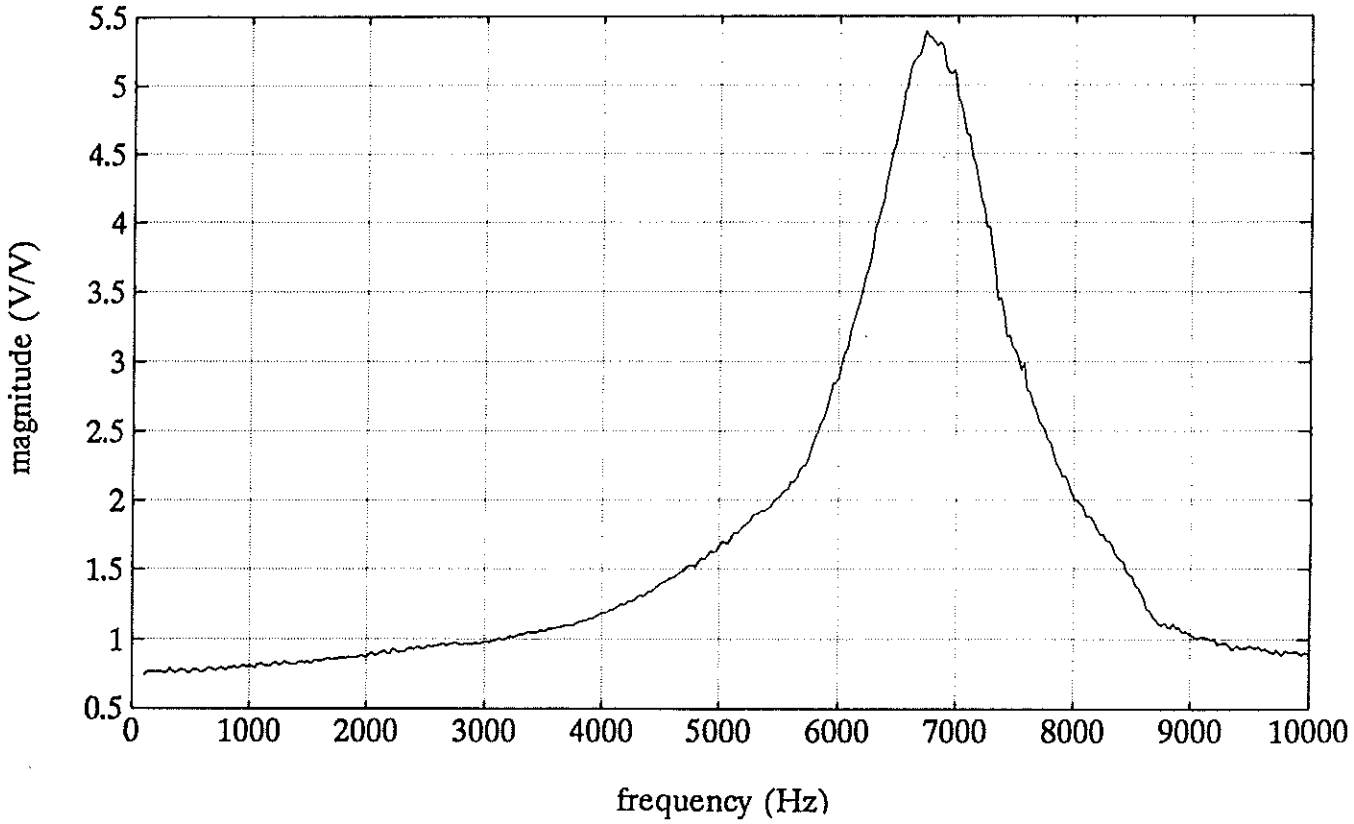

Figure 25a. Magnitude of coupler transfer function.

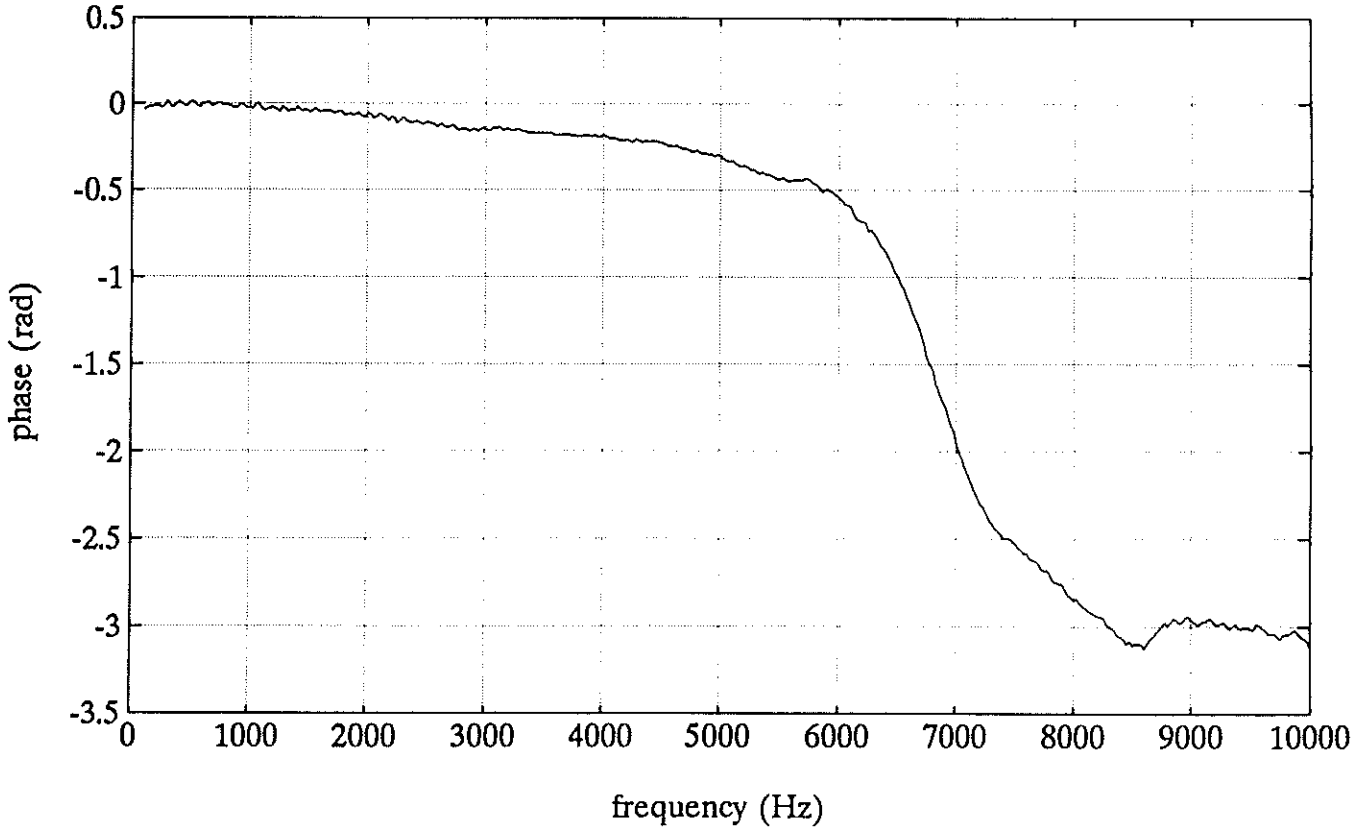

Figure 25b. Phase of coupler transfer function.

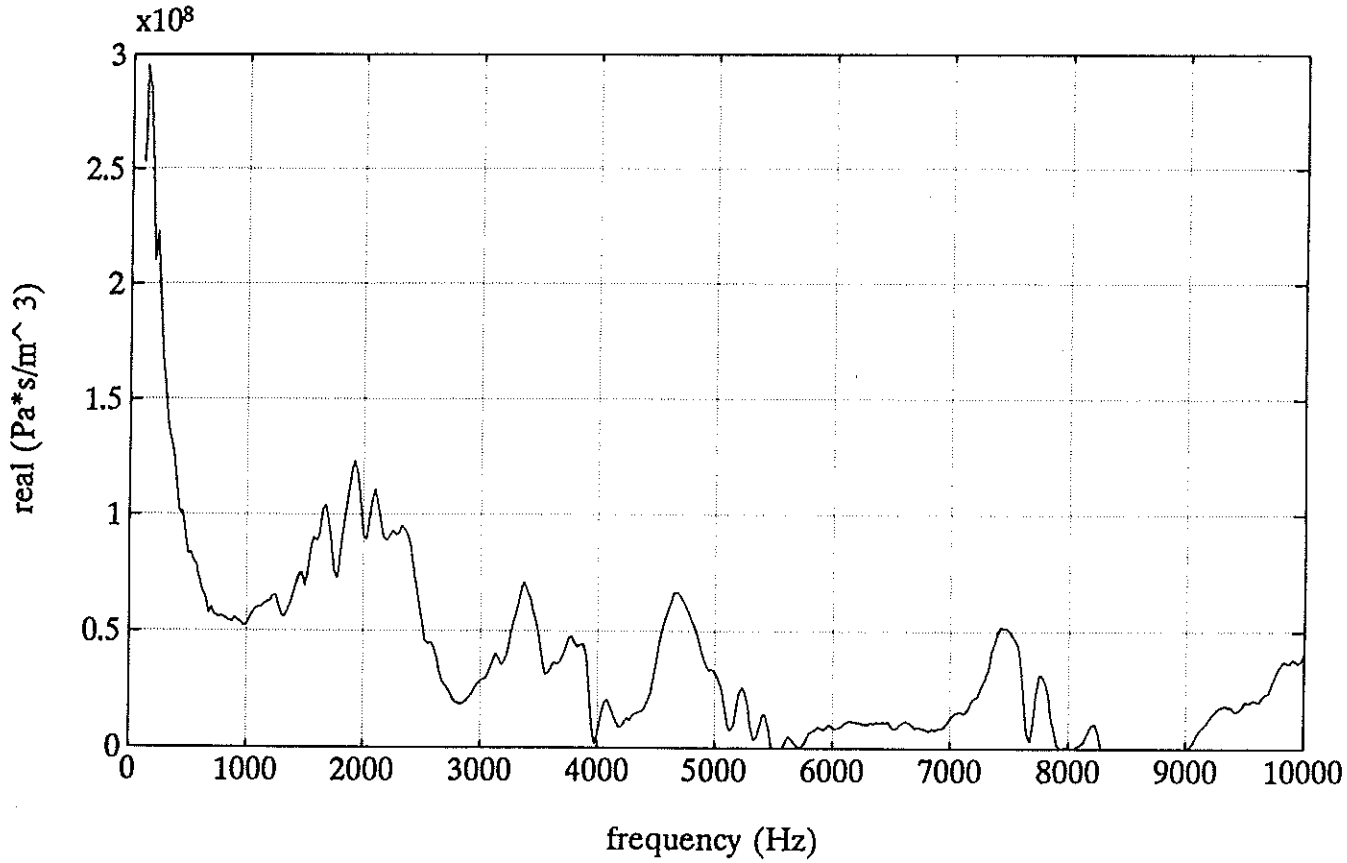

Figure 26a. Real part of hearing aid Thevenin impedance in prediction-in-coupler experiment.

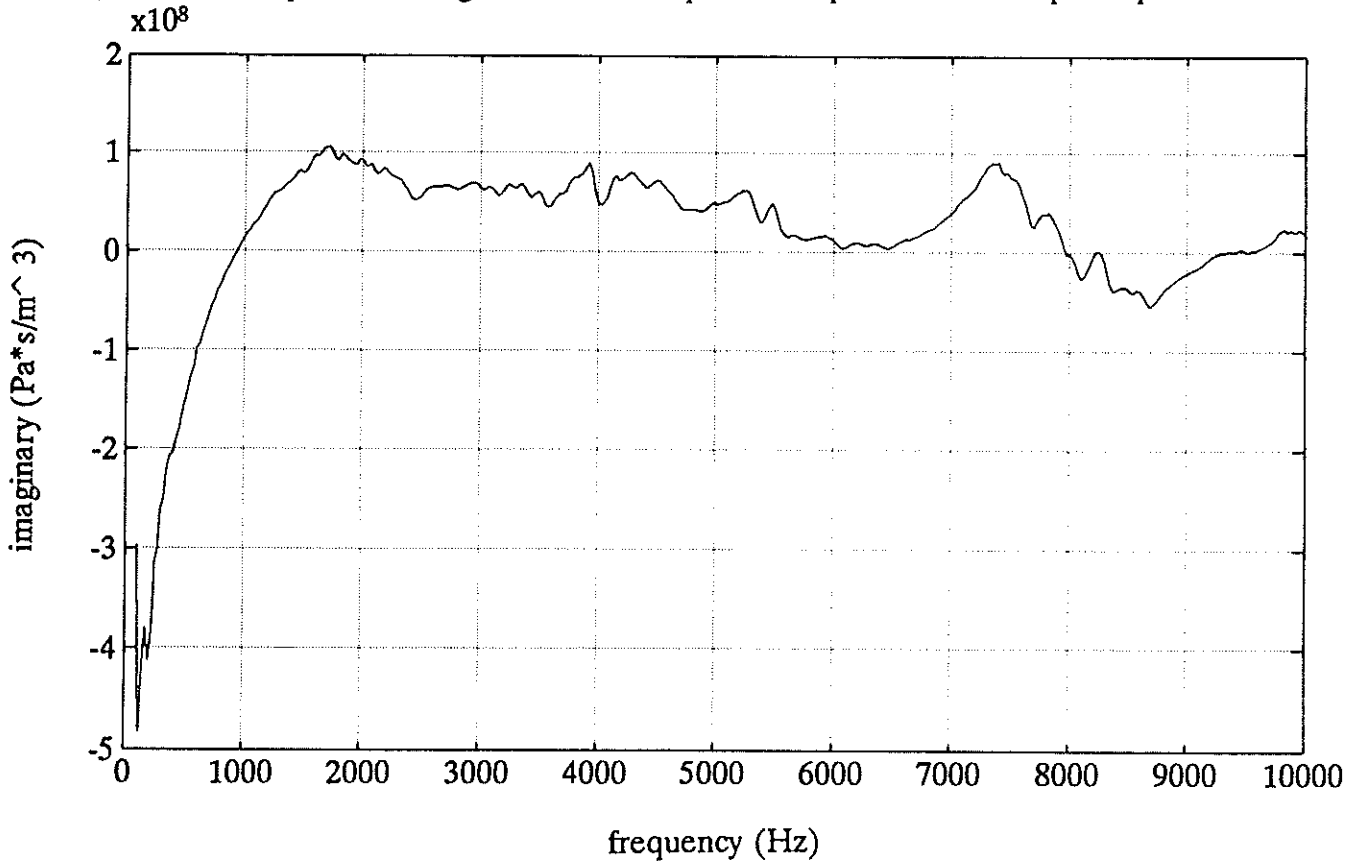

Figure 26b. Imaginary part of hearing aid Thevenin impedance in prediction-in-coupler experiment.

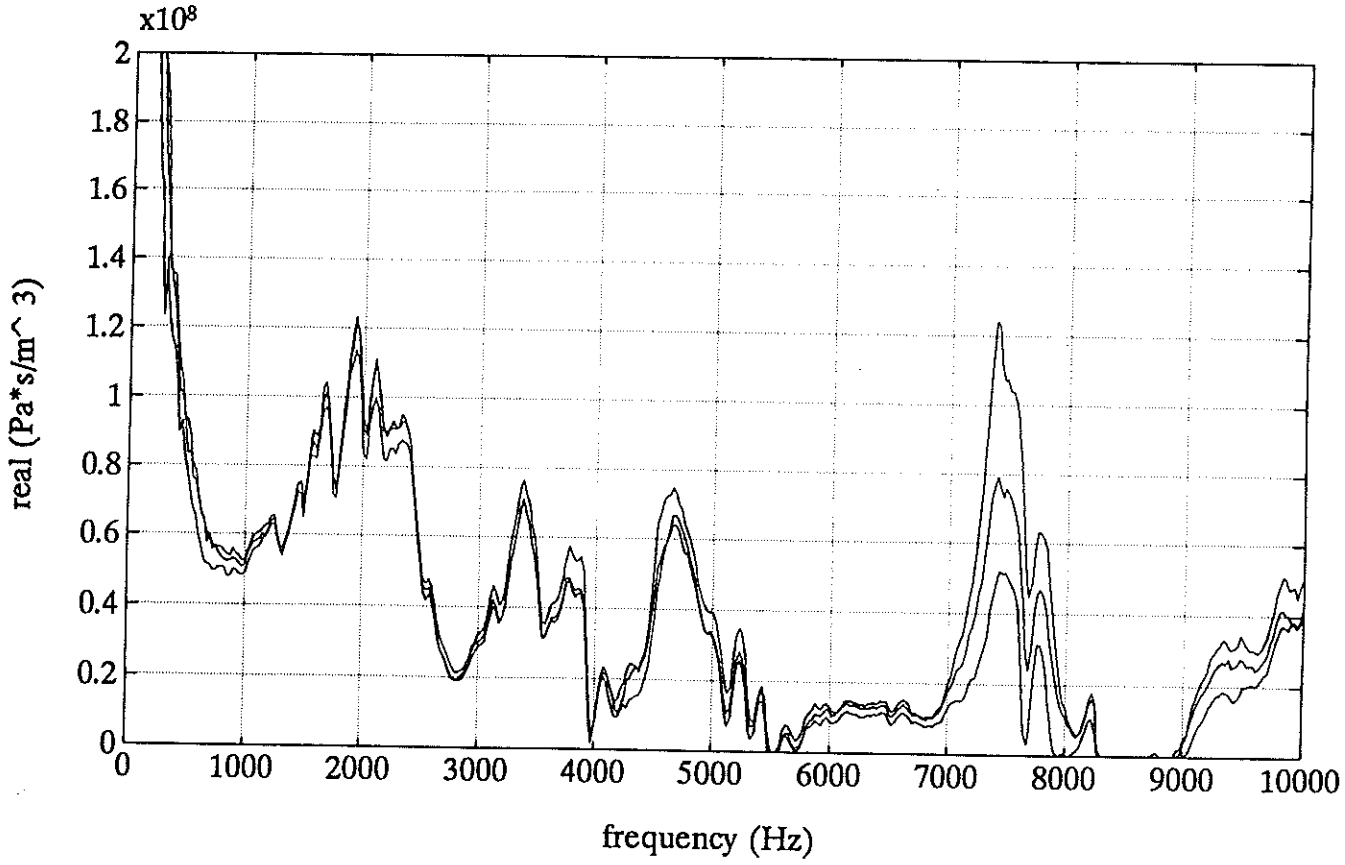

Figure 27a. Three measurements of the real part of hearing aid Thevenin impedance.

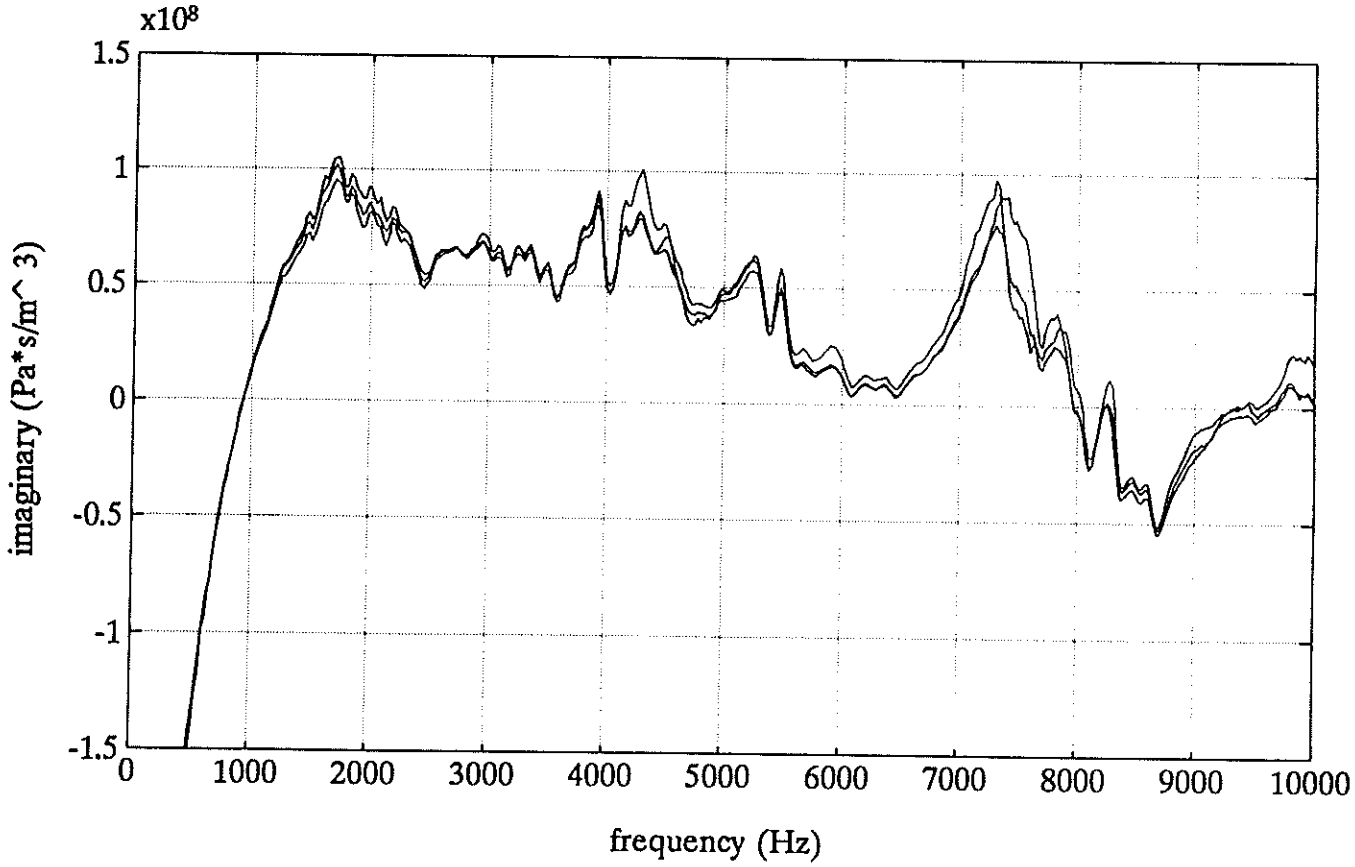

Figure 27b. Three measurements of the imaginary part of hearing aid Thevenin impedance.

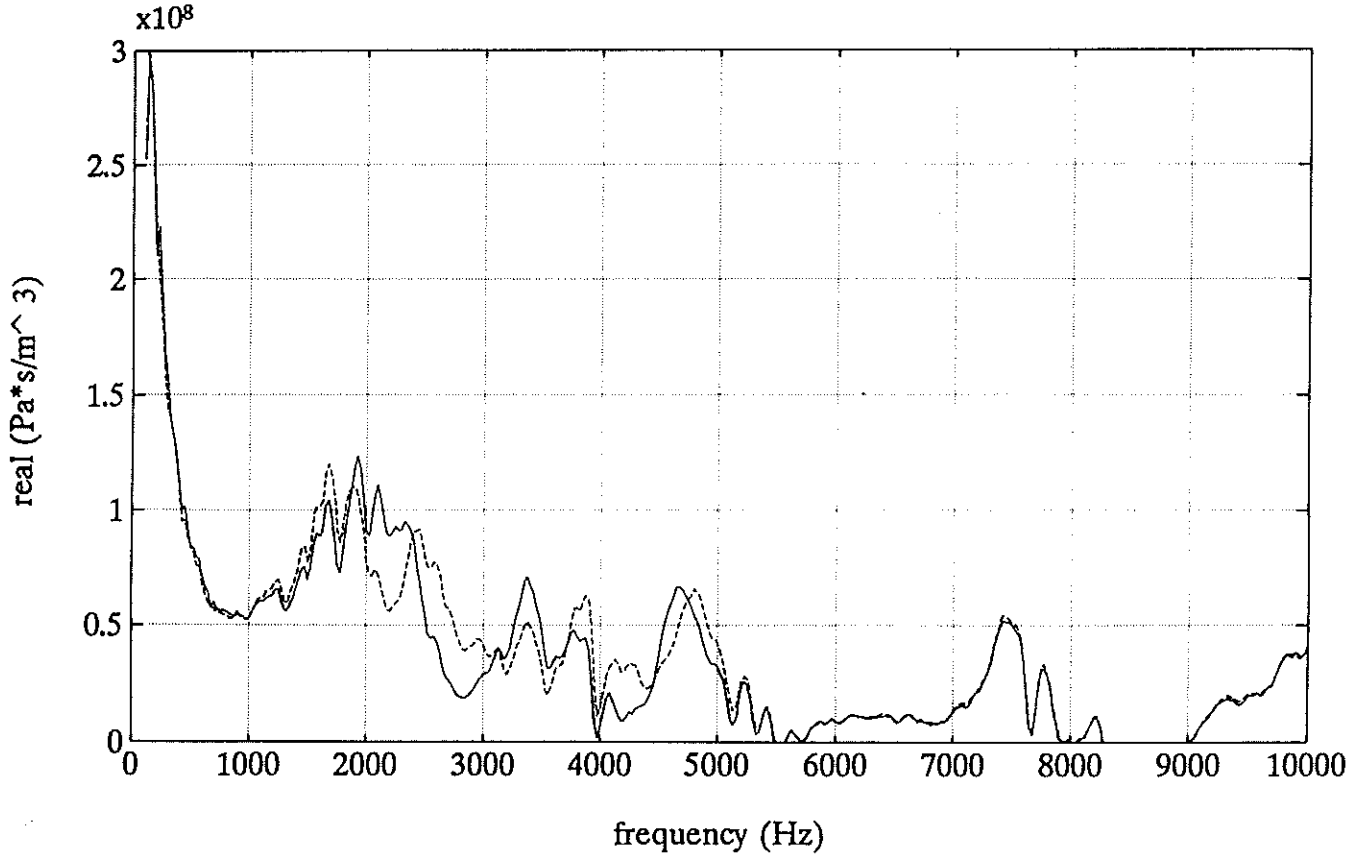

Figure 28a. Real part of hearing aid Thevenin impedance with power turned on (solid) and power turned off (dashed).

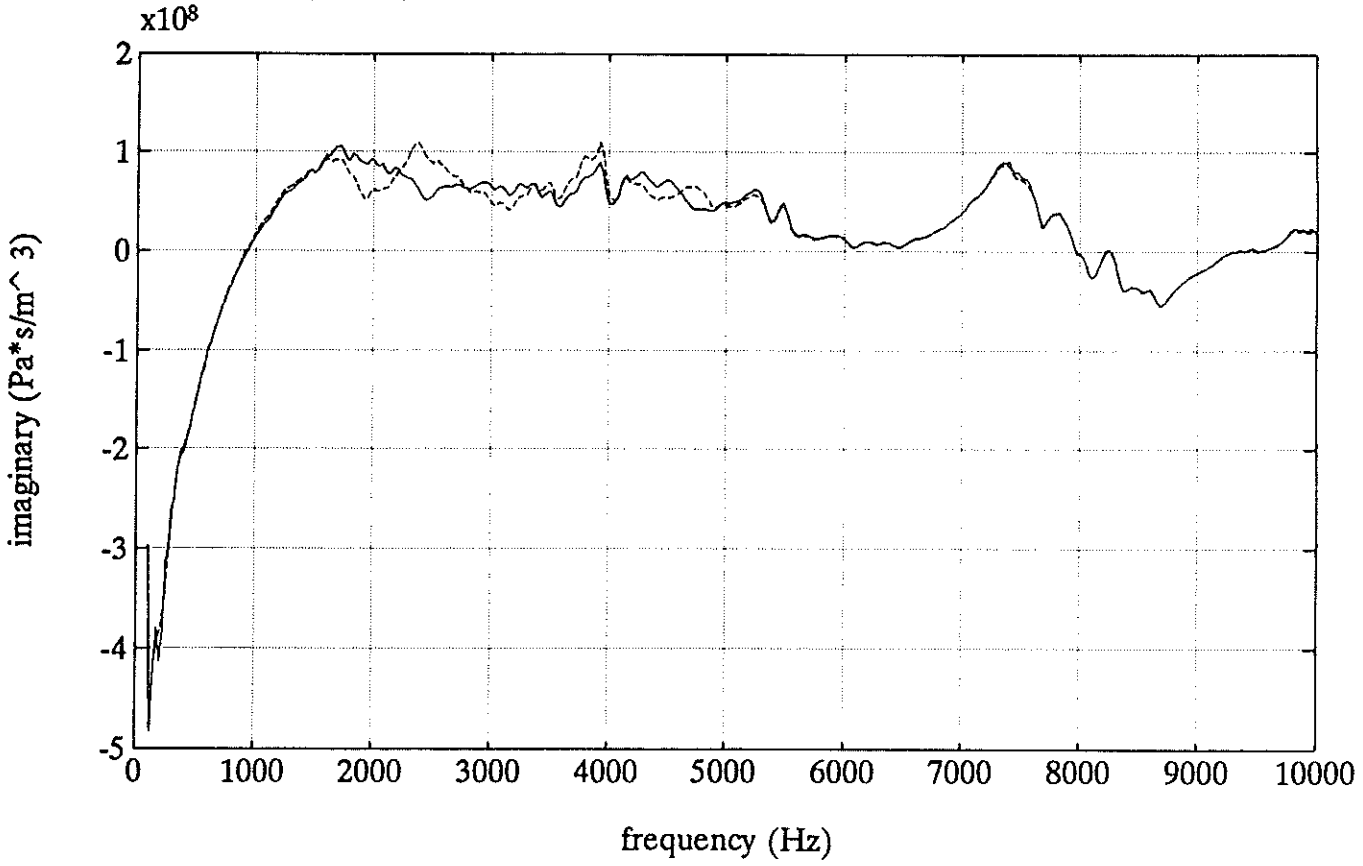

Figure 28b. Imaginary part of hearing aid Thevenin impedance with power turned on (solid) and power turned off (dashed).

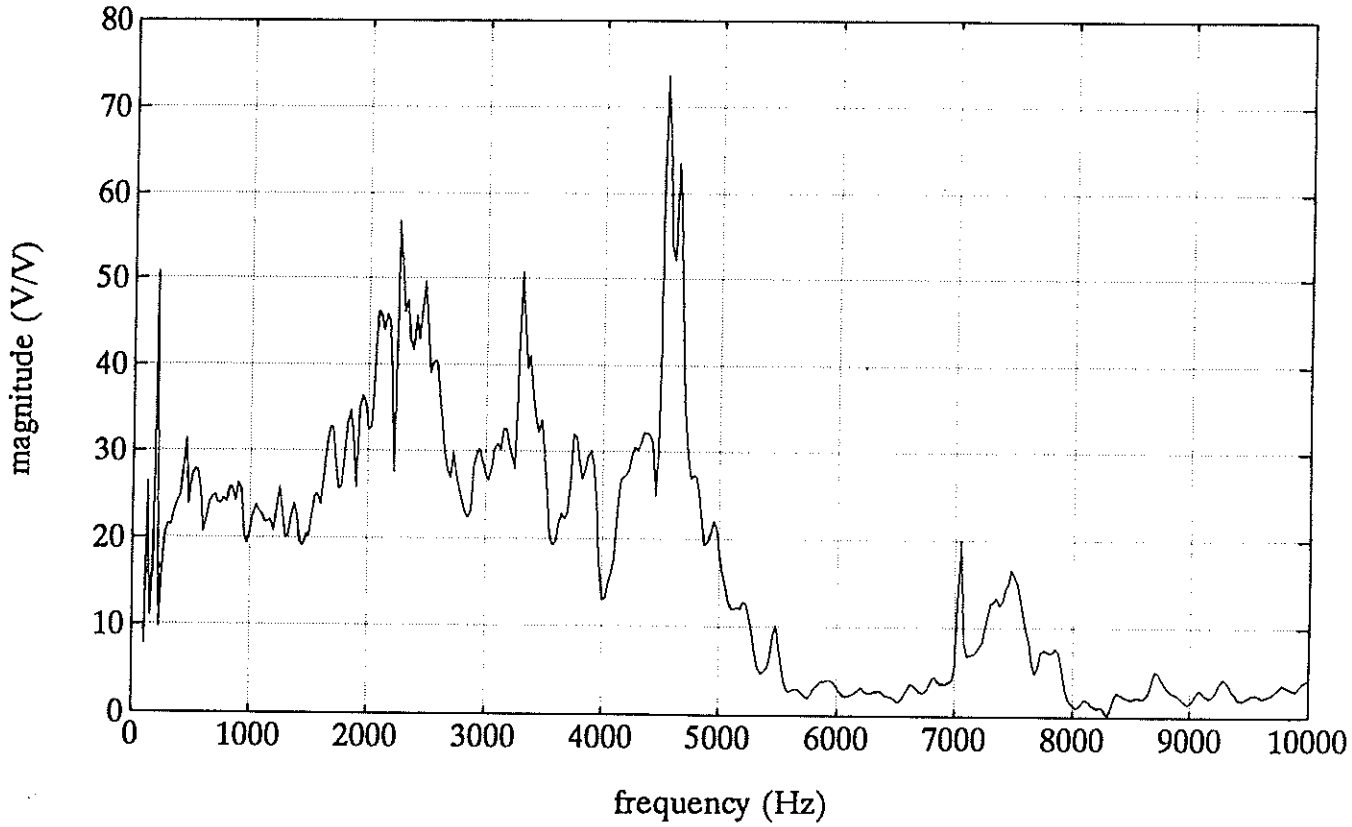

Figure 29a. Magnitude of hearing aid Thevenin pressure transfer function in prediction-in-coupler experiment.

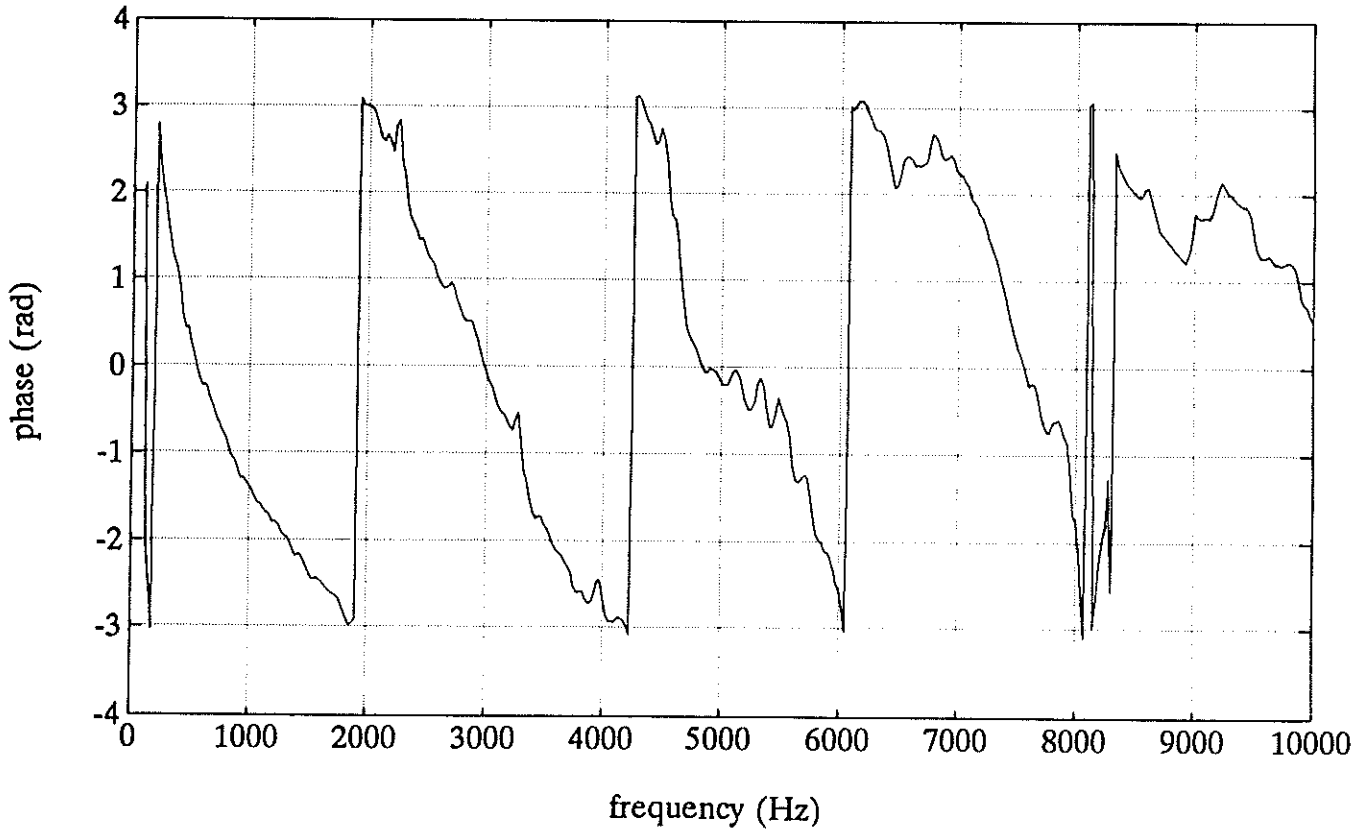

Figure 29b. Phase of hearing aid Thevenin pressure transfer function in prediction-in-coupler experiment.

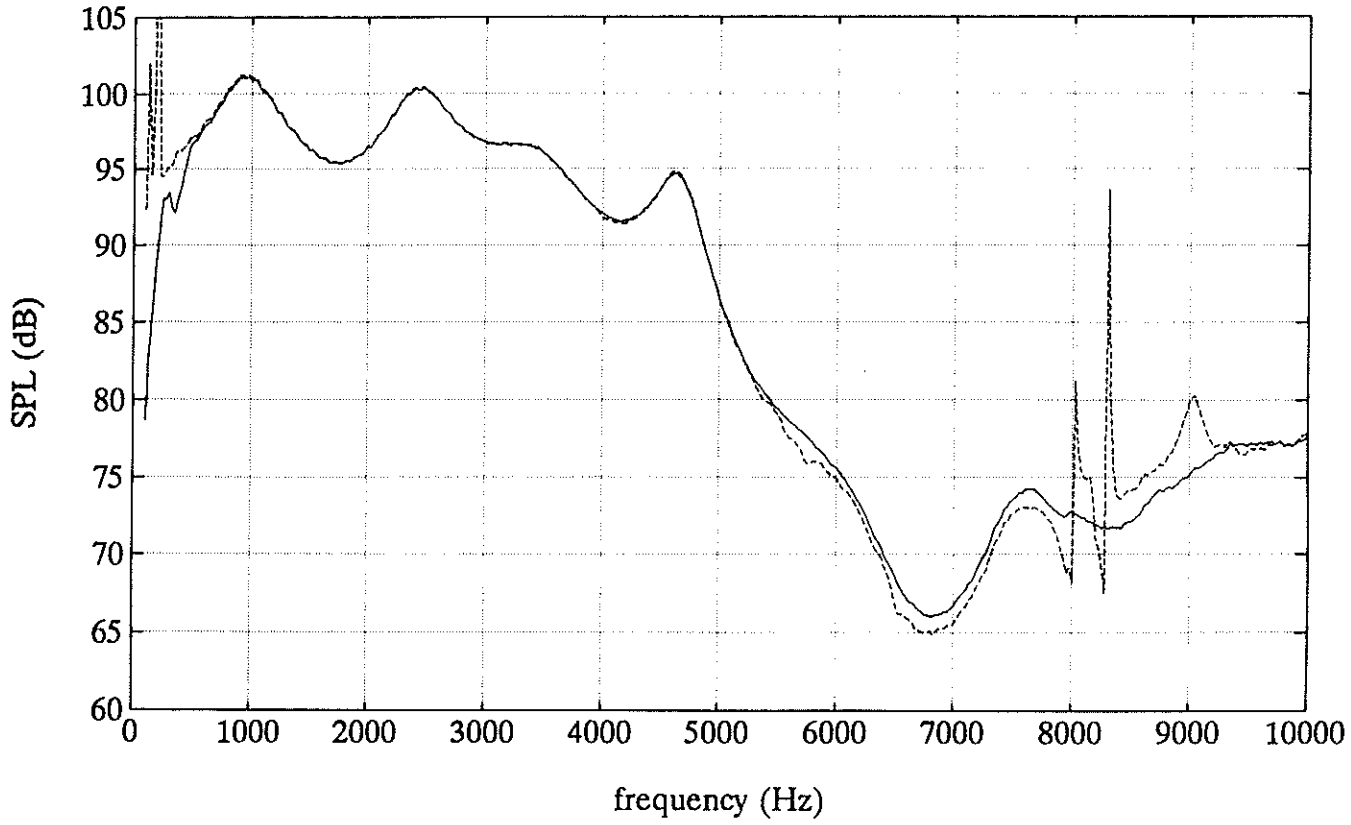

Figure 30. Measured (solid) and predicted (dashed) sound pressure levels from second measurement in prediction-in-coupler experiment.

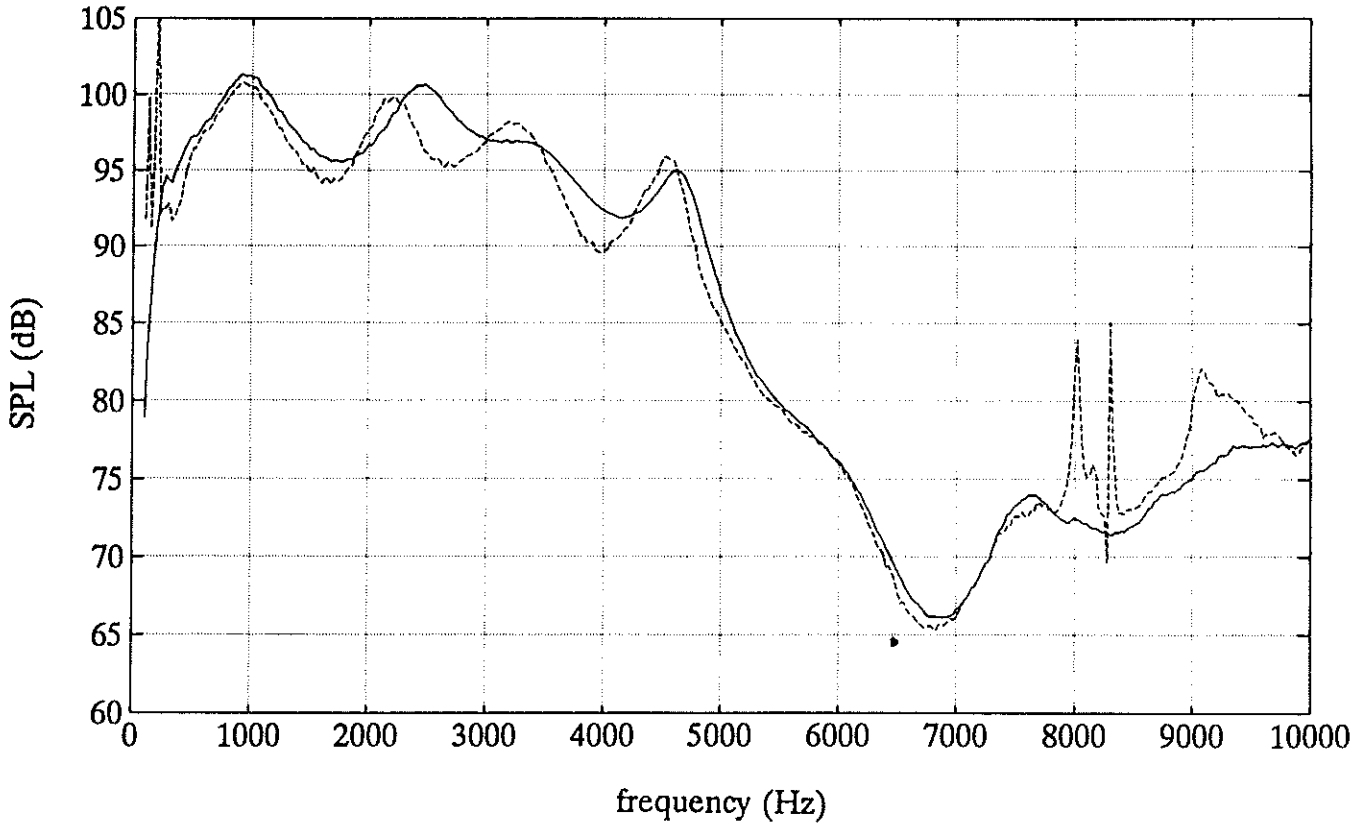

Figure 31. Measured (solid) and predicted (dashed) sound pressure levels from third measurement in prediction-in-coupler experiment.

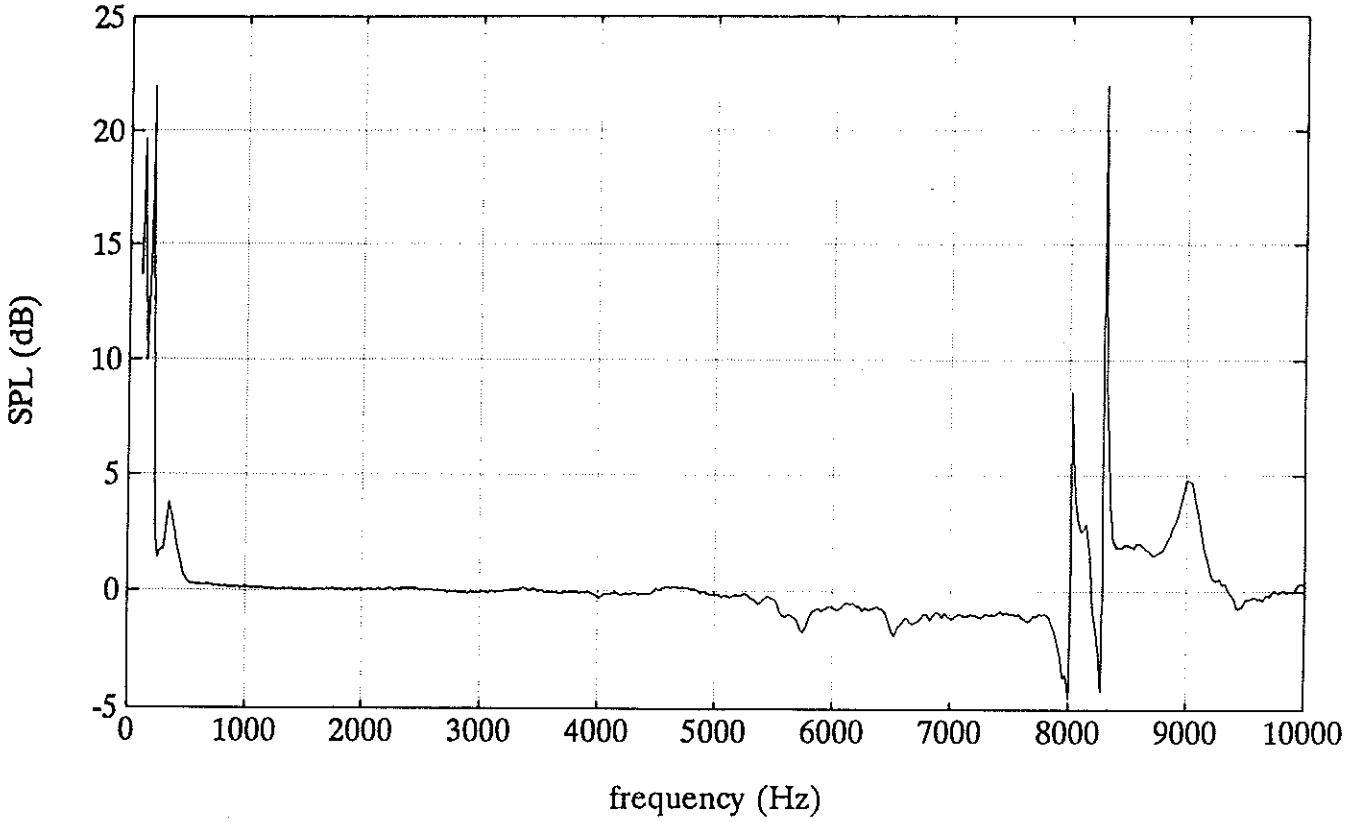

Figure 32. Predicted - measured sound pressure level from second measurement in prediction-in-coupler experiment.

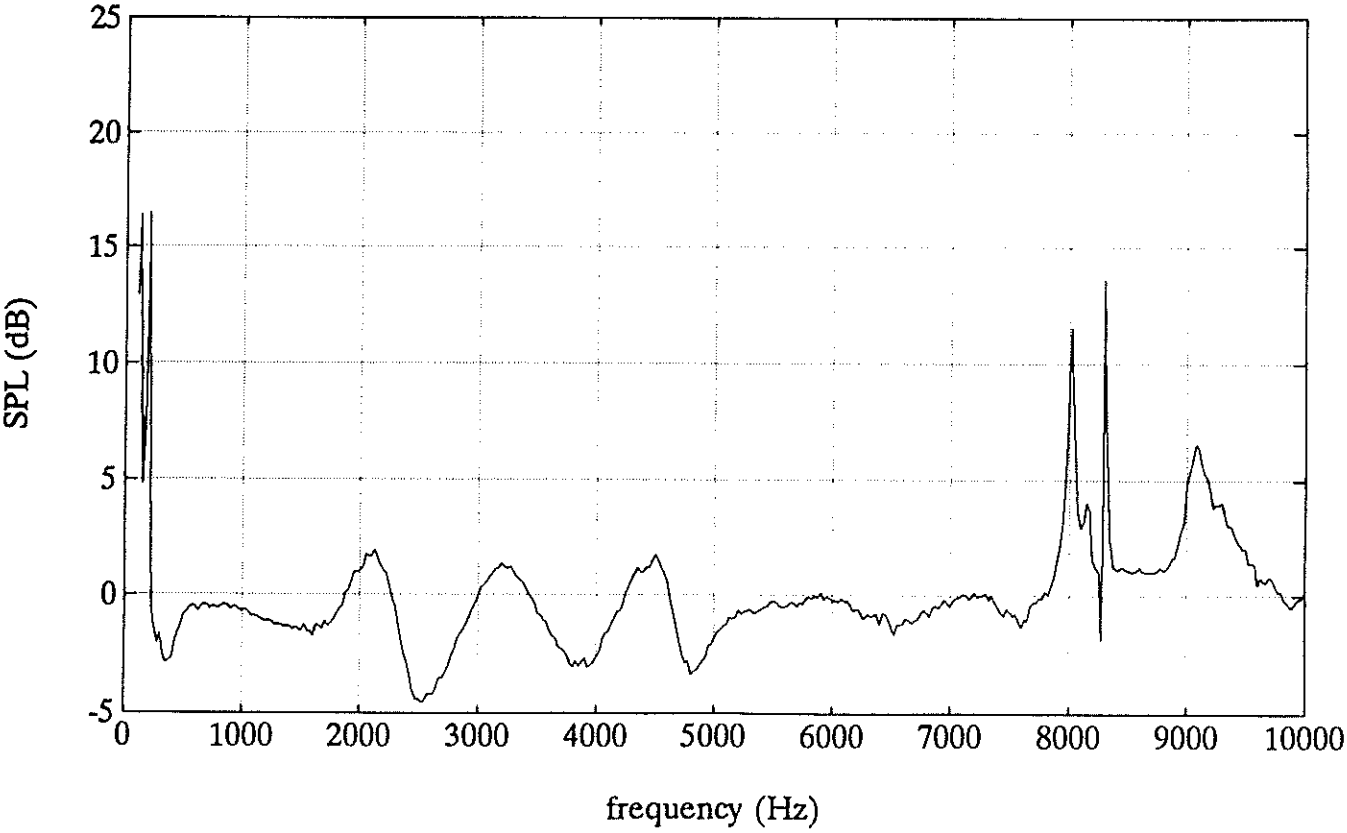

Figure 33. Predicted - measured sound pressure level from third measurement in prediction-in-coupler experiment.

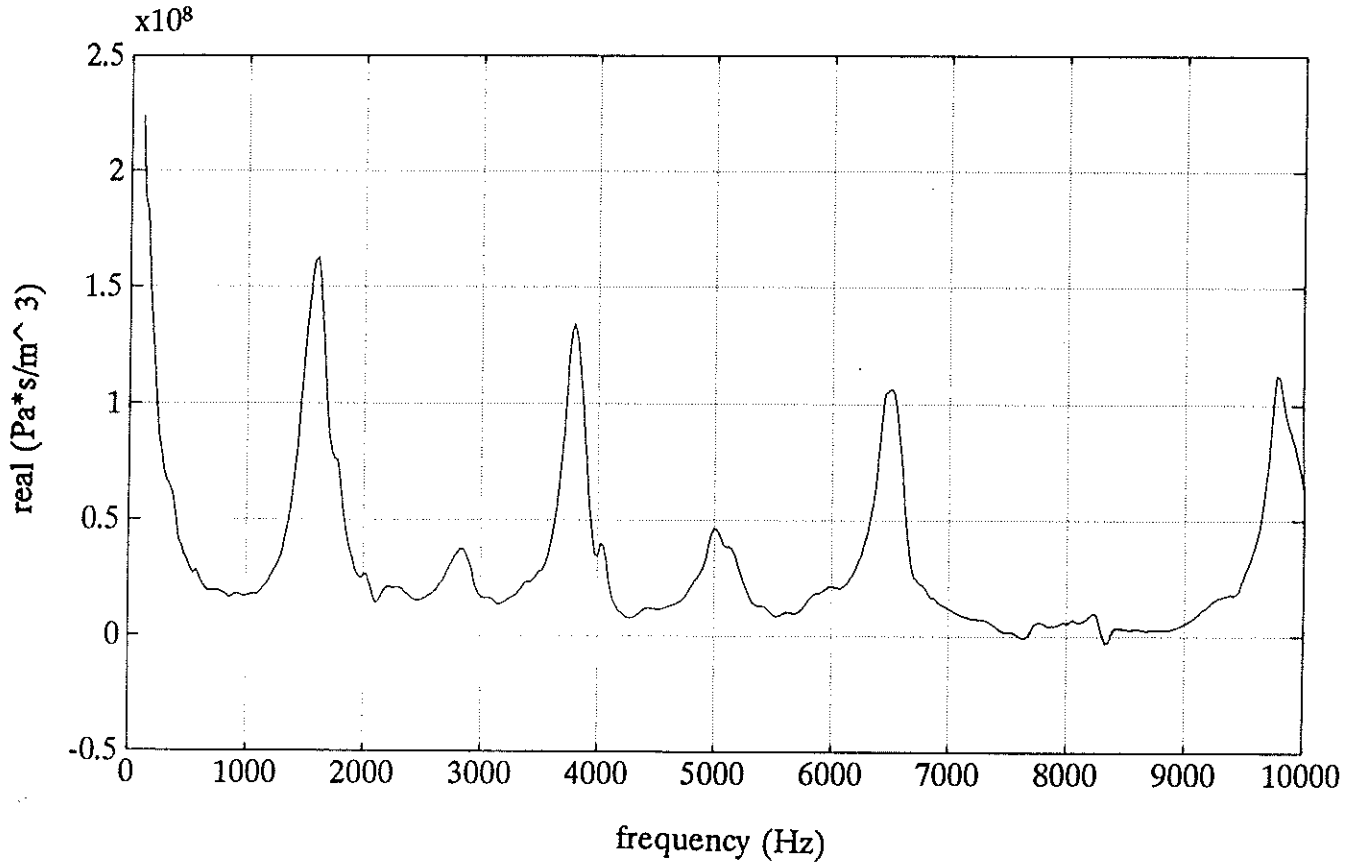

Figure 34a. Real part of hearing aid Thevenin impedance for the Widex ES1 hearing aid.

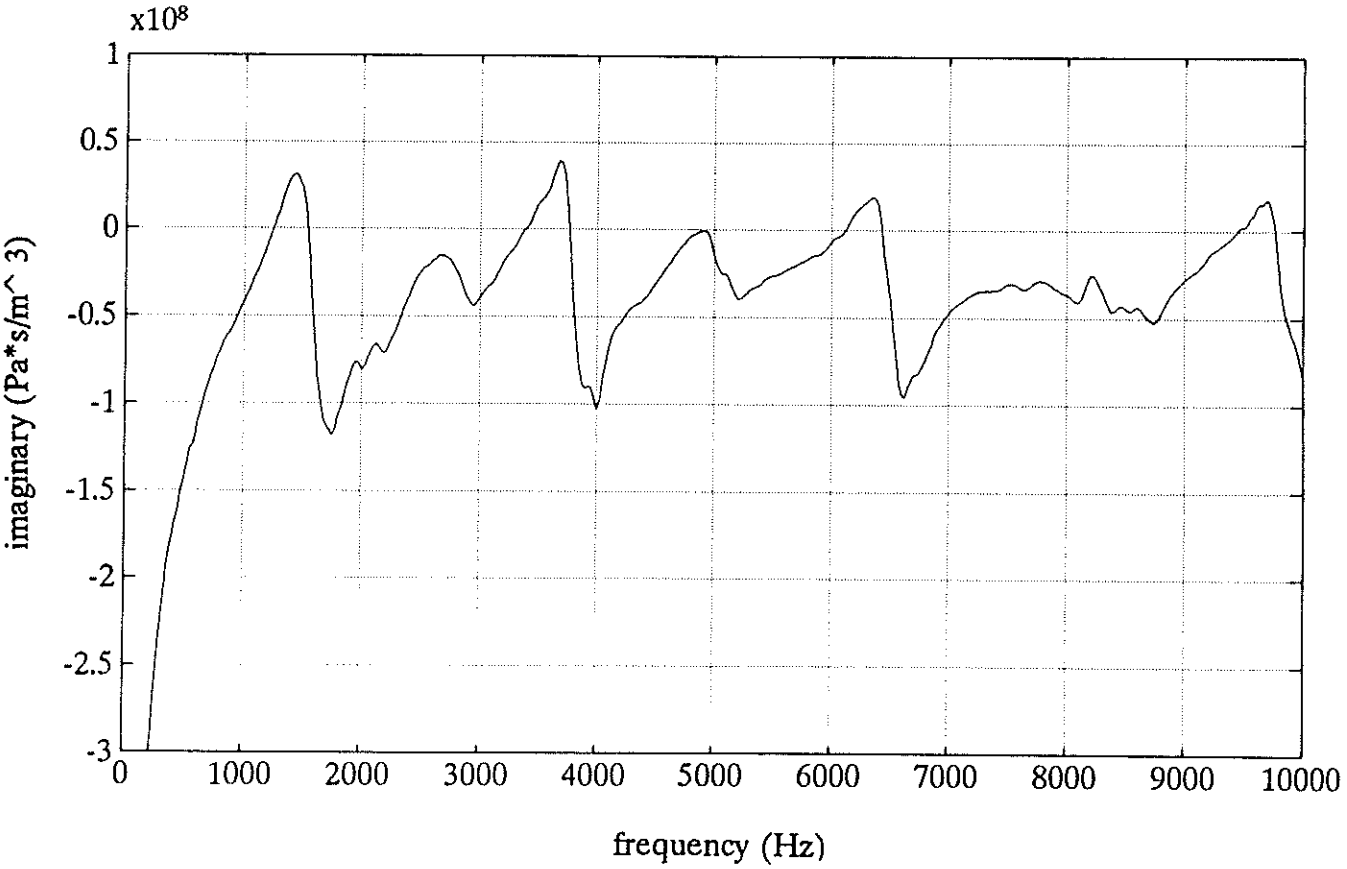

Figure 34b. Imaginary part of hearing aid Thevenin impedance for the Widex ES1 hearing aid.

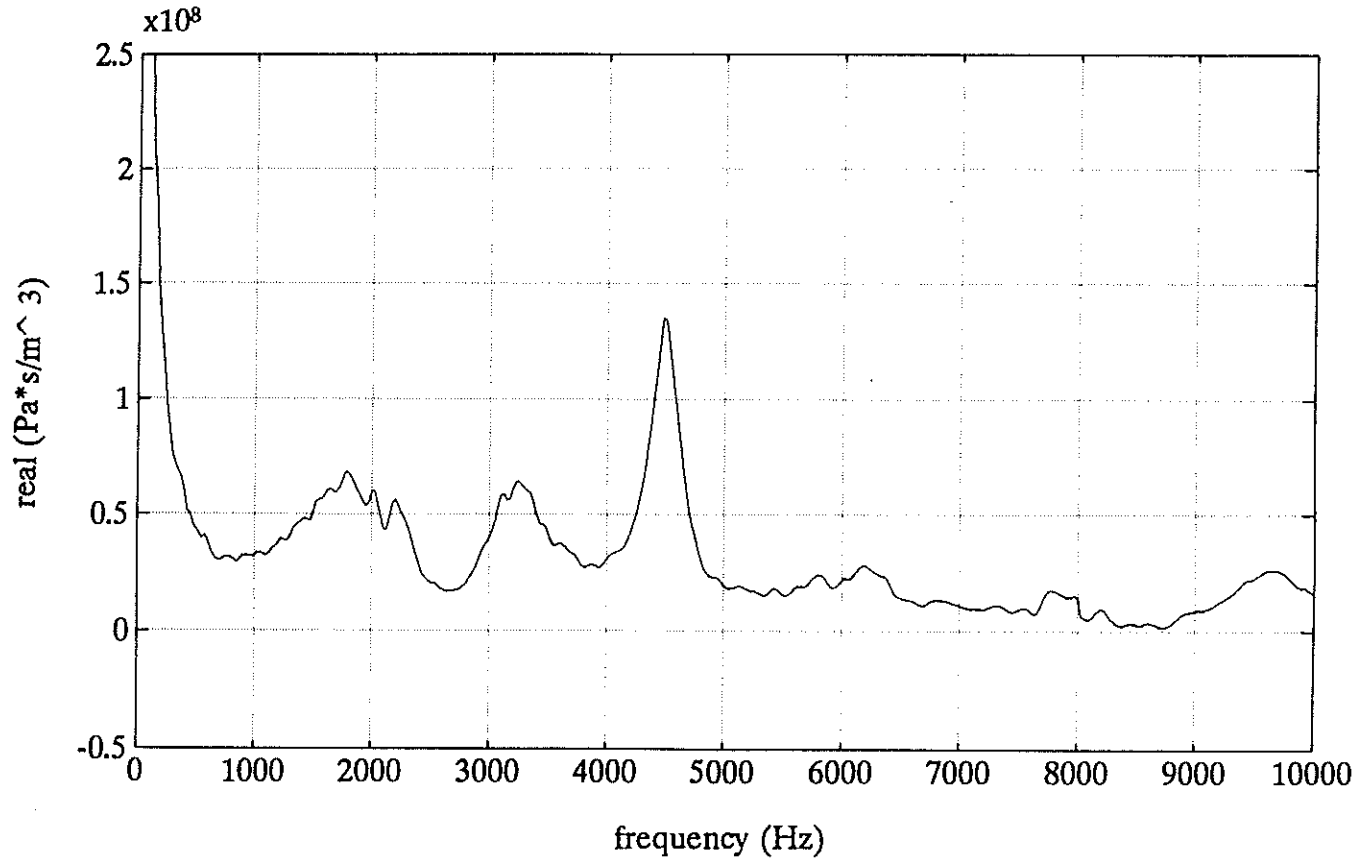

Figure 35a. Real part of hearing aid Thevenin impedance for the Philips M49 hearing aid.

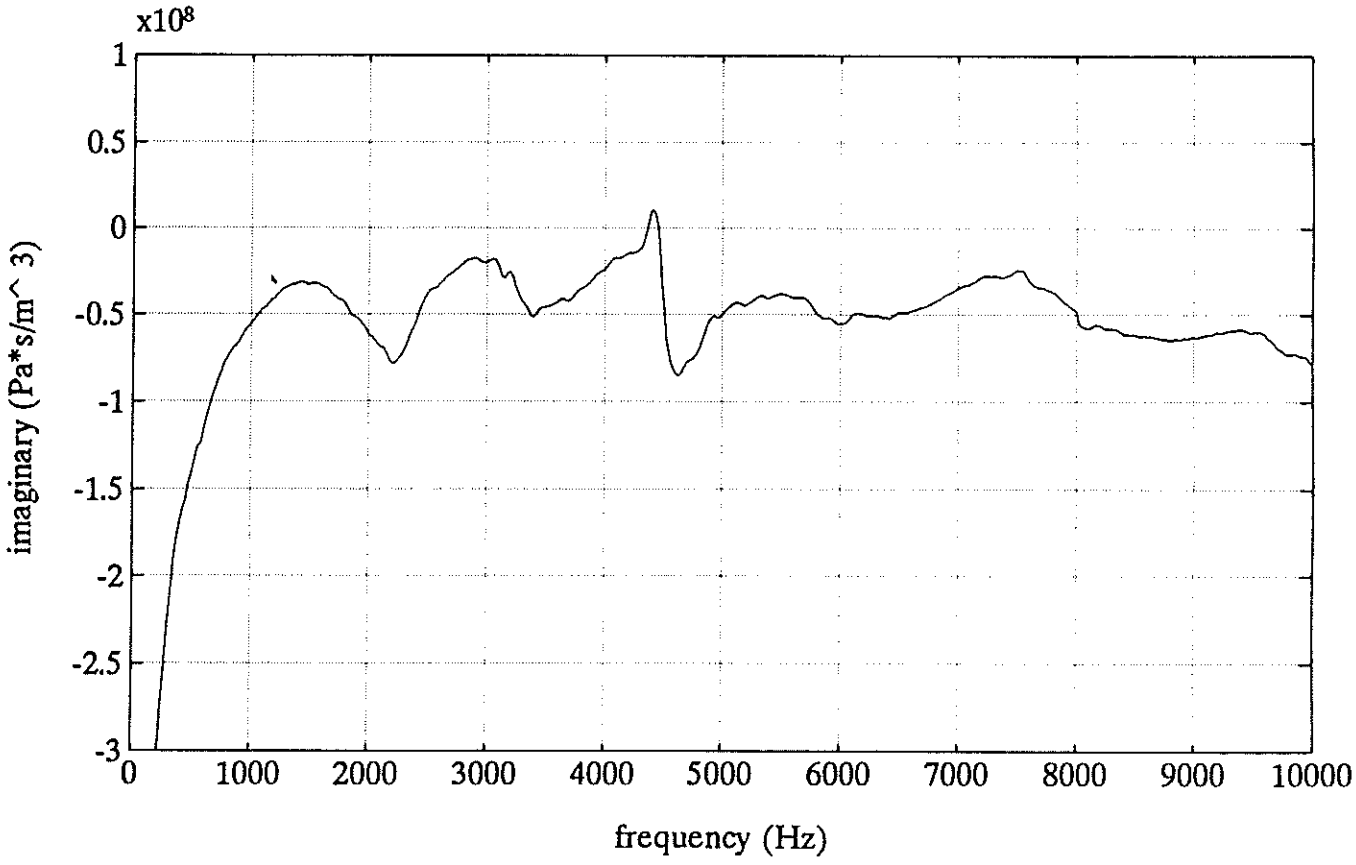

Figure 35b. Imaginary part of hearing aid Thevenin impedance for the Philips M49 hearing aid.

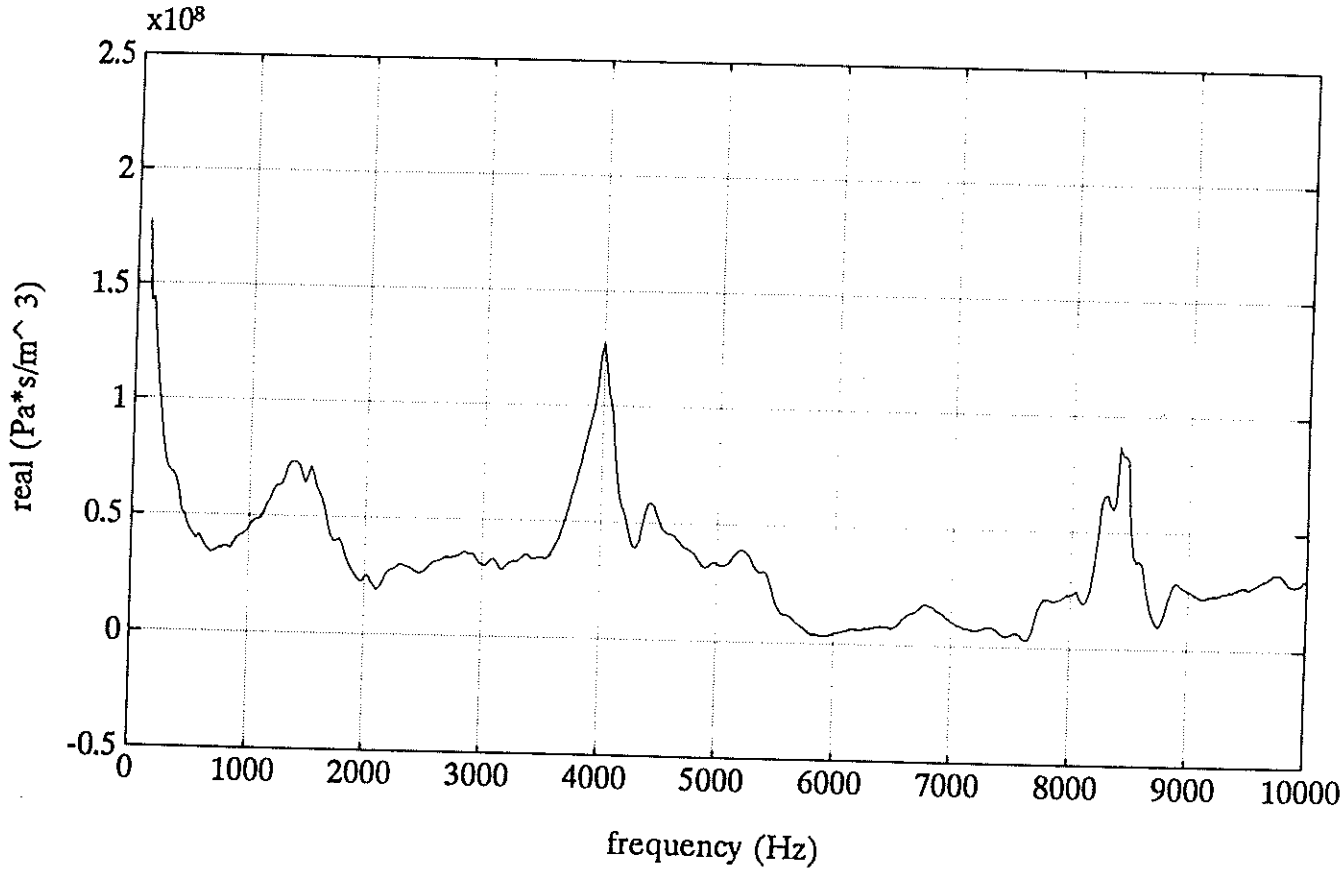

Figure 36a. Real part of hearing aid Thevenin impedance for the Phonak Pico SC hearing aid.

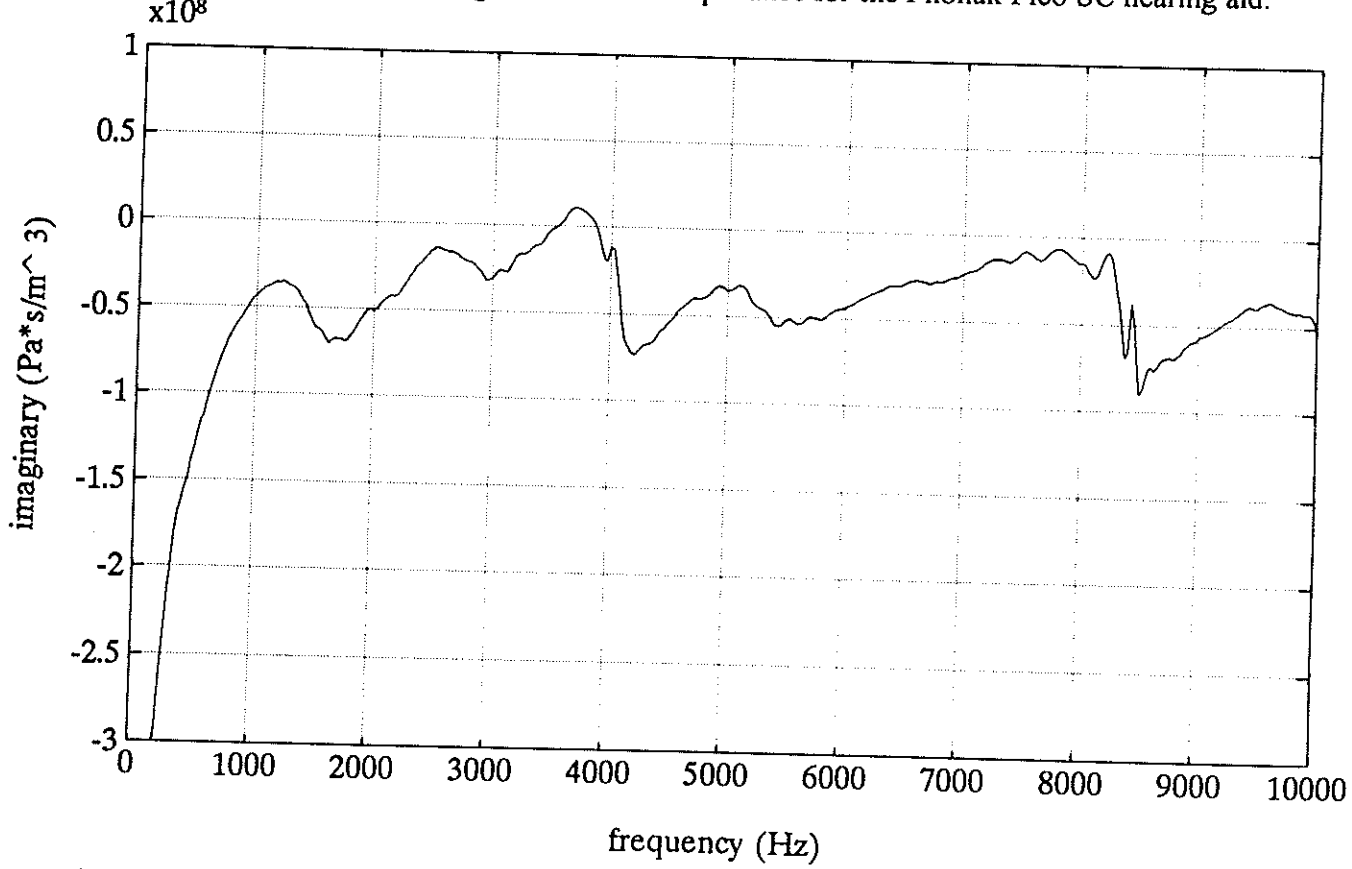

Figure 36b. Imaginary part of hearing aid Thevenin impedance for the Phonak Pico SC hearing aid.

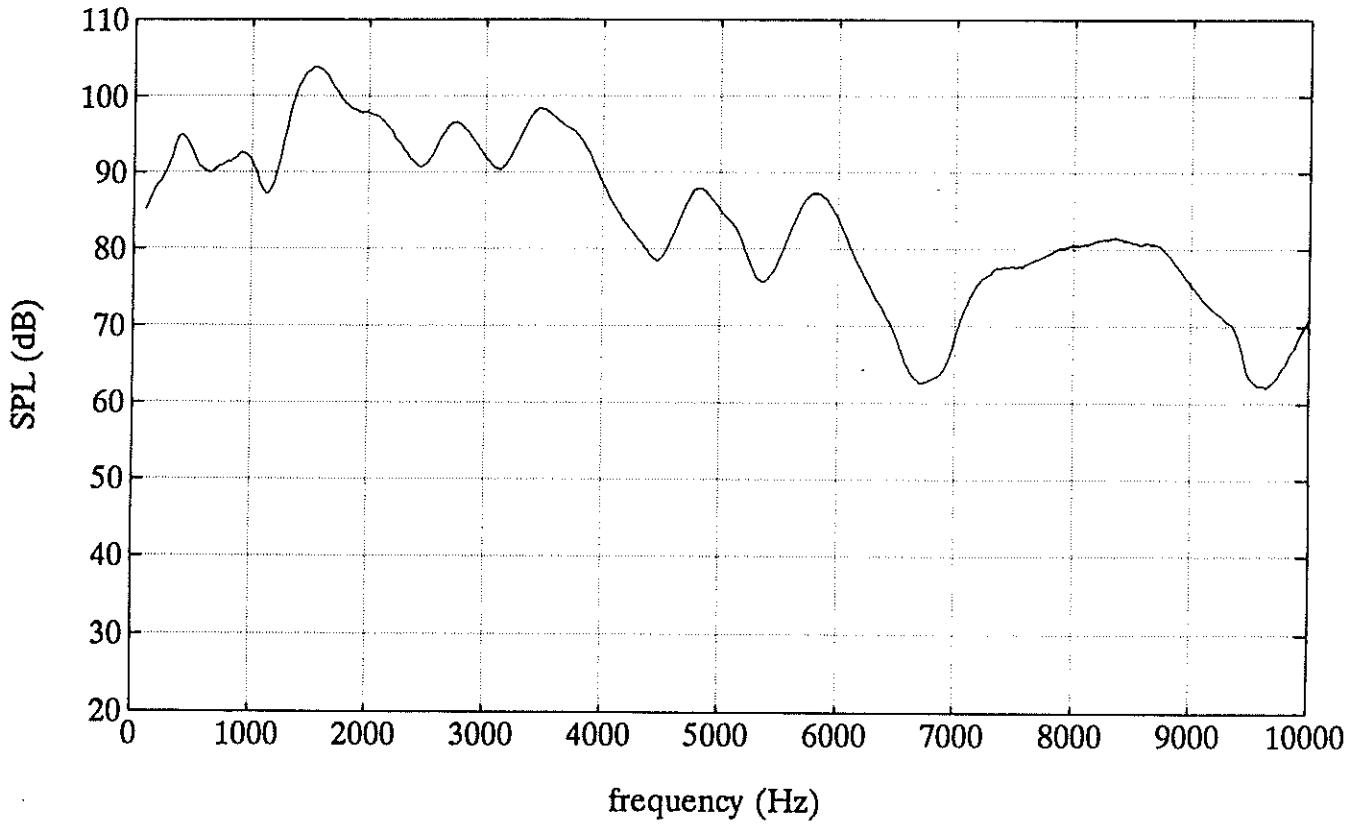

Figure 37a. Example of sound pressure level from measurement of hearing aid Thevenin impedance on Widex ES1.

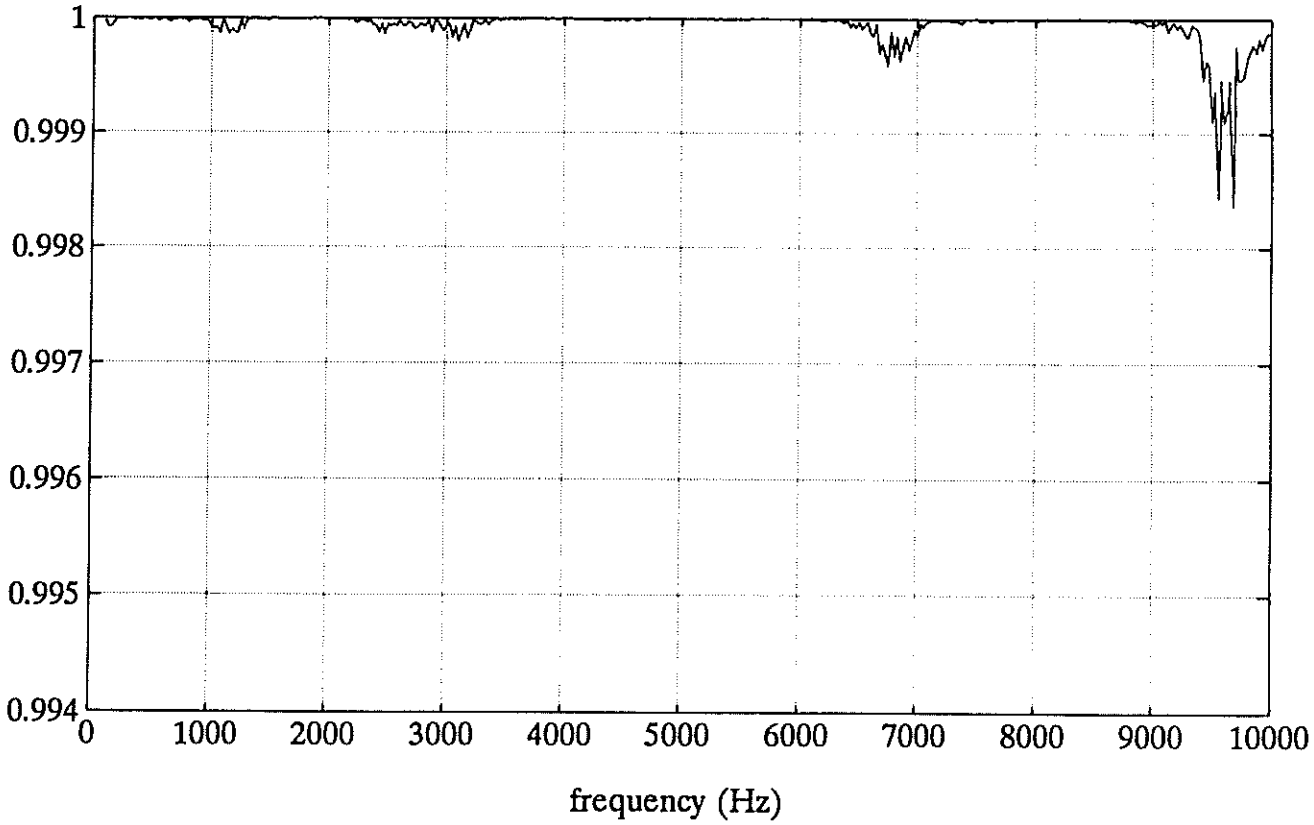

Figure 37b. Example of coherence function from measurement of hearing aid Thevenin impedance on Widex ES1.

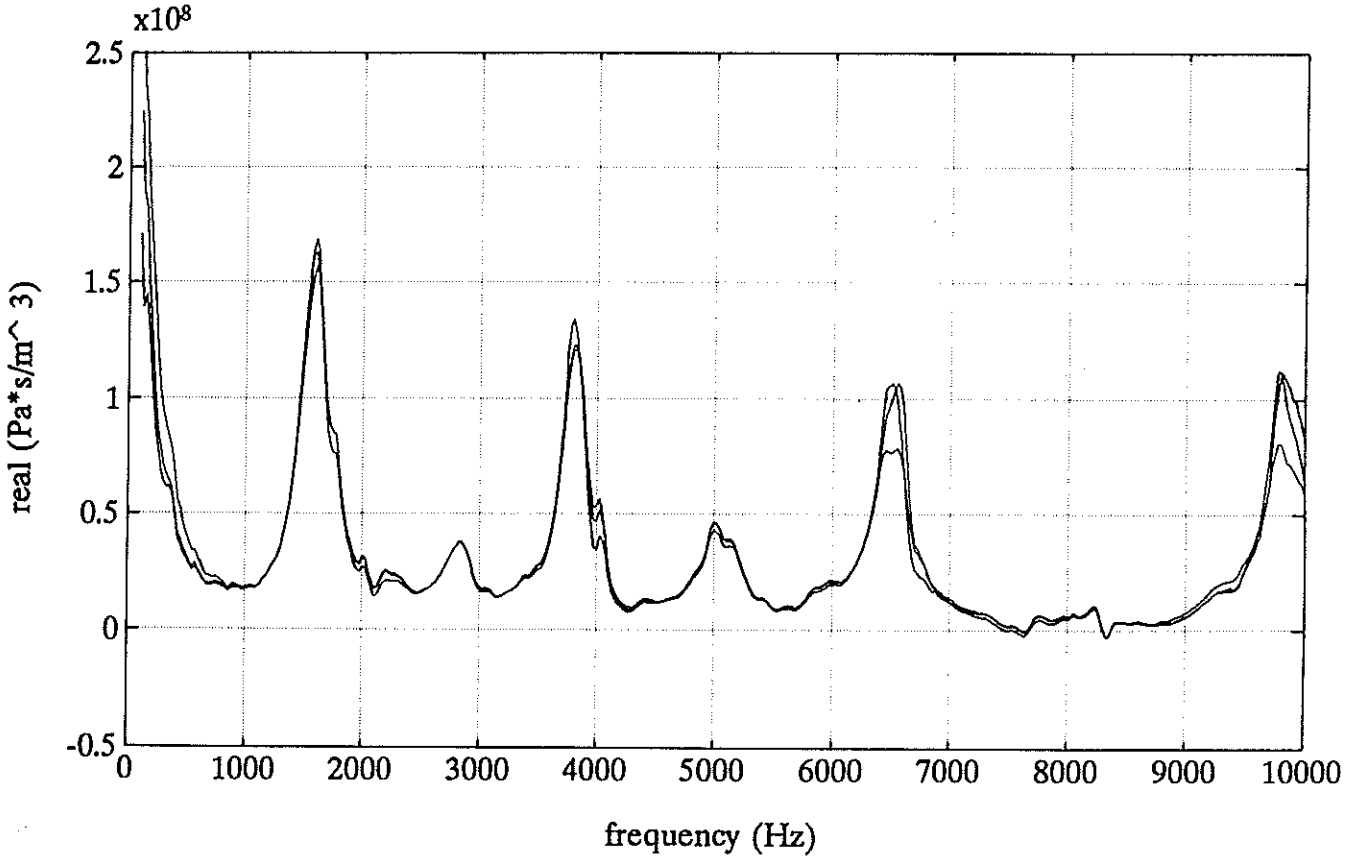

Figure 38a. Example of reproducibility in measurements of hearing aid Thevenin impedance on Widex ES1, real part.

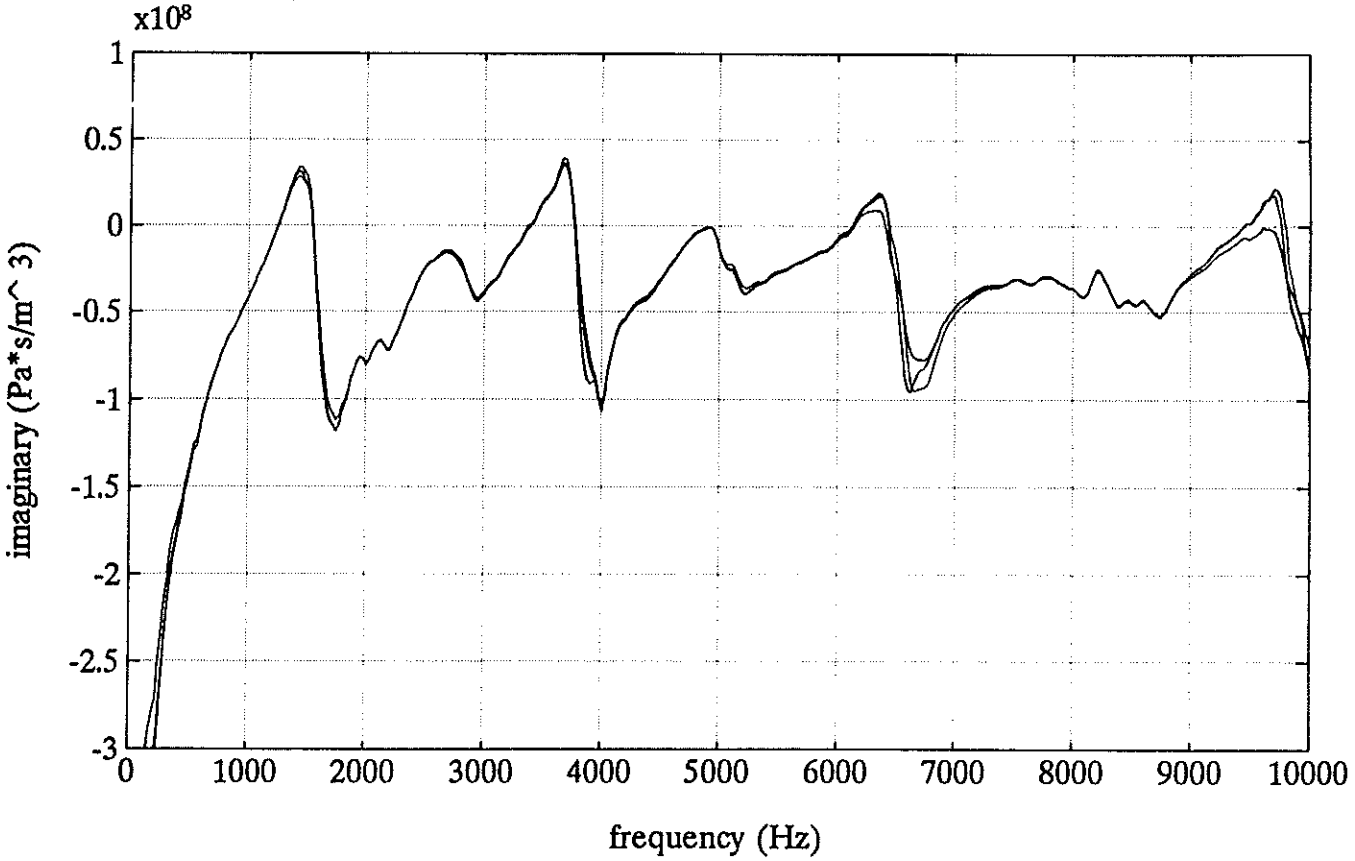

Figure 38b. Example of reproducibility in measurements of hearing aid Thevenin impedance on Widex ES1, imaginary part.

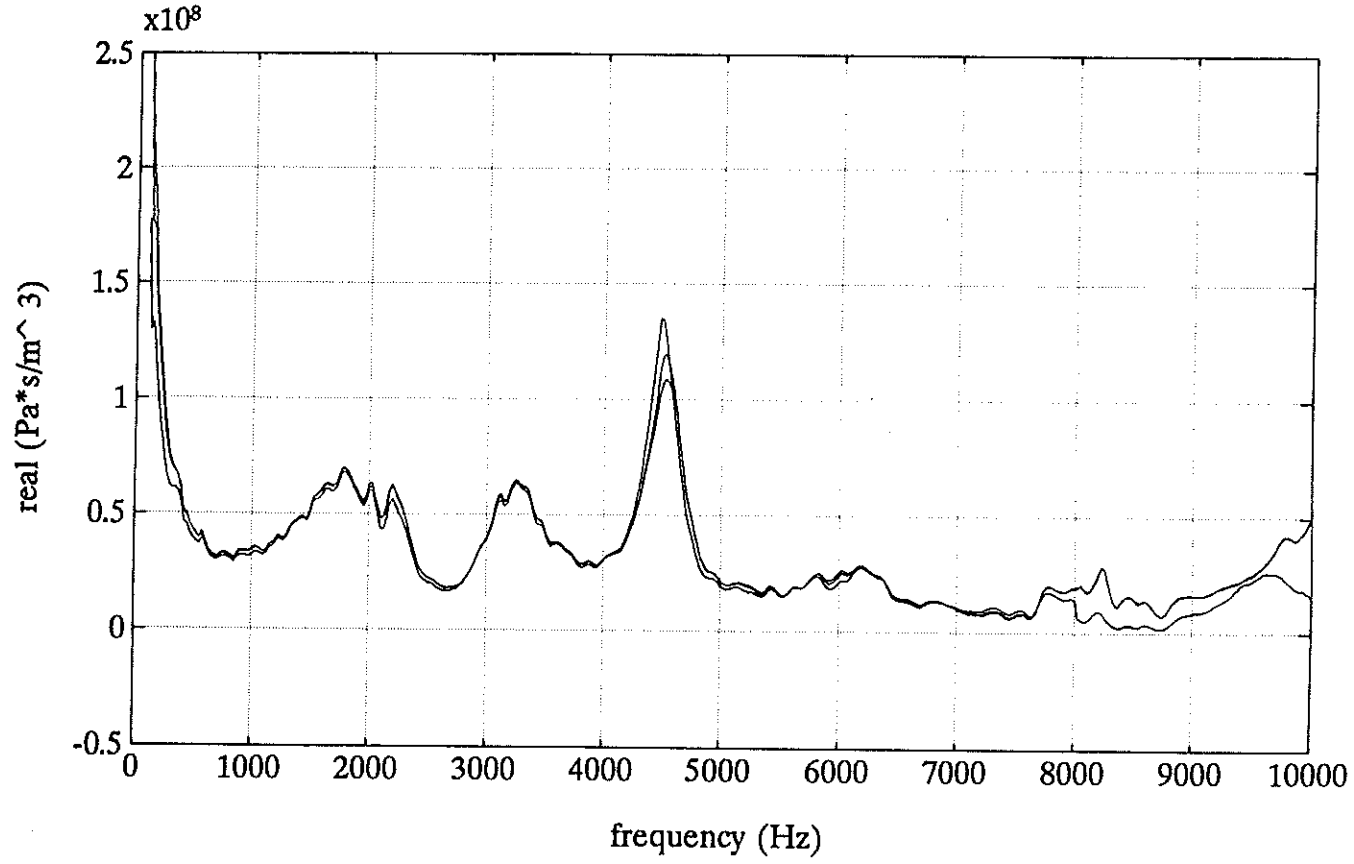

Figure 39a. Example of reproducibility in measurements of hearing aid Thevenin impedance on Philips M49, real part.

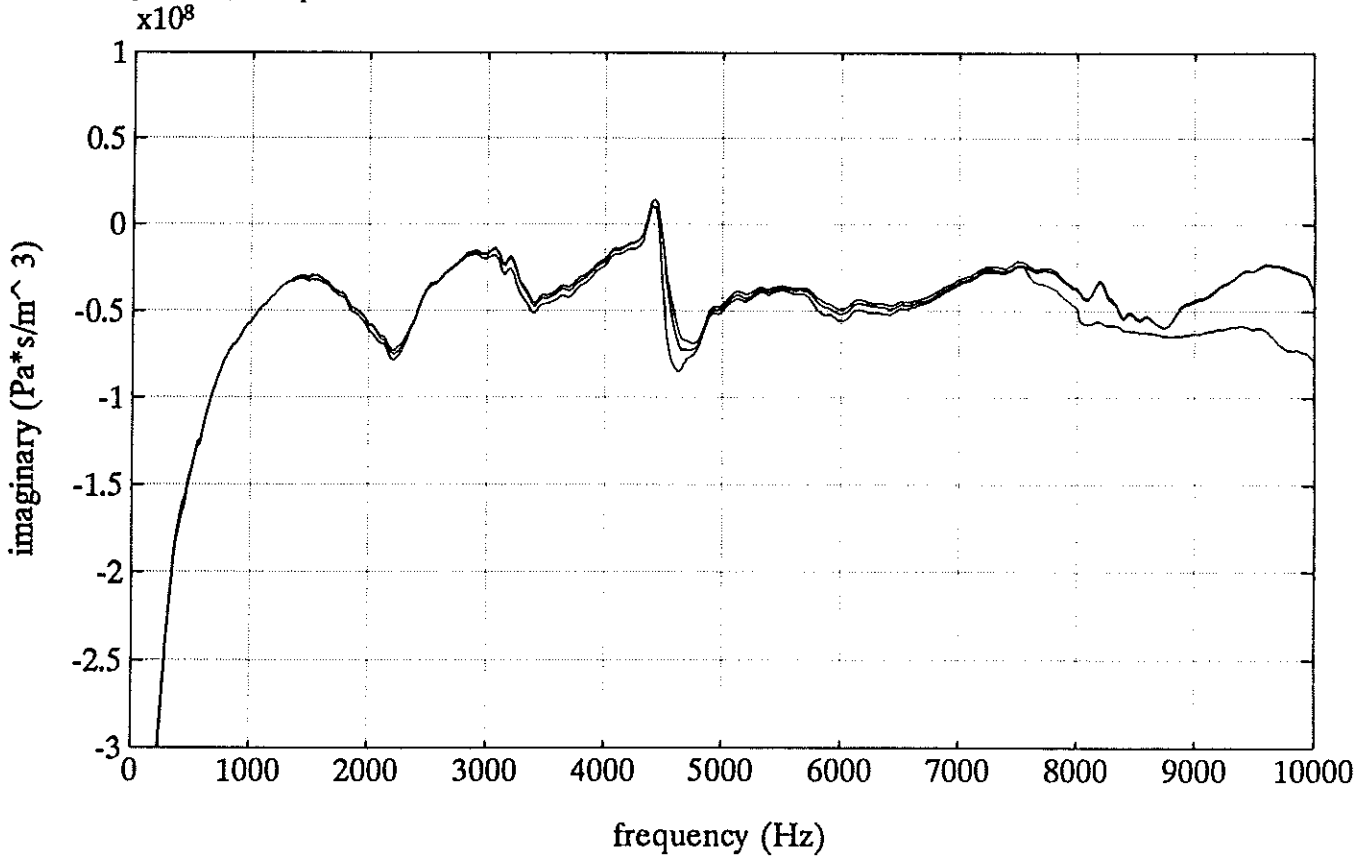

Figure 39b. Example of reproducibility in measurements of hearing aid Thevenin impedance on Philips M49, imaginary part.

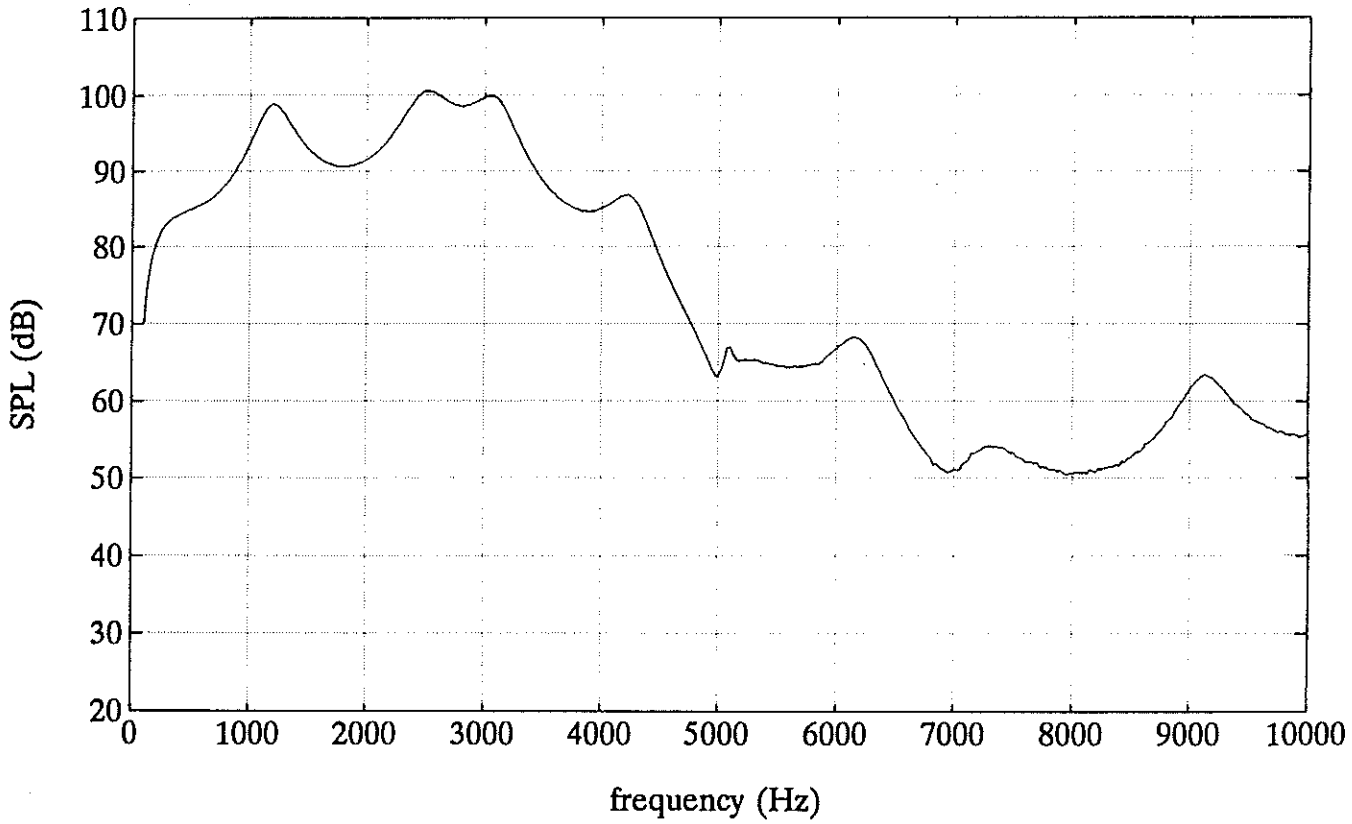

Figure 40a. Example of sound pressure level from measurement of hearing aid Thevenin pressure transfer function on Widex ES1.

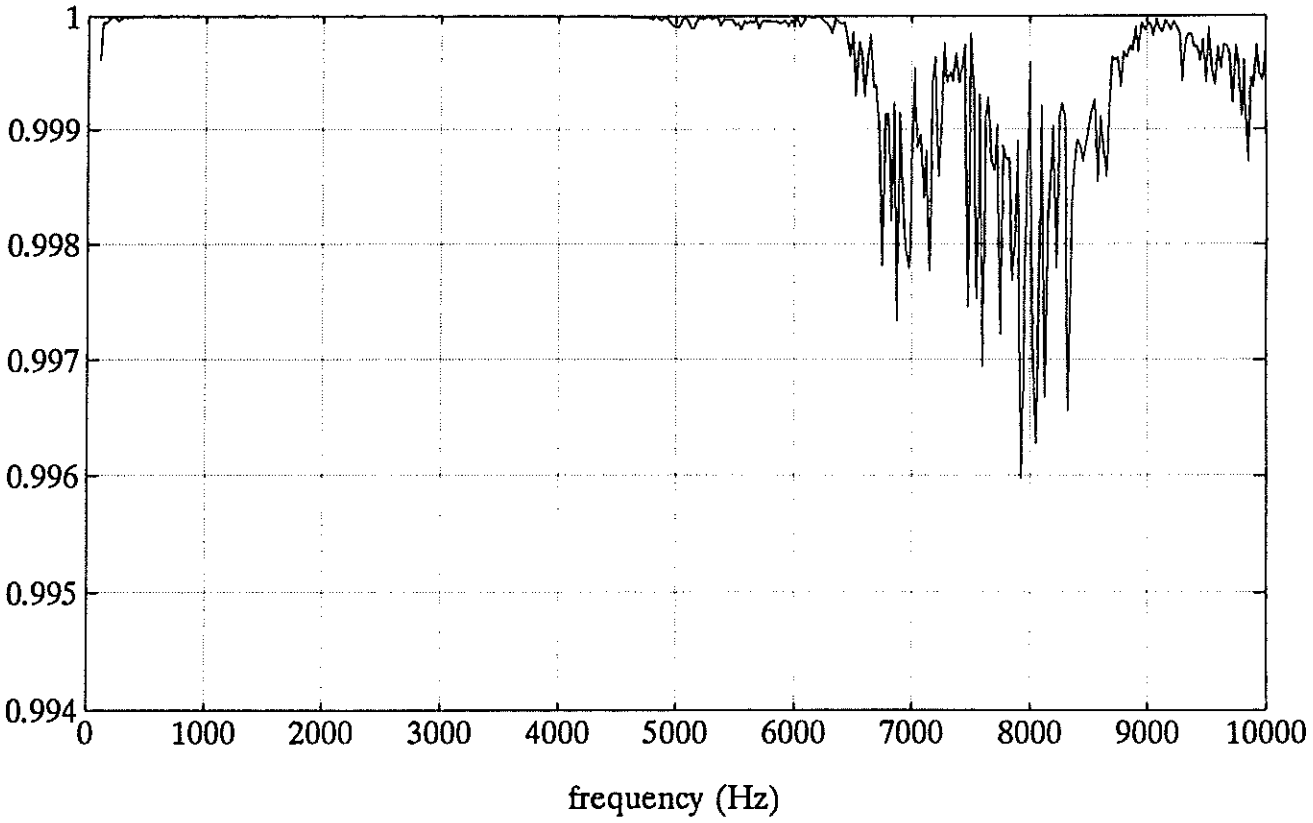

Figure 40b. Example of coherence function from measurement of hearing aid Thevenin pressure transfer function on Widex ES1.

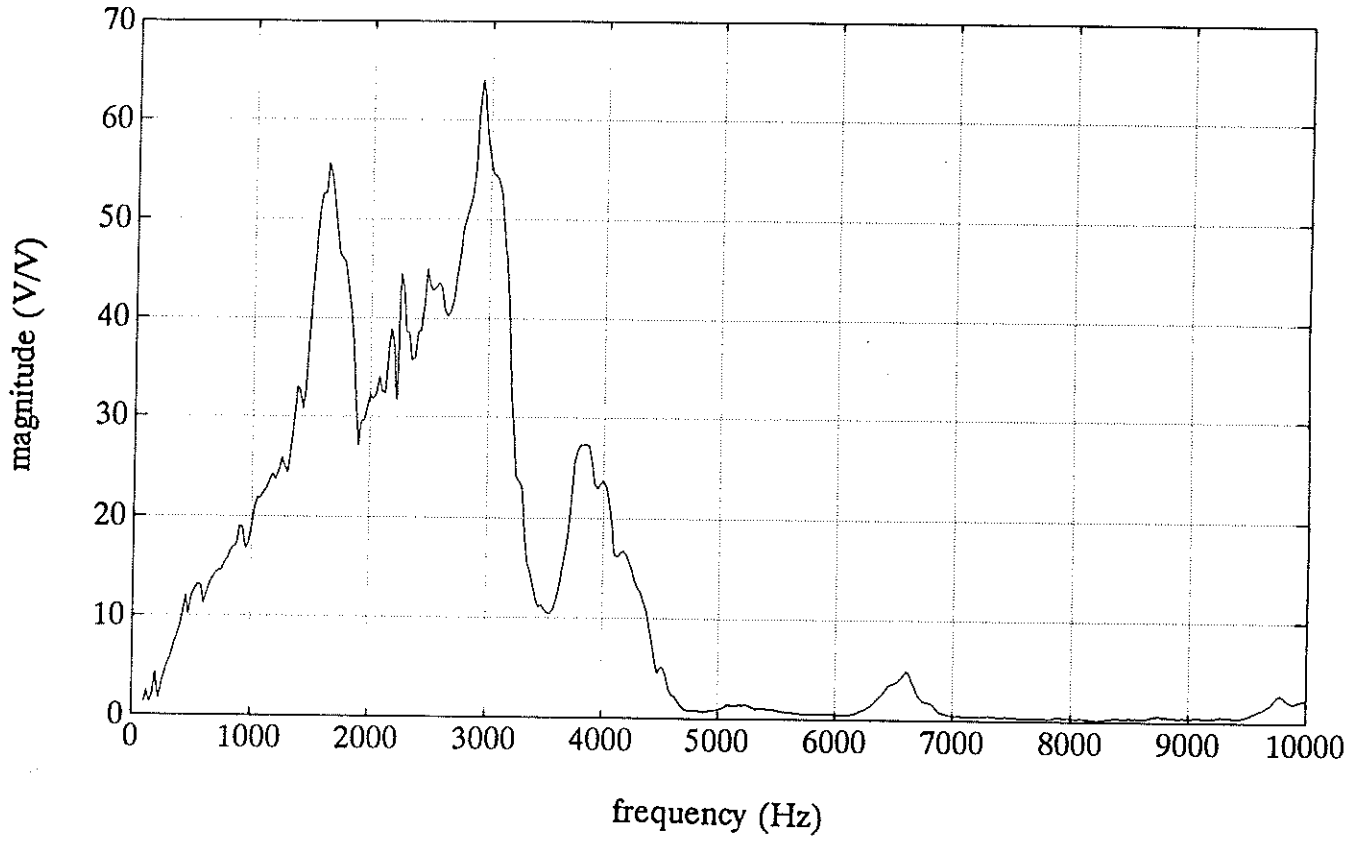

Figure 41a. Magnitude of hearing aid Thevenin pressure transfer function for Widex ES1.

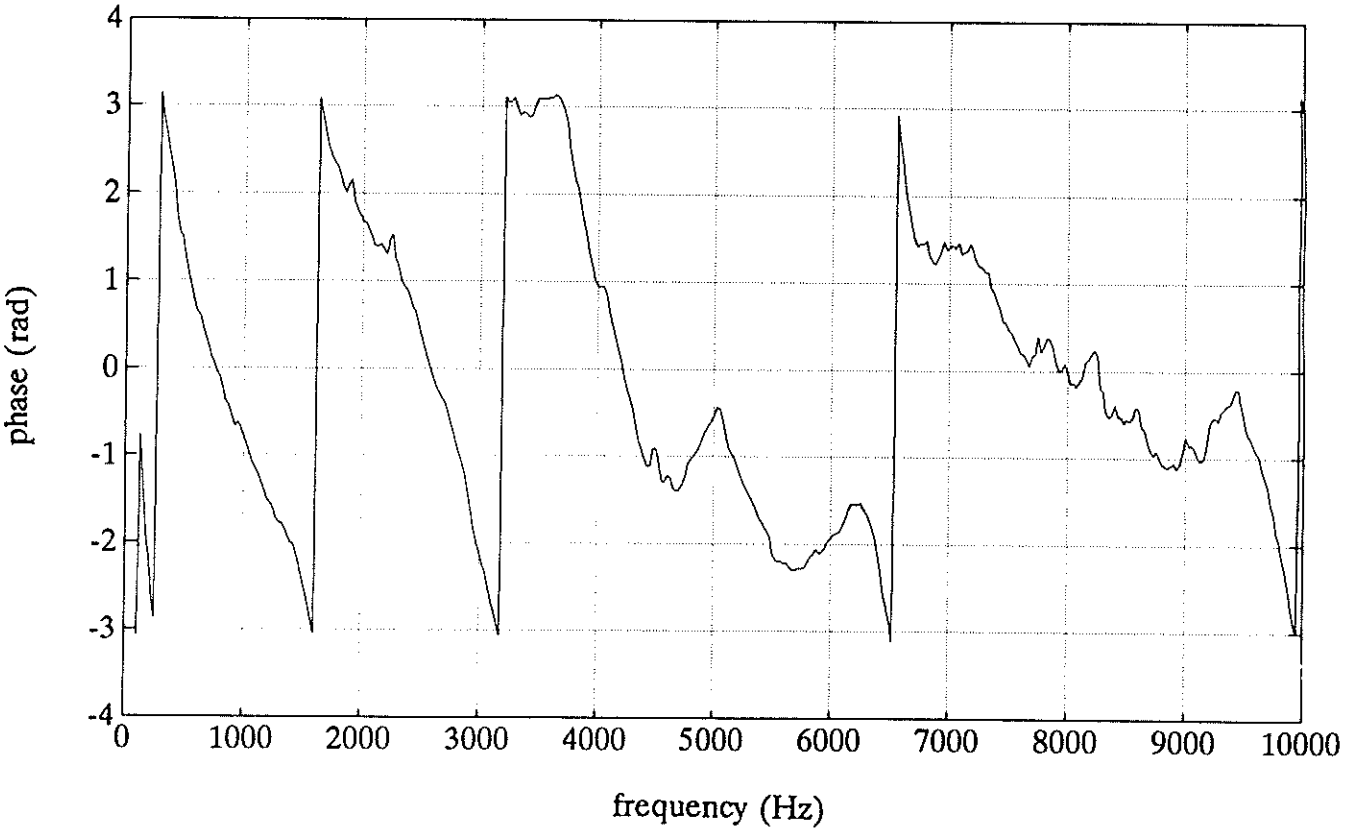

Figure 41b. Phase of hearing aid Thevenin pressure transfer function for Widex ES1.

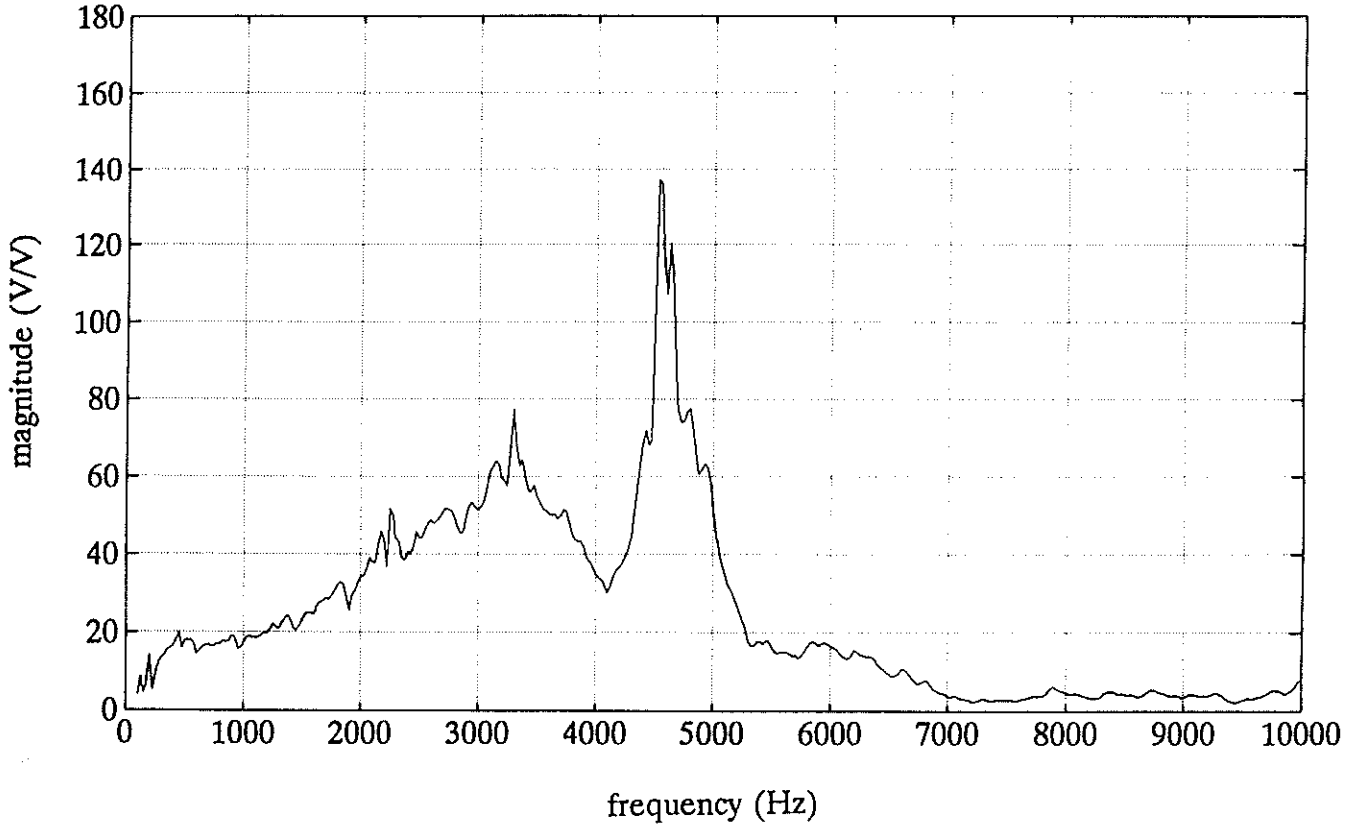

Figure 42a. Magnitude of hearing aid Thevenin pressure transfer function for Philips M49.

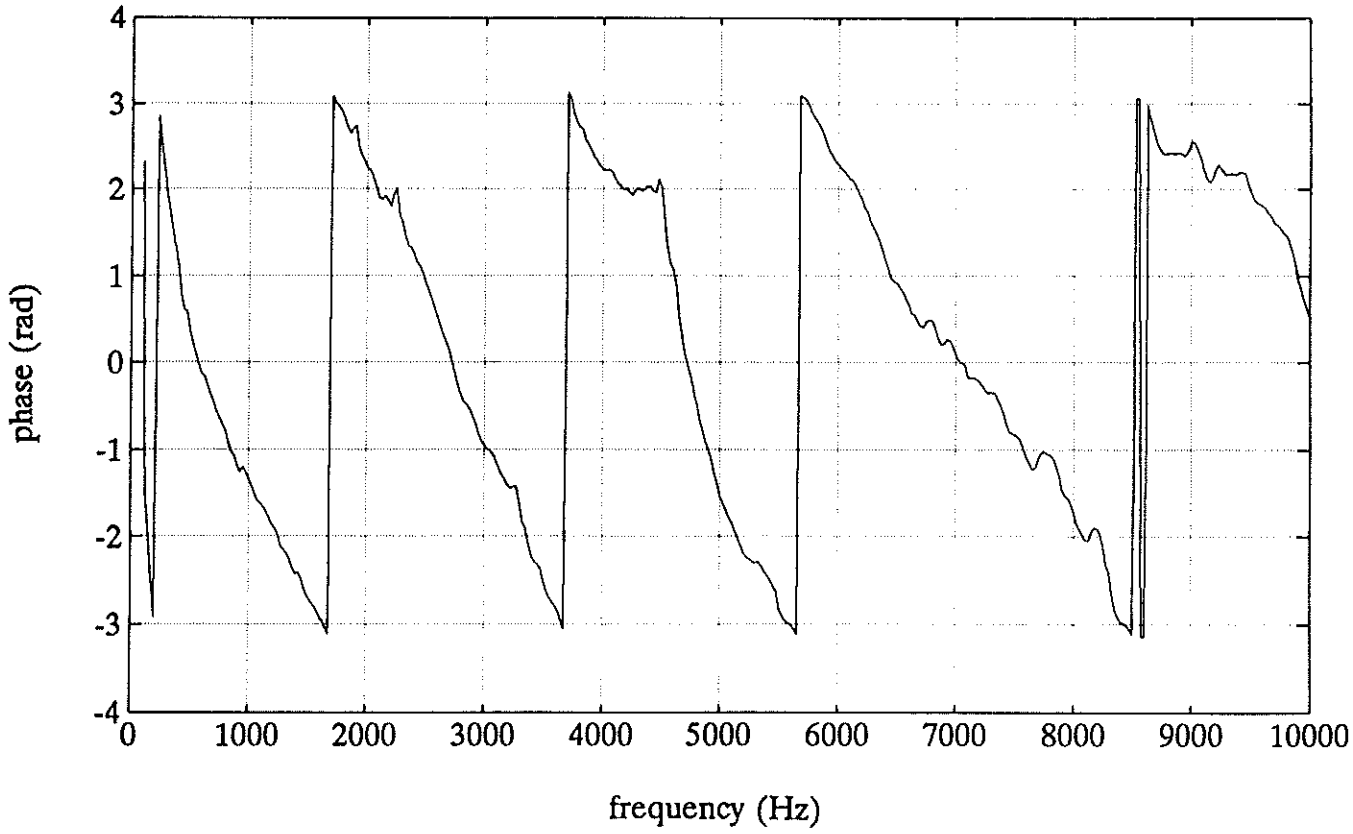

Figure 42b. Phase of hearing aid Thevenin pressure transfer function for Philips M49.

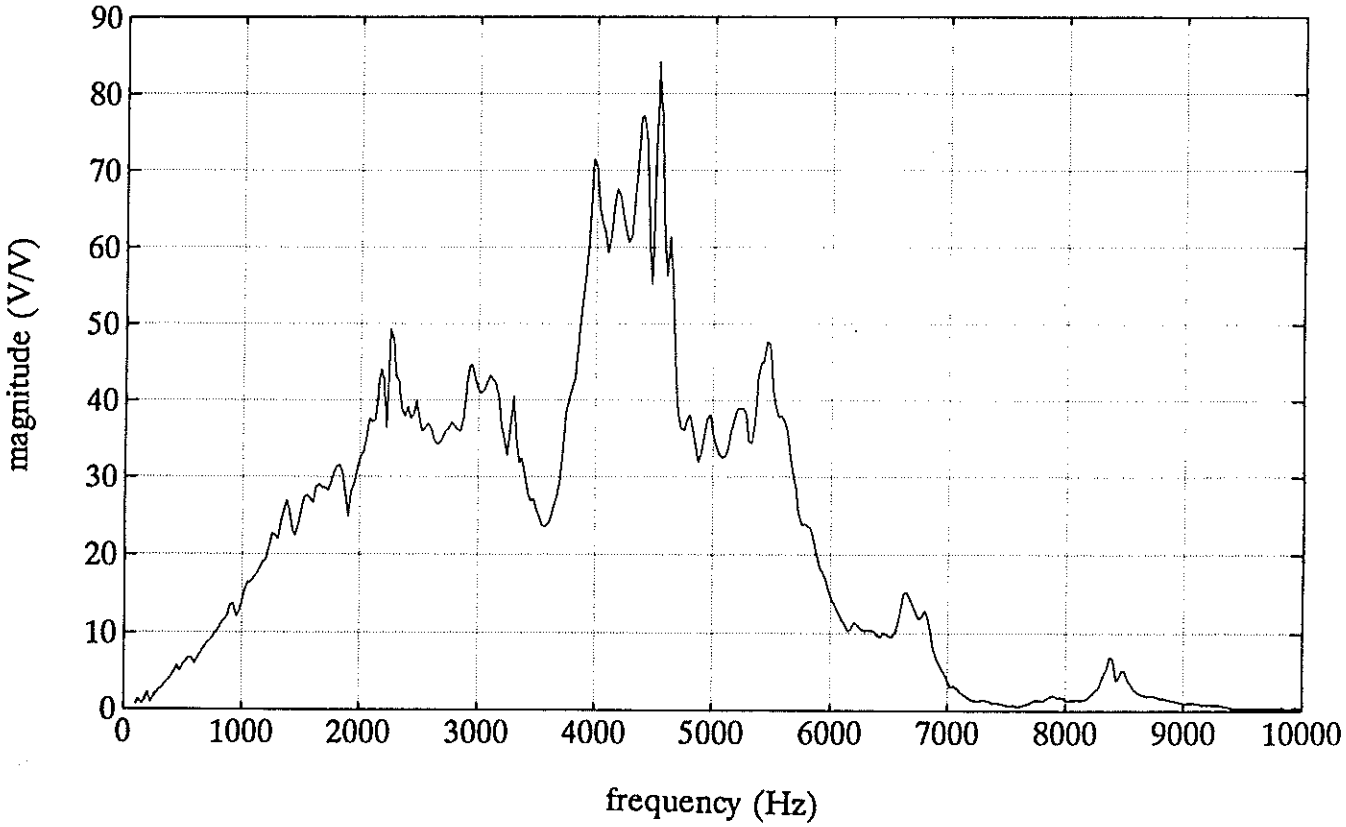

Figure 43a. Magnitude of hearing aid Thevenin pressure transfer function for Phonak Pico SC.

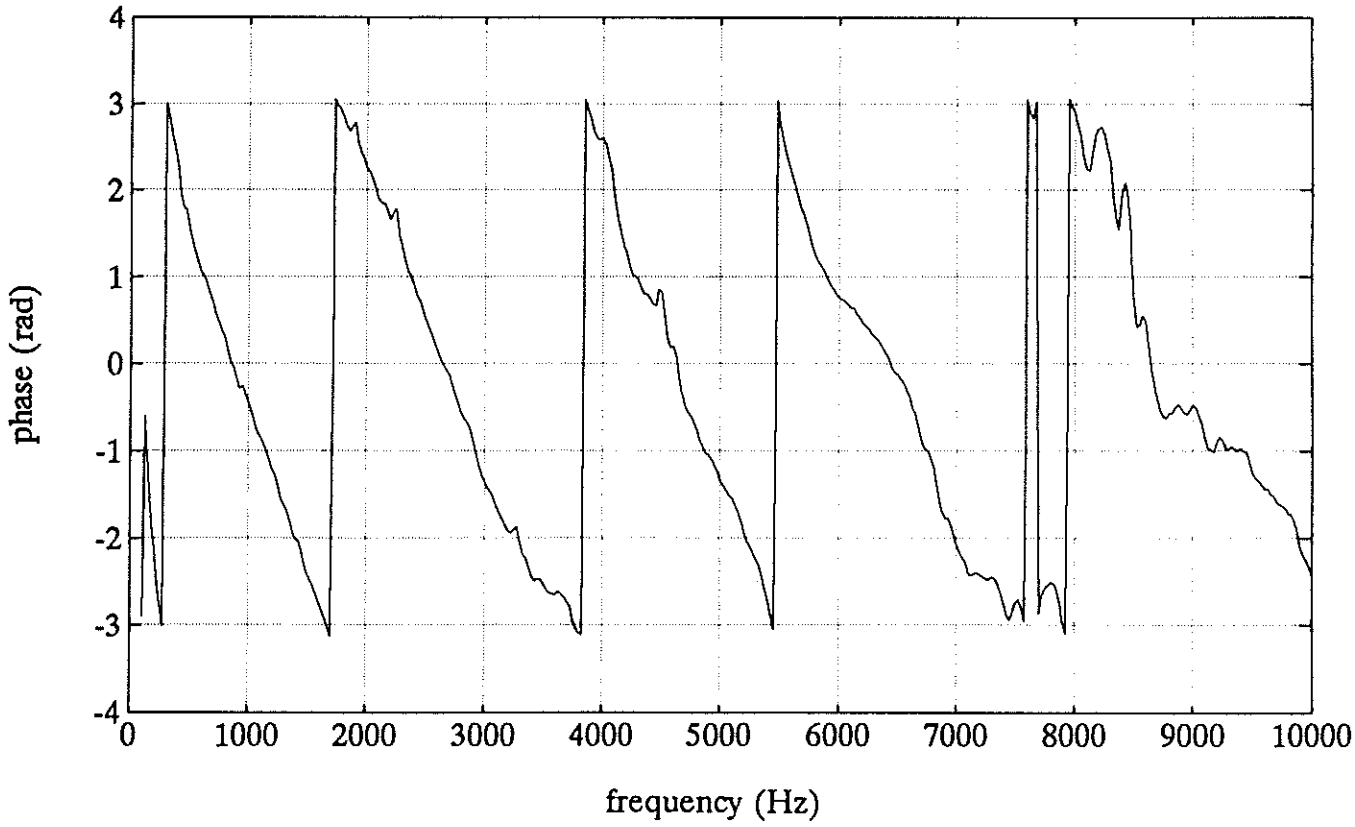

Figure 43b. Phase of hearing aid Thevenin pressure transfer function for Phonak Pico SC.

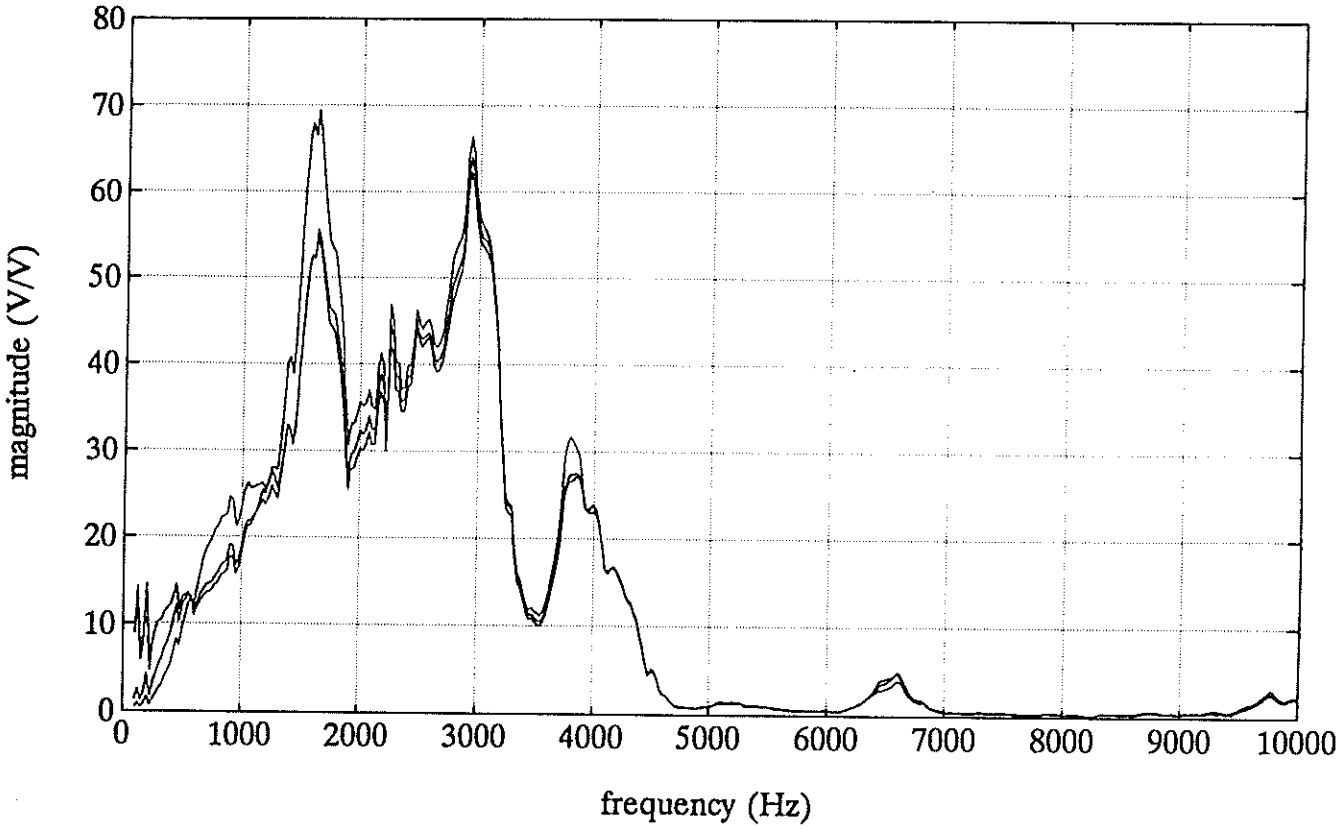

Figure 44a. Example of reproducibility in measurements of hearing aid Thevenin pressure transfer function on Widex ES1, magnitude.

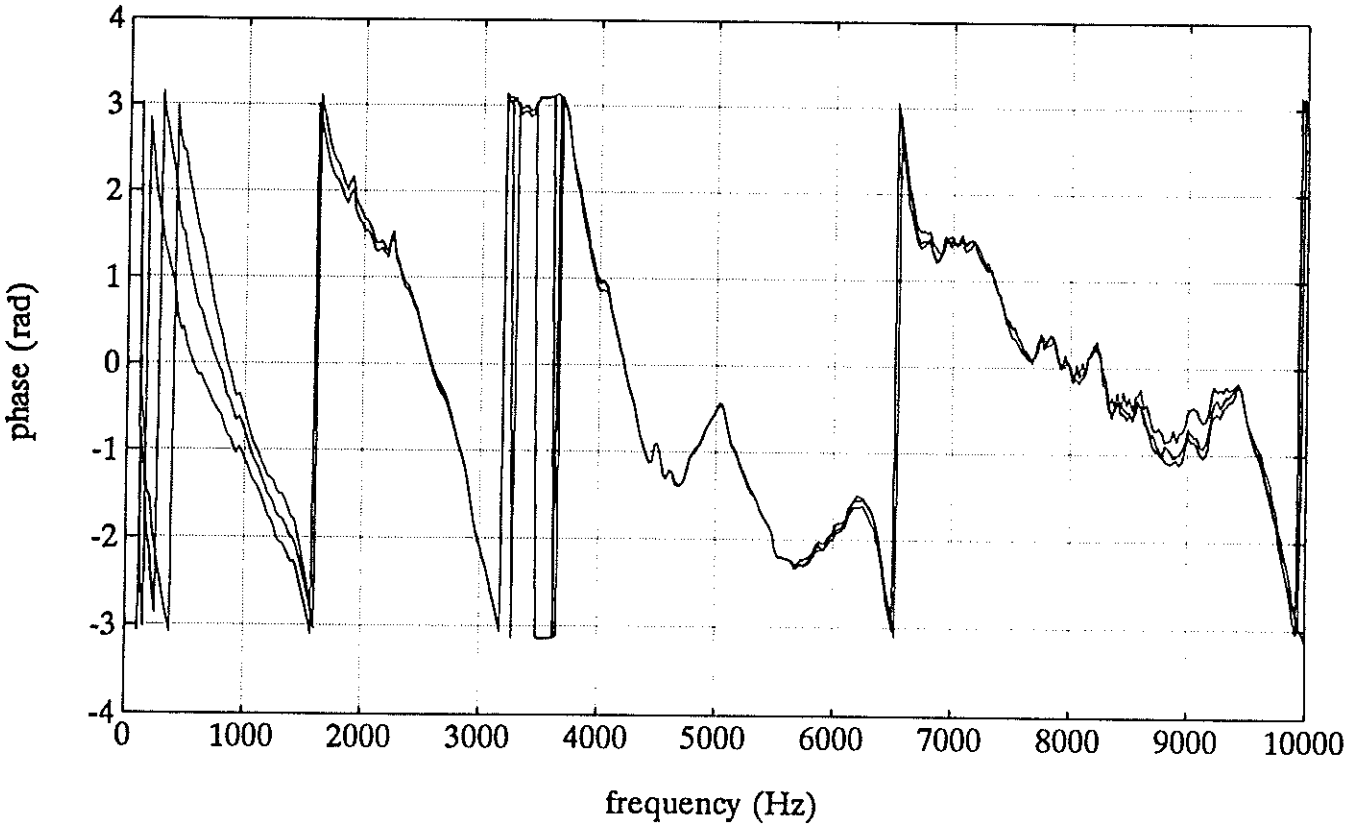

Figure 44b. Example of reproducibility in measurements of hearing aid Thevenin pressure transfer function on Widex ES1, phase.

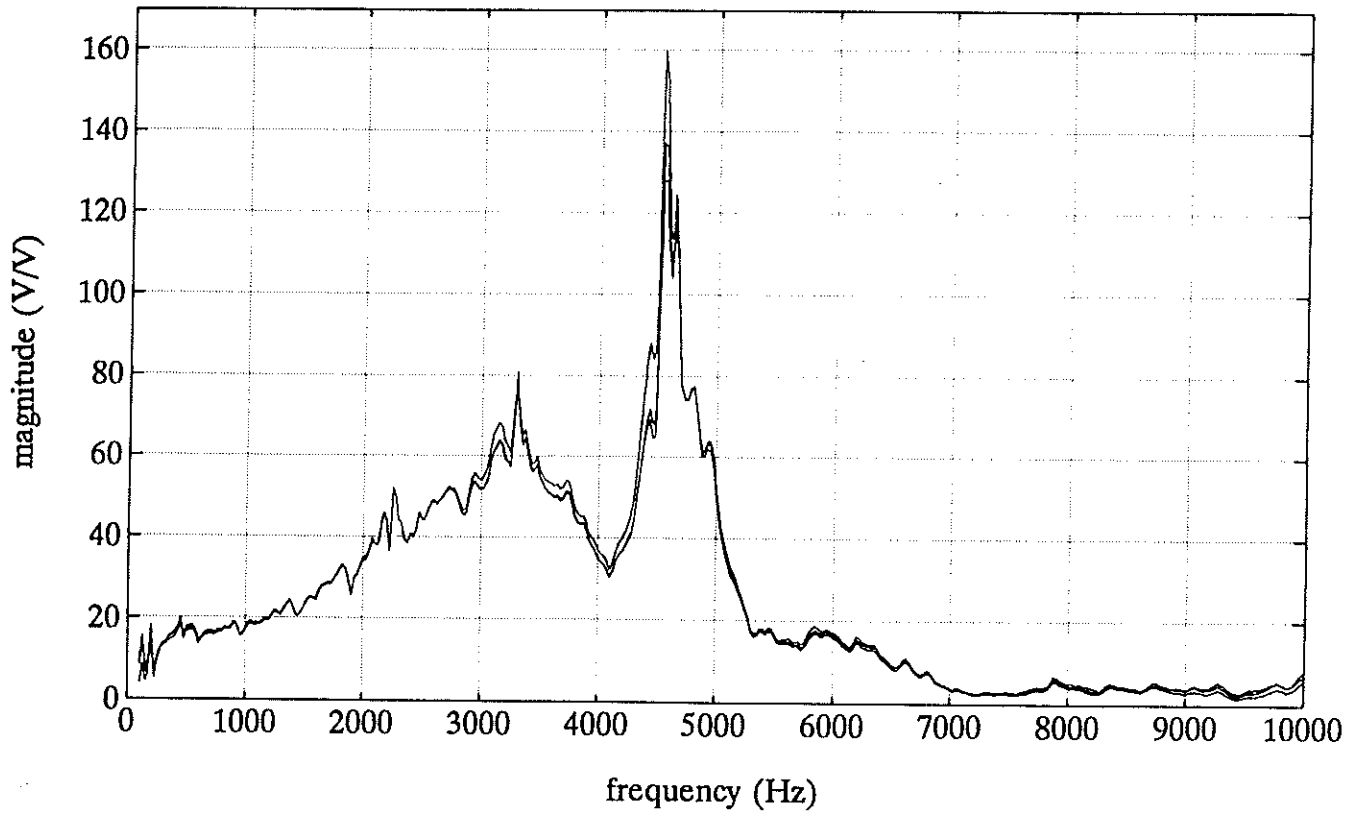

Figure 45a. Example of reproducibility in measurements of hearing aid Thevenin pressure transfer function on Philips M49, magnitude.

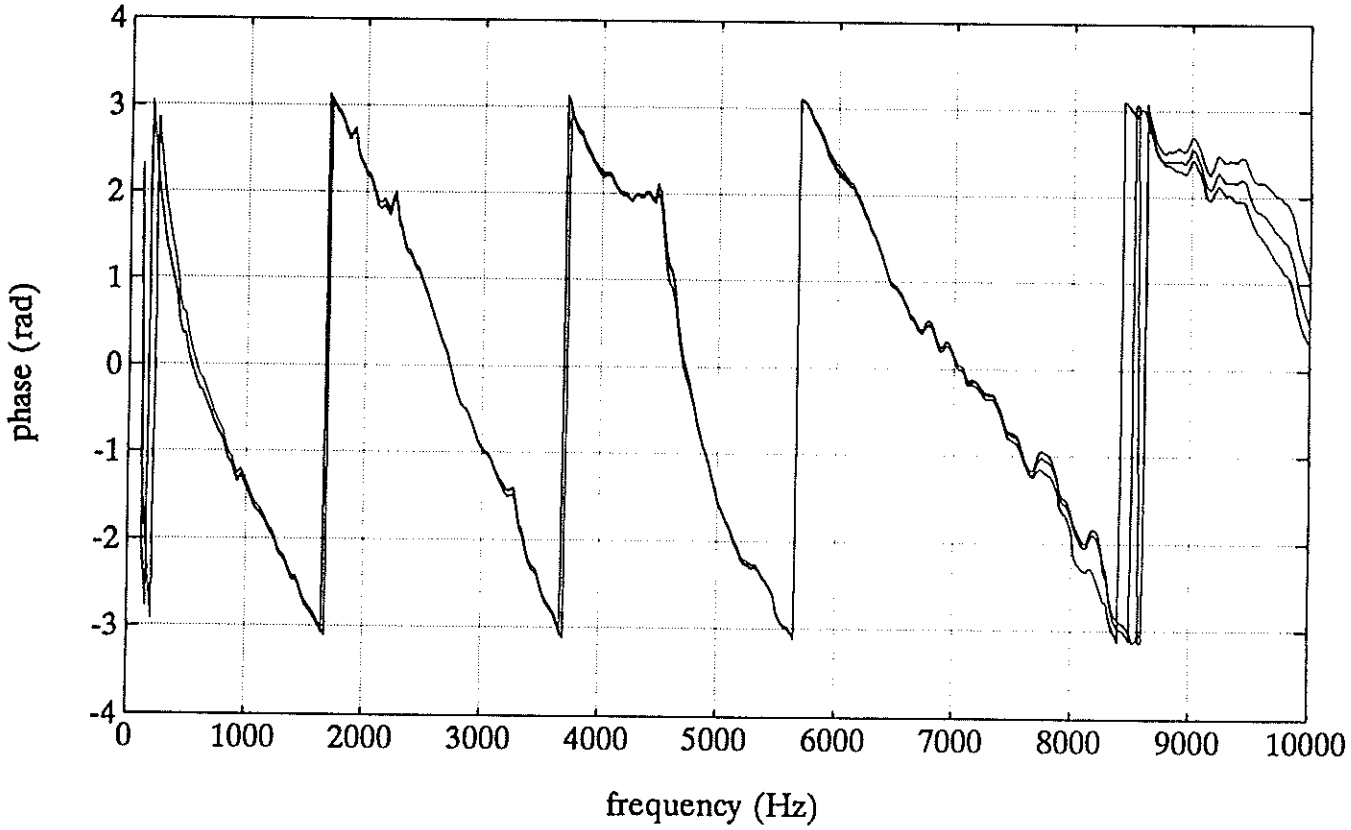

Figure 45b. Example of reproducibility in measurements of hearing aid Thevenin pressure transfer function on Philips M49, phase.

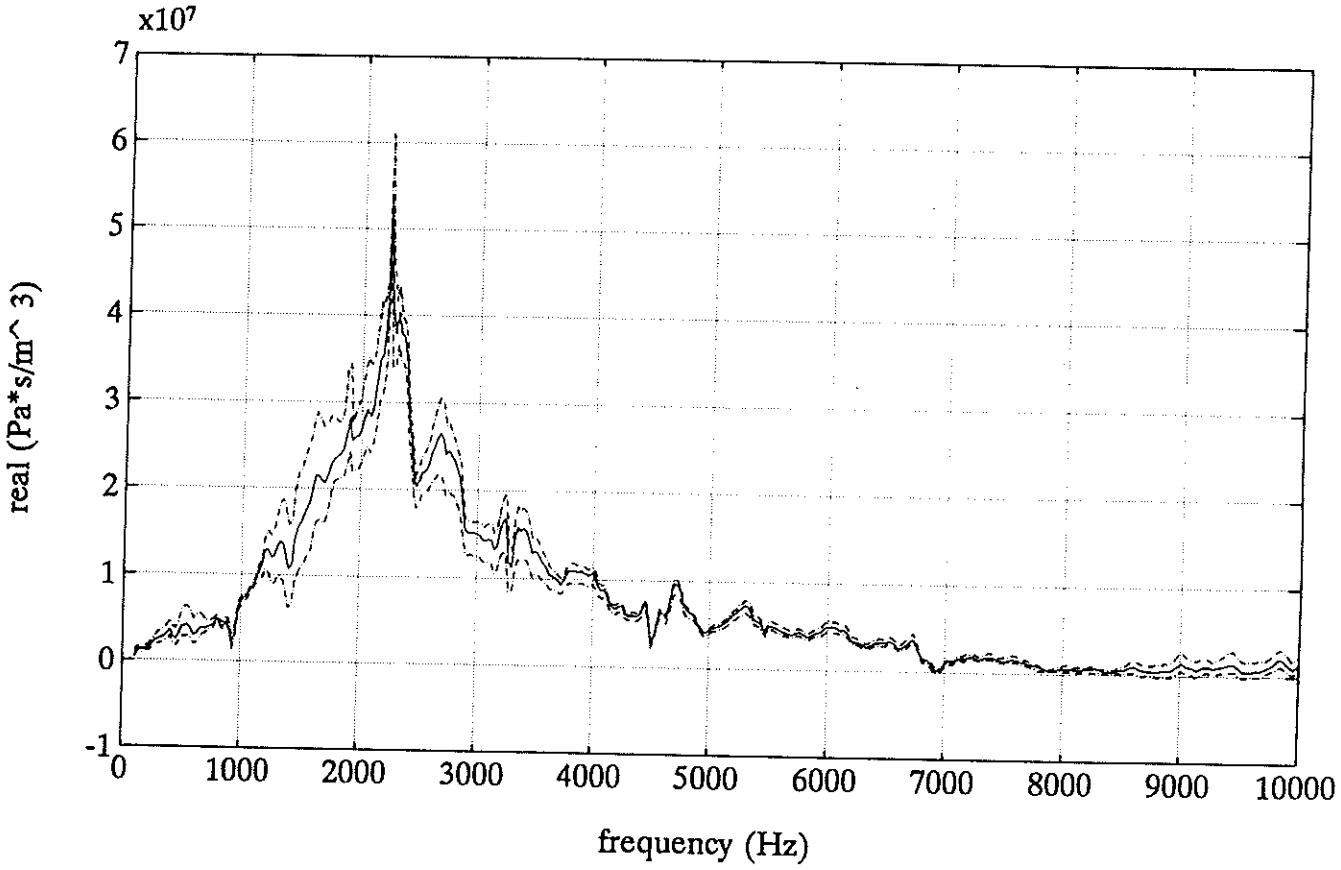

Figure 46a. Real part of ear input impedance at 100-105 dB(max), subject A.

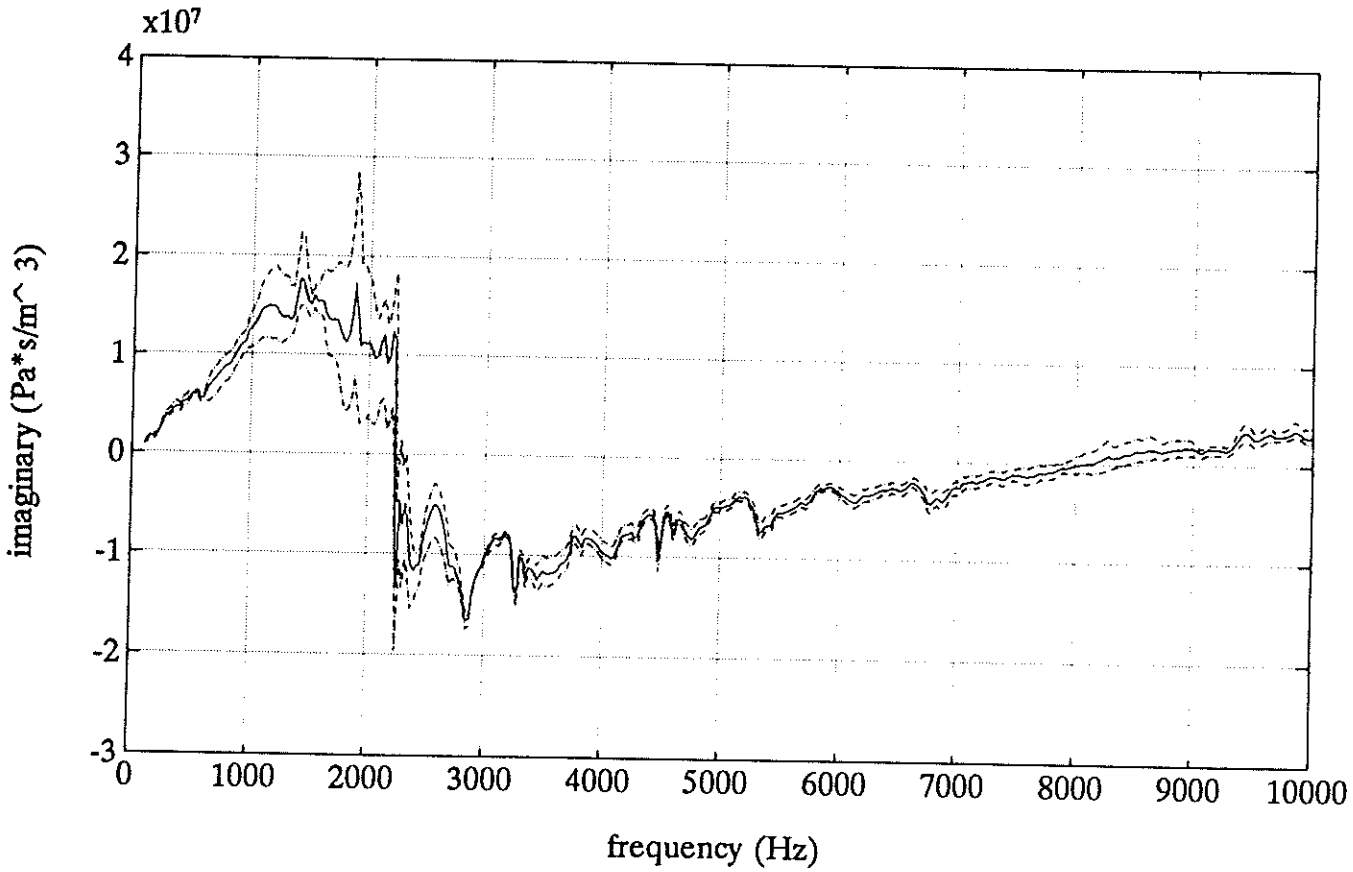

Figure 46b. Imaginary part of ear input impedance at 100-105 dB(max), subject A.

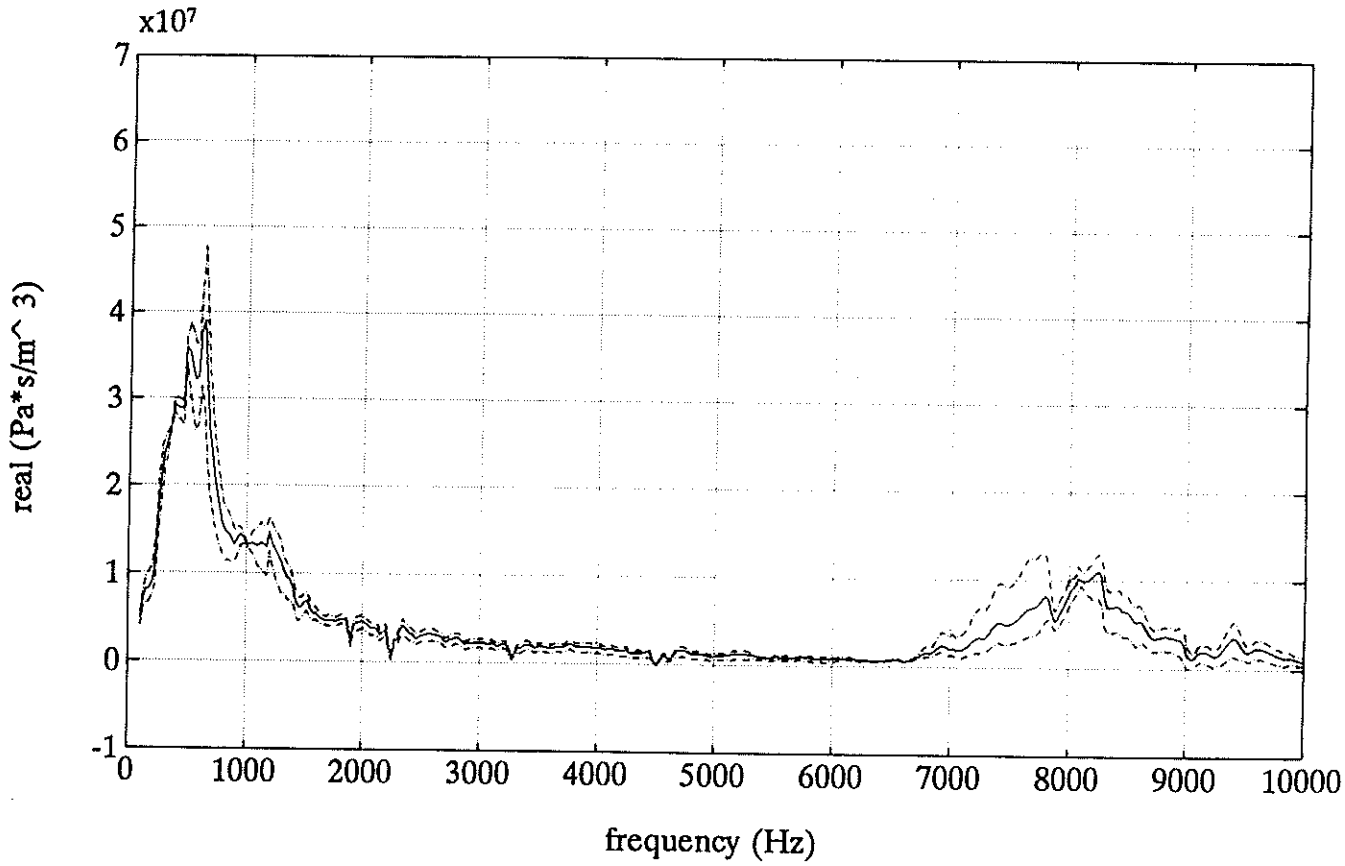

Figure 47a. Real part of ear input impedance at 100-105 dB(max), subject B.

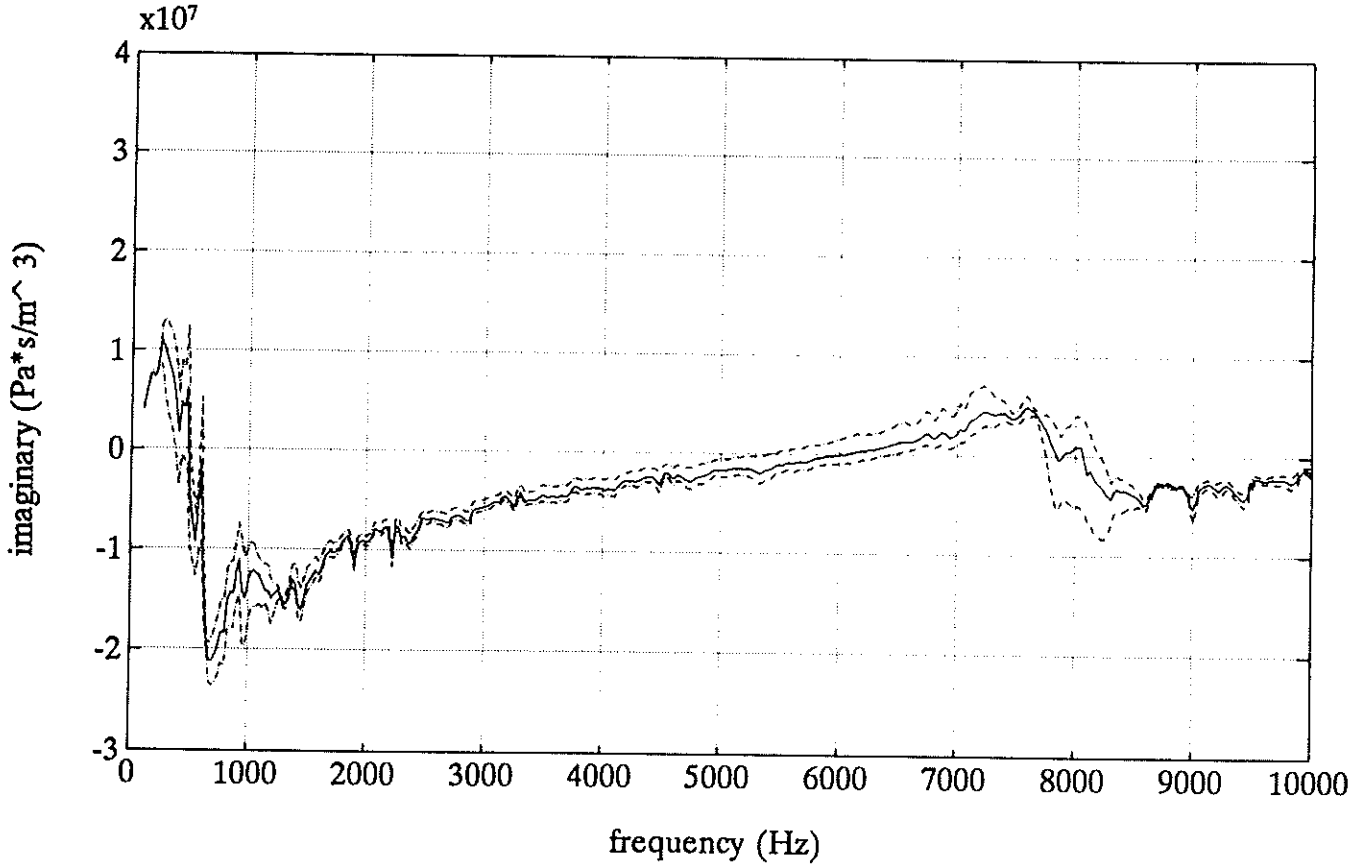

Figure 47b. Imaginary part of ear input impedance at 100-105 dB(max), subject B.

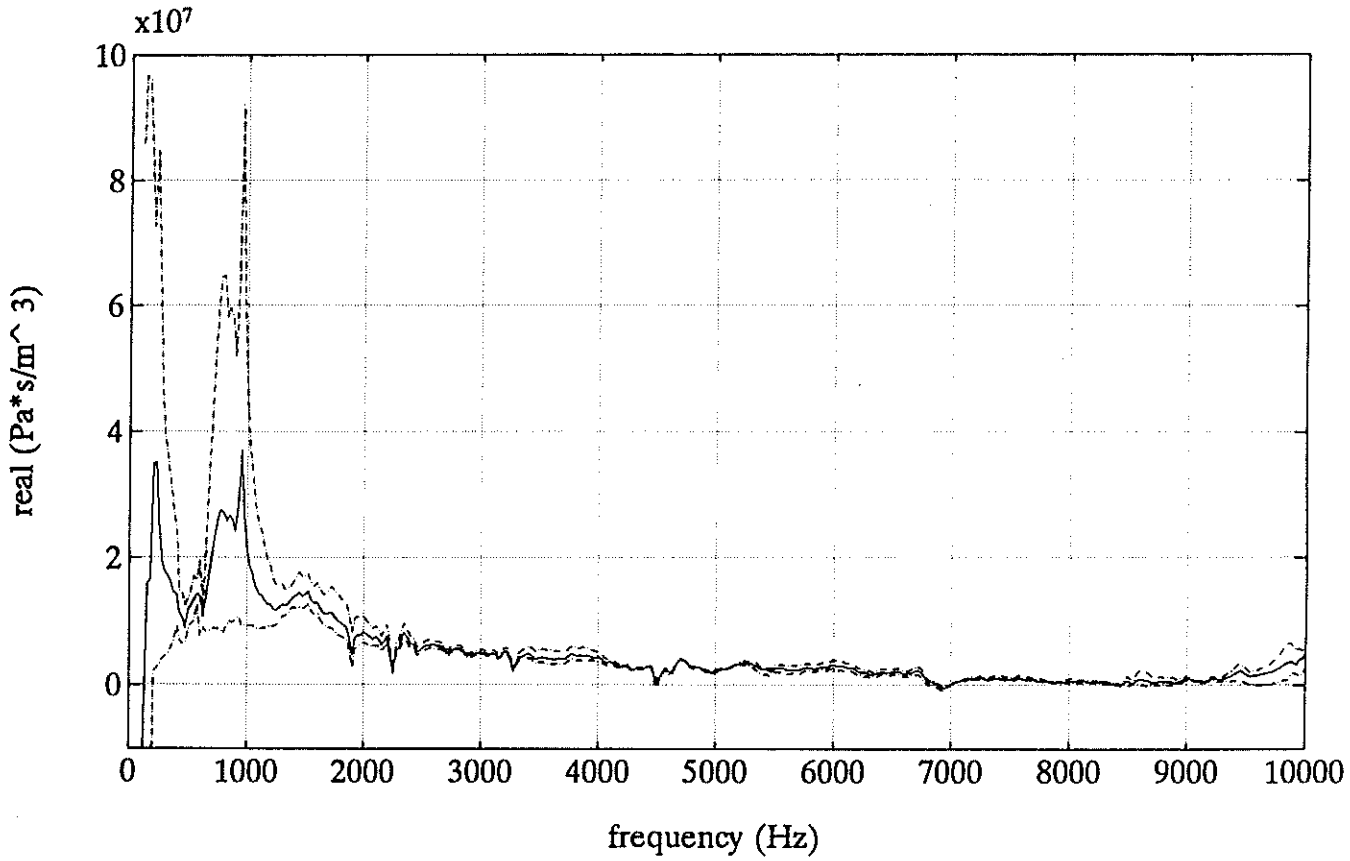

Figure 48a. Real part of ear input impedance at 100-105 dB(max), subject C.

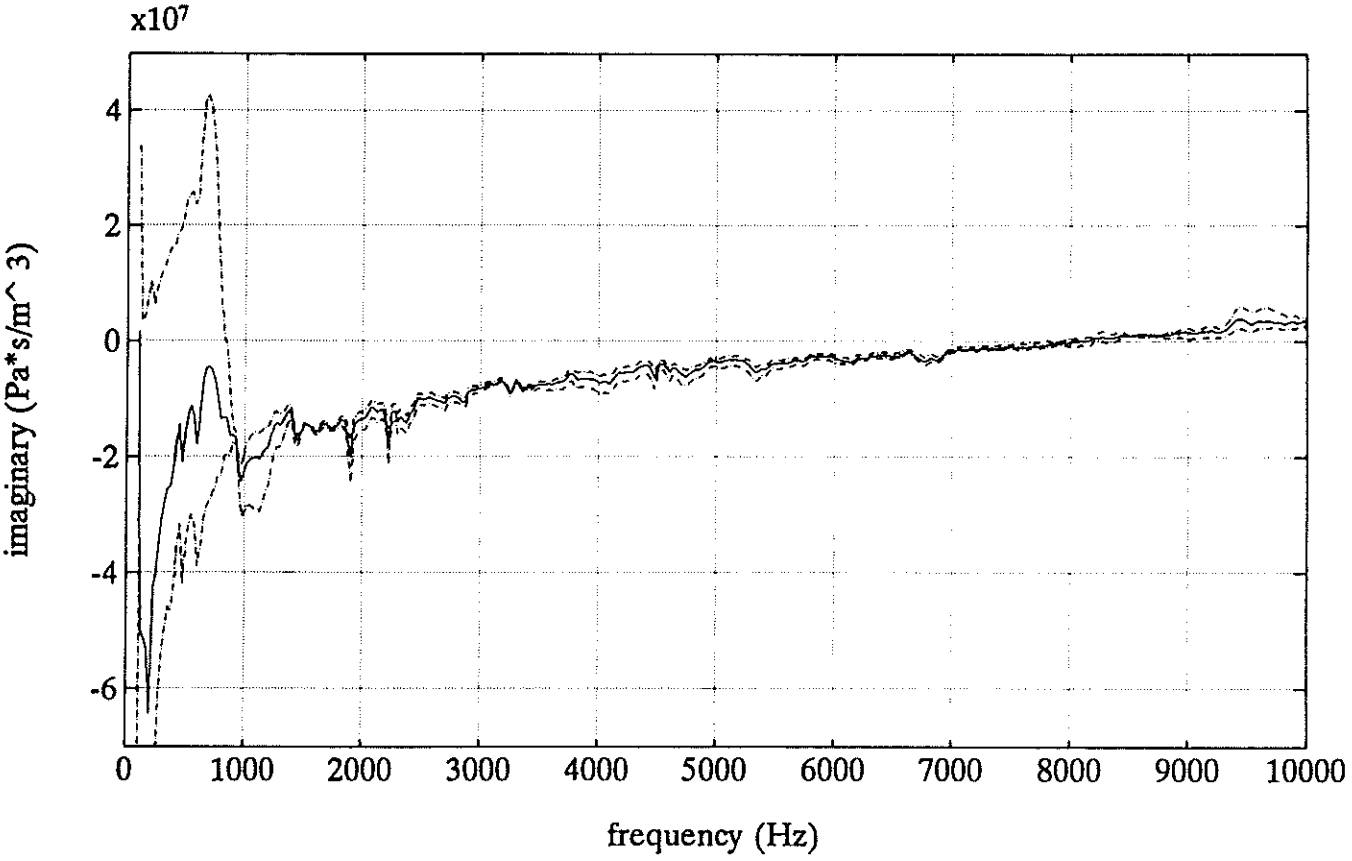

Figure 48b. Imaginary part of ear input impedance at 100-105 dB(max), subject C.

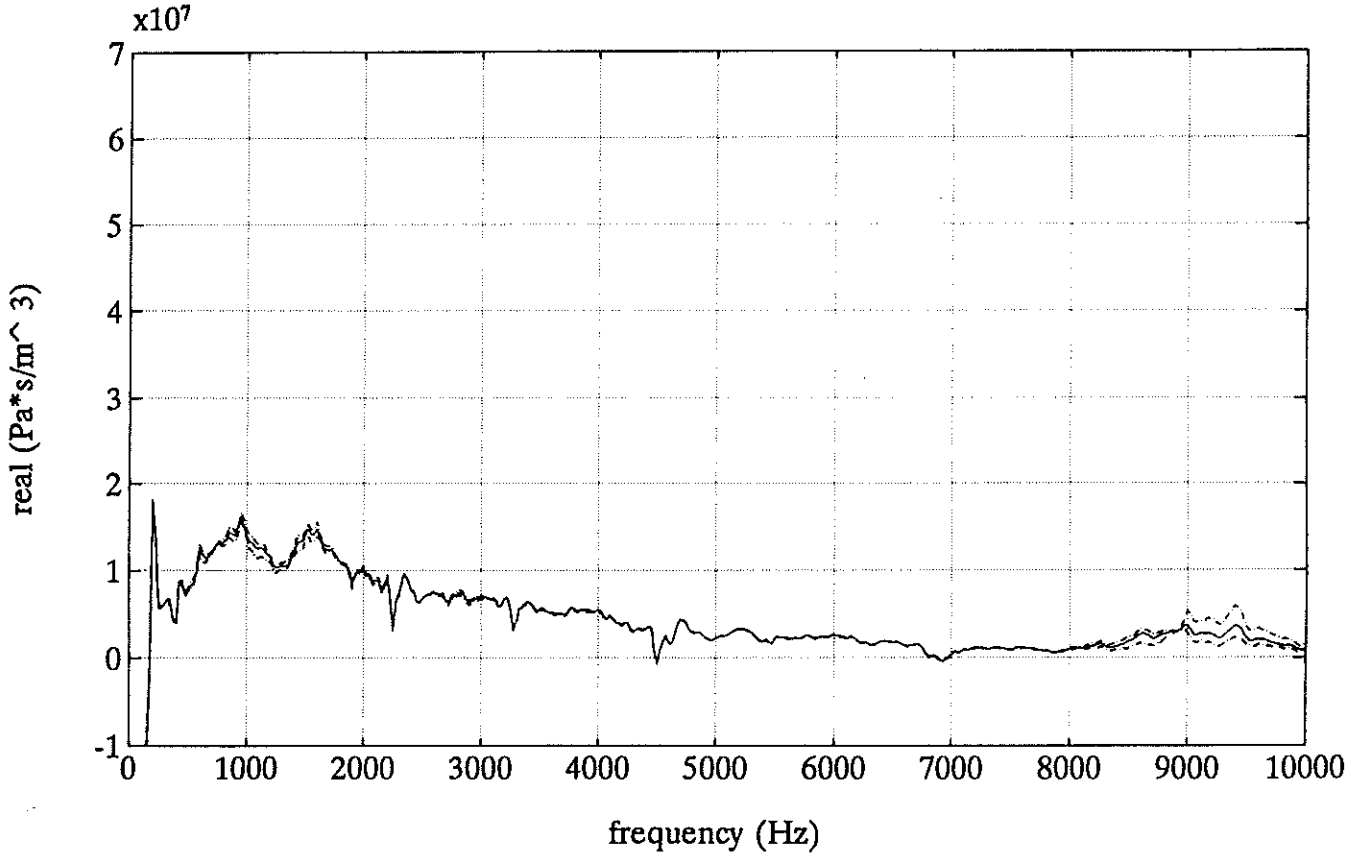

Figure 49a. Real part of ear input impedance at 100-105 dB(max), subject D.

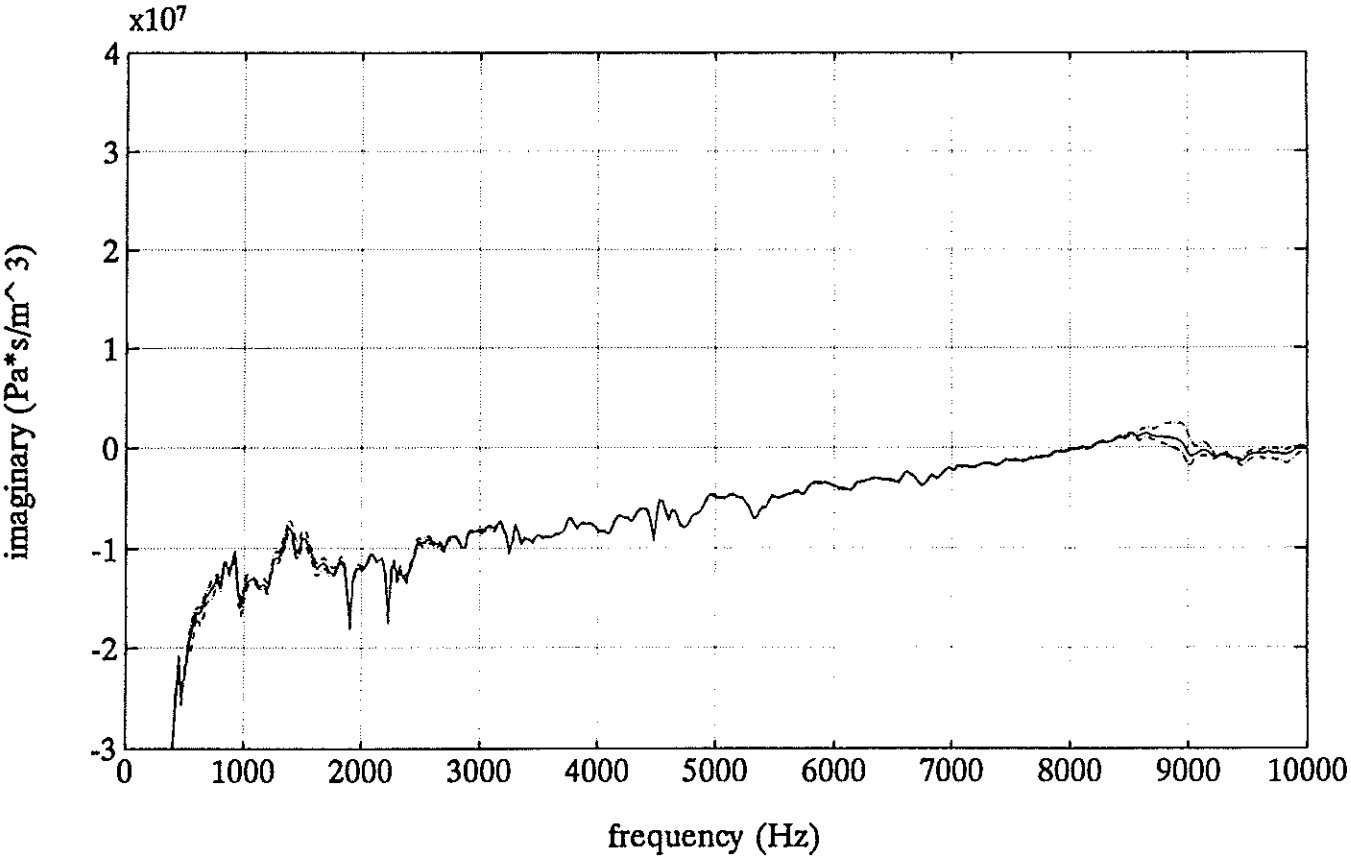

Figure 49b. Imaginary part of ear input impedance at 100-105 dB(max), subject D.

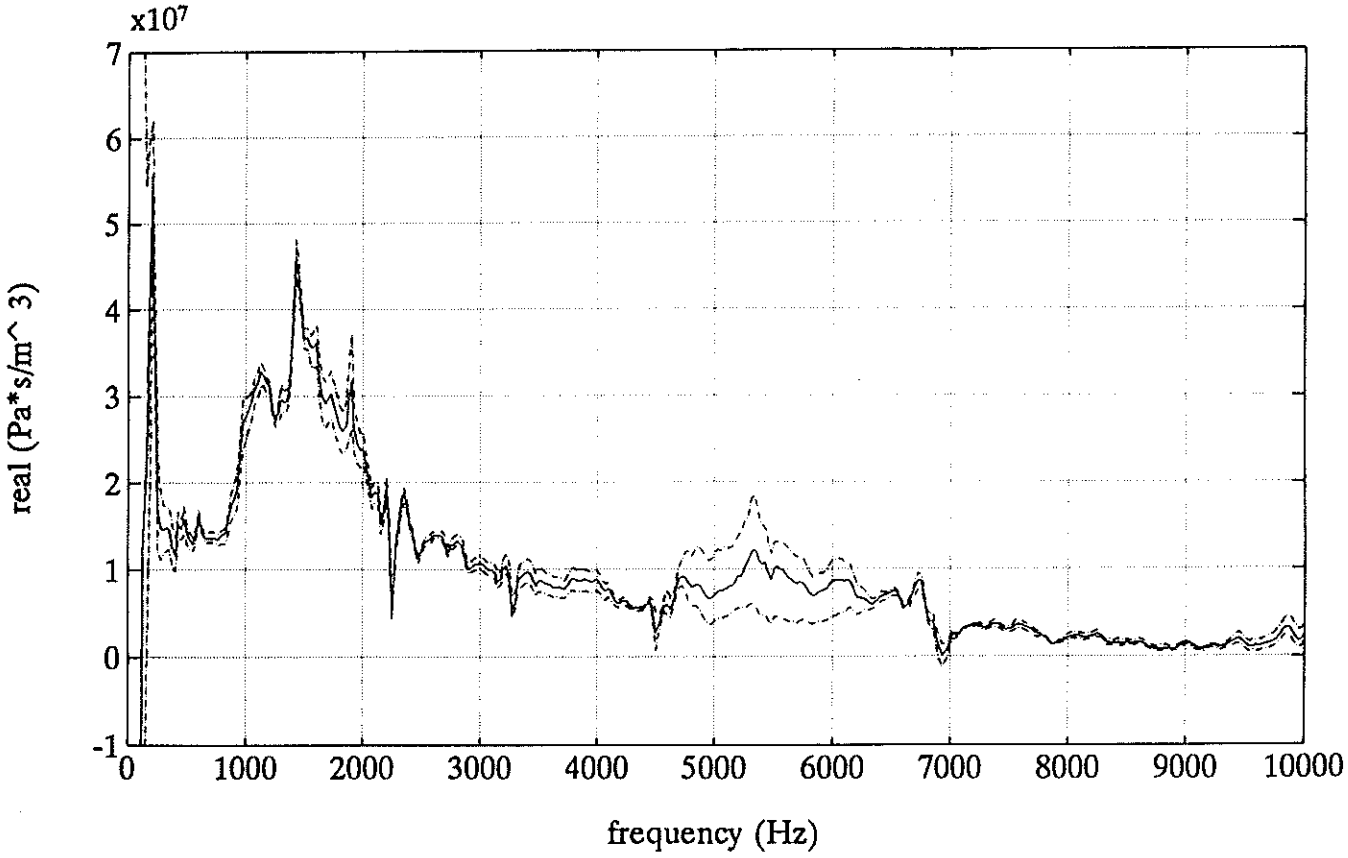

Figure 50a. Real part of ear input impedance at 100-105 dB(max), subject E.

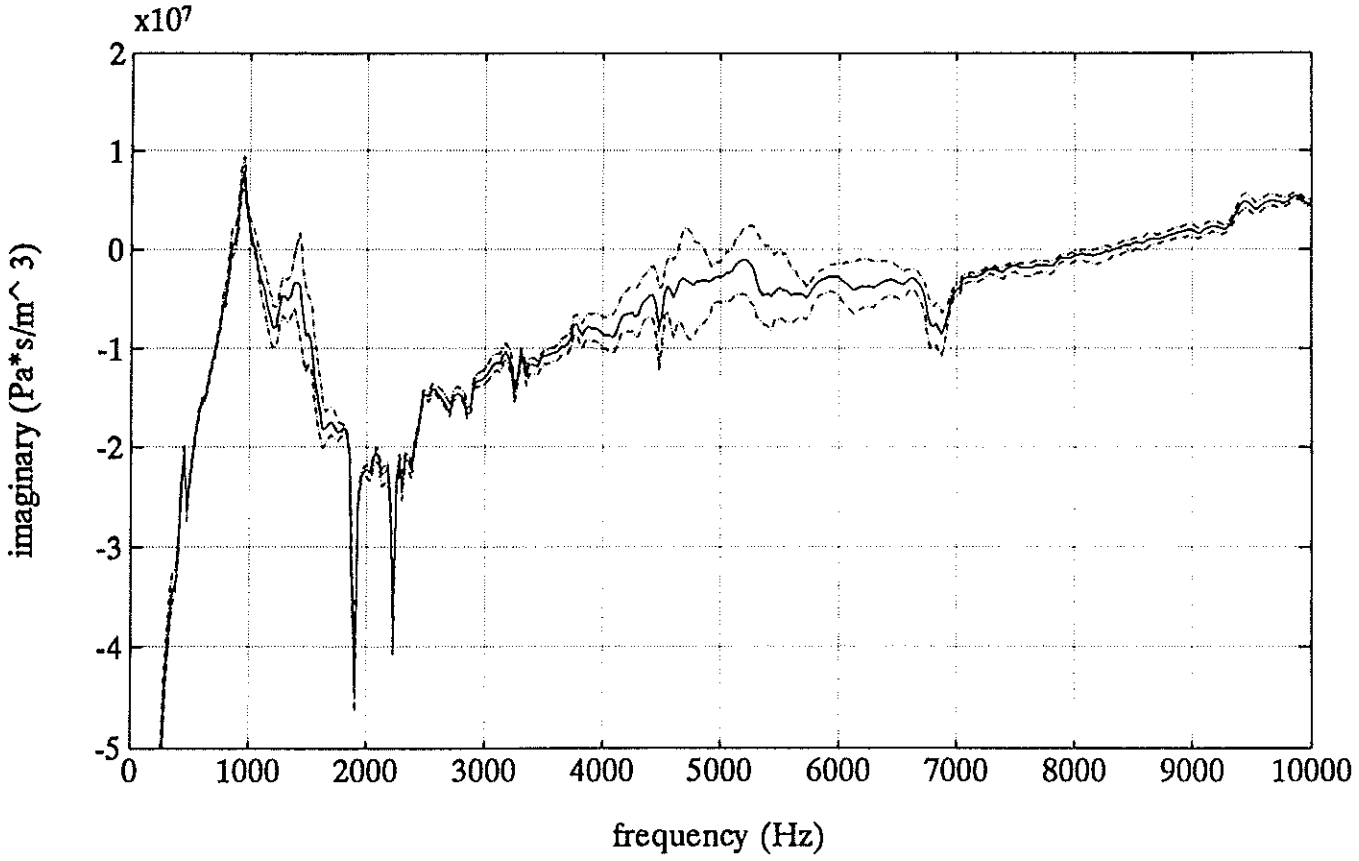

Figure 50b. Imaginary part of ear input impedance at 100-105 dB(max), subject E.

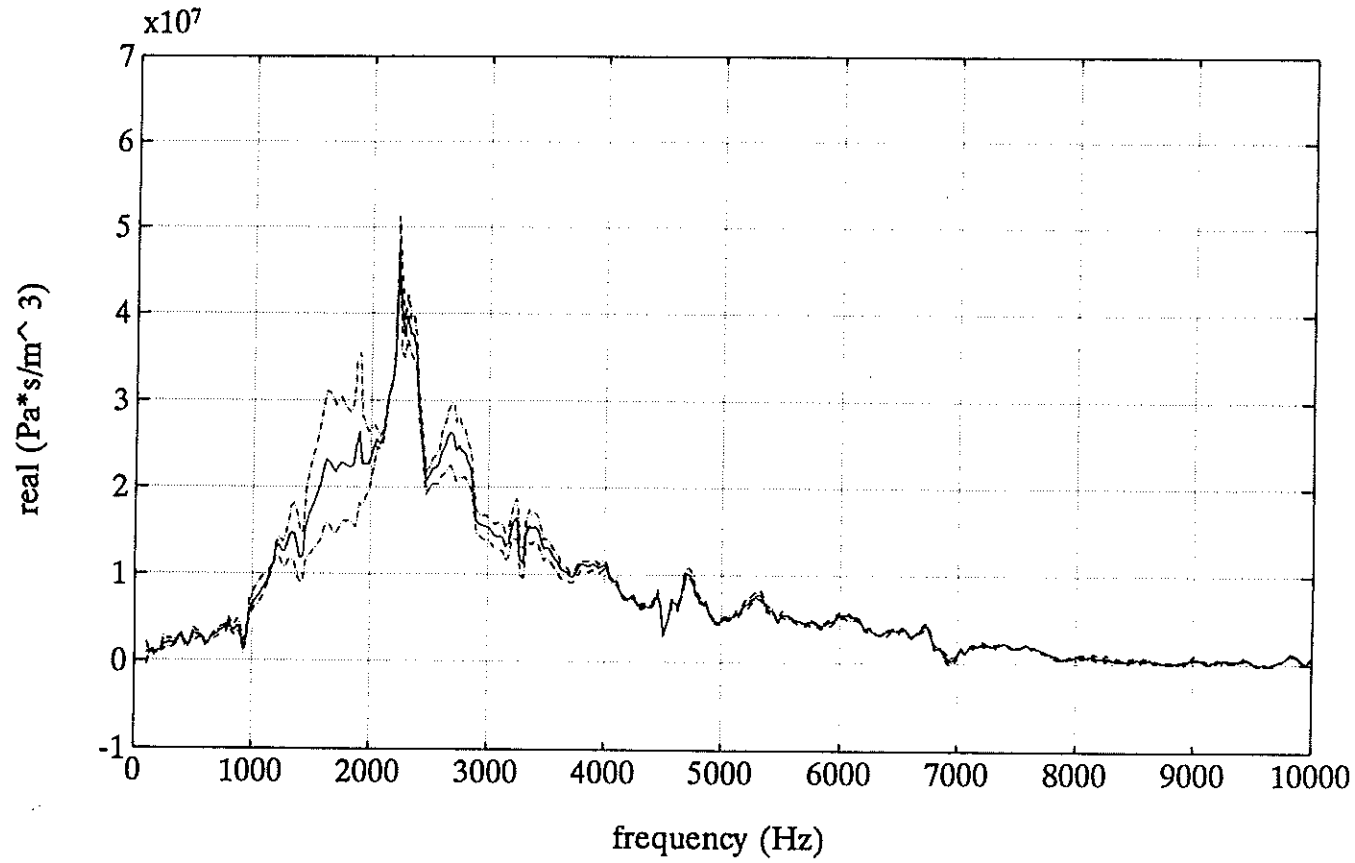

Figure 51a. Real part of ear input impedance at 80-85 dB(max), subject A.

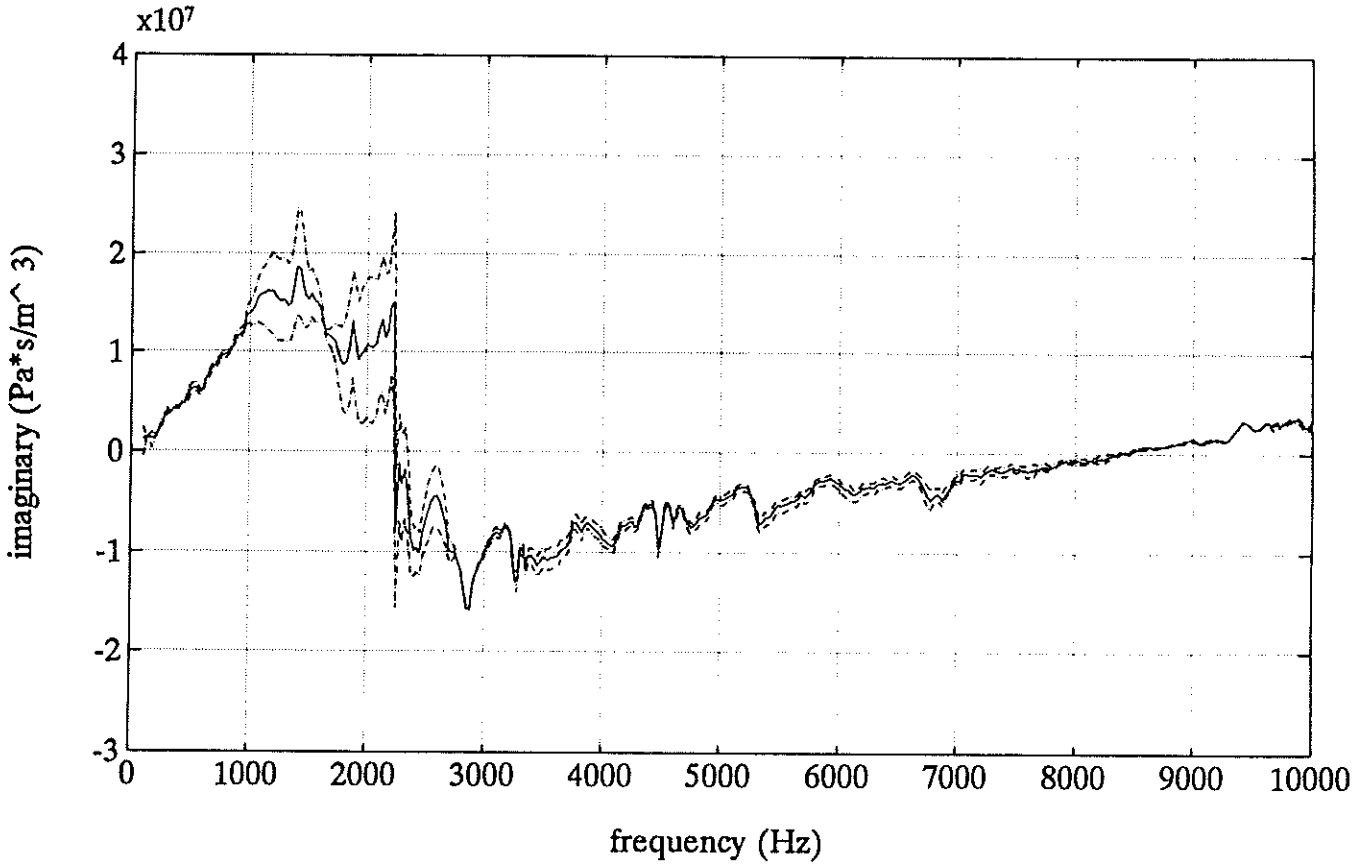

Figure 51b. Imaginary part of ear input impedance at 80-85 dB(max), subject A.

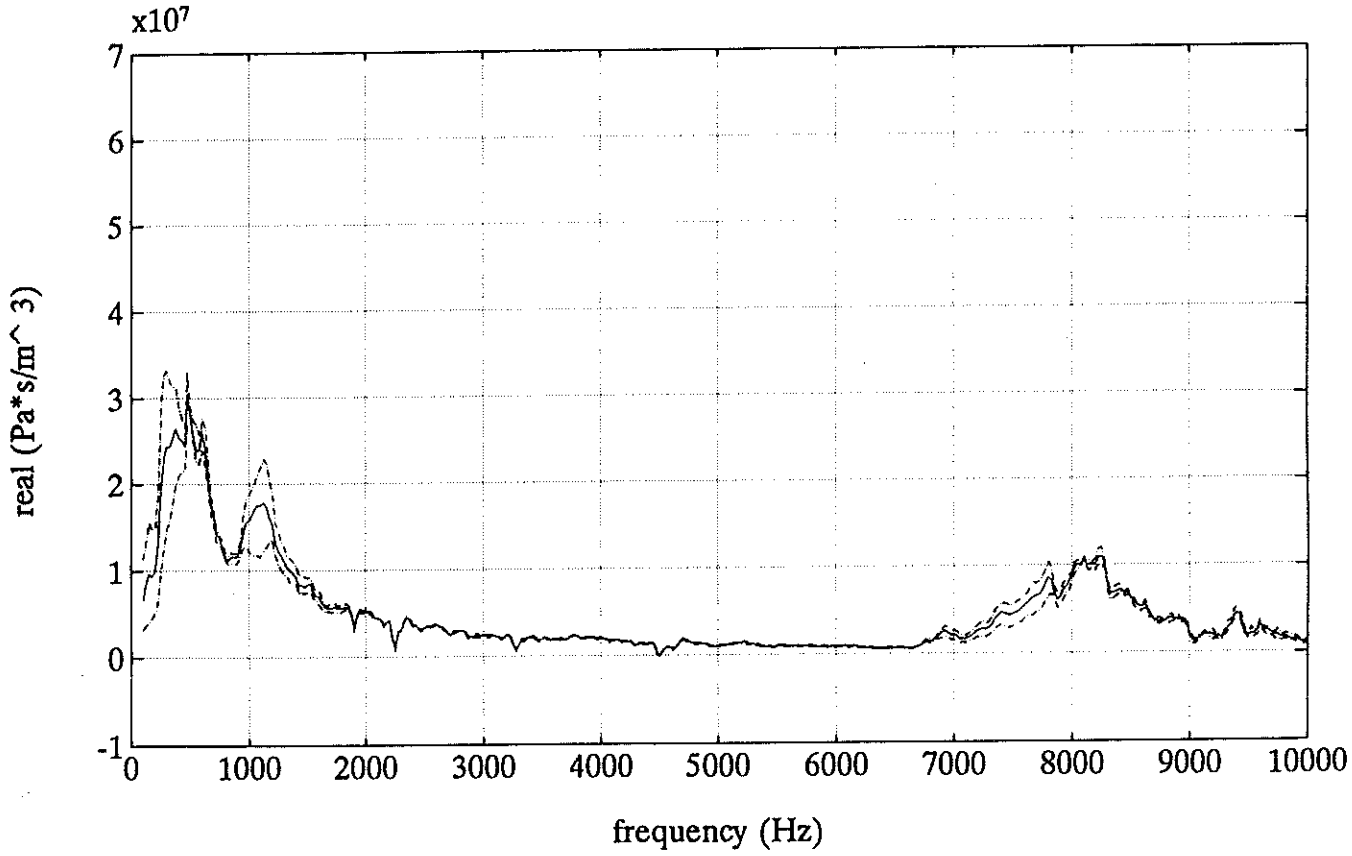

Figure 52a. Real part of ear input impedance at 80-85 dB(max), subject B.

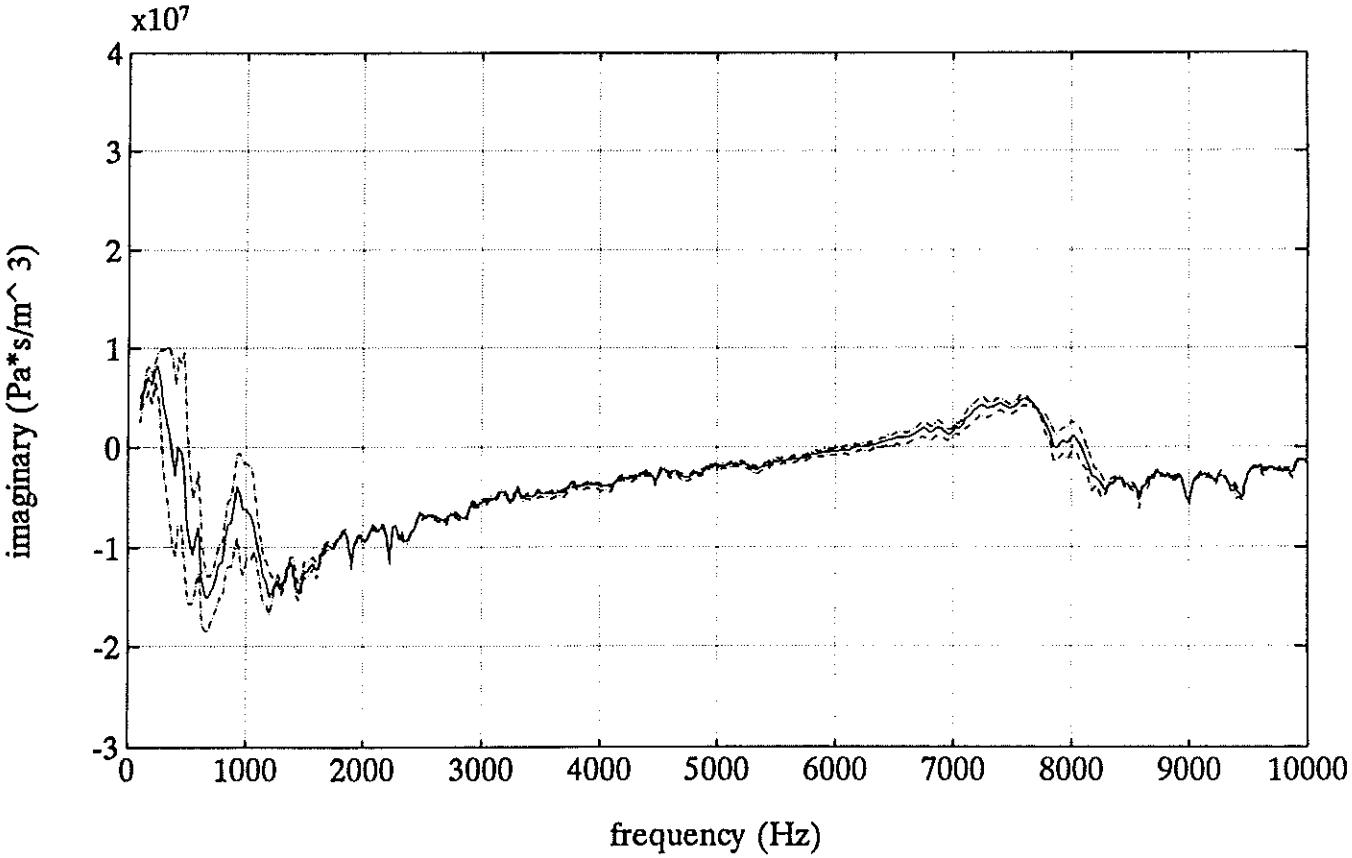

Figure 52b. Imaginary part of ear input impedance at 80-85 dB(max), subject B.

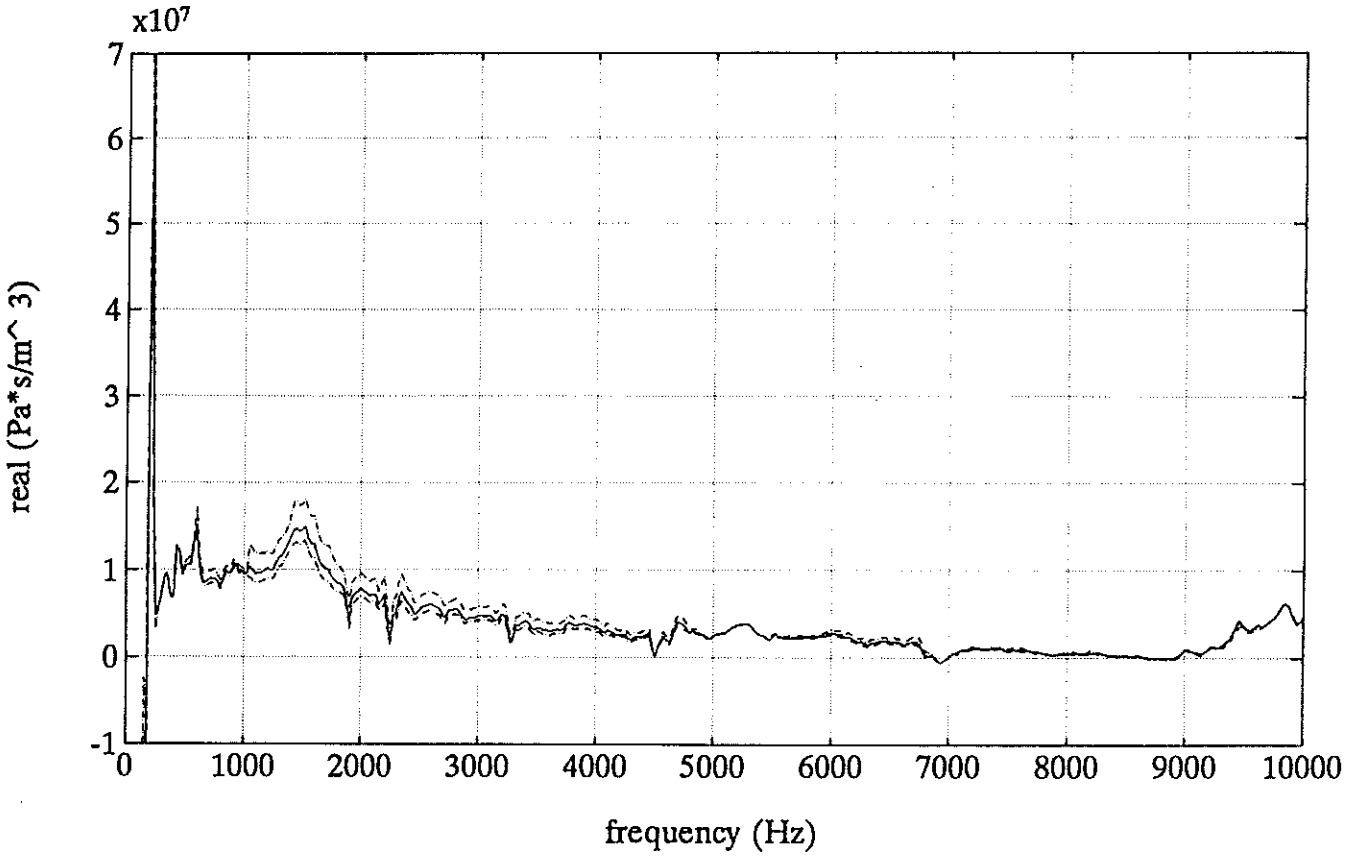

Figure 53a. Real part of ear input impedance at 80-85 dB(max), subject C.

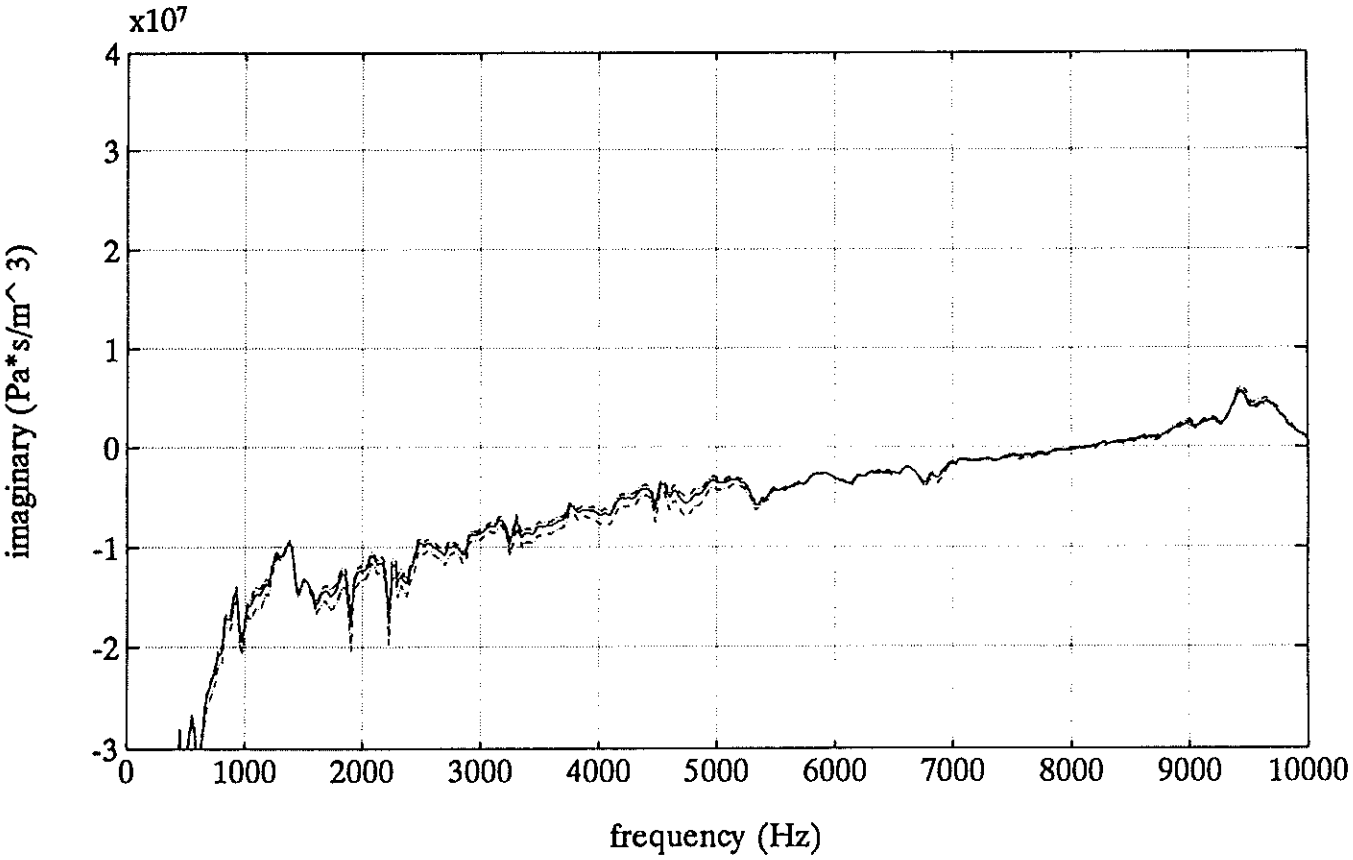

Figure 53b. Imaginary part of ear input impedance at 80-85 dB(max), subject C.

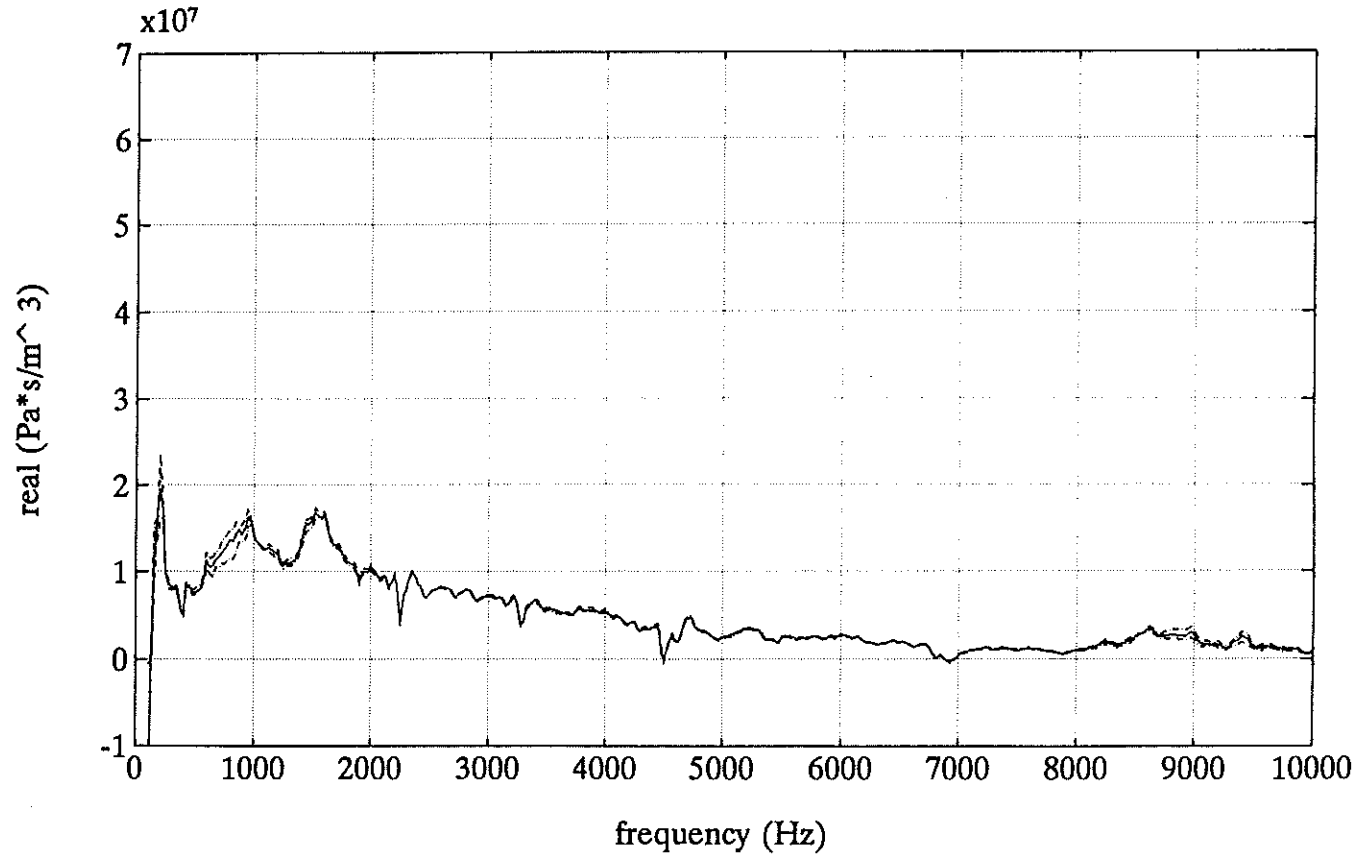

Figure 54a. Real part of ear input impedance at 80-85 dB(max), subject D.

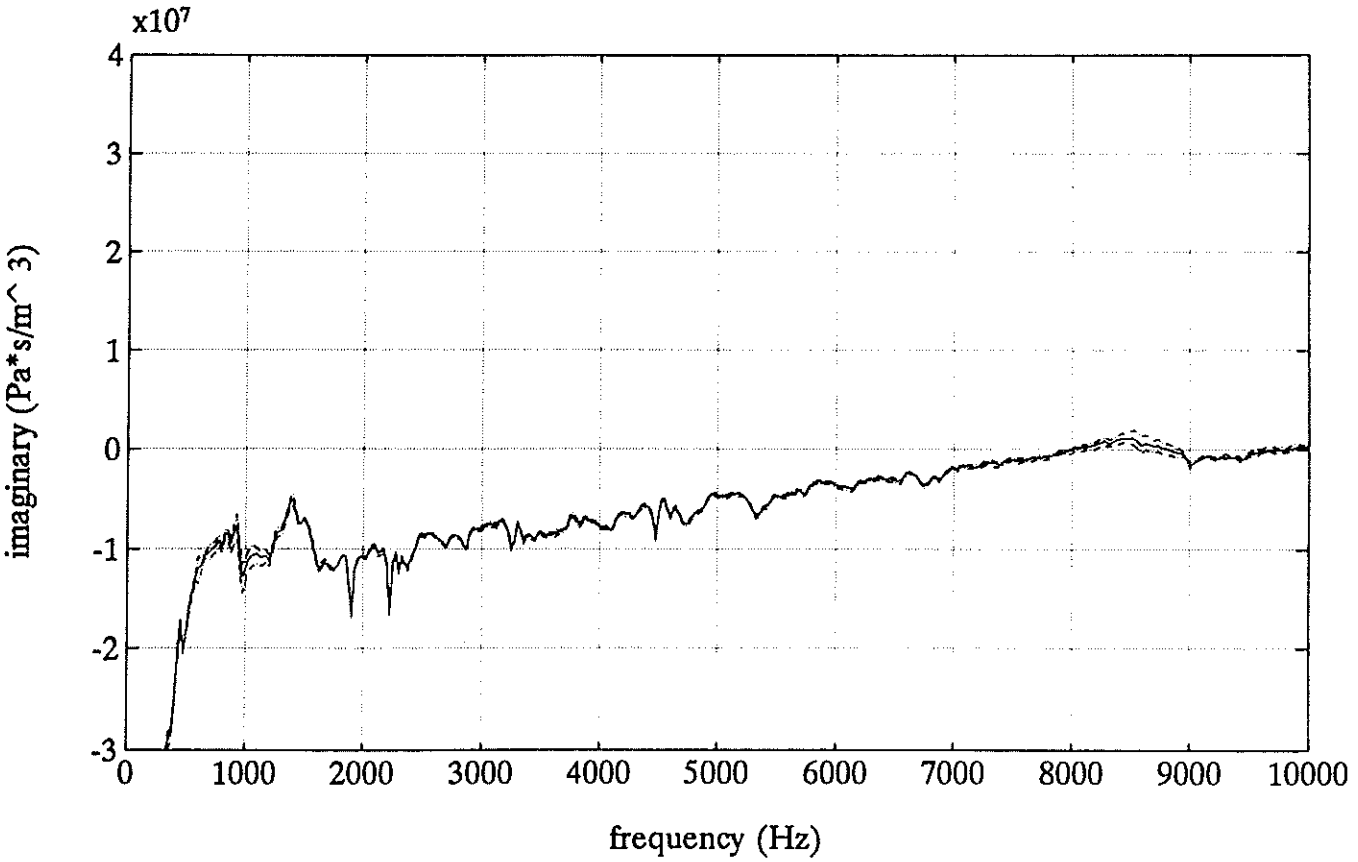

Figure 54b. Imaginary part of ear input impedance at 80-85 dB(max), subject D.

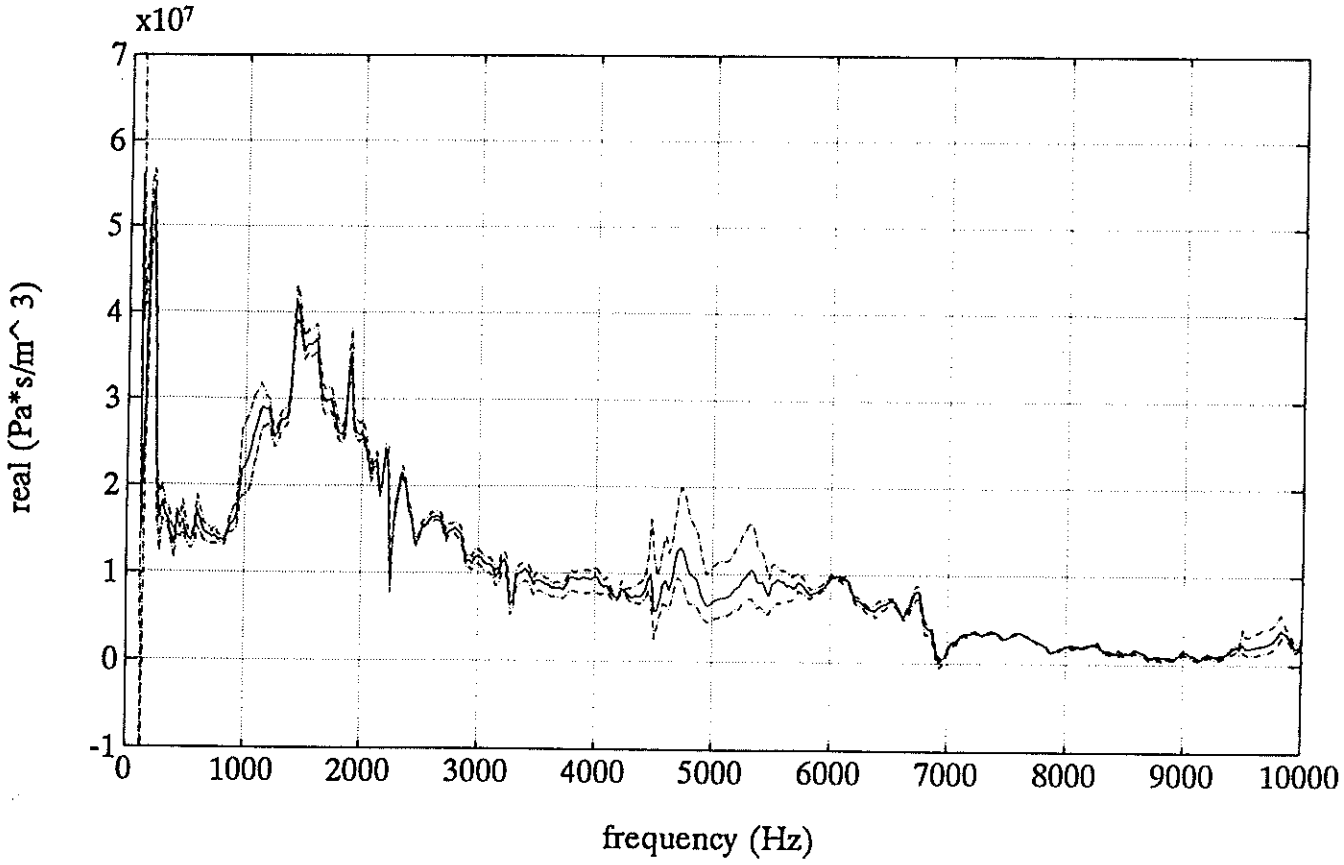

Figure 55a. Real part of ear input impedance at 80-85 dB(max), subject E.

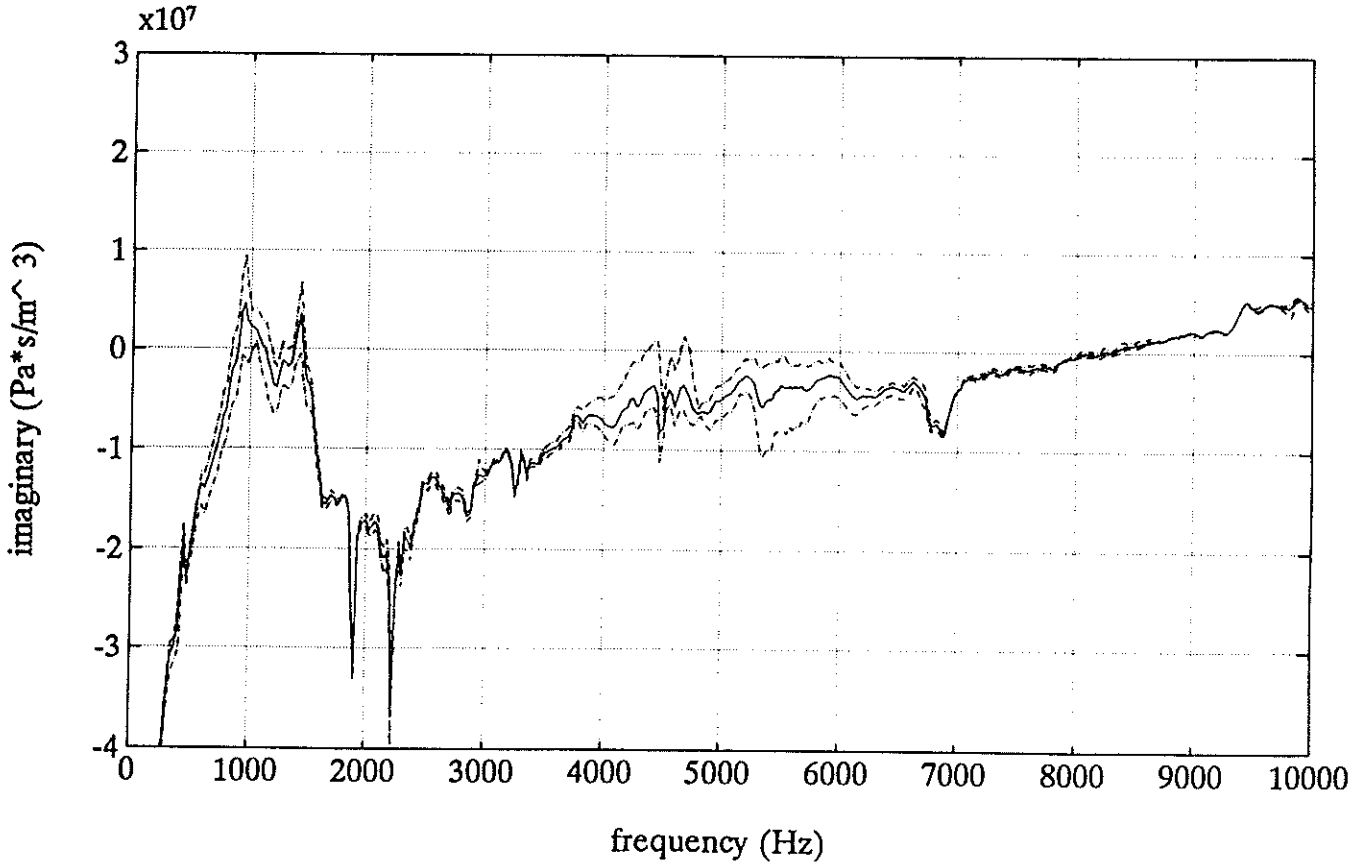

Figure 55b. Imaginary part of ear input impedance at 80-85 dB(max), subject E.

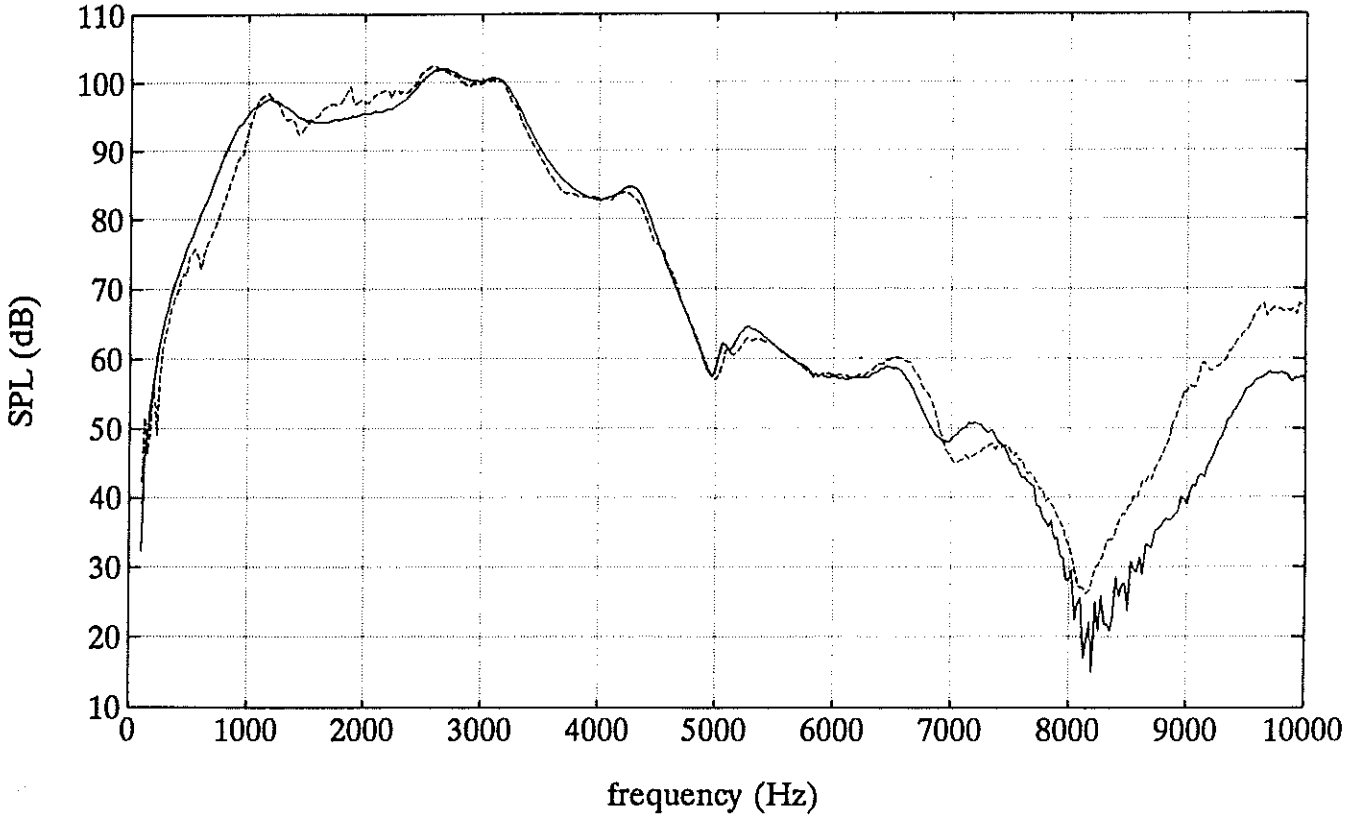

Figure 56. Measured (solid) and predicted (dashed) sound pressure level from Widex ES1 on subject A.

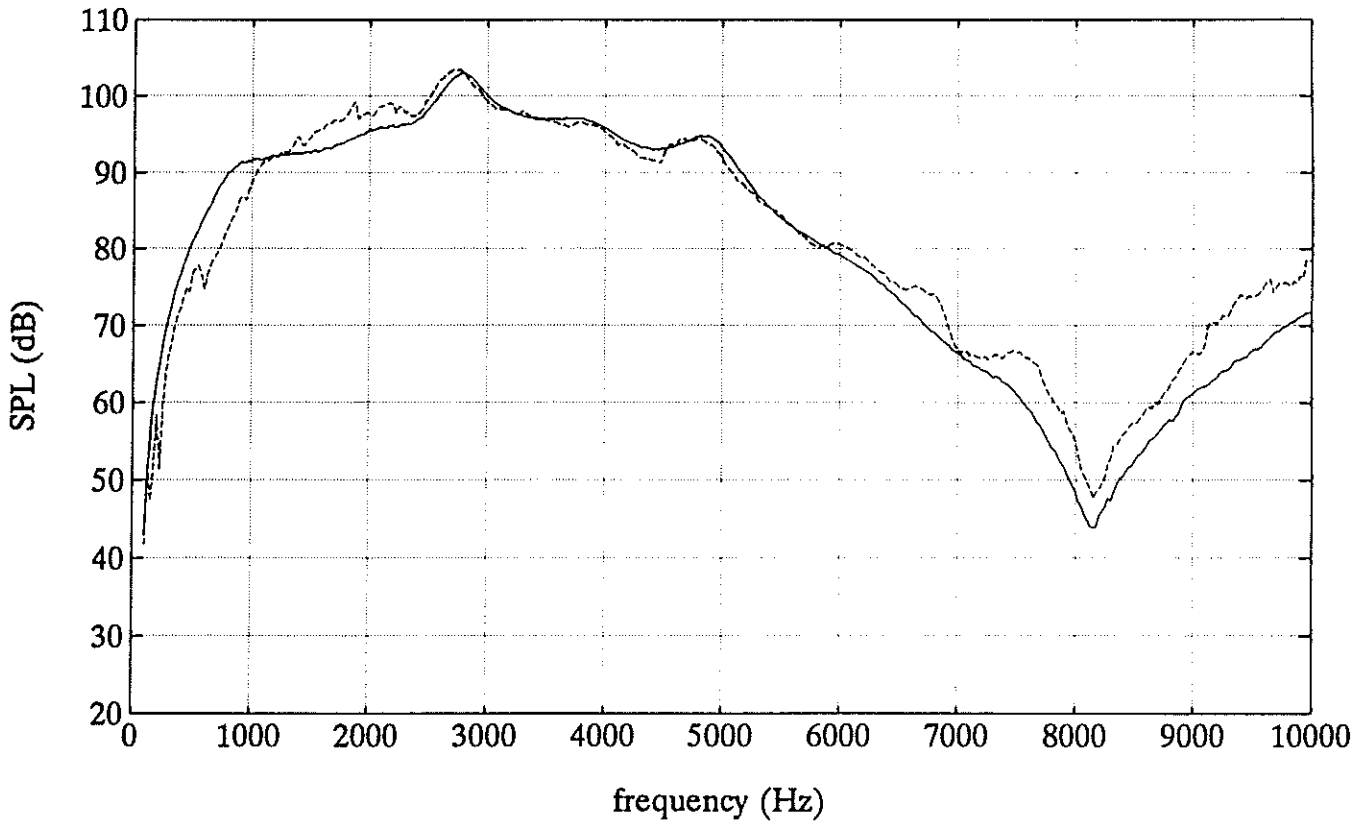

Figure 57. Measured (solid) and predicted (dashed) sound pressure level from Philips M49 on subject A.

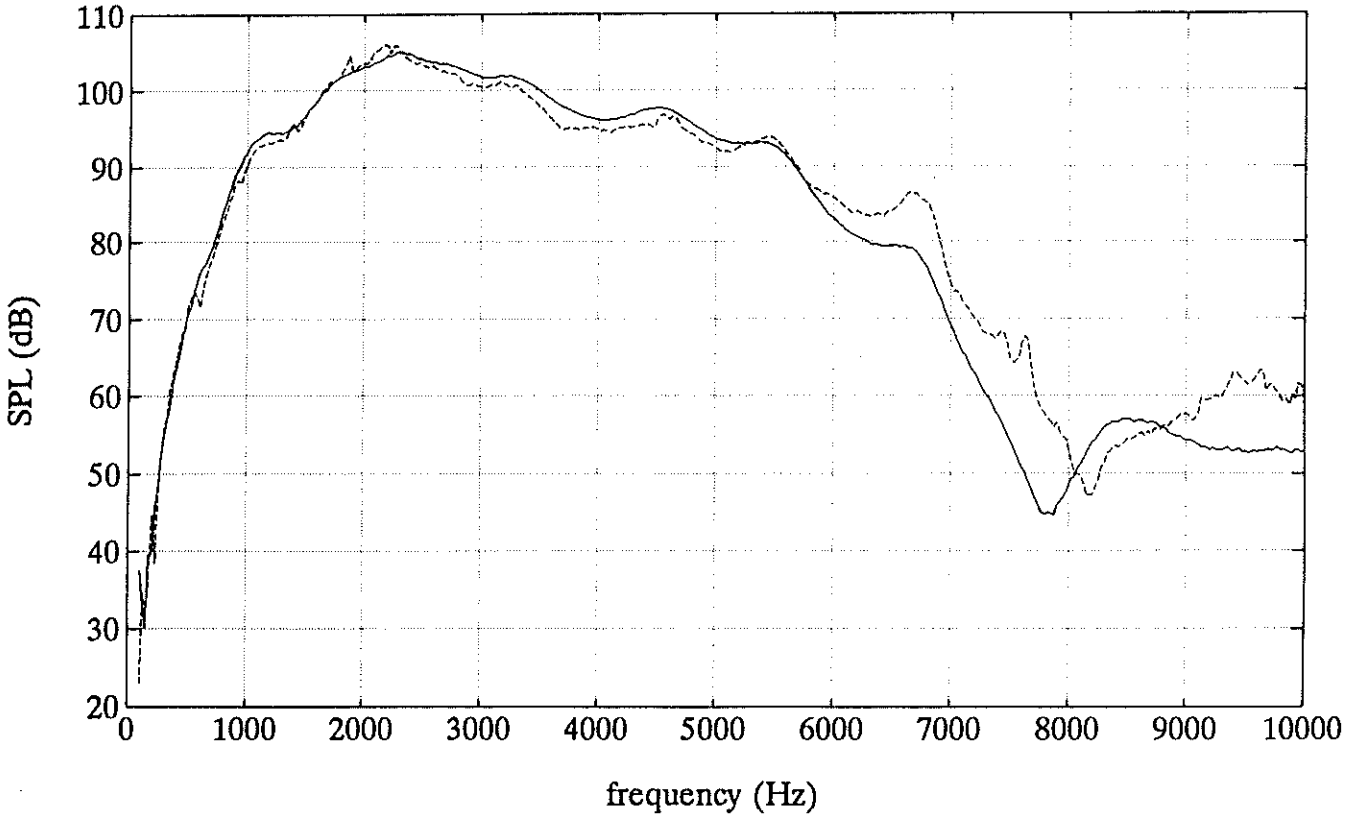

Figure 58. Measured (solid) and predicted (dashed) sound pressure level from Phonak Pico SC on subject A.

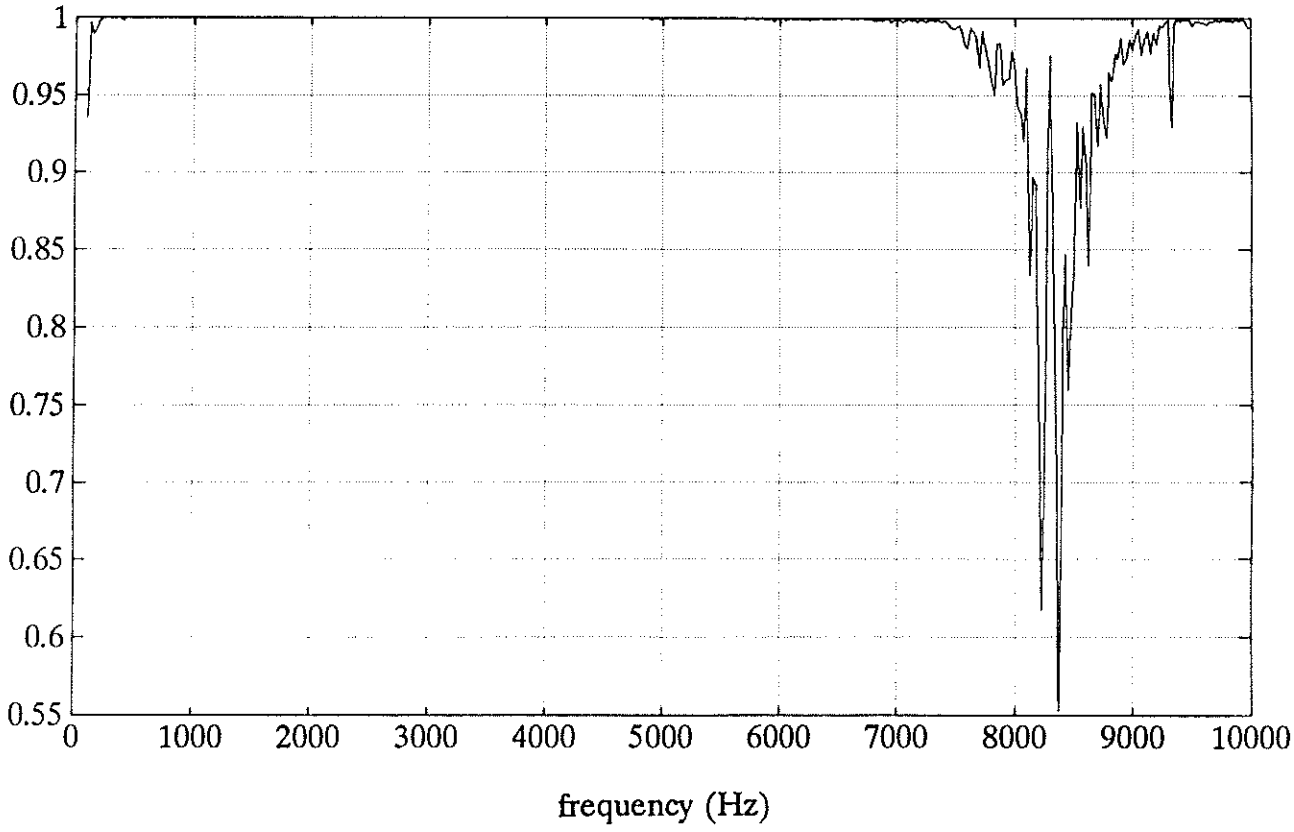

Figure 59. Coherence function of a prediction check measurement of Widex ES1 on subject A.

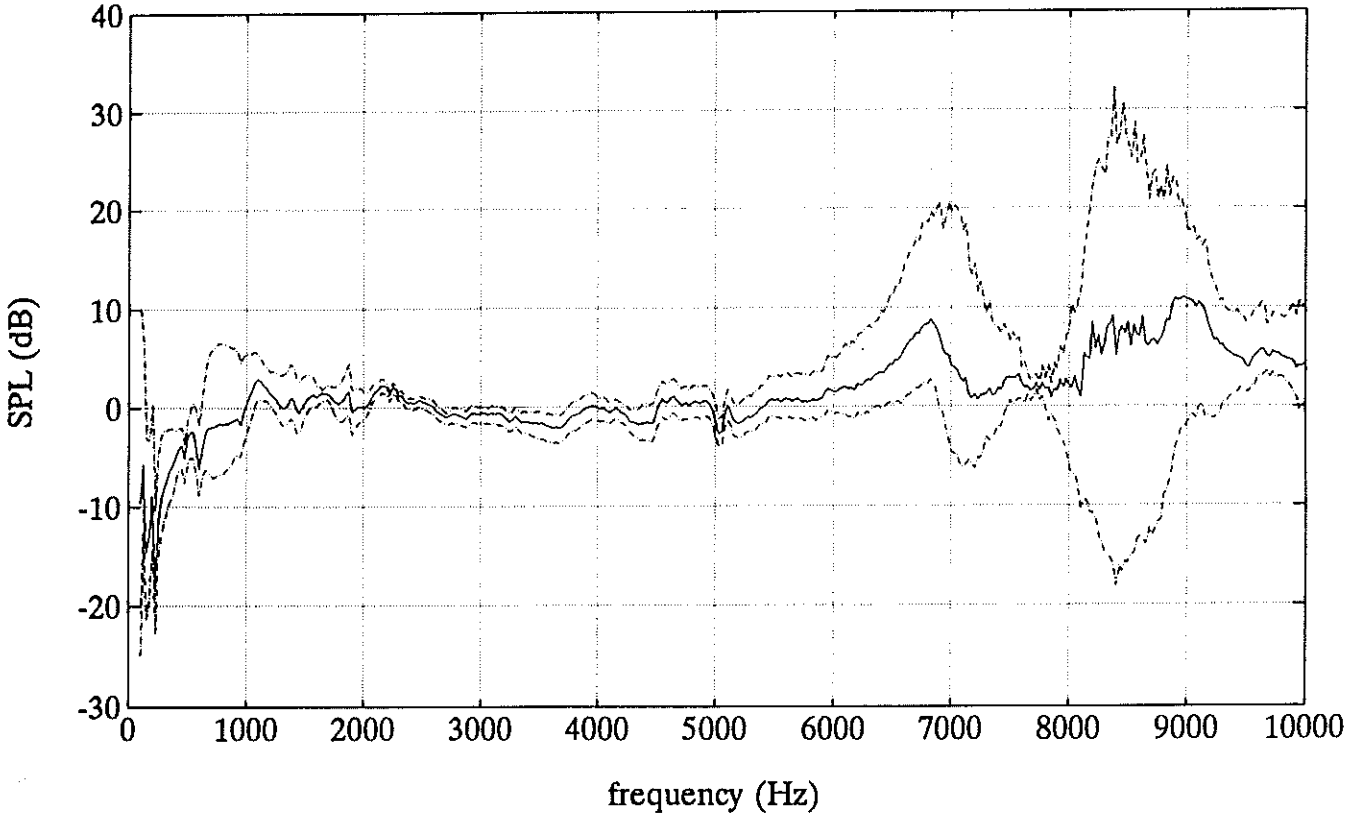

Figure 60. Predicted minus measured sound pressure level of Widex ES1 on subject A. Maximum, average and minimum of three measurements.

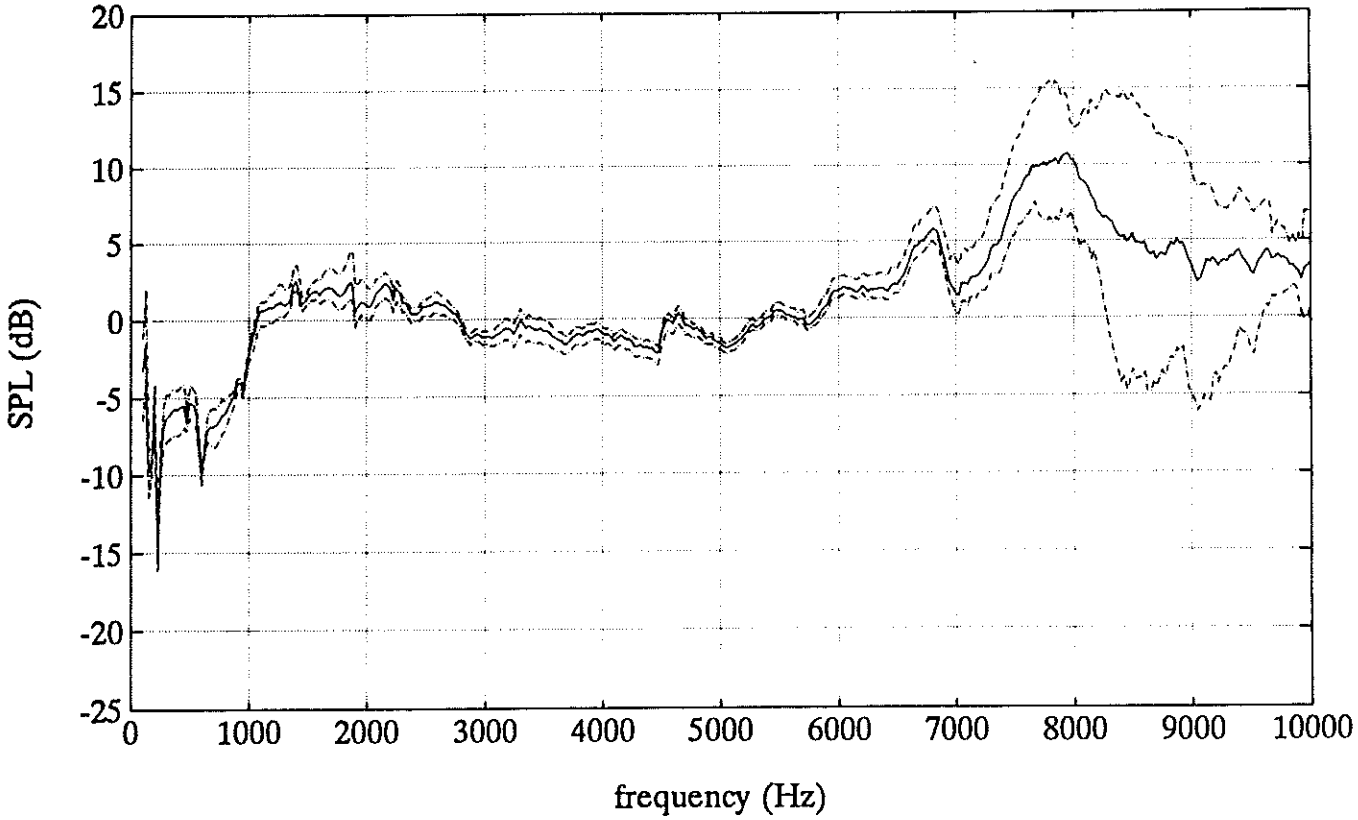

Figure 61. Predicted minus measured sound pressure level of Philips M49 on subject A. Maximum, average and minimum of three measurements.

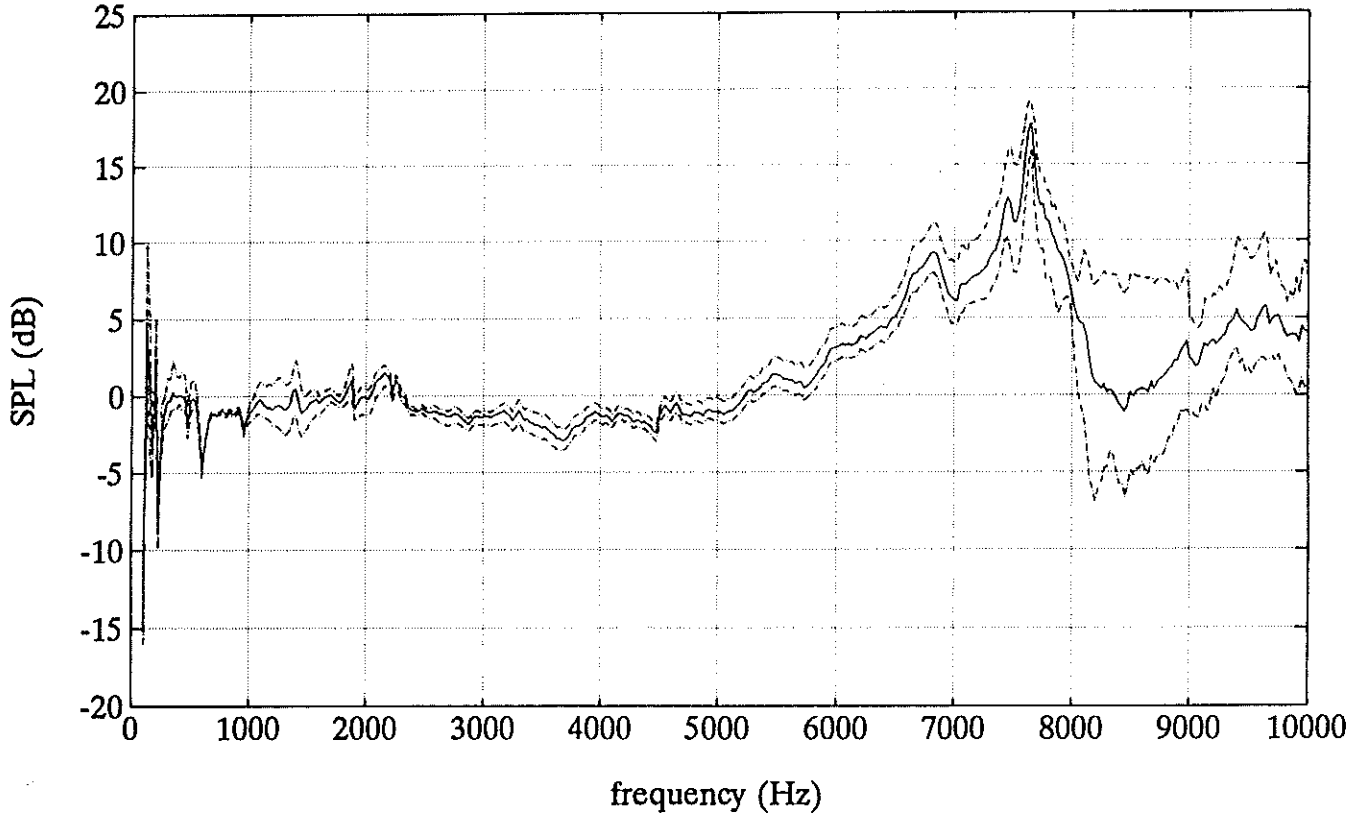

Figure 62. Predicted minus measured sound pressure level of Phonak Pico SC on subject A. Maximum, average and minimum of three measurements.

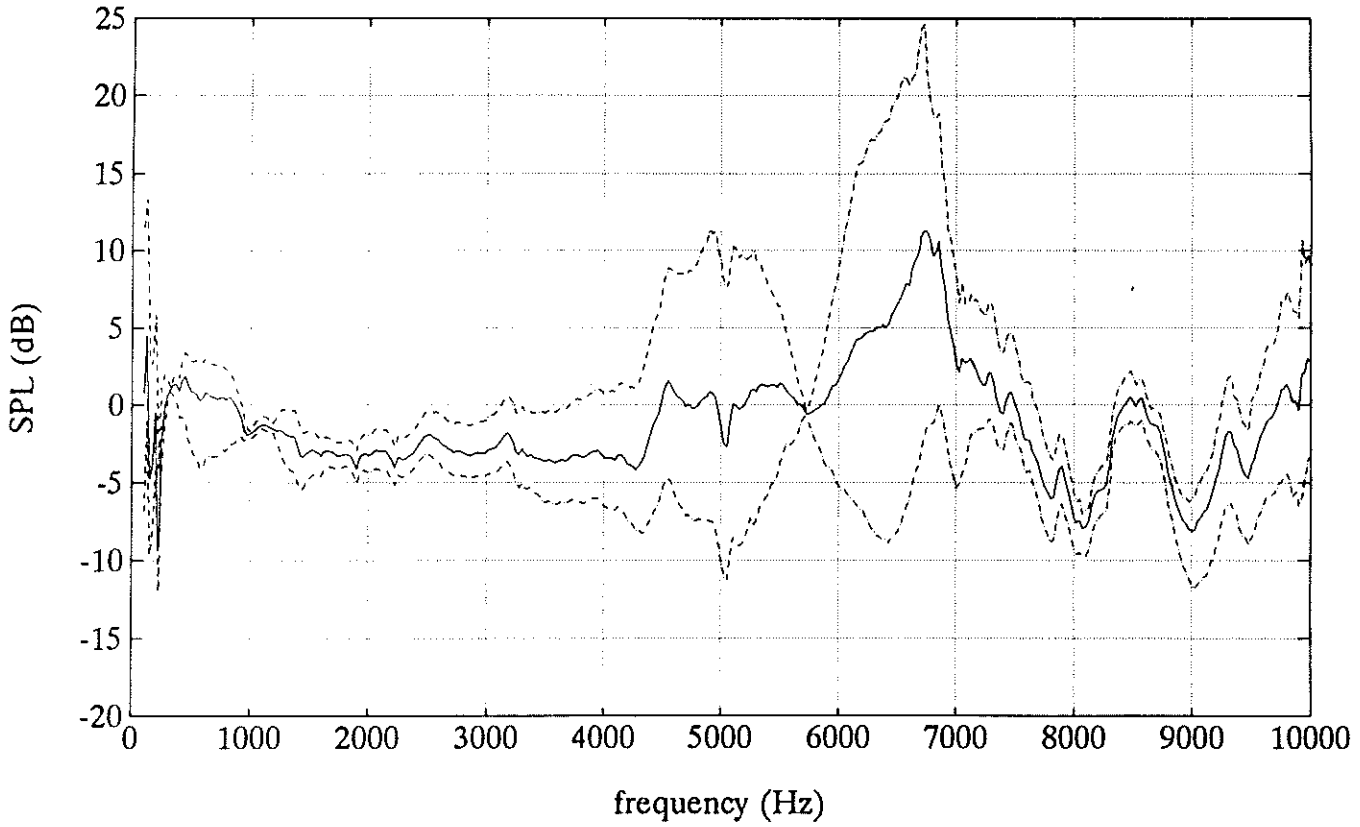

Figure 63. Predicted minus measured sound pressure level of Widex ES1 on subject B. Maximum, average and minimum of three measurements.

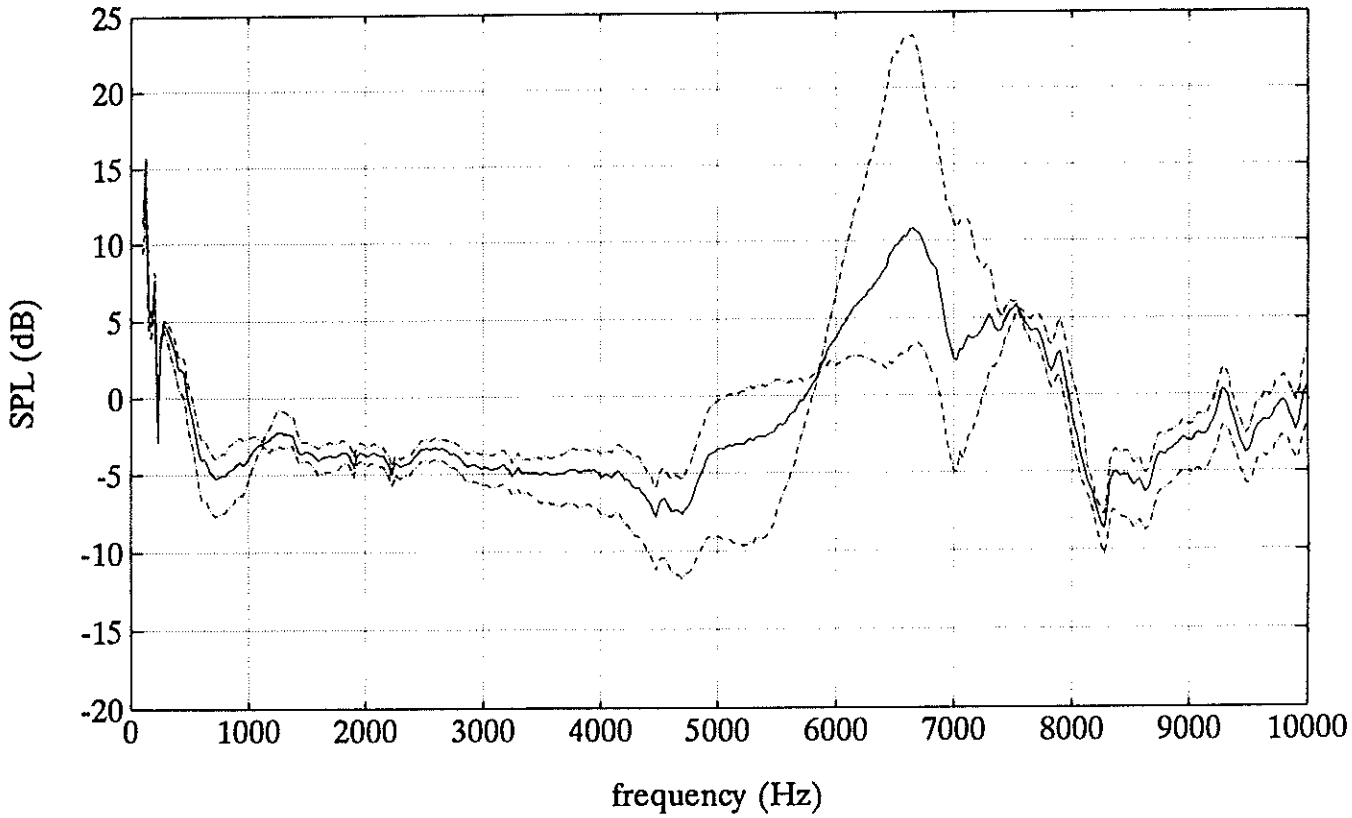

Figure 64. Predicted minus measured sound pressure level of Philips M49 on subject B. Maximum, average and minimum of three measurements.

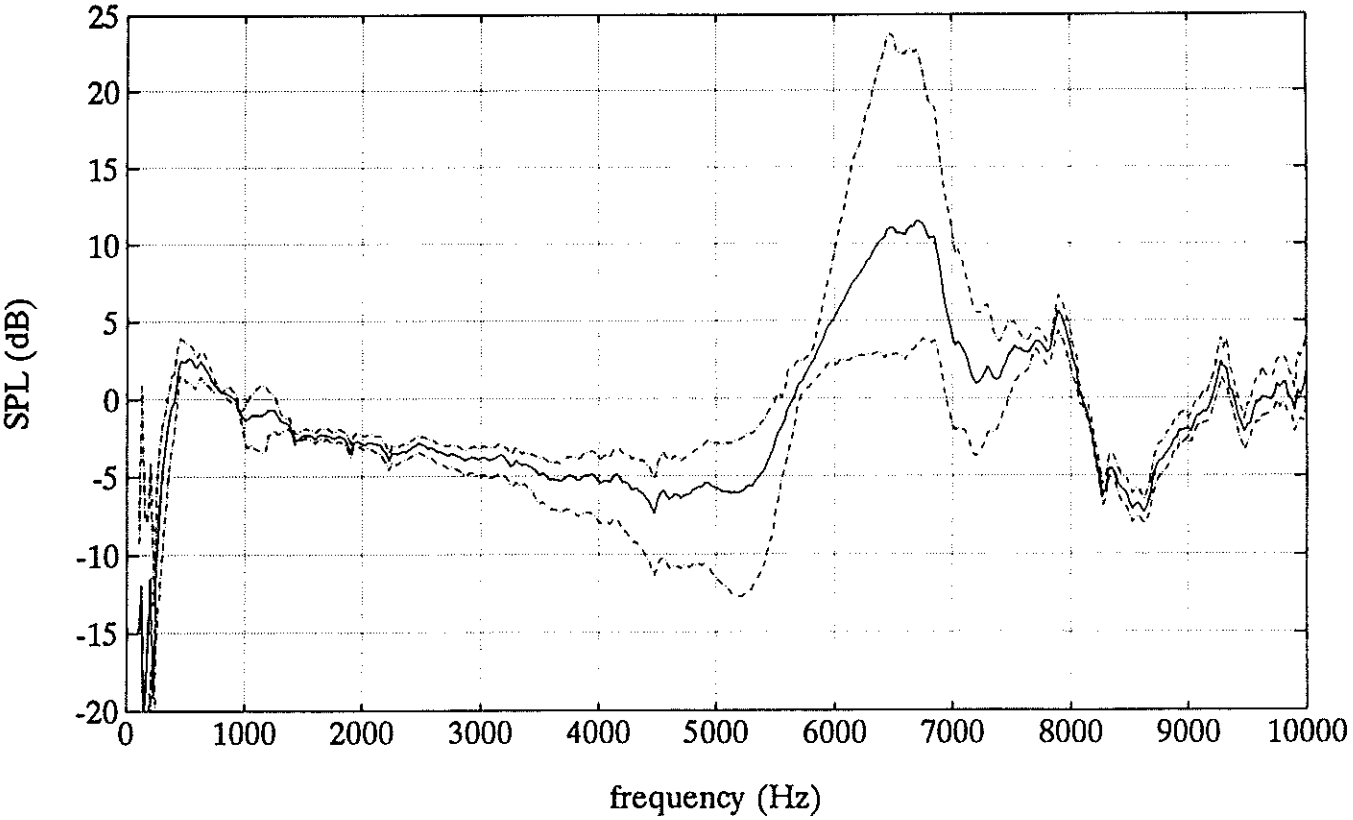

Figure 65. Predicted minus measured sound pressure level of Phonak Pico SC on subject B. Maximum, average and minimum of three measurements.

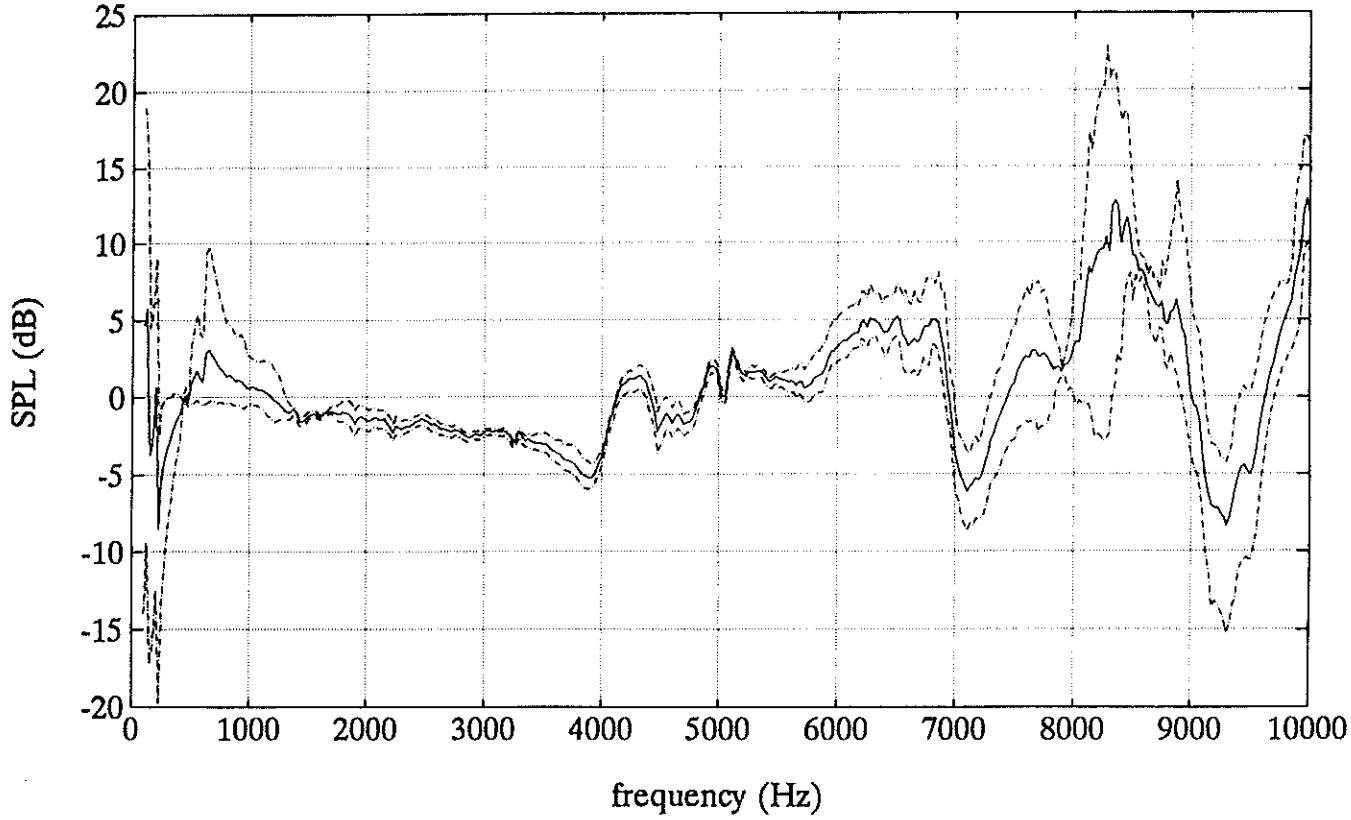

Figure 66. Predicted minus measured sound pressure level of Widex ES1 on subject C. Maximum, average and minimum of three measurements.

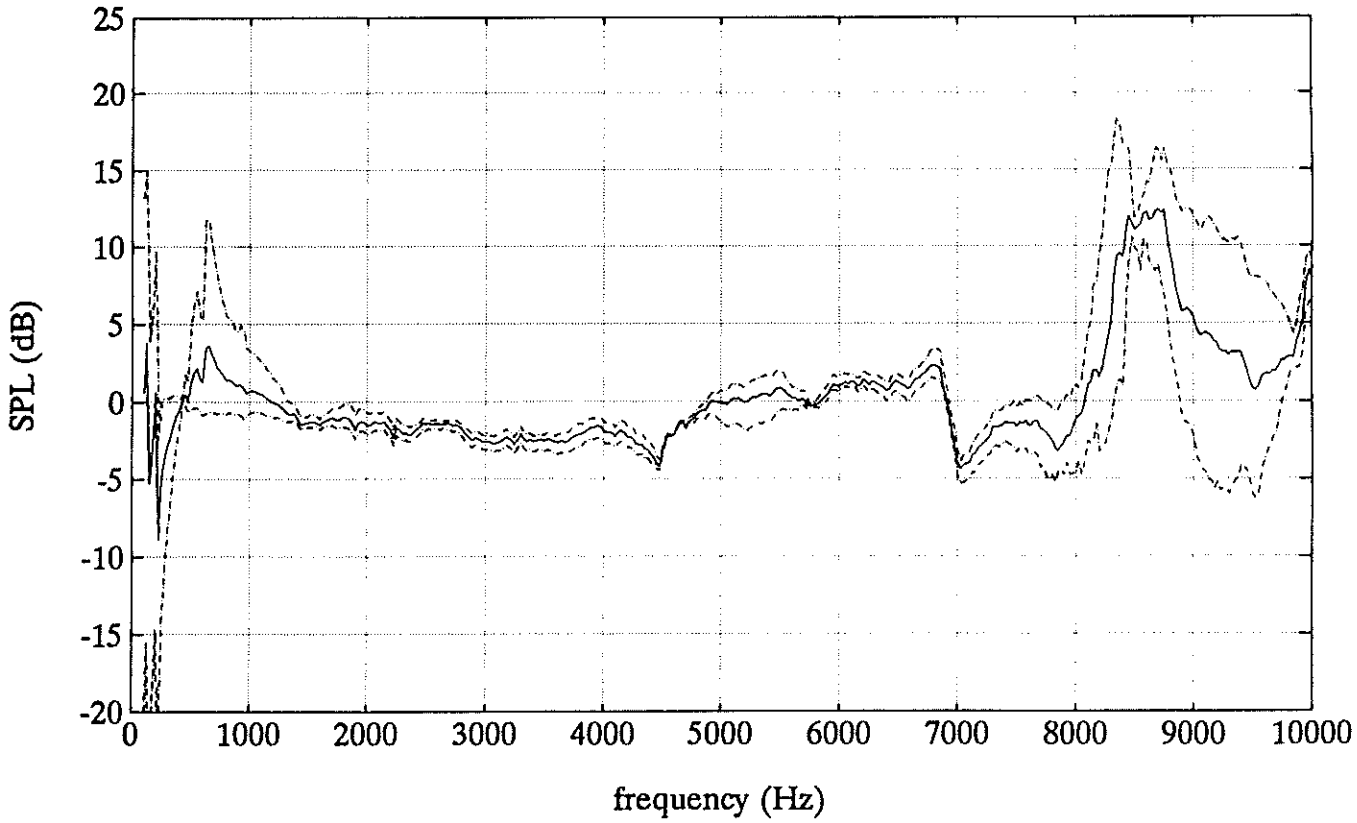

Figure 67. Predicted minus measured sound pressure level of Philips M49 on subject C. Maximum, average and minimum of three measurements.

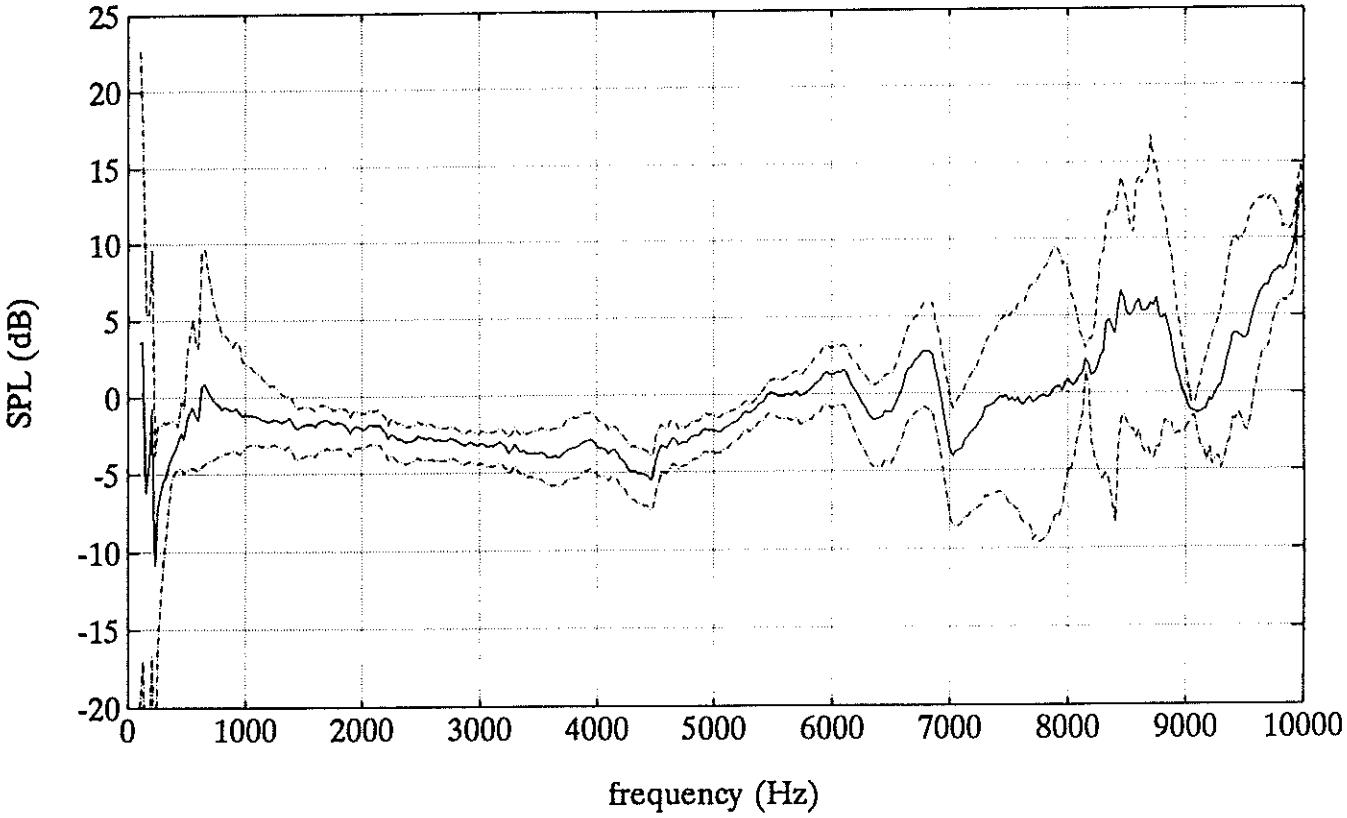

Figure 68. Predicted minus measured sound pressure level of Phonak Pico SC on subject C. Maximum, average and minimum of three measurements.

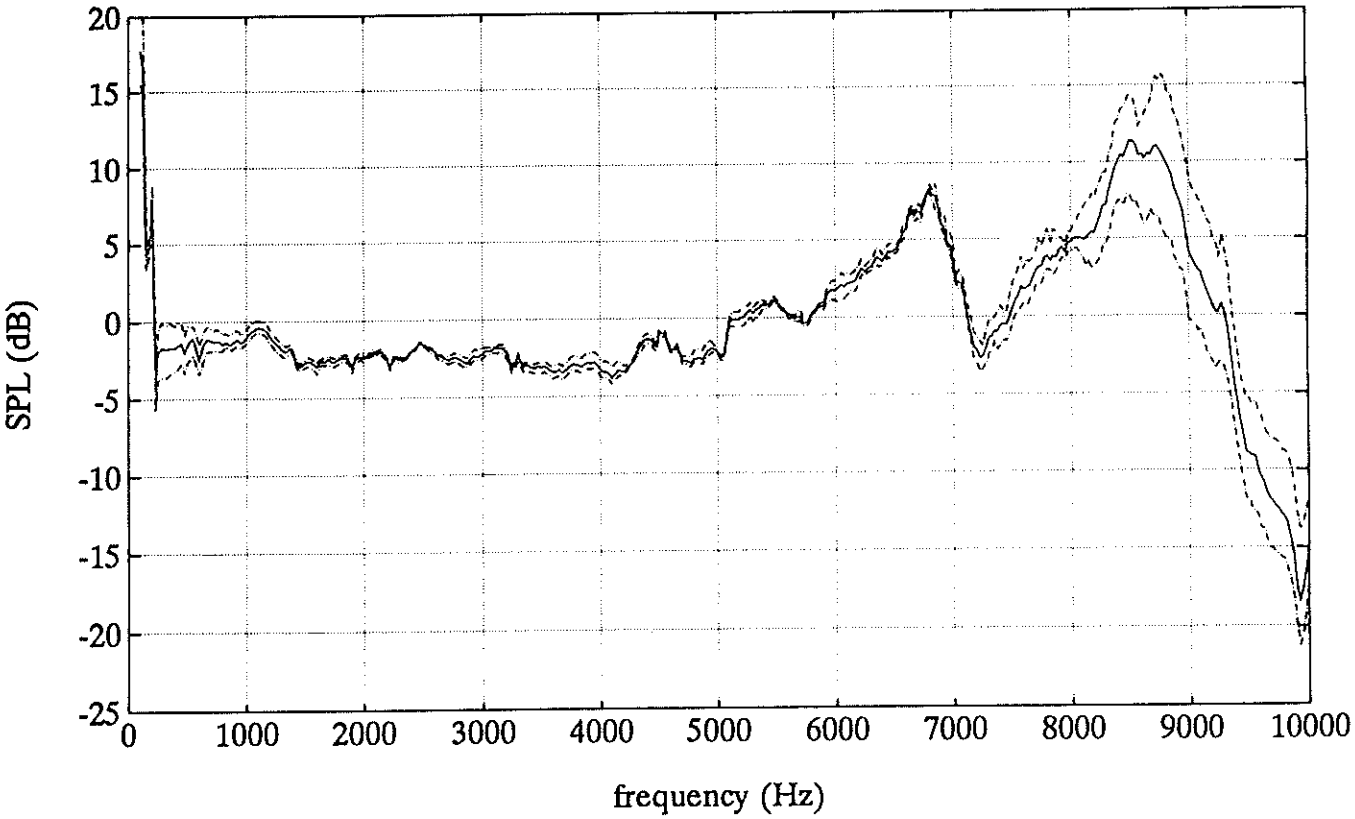

Figure 69. Predicted minus measured sound pressure level of Widex ES1 on subject D. Maximum, average and minimum of three measurements.

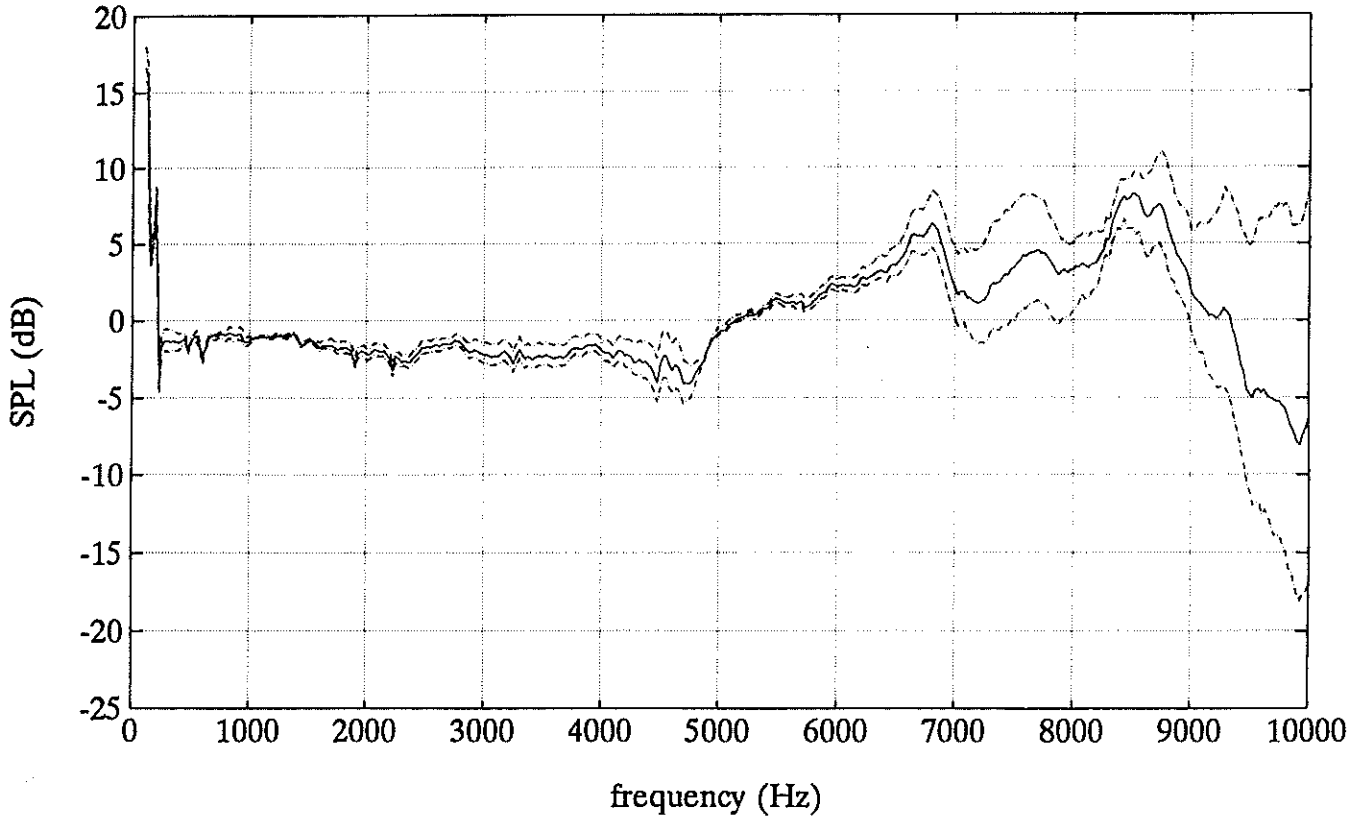

Figure 70. Predicted minus measured sound pressure level of Philips M49 on subject D. Maximum, average and minimum of three measurements.

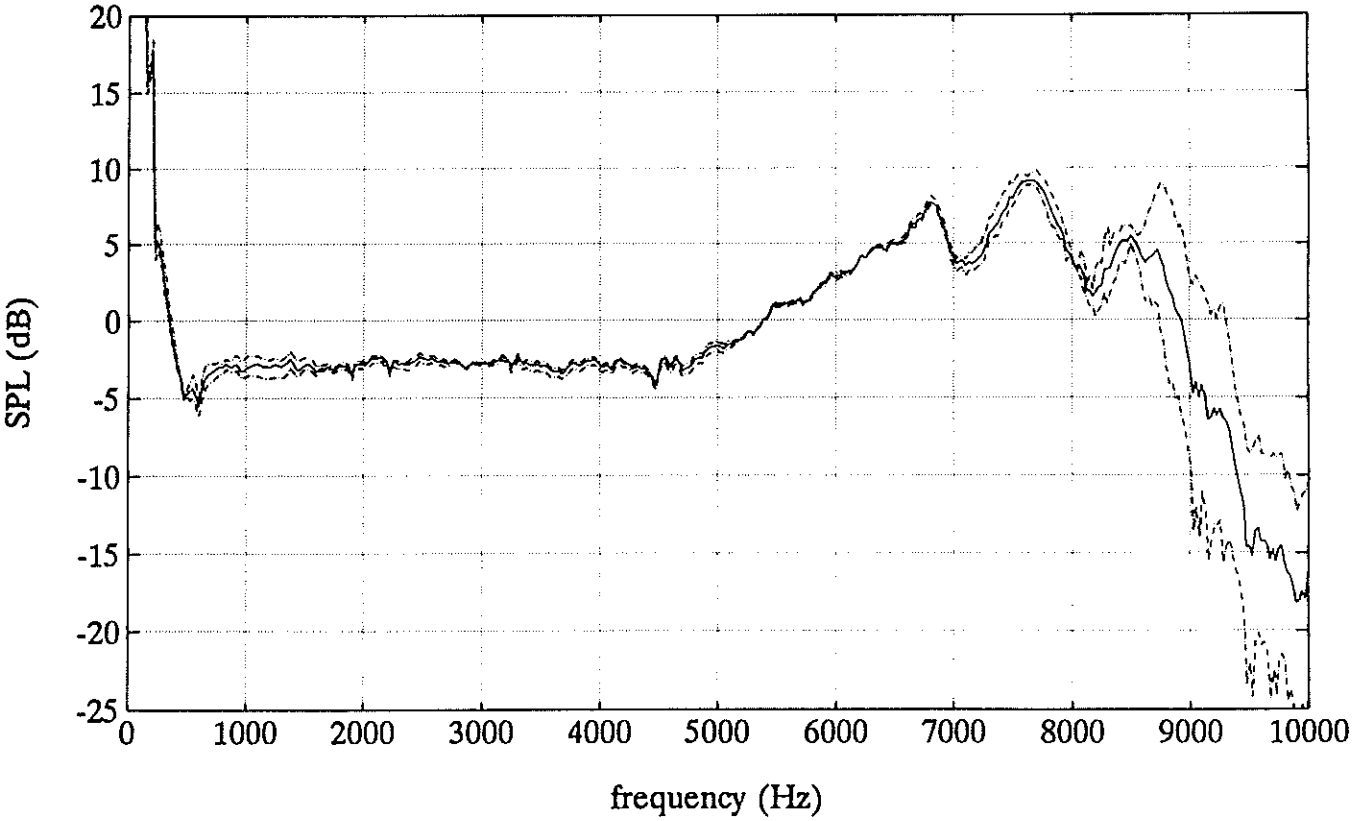

Figure 71. Predicted minus measured sound pressure level of Phonak Pico SC on subject D. Maximum, average and minimum of three measurements.

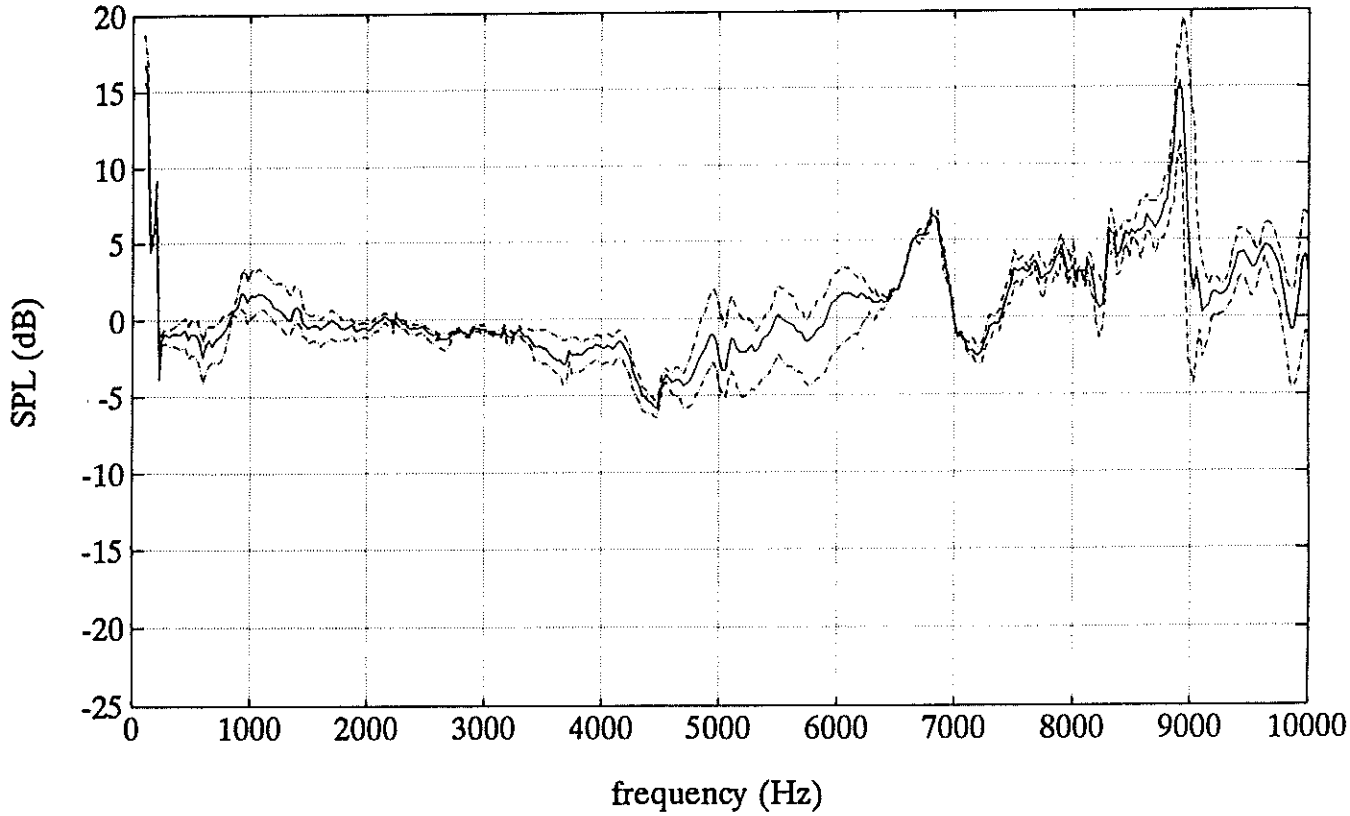

Figure 72. Predicted minus measured sound pressure level of Widex ES1 on subject E. Maximum, average and minimum of three measurements.

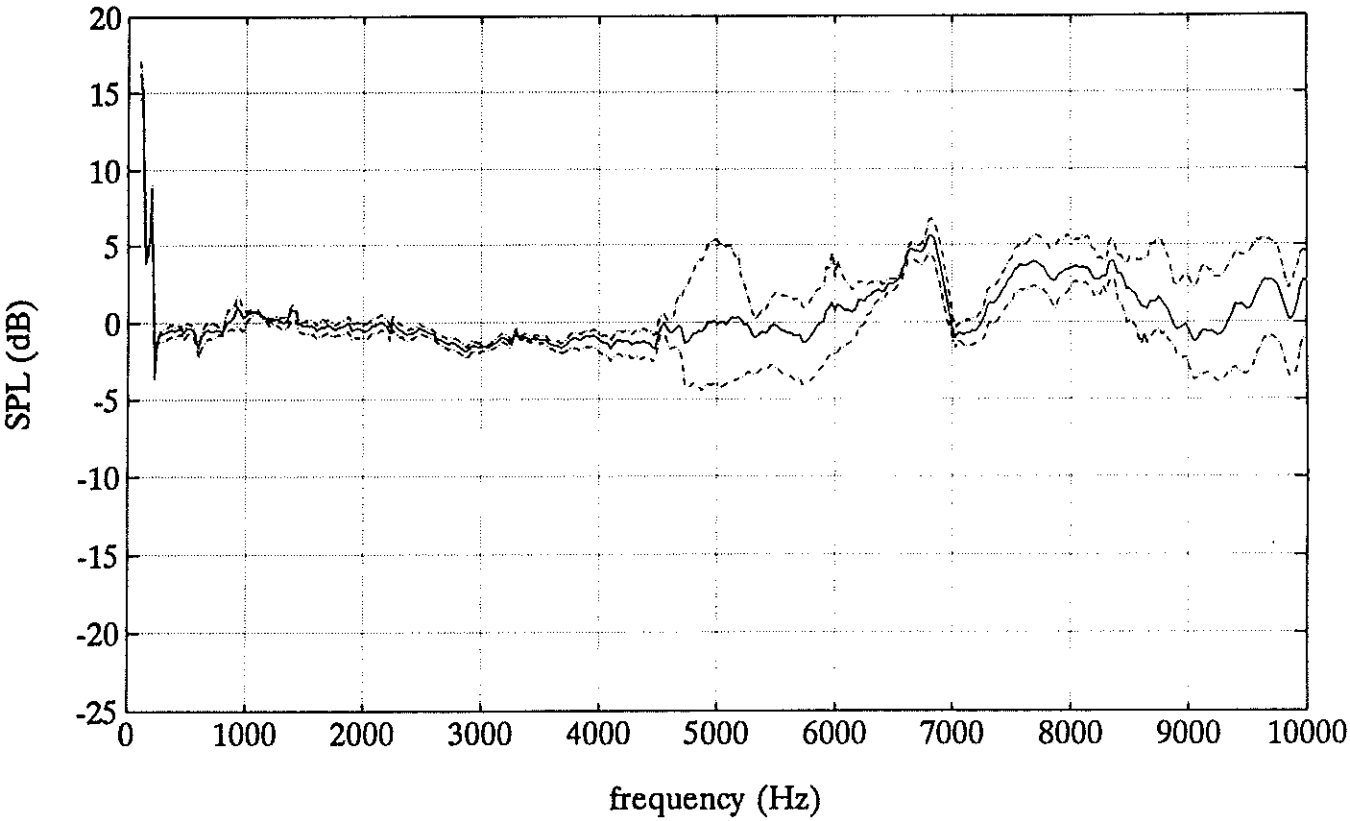

Figure 73. Predicted minus measured sound pressure level of Philips M49 on subject E. Maximum, average and minimum of three measurements.

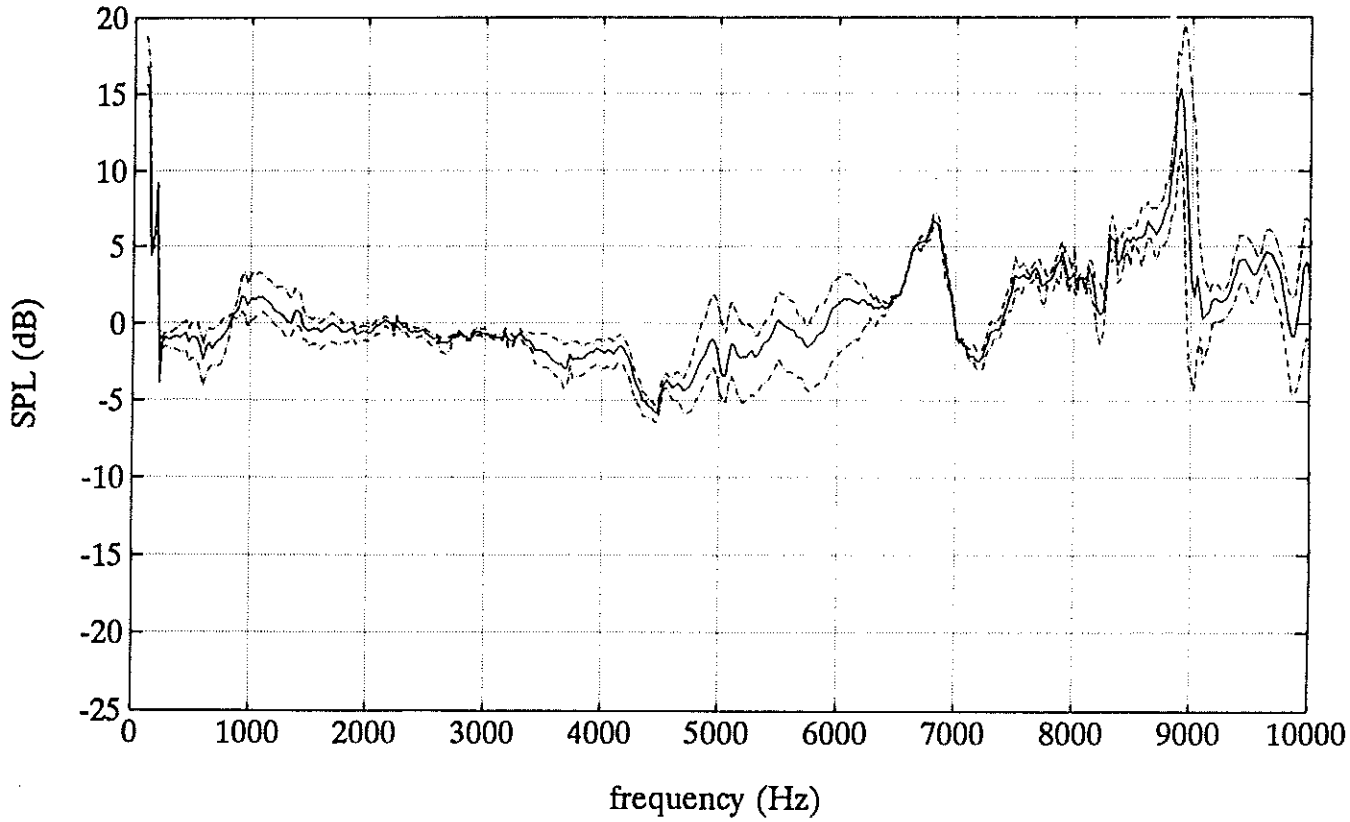

Figure 74. Predicted minus measured sound pressure level of Phonak Pico SC on subject E. Maximum, average and minimum of three measurements.

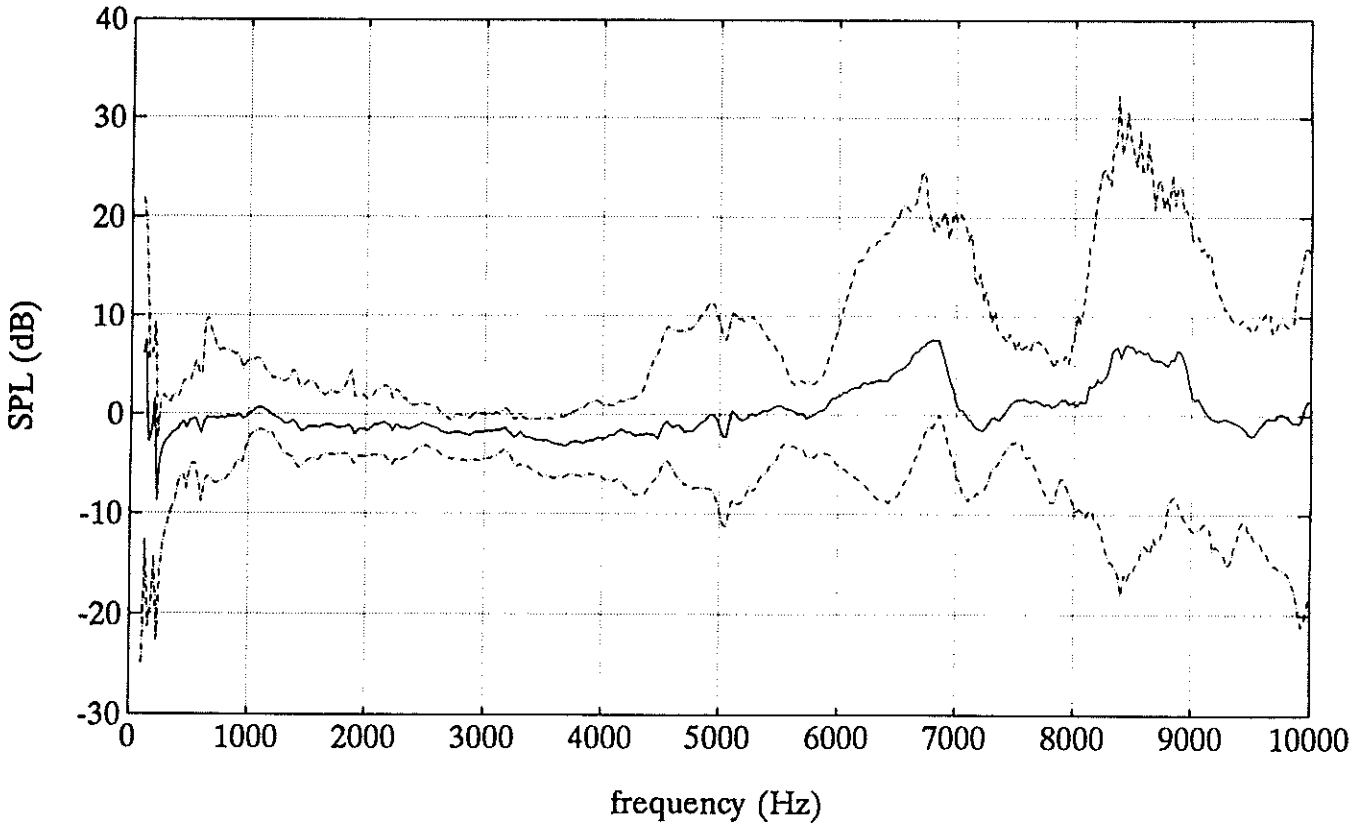

Figure 75. Maximum, average and minimum of prediction error with Widex ES1 over all subjects.

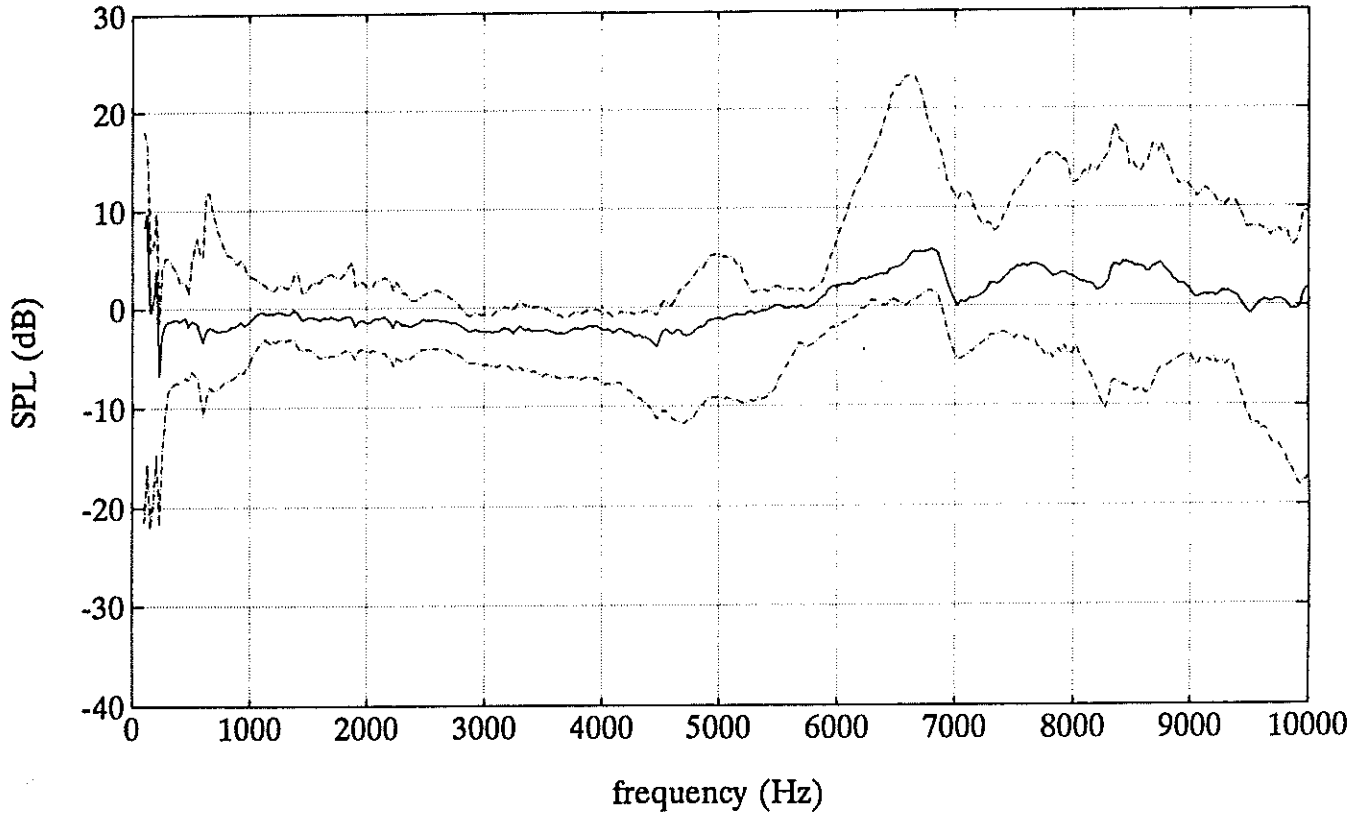

Figure 76. Maximum, average and minimum of prediction error with Philips M49 over all subjects.

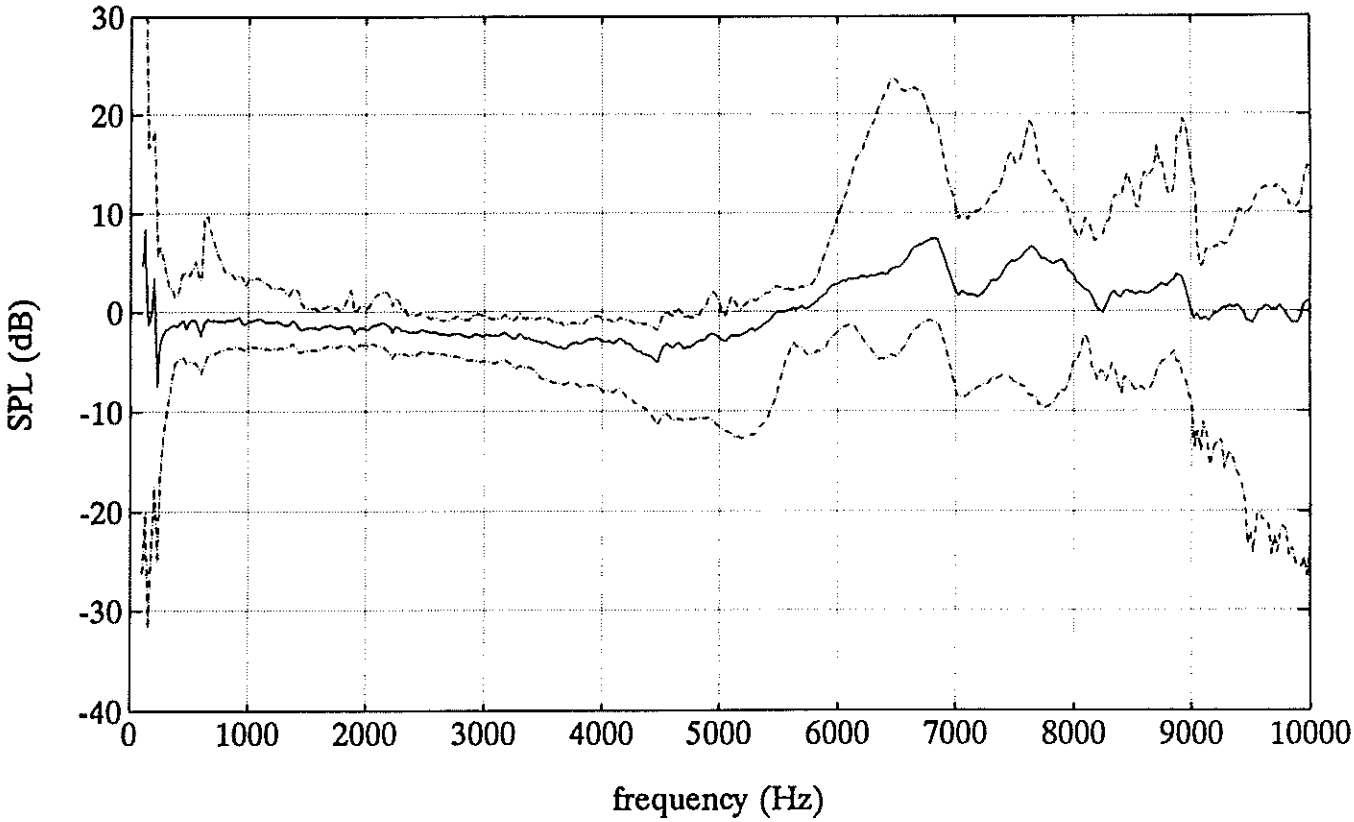

Figure 77. Maximum, average and minimum of prediction error with Phonak Pico SC over all subjects.

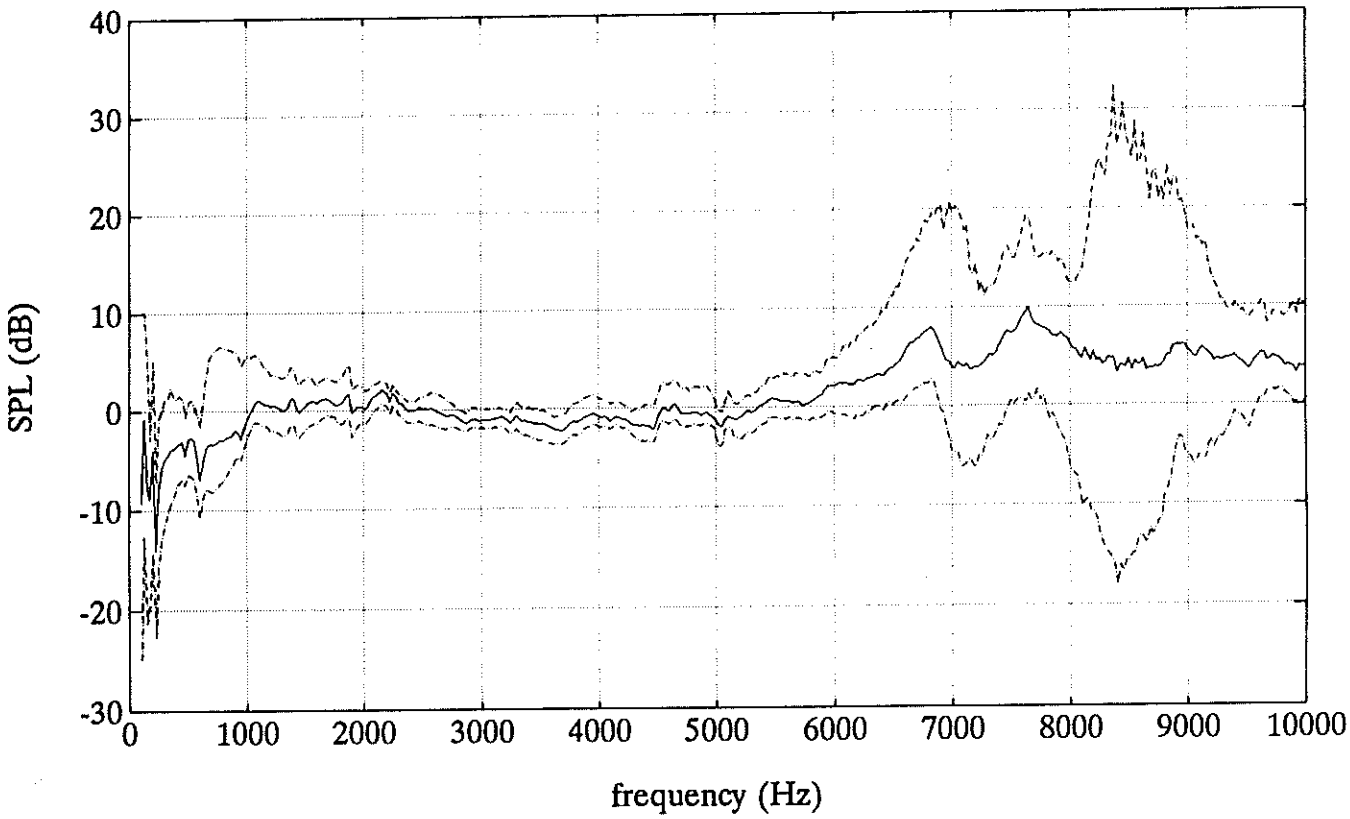

Figure 78. Maximum, average and minimum of prediction error on subject A over all hearing aids.

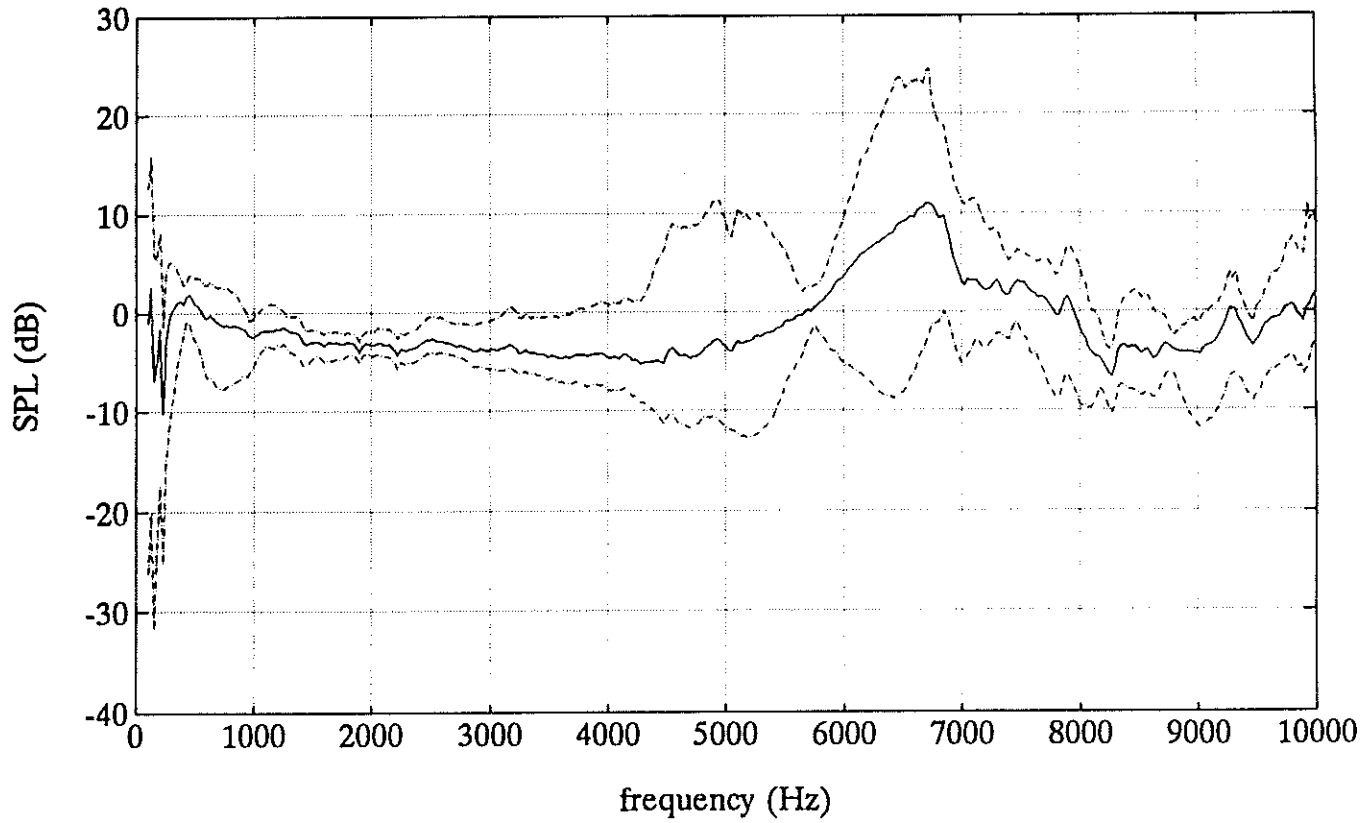

Figure 79. Maximum, average and minimum of prediction error on subject B over all hearing aids.

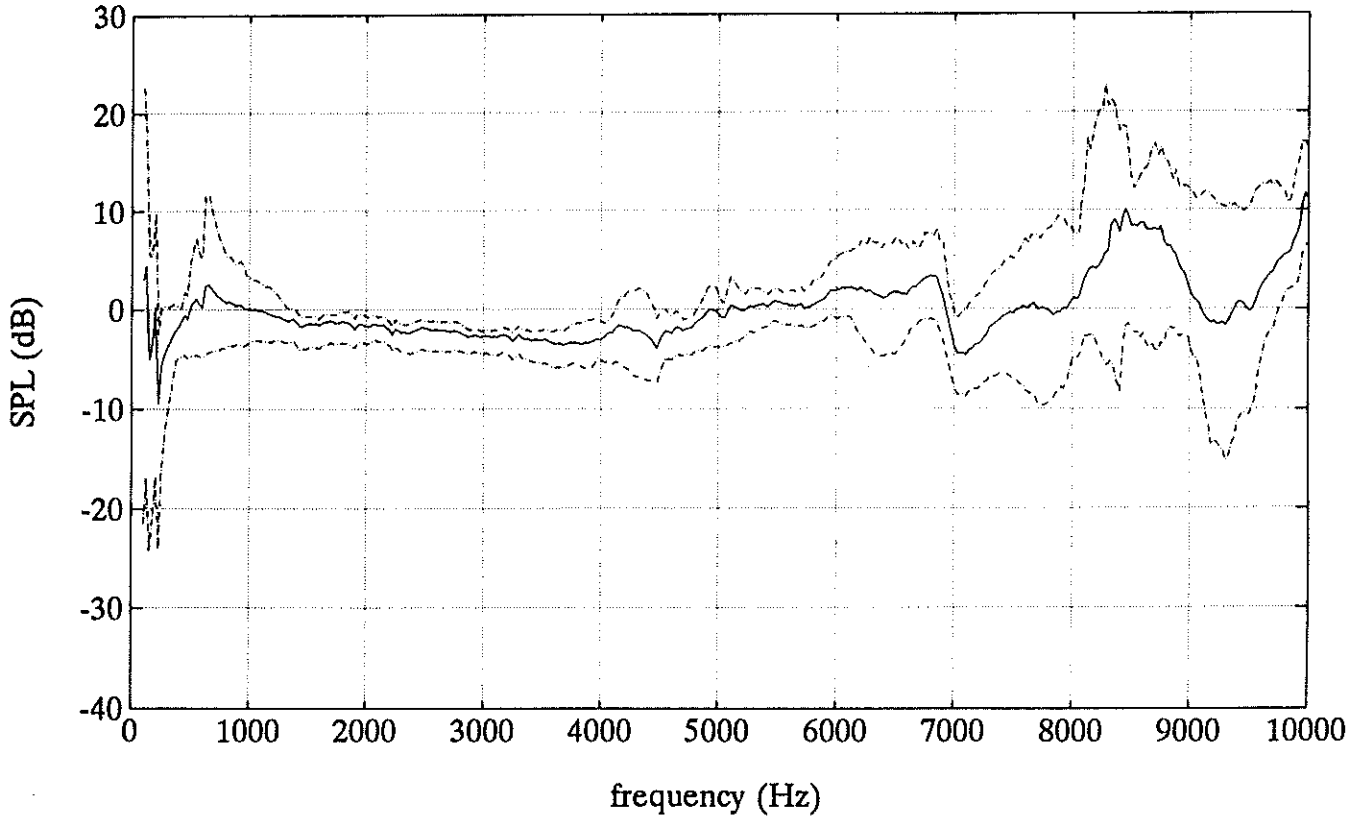

Figure 80. Maximum, average and minimum of prediction error on subject C over all hearing aids.

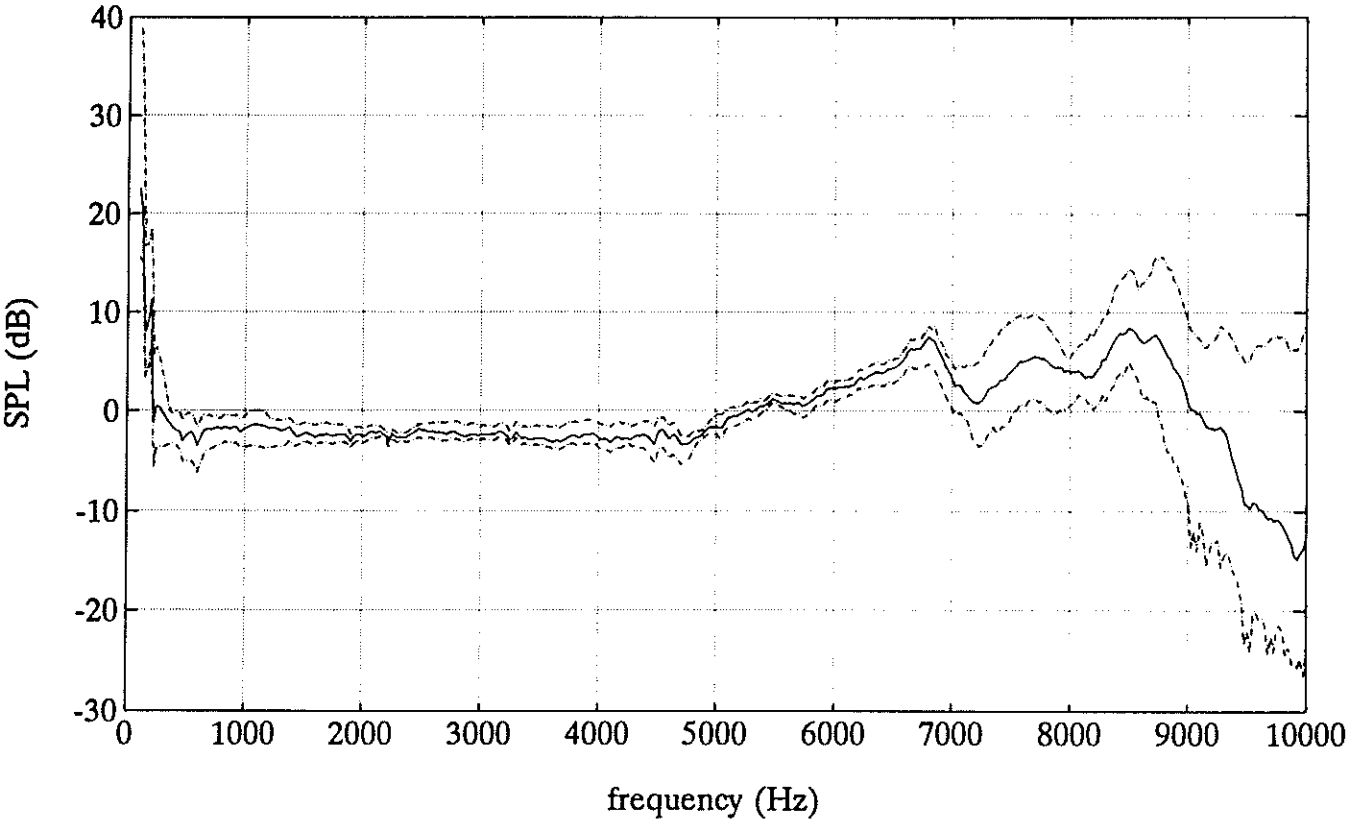

Figure 81. Maximum, average and minimum of prediction error on subject D over all hearing aids.

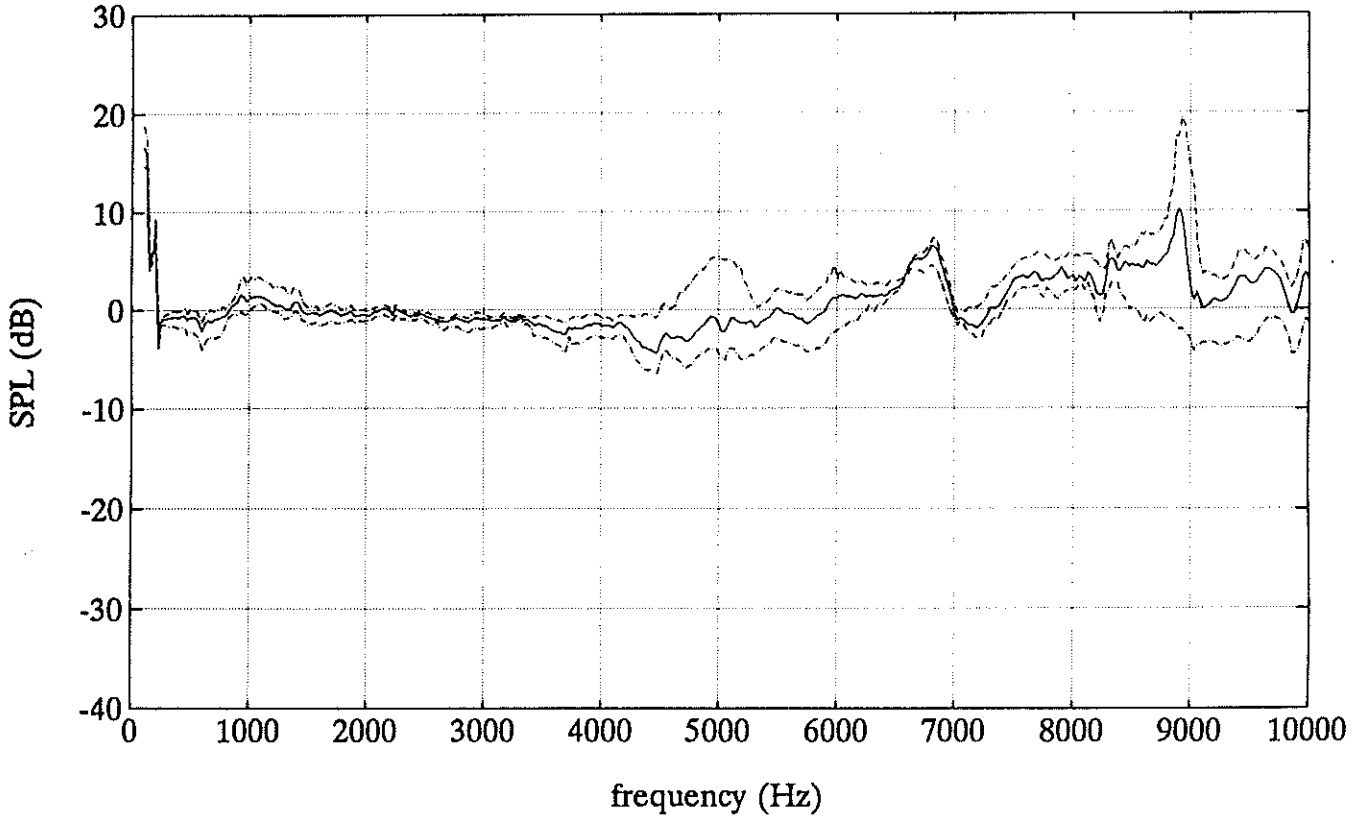

Figure 82. Maximum, average and minimum of prediction error on subject E over all hearing aids.

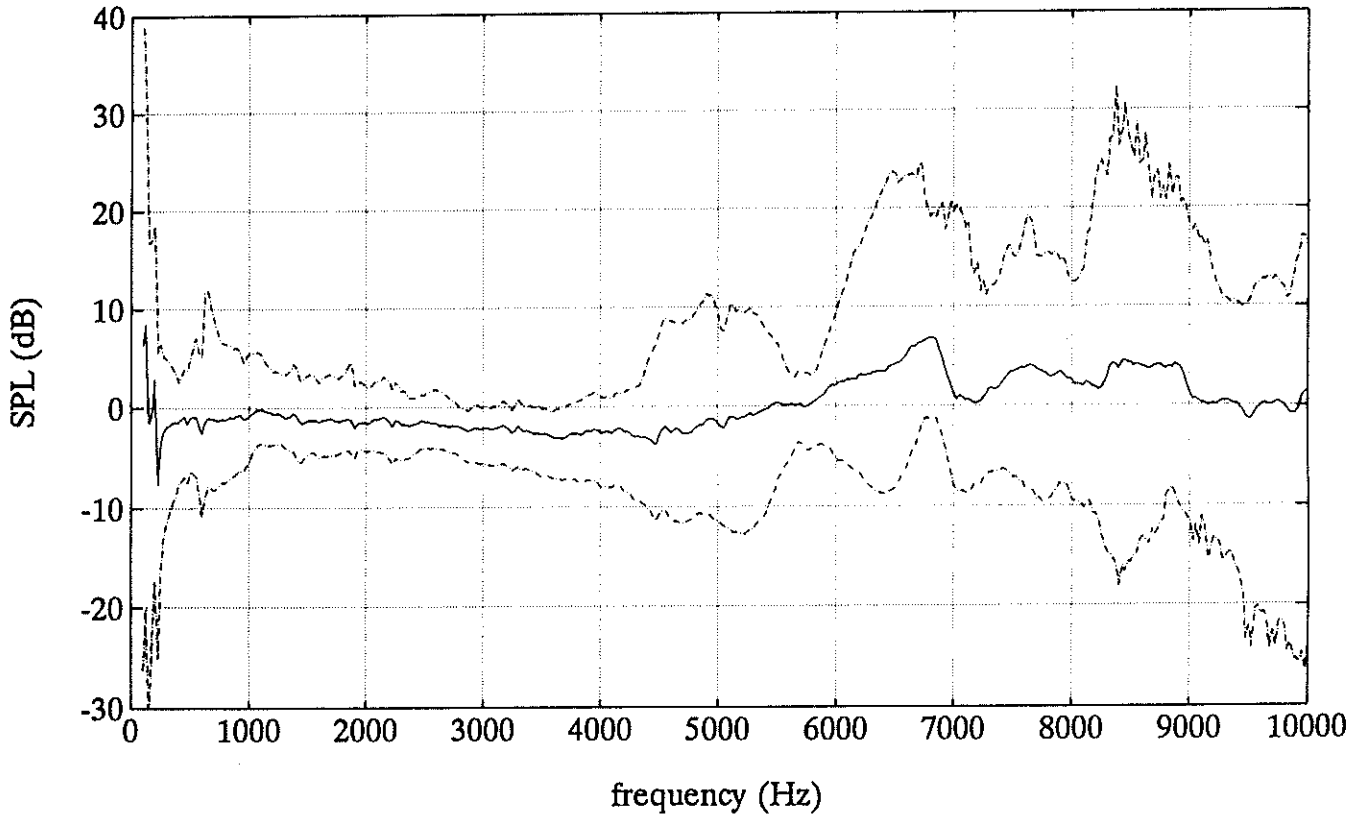

Figure 83. Maximum, average and minimum of prediction error over all hearing aids and subjects, with ear impedance measured at 100-105 dB(max).

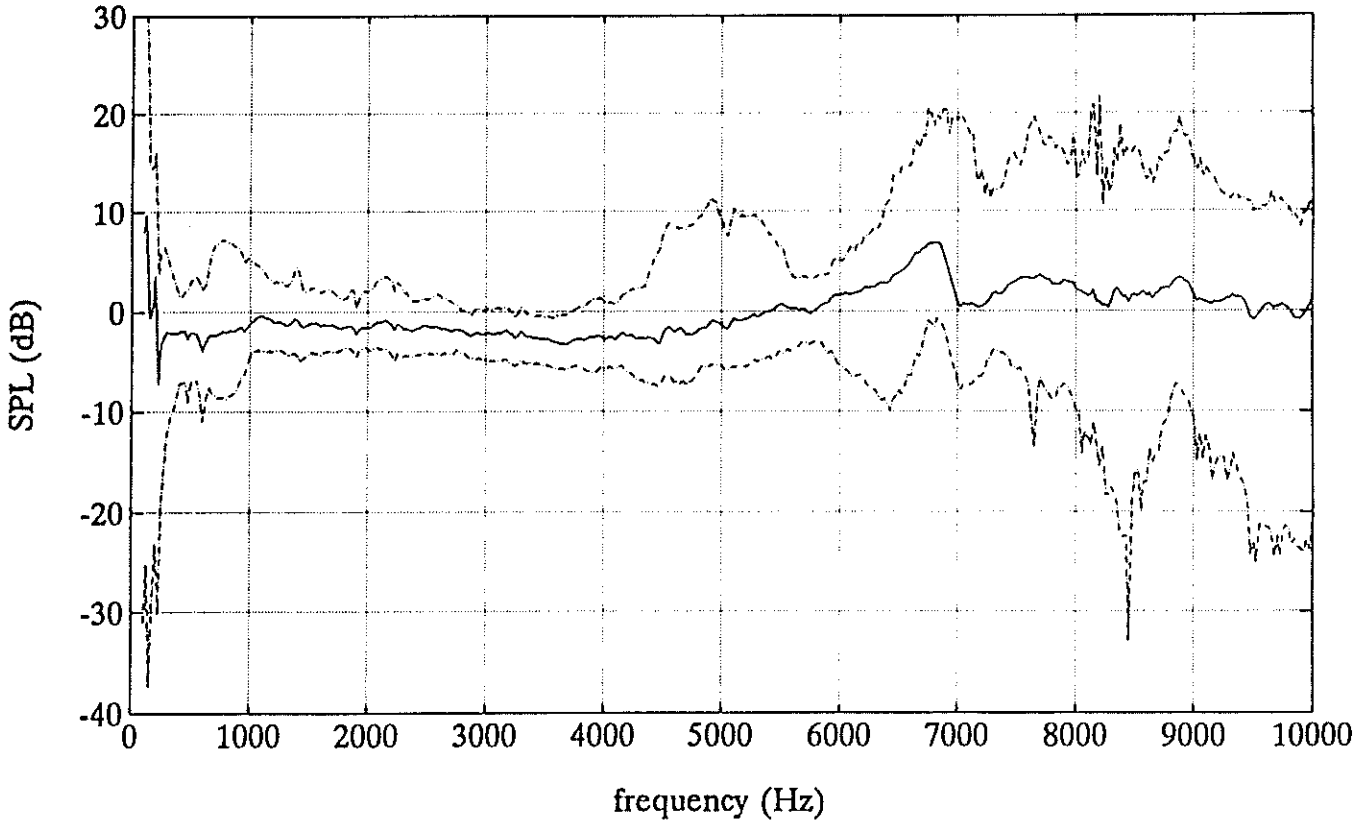

Figure 84. Maximum, average and minimum of prediction error over all hearing aids and subjects, with ear impedance measured at 80-85 dB(max).

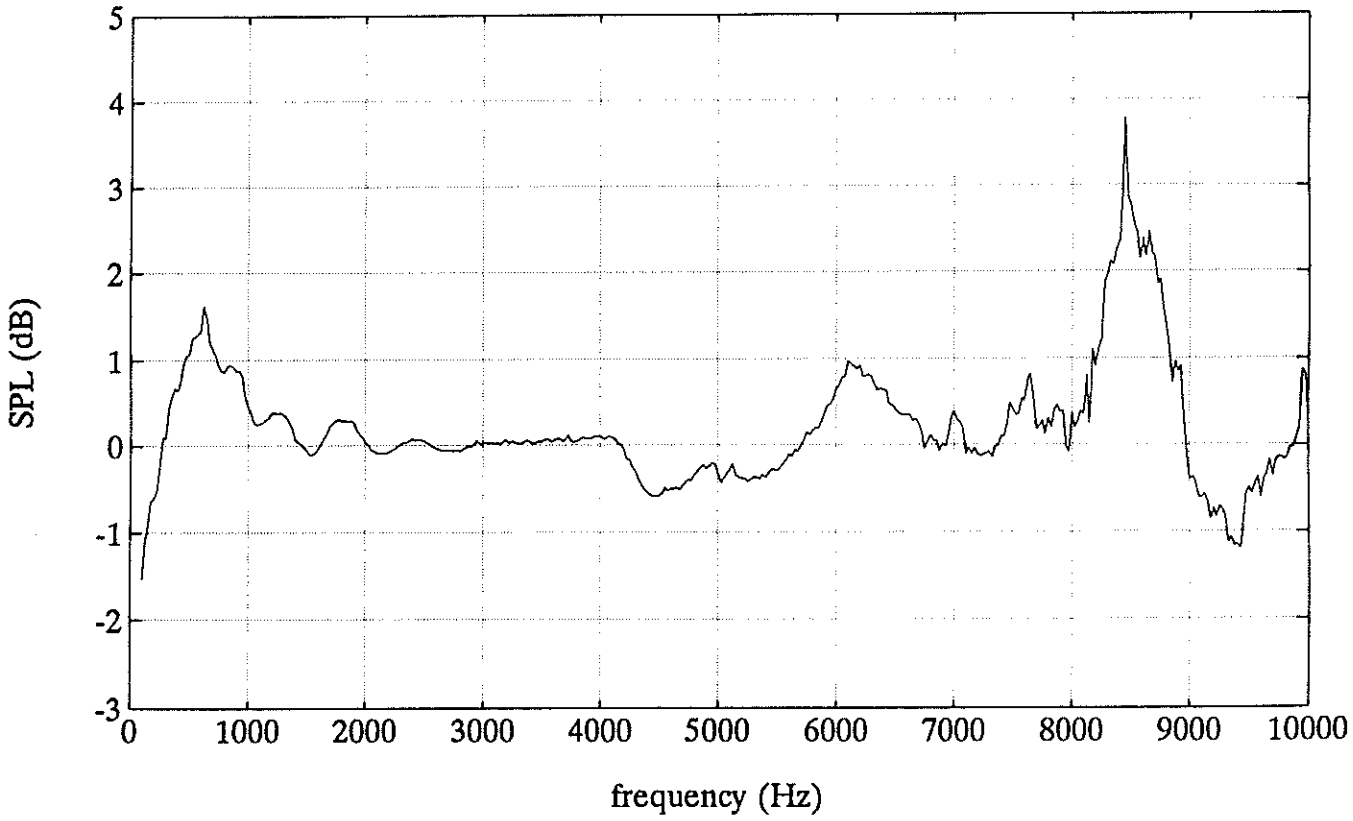

Figure 85. Average over hearing-aids and subjects of prediction error with ear impedance measured at 100-105 dB(max) minus average over hearing aids and subjects of prediction error with ear impedance measured at 80-85 dB(max)

SIMULATED PROBE POSITION ERROR
IN HEARING-AID THEVENIN IMPEDANCE MEASUREMENT
(APPEND1.MCD, 930920)

$i := \sqrt{-1}$

pi := 3.141593

Time factor: $-i\omega t$

Frequency points: fp := 1 ..100

Frequency factor: ff := 100 => 100Hz - 10kHz

HEARING-AID THEVENIN IMPEDANCE

Receiver output impedance (Pa*s/m^3): $ZR := 10^{9}$

Viscousity of air (kg/m*s): $\mu := 1.7 \cdot 10^{-5}$

Speed of sound (m/s): c := 340

Air density (kg/m^3): $\rho := 1.3$

Tygon tube radius (m): r := 0.001

Tygon tube length (m): l := 0.06

Specific heat at constant pressure (m^2/(s^2*K)): $cp := 1.0 \cdot 10^{3}$

cp/cv: $\Gamma := 1.40$

Thermal conductivity (W/(K*m)): ka := 0.024

Prandtls number: $Pr := \mu \cdot \frac{cp}{ka}$

The complex wavenumber for the case of wide ducts with losses is
(Pierce: ACOUSTICS, eq.10-5.10):

$$K(fp) := 2 \cdot pi \cdot fp \cdot \frac{ff}{c} + (1 + i) \cdot 0.353 \cdot \left[2 \cdot pi \cdot fp \cdot ff \cdot \frac{\mu}{\rho \cdot c^{2}}\right]^{0.5} \cdot \left[1 + \frac{\Gamma - 1}{\sqrt{Pr}}\right] \cdot \frac{2}{r}$$

$KL(fp) := K(fp) \cdot l$

The characteristic impedance is given by Pierce: ACOUSTICS, eq.3-7.3:

$$ZKAR(fp) := 2 \cdot pi \cdot fp \cdot ff \cdot \frac{\rho}{K(fp) \cdot pi \cdot r^{2}}$$

The hearing-aid output impedance is given by
(Pierce: ACOUSTICS, eq.3-7.2):

$$HAOI(fp) := ZKAR(fp)\cdot\frac{ZR\cdot\cos(KL(fp)) - i\cdot ZKAR(fp)\cdot\sin(KL(fp))}{ZKAR(fp)\cdot\cos(KL(fp)) - i\cdot ZR\cdot\sin(KL(fp))}$$

Probe position error in measurement (m): $dl := 0.001$

Tygon tube cross-section (m^2): $A := \pi\cdot r^2$

Hearing-aid Thevenin impedance measured with probe position error dl, for the case of no losses in dl, is given by
(Pierce: ACOUSTICS, eq.7-7.2):

$$K11(fp) := \cos(K(fp)\cdot dl) \qquad K12(fp) := -i\cdot\frac{\rho\cdot c}{A}\cdot\sin(K(fp)\cdot dl)$$

$$K21(fp) := -i\cdot\frac{A}{\rho\cdot c}\cdot\sin(K(fp)\cdot dl) \qquad K22(fp) := \cos(K(fp)\cdot dl)$$

$$HAOIE(fp) := \frac{K11(fp)\cdot HAOI(fp) + K12(fp)}{K21(fp)\cdot HAOI(fp) + K22(fp)}$$

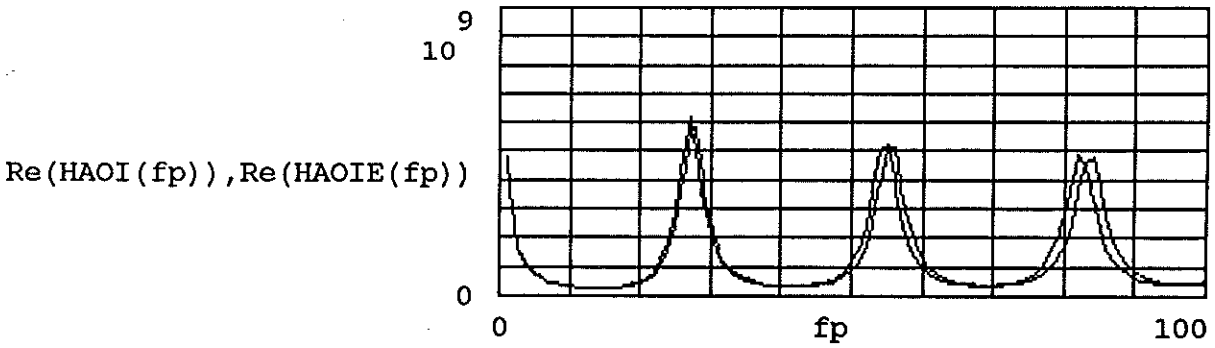

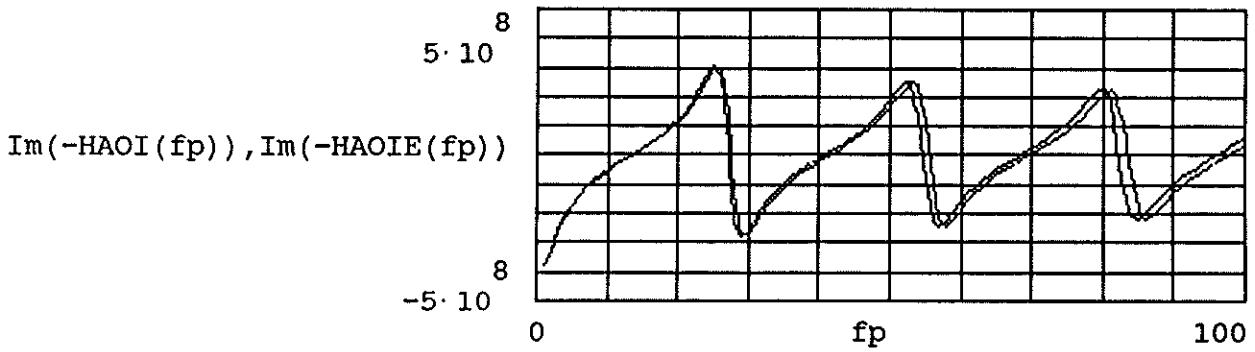

EAR INPUT IMPEDANCE

The ear input impedance (cgs-units) at the eardrum is given by the electrical analog in "Shaw, Stinson: Network concepts and energy flow in the human middle-ear", The 101st meeting of the Acoustical Society of America, 19-22 May 1981, Invited paper T2.

The middle-ear cavities:

$La := 20 \cdot 10^{-3}$ $Ra := 10$ $Cp := 5.1 \cdot 10^{-6}$

$Rm := 200$ $Ct := 0.35 \cdot 10^{-6}$

Eardrum area coupling system:

$Rdo := 170$ $Cdo := 0.2 \cdot 10^{-6}$ $SdSo := 9$

"Outer" eardrum:

$Rd := 10$ $Ld := 12 \cdot 10^{-3}$ $Cd := 3.0 \cdot 10^{-6}$

Incudo - stapedial joint:

$Rs := 3.0 \cdot 10^{5}$ $Cs := 3.0 \cdot 10^{-9}$

"Centre" eardrum, malleus and incus:

$Ro := 9.0 \cdot 10^{3}$ $Lo := 3.0$ $Co := 15.0 \cdot 10^{-9}$

Stapes, oval window and cochlea:

$Rc := 6.0 \cdot 10^{4}$ $Lc := 2.0$ $Cc := 5.0 \cdot 10^{-9}$

$b := 2 \cdot pi \cdot ff$

Impedance of stapes, oval window and cochlea:

$$Zsowc(fp) := Rc + i \cdot b \cdot fp \cdot Lc + \frac{1}{i \cdot b \cdot fp \cdot Cc}$$

Impedance of "centre" eardrum. malleus and incus:

$$Zcemi(fp) := Ro + i \cdot b \cdot fp \cdot Lo + \frac{1}{i \cdot b \cdot fp \cdot Co}$$

Impedance of incudo-stapedial loint:

$$Zisj(fp) := Rs + \frac{1}{i \cdot b \cdot fp \cdot Cs}$$

Transformed impedance of "centre" eardrum:

$$Zsot(fp) := \frac{1}{SdSo} \cdot \left[Zcemi(fp) + Zsowc(fp) \cdot \left[\frac{Zisj(fp)}{Zsowc(fp) + Zisj(fp)} \right] \right]$$

Shunt impedance of eardrum area coupling system:

$$Zeacs(fp) := Rdo + \frac{1}{i \cdot b \cdot fp \cdot Cdo}$$

Impedance of outer eardrum:

$$Zoe(fp) := Rd + i \cdot b \cdot fp \cdot Ld + \frac{1}{i \cdot b \cdot fp \cdot Cd}$$

Impedance of middle-ear cavities:

$$Zmec(fp) := \frac{1}{\frac{1}{Rm} + i \cdot b \cdot fp \cdot Ct + \frac{1}{Ra + i \cdot b \cdot fp \cdot La + \frac{1}{i \cdot b \cdot fp \cdot Cp}}}$$

Ear input impedance at the eardrum:

$$ZShaw(fp) := Zmec(fp) + Zoe(fp) + Zsot(fp) \cdot \frac{Zeacs(fp)}{Zsot(fp) + Zeacs(fp)}$$

In MKS-units:

$$ZED(fp) := 10^{5} \cdot (Re(ZShaw(fp)) - i \cdot Im(ZShaw(fp)))$$

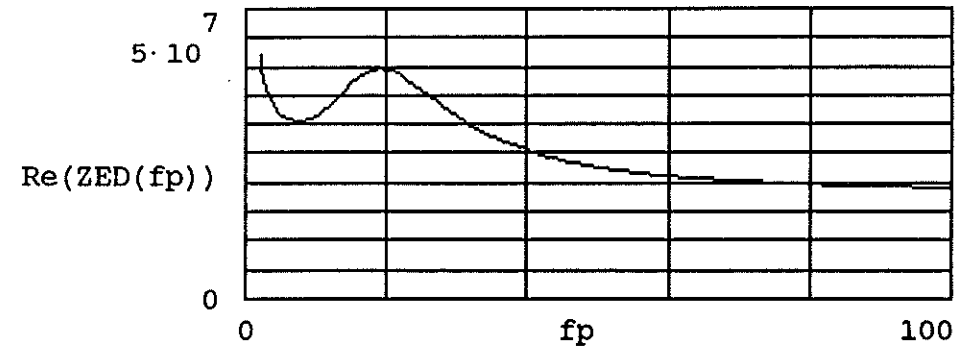

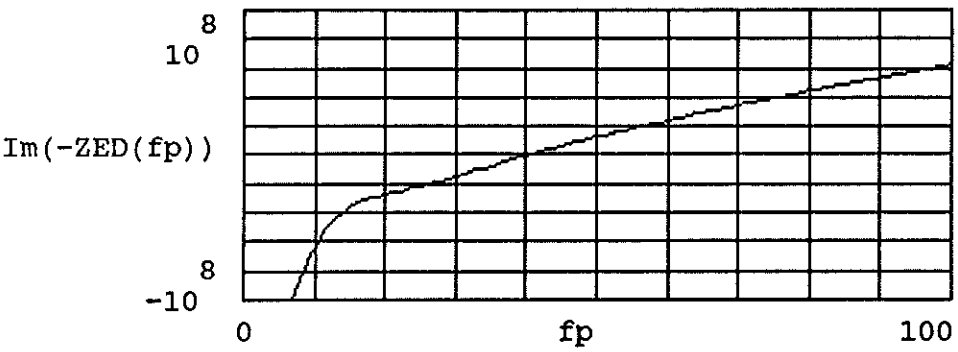

Ear input impedance at mold end (Pa*s/m^3):

Ear canal radius (m): rec := 0.00375

Length of ear canal from mold end (m): lec := 0.015

Complex wave number in ear canal:

$$K(fp) := 2\cdot pi\cdot fp\cdot\frac{ff}{c} + (1 + i)\cdot 0.353\cdot\left[2\cdot pi\cdot fp\cdot ff\cdot\frac{\mu}{\rho\cdot c^2}\right]^{0.5}\cdot\left[1 + \frac{\Gamma - 1}{\sqrt{Pr}}\right]\cdot\frac{2}{rec}$$

Characteristic impedance in ear canal:

$$ZKEC(fp) := 2\cdot pi\cdot ff\cdot fp\cdot\frac{\rho}{K(fp)\cdot pi\cdot rec^2}$$

$$KLEC(fp) := lec\cdot K(fp)$$

Ear input impedance at mold end:

$$ZEar(fp) := ZKEC(fp)\cdot\frac{ZED(fp)\cdot\cos(KLEC(fp)) - i\cdot ZKEC(fp)\cdot\sin(KLEC(fp))}{ZKEC(fp)\cdot\cos(KLEC(fp)) - i\cdot ZED(fp)\cdot\sin(KLEC(fp))}$$

Ratio "ear canal pressure"/"hearing-aid Thevenin pressure", with error:

$$REPTPE(fp) := \frac{ZEar(fp)}{ZEar(fp) + HAOIE(fp)}$$

Ratio "ear canal pressure"/"hearing-aid Thevenin pressure", without error:

$$REPTP(fp) := \frac{ZEar(fp)}{ZEar(fp) + HAOI(fp)}$$

$$LPE(fp) := 10\cdot\log\left[(Re(REPTPE(fp)))^2 + (Im(REPTPE(fp)))^2 + 10^{-9}\right]$$

$$LP(fp) := 10\cdot\log\left[(Re(REPTP(fp)))^2 + (Im(REPTP(fp)))^2 + 10^{-9}\right]$$

$$LPDIFF(fp) := LPE(fp) - LP(fp)$$

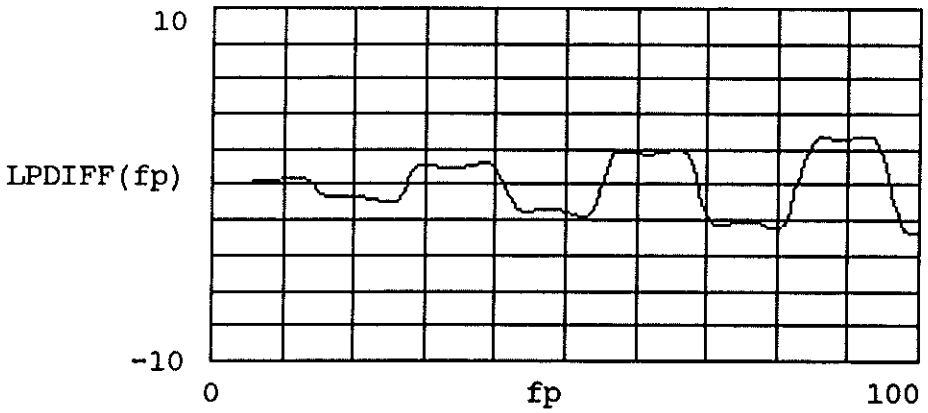

SIMULATED PROBE POSITION ERROR IN EAR IMPEDANCE MEASUREMENT
(APPEND2.MCD, 930921)

$i := \sqrt{-1}$

pi := 3.141593

Time dependece: -iωt

Frequency points: fp := 1 ..100

Frequency factor: ff := 100 => 100Hz - 10kHz

HEARING-AID THEVENIN IMPEDANCE

Receiver output impedance (Pa*s/m^3): $ZR := 10^{9}$

Viscousity of air (kg/m*s): $\mu := 1.7 \cdot 10^{-5}$

Speed of sound (m/s): c := 340

Air density (kg/m^3): ρ := 1.3

Tygon tube radius (m): r := 0.001

Tygon tube length (m): l := 0.06

Specific heat at constant pressure (m^2/(s^2*K)): $cp := 1.0 \cdot 10^{3}$

cp/cv: Γ := 1.40

Thermal conductivity (W/(K*m)): ka := 0.024

Prandtls number: $Pr := \mu \cdot \frac{cp}{ka}$

The complex wavenumber for the case of wide ducts with losses is
(Pierce: ACOUSTICS, eq.10-5.10):

$$K(fp) := 2 \cdot pi \cdot fp \cdot \frac{ff}{c} + (1 + i) \cdot 0.353 \cdot \left[2 \cdot pi \cdot fp \cdot ff \cdot \frac{\mu}{\rho \cdot c^{2}}\right]^{0.5} \cdot \left[1 + \frac{\Gamma - 1}{\sqrt{Pr}}\right] \cdot \frac{2}{r}$$

KL(fp) := K(fp)·l

The characteristic impedance is given by Pierce: ACOUSTICS, eq.3-7.3:

$$ZKAR(fp) := 2 \cdot pi \cdot fp \cdot ff \cdot \frac{\rho}{K(fp) \cdot pi \cdot r^{2}}$$

The hearing-aid output impedance is given by
(Pierce: ACOUSTICS, eq.3-7.2):

$$HAOI(fp) := ZKAR(fp) \cdot \frac{ZR \cdot \cos(KL(fp)) - i \cdot ZKAR(fp) \cdot \sin(KL(fp))}{ZKAR(fp) \cdot \cos(KL(fp)) - i \cdot ZR \cdot \sin(KL(fp))}$$

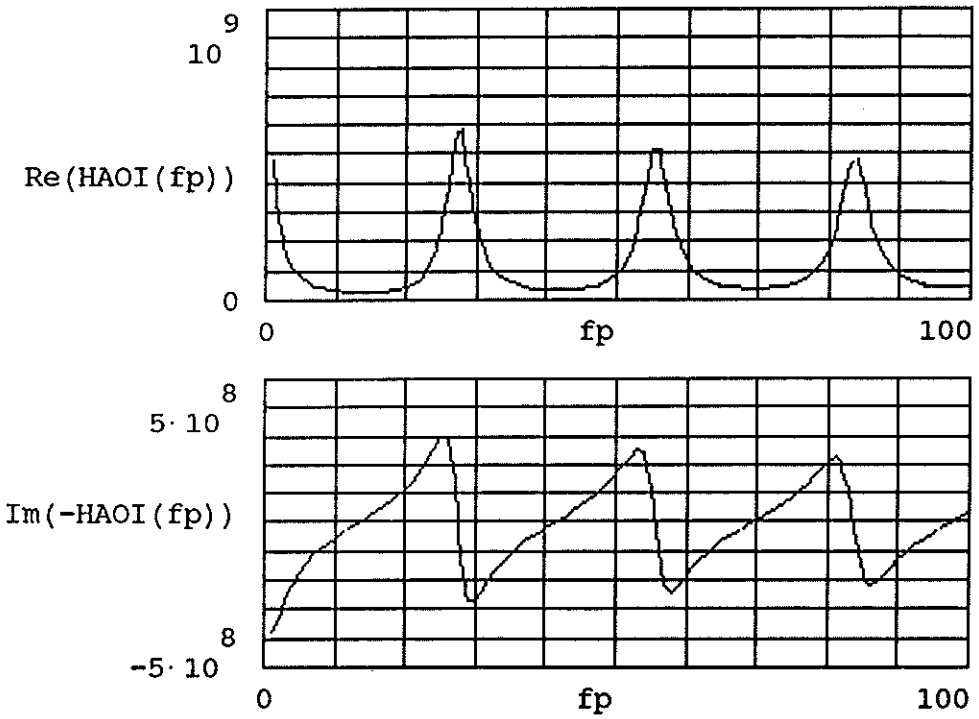

EAR INPUT IMPEDANCE

The ear input impedance (cgs-units) at the eardrum is given by the electrical analog in "Shaw, Stinson: Network concepts and energy flow in the human middle-ear", The 101st meeting of the Acoustical Society of America, 19-22 May 1981, Invited paper T2.

The middle-ear cavities:

$La := 20 \cdot 10^{-3}$ $Ra := 10$ $Cp := 5.1 \cdot 10^{-6}$

$Rm := 200$ $Ct := 0.35 \cdot 10^{-6}$

Eardrum area coupling system:

$Rdo := 170$ $Cdo := 0.2 \cdot 10^{-6}$ $SdSo := 9$

"Outer" eardrum:

$Rd := 10$ $Ld := 12 \cdot 10^{-3}$ $Cd := 3.0 \cdot 10^{-6}$

Incudo - stapedial joint:

$Rs := 3.0 \cdot 10^{5}$ $Cs := 3.0 \cdot 10^{-9}$

"Centre" eardrum, malleus and incus:

$Ro := 9.0 \cdot 10^{3}$ $Lo := 3.0$ $Co := 15.0 \cdot 10^{-9}$

Stapes, oval window and cochlea:

$Rc := 6.0 \cdot 10^{4}$ $Lc := 2.0$ $Cc := 5.0 \cdot 10^{-9}$

$b := 2 \cdot pi \cdot ff$

Impedance of stapes, oval window and cochlea:

$$Zsowc(fp) := Rc + i \cdot b \cdot fp \cdot Lc + \frac{1}{i \cdot b \cdot fp \cdot Cc}$$

Impedance of "centre" eardrum. malleus and incus:

$$Zcemi(fp) := Ro + i \cdot b \cdot fp \cdot Lo + \frac{1}{i \cdot b \cdot fp \cdot Co}$$

Impedance of incudo-stapedial loint:

$$Zisj(fp) := Rs + \frac{1}{i \cdot b \cdot fp \cdot Cs}$$

Transformed impedance of "centre" eardrum:

$$Zsot(fp) := \frac{1}{SdSo} \cdot \left[Zcemi(fp) + Zsowc(fp) \cdot \left[\frac{Zisj(fp)}{Zsowc(fp) + Zisj(fp)} \right] \right]$$

Shunt impedance of eardrum area coupling system:

$$Zeacs(fp) := Rdo + \frac{1}{i \cdot b \cdot fp \cdot Cdo}$$

Impedance of outer eardrum:

$$Zoe(fp) := Rd + i \cdot b \cdot fp \cdot Ld + \frac{1}{i \cdot b \cdot fp \cdot Cd}$$

Impedance of middle-ear cavities:

$$Zmec(fp) := \frac{1}{\frac{1}{Rm} + i \cdot b \cdot fp \cdot Ct + \frac{1}{Ra + i \cdot b \cdot fp \cdot La + \frac{1}{i \cdot b \cdot fp \cdot Cp}}}$$

Ear input impedance at the eardrum:

$$ZShaw(fp) := Zmec(fp) + Zoe(fp) + Zsot(fp) \cdot \frac{Zeacs(fp)}{Zsot(fp) + Zeacs(fp)}$$

In MKS-units:

$ZED(fp) := 10^{5} \cdot (Re(ZShaw(fp)) - i \cdot Im(ZShaw(fp)))$

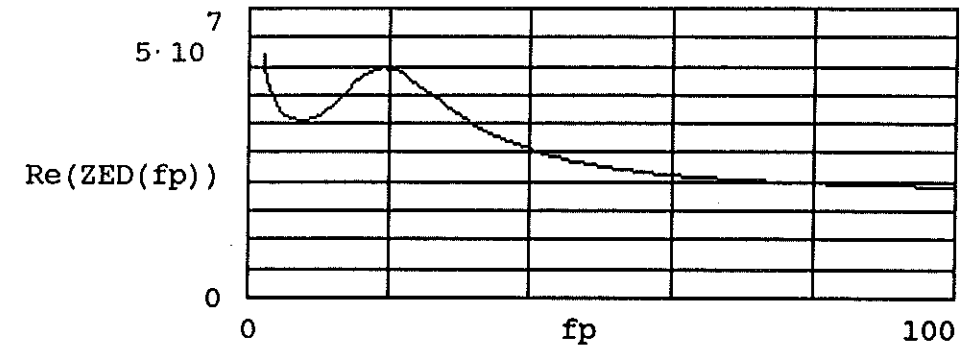

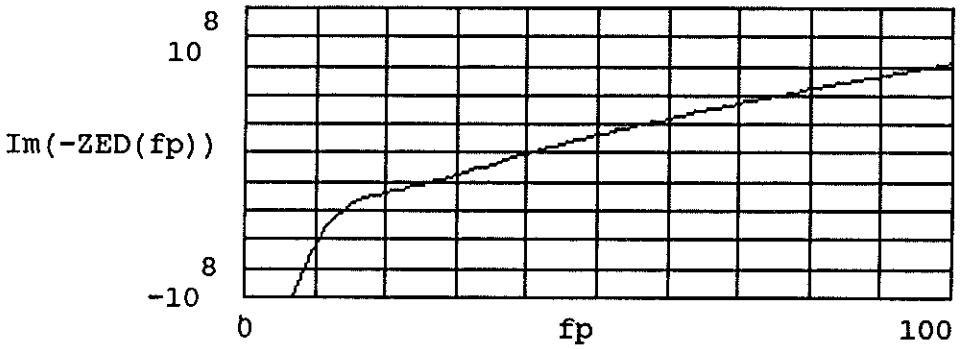

Ear canal radius (m): $rec := 0.00375$

Length of ear canal from mold end (m): $lec := 0.015$

Complex wave number in ear canal:

$$K(fp) := 2 \cdot pi \cdot fp \cdot \frac{ff}{c} + (1 + i) \cdot 0.353 \cdot \left[2 \cdot pi \cdot fp \cdot ff \cdot \frac{\mu}{\rho \cdot c^{2}}\right]^{0.5} \cdot \left[1 + \frac{\Gamma - 1}{\sqrt{Pr}}\right] \cdot \frac{2}{rec}$$

Characteristic impedance in ear canal:

$$ZKEC(fp) := 2 \cdot pi \cdot ff \cdot fp \cdot \frac{\rho}{K(fp) \cdot pi \cdot rec^{2}}$$

$KLEC(fp) := lec \cdot K(fp)$

Ear input impedance at mold end:

$$ZEar(fp) := ZKEC(fp) \cdot \frac{ZED(fp) \cdot \cos(KLEC(fp)) - i \cdot ZKEC(fp) \cdot \sin(KLEC(fp))}{ZKEC(fp) \cdot \cos(KLEC(fp)) - i \cdot ZED(fp) \cdot \sin(KLEC(fp))}$$

Probe position error in measurement (m): $dl := 0.001$

Ear canal cross-section (m^2): $A := pi \cdot rec^{2}$

Ear input impedance measured with probe position error dl, for the case of no losses in dl, is given by (Pierce: ACOUSTICS, eq.7-7.2):

$$K11(fp) := \cos(K(fp)\cdot dl) \qquad K12(fp) := -i\cdot\frac{\rho\cdot c}{A}\cdot\sin(K(fp)\cdot dl)$$

$$K21(fp) := -i\cdot\frac{A}{\rho\cdot c}\cdot\sin(K(fp)\cdot dl) \qquad K22(fp) := \cos(K(fp)\cdot dl)$$

$$ZEare(fp) := \frac{K11(fp)\cdot ZEar(fp) + K12(fp)}{K21(fp)\cdot ZEar(fp) + K22(fp)}$$

Ratio "ear canal pressure"/"hearing-aid Thevenin pressure", with error:

$$REPTPE(fp) := \frac{ZEare(fp)}{ZEare(fp) + HAOI(fp)}$$

Ratio "ear canal pressure"/"hearing-aid Thevenin pressure", without error:

$$REPTP(fp) := \frac{ZEar(fp)}{ZEar(fp) + HAOI(fp)}$$

$$LPE(fp) := 10\cdot\log\left[(Re(REPTPE(fp)))^2 + (Im(REPTPE(fp)))^2 + 10^{-9}\right]$$

$$LP(fp) := 10\cdot\log\left[(Re(REPTP(fp)))^2 + (Im(REPTP(fp)))^2 + 10^{-9}\right]$$

$$LPDIFF(fp) := LPE(fp) - LP(fp)$$

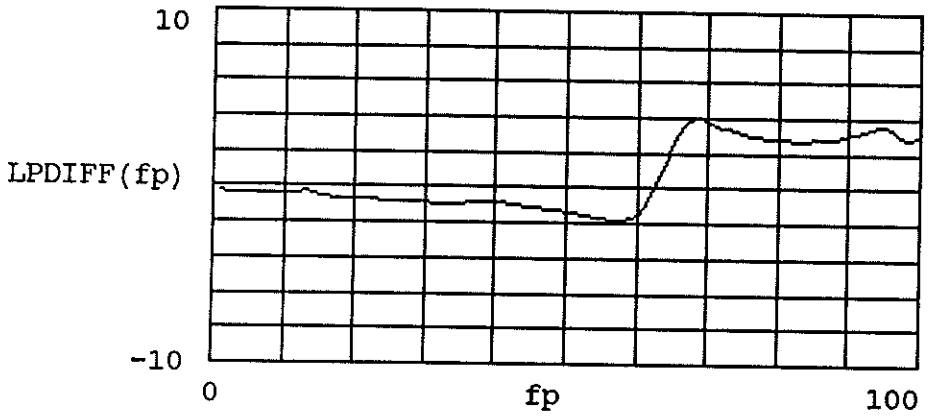

APPENDIX 3
DERIVATION OF THE LMS-SOLUTION
(APPEND3.MCD, 930921)

The overdetermined system is given by A*s=f or

$$\begin{bmatrix} Z_1 & -P_1 \\ Z_2 & -P_2 \\ \vdots & \vdots \\ Z_M & -P_M \end{bmatrix} \cdot \begin{bmatrix} P_0 \\ Z_0 \end{bmatrix} = \begin{bmatrix} P_1 \cdot Z_1 \\ P_2 \cdot Z_2 \\ \vdots \\ P_M \cdot Z_M \end{bmatrix}$$

To find the LMS-solution we multiply with A transposed. Below dash indicates conjugate quantity.

$$\begin{bmatrix} \overline{Z_1} & \overline{Z_2} & \cdots & \overline{Z_M} \\ -\overline{P_1} & -\overline{P_2} & \cdots & -\overline{P_M} \end{bmatrix} \cdot \begin{bmatrix} Z_1 & -P_1 \\ Z_2 & -P_2 \\ \vdots & \vdots \\ Z_M & -P_M \end{bmatrix} \cdot \begin{bmatrix} P_0 \\ Z_0 \end{bmatrix} = \begin{bmatrix} \overline{Z_1} & \overline{Z_2} & \cdots & \overline{Z_M} \\ -\overline{P_1} & -\overline{P_2} & \cdots & -\overline{P_M} \end{bmatrix} \cdot \begin{bmatrix} P_1 \cdot Z_1 \\ P_2 \cdot Z_2 \\ \vdots \\ P_M \cdot Z_M \end{bmatrix}$$

$$\begin{bmatrix} \Sigma\left[\left|Z_i\right|\right]^2 & -\Sigma\overline{Z_i} \cdot P_i \\ -\Sigma Z_i \cdot \overline{P_i} & \Sigma\left[\left|P_i\right|\right]^2 \end{bmatrix} \cdot \begin{bmatrix} P_0 \\ Z_0 \end{bmatrix} = \begin{bmatrix} \Sigma\left[\left|Z_i\right|\right]^2 \cdot P_i \\ -\Sigma Z_i \cdot \left[\left|P_i\right|\right]^2 \end{bmatrix}$$

In order to invert the 2*2- matrix we use the simplified notation:

$$\begin{bmatrix} B_{11} \cdot P_0 & B_{21} \cdot Z_0 \\ B_{12} \cdot P_0 & B_{22} \cdot Z_0 \end{bmatrix} = \begin{bmatrix} E_1 \\ E_2 \end{bmatrix}$$

Substituting P0 in the second row we get:

$$B_{11} \cdot P_0 + B_{21} \cdot Z_0 = E_1$$

$$B_{12} \cdot \left[\frac{1}{B_{11}} \cdot \left[-B_{21} \cdot Z_0 + E_1\right]\right] + B_{22} \cdot Z_0 = E_2$$

From this we obtain:

$$Z_0 = \frac{1}{\delta} \cdot \left[\Sigma Z_i \cdot \overline{P_i} \cdot \Sigma\left[\left|Z_i\right|\right]^2 \cdot P_i - \Sigma Z_i \cdot \left[\left|P_i\right|\right]^2 \cdot \Sigma\left[\left|Z_i\right|\right]^2\right]$$

and

$$P_0 = \frac{1}{\delta} \cdot \left[\Sigma \left[\left| P_i \right| \right]^2 \cdot \Sigma \left[\left| Z_i \right| \right]^2 \cdot P_i - \Sigma Z_i \cdot \left[\left| P_i \right| \right]^2 \cdot \Sigma \overline{Z}_i \cdot P_i \right]$$

or

$$\begin{bmatrix} P_0 \\ Z_0 \end{bmatrix} = \frac{1}{\delta} \cdot \begin{bmatrix} \Sigma \left[\left| P_i \right| \right]^2 & -\Sigma \overline{Z}_i \cdot P_i \\ \Sigma \overline{P}_i \cdot Z_i & -\Sigma \left[\left| Z_i \right| \right]^2 \end{bmatrix} \cdot \begin{bmatrix} \Sigma \left[\left| Z_i \right| \right]^2 \cdot P_i \\ \Sigma \left[\left| P_i \right| \right]^2 \cdot Z_i \end{bmatrix}$$

with

$$\delta = \left[\Sigma \left[\left| Z_i \right| \right]^2 \cdot \Sigma \left[\left| P_i \right| \right]^2 - \Sigma Z_i \cdot \overline{P}_i \cdot \Sigma \overline{Z}_i \cdot P_i \right]$$